Studies into host macrophage transcriptional control by the African Swine Fever Virus protein A238L

Rhiannon Nicola Silk

Thesis submitted for the degree of
Doctor of Philosophy

Institute of Animal Health
Pirbright Laboratory

The University of Edinburgh

2008

Declaration

I hereby declare that, unless otherwise indicated in the text or references, the research described within this thesis is my own work. The work presented has never been submitted for any other degree or professional qualification.

Rhiannon Silk

Abstract

African swine fever virus (ASFV) is a large double-stranded DNA virus which causes a lethal haemorrhagic fever in domestic pigs. This virus primarily infects cells from the monocyte/macrophage lineage and its ability to manipulate the function of these cells is key to the pathogenesis of this disease. ASFV encodes several proteins involved in immune evasion. One of these proteins, A238L, has been shown to inhibit host macrophage gene transcription. This protein has been shown to interact with several cellular proteins involved in signal transduction: a serine/threonine protein phosphatase, calcinerurin (CaN), the transcription factor NF-κB, and most recently the transcriptional co-activator CREB binding protein (CBP/P300). However its exact mechanism of action is not fully understood. Previous work has been limited to the investigation of individual signaling pathways and/or the expression of individual host genes. The aim of this study was to investigate the global effect of A238L on host macrophage gene transcription and also to carry out further investigation into the mechanism by which this protein functions.

To determine the global effect of A238L on host macrophage gene transcription differential gene expression between porcine cells expressing A238L and control cells was examined using a porcine oligonucleotide microarray. These results demonstrated that A238L was a potent inhibitor of host macrophage gene expression. Functional characterisation of the annotated genes showed that a large proportion of A238L down-regulated genes are typically induced in response to cell stress. Significantly, genes regulated by the I kappa B kinase (IKK), mitogen-activated protein kinase **(**MAPK) and janus kinase/signal transducers and activators of transcription (JAK/STAT) signaling pathways were all shown to be down regulated by A238L. Genes associated with the MAPK pathways were particularly enriched. The transcription of A238L-regulated genes is controlled by numerous different transcription factors, including NF-κB. All of the transcription factors identified interact with the transcription co-activator CBP/P300. This provides a common link between these factors, and indicates that A238L may target CBP/P300 to inhibit gene transcription. This observation supports recent work demonstrating that A238L interacts with and inhibits CBP/P300 function.

To explore the potential mechanisms involved in the nuclear localisation of A238L, ASFV-infected Vero cells, expressing A238L under the control of its own promoter, were examined under a range of conditions using confocal microscopy. The results demonstrated that A238L was actively imported into the nucleus and exported by a CRM 1 mediated pathway, although a pool of A238L protein remained in the cytoplasm. Sequence analysis of A238L identified the presence of two putative nuclear localisation signals (NLS-1 and NLS-2). NLS-2 was located within A238L's CaN docking motif. Mutation of these motifs indicated that both NLS-1 and NLS-2 are active and exhibit functional redundancy. Mutation of the CaN docking motif alone, in the presence of intact NLS-2, resulted in a dramatic increase in the nuclear localisation of A238L. These results are consistent with a model in which A238L functions within both the nucleus and the cytoplasm and suggest that binding of CaN to A238L masks NLS-2, contributing to the cytoplasmic retention of A238L.

Publications arising from this thesis

Rhiannon N. Silk, Gavin C. Bowick, Charles C. Abrams and Linda K. Dixon

African swine fever virus A238L inhibitor of NF-kappaB and of calcineurin phosphatase is imported actively into the nucleus and exported by a CRM1-mediated pathway. *Journal of general Virology*. (2007) 88; (Pt 2): 411-9.

Charles C. Abrams, Dave A.G. Chapman, Rhiannon Silk, Elisabetta Liverani and Linda K. Dixon.

Domains involved in calcineurin phosphatase inhibition and nuclear localisation in the African swine fever virus A238L protein. *Virology*. (2008) 374; (2): 477-86.

Copies of these publications can be found in Appendix I.

Table of Contents

List of Tables

List of Figures

Chapter 7

Acknowledgements

First of all I would like to thank my supervisor, Dr Linda Dixon, whose expertise, sound advice and guidance was invaluable throughout the duration of this thesis. In particular her ability to plough through tedious pages of text and still appear relatively cheerful at the end of it is particularly impressive. I would also like to thank Dr Jeremy Bradshaw at the University of Edinburgh, for his help and interest throughout this project, it is much appreciated.

Special thanks go to Dr. Fuqan Zhang for providing the tools, help and expertise essential for the microarray data capture, processing and analysis and also to Dr Charles Abrams for providing the microarray chips in the first place. I would also like to thank the members of the ASFV group and all the staff at Pirbright for making it such a great place to work over the last seven years. I would especially like to thank Dr Rebecca Rowlands for her very helpful advice on all matters and for being such a great friend.

As for my family, I would like to thank my Mum and Dad, with a special thank you to my brilliant Mum, for all her endless hours of baby sitting, Stewart for all his support, and finally to Tom and Poppy for always making me grin and for putting things into their proper perspective.

Thank you to The Biotechnology and Biological Sciences Research Council (BBSRC) for funding this project.

Chapter 1

Introduction

1.1 African swine fever

African swine fever (ASF) is a devastating disease of domestic swine. The disease is characterised as a severe haemorrhagic fever with up to 100 % mortality in infected herds (Montgomery, 1921). ASF was first described in Kenya in the 1920s and contact of domestic pigs with warthogs was identified as the source of infection. The infectious agent was identified as a virus named African swine fever virus (ASFV). Since then ASF has been reported from most sub-Saharan countries in Africa. In 1957 and 1960 ASF was introduced to Portugal via infected meat products from airline waste. The disease spread throughout the Iberian peninsula and remained endemic there between 1960 and the mid-1990s (Perez-Sanchez *et al.*, 1994; Wilkinson, 1989). Outbreaks in France, Italy, Malta, Belgium, Holland, Sardinia, Cuba, Dominican Republic, Haiti and Brazil were thought to have been introduced from the Iberian peninsula. These outbreaks were eradicated with the exception of Sardinia where disease has remained endemic since its introduction in 1982 (Perez-Sanchez *et al.*, 1994; Dixon, 2005). In Africa ASF remains endemic in many sub-saharan countries and more recently has spread to previously uninfected countries including Madagascar. Recent outbreaks of ASFV in Georgia and surrounding countries in the Caucasus have lead to the slaughter of over 20,000 animals (Northoff, 2007). There is no vaccine available and control methods rely on quarantine and slaughter, which are difficult to implement in many developing countries due to the lack of appropriate infrastructure.

In Africa ASFV is maintained in a natural transmission cycle between its natural hosts, warthogs (*Phacochoerus aethiopicus*), bushpigs (*Potomochorus porus*) and soft ticks of the *Ornithodoros* species, and these provide a reservoir of disease. The virus is highly

adapted to these hosts and causes a sub-clinical persistent infection. In the transmission cycle involving these wildlife hosts the tick vector is thought to play a very important and possibly essential role since direct transmission between warthogs is thought to occur rarely. In contrast the virus can be transmitted directly between domestic pigs without the need for a tick vector and therefore is a risk to pig populations even in countries which do not contain the arthropod vector (reviewed in Wilkinson 1989).

1.2 African swine fever virus

1.2.1 Classification

African swine fever virus (ASFV) is the etiological agent of ASF. It is a large, enveloped, double-stranded DNA virus which replicates predominantly in the cytoplasm of infected cells. The virus is morphologicaly similar to the *Iridoviridae* virus family but has a similar genome structure and replication strategy to the *Poxviridae* and therefore has been placed in a separate virus family the *Asfarviridae*, genus Asfivirus (Dixon, 2000) in which it is the only member**.** ASFV is currently the only known DNA arbovirus. The *Iridoviridae*, *Poxviridae* and *Asfarviridae* virus families all belong to a group of nucleocytoplasmic large DNA viruses (NCLDV) which also includes the *Phycodnaviridae*, and *Mimivirus* (Iyer *et al*., 2001; Raoult *et al*., 2004; Iver *et al*., 2006). All of these virus families either replicate exclusively in the cytoplasm of the host cell or start their life cycle in the host nucleus but complete in the cytoplasm. Typically these viruses do not depent on the host replication or transcription systems for completing their replication cycle and encode several conserved proteins responsible for DNA replication and transcription. Comparative analysis between the genome sequences of viruses belonging to these virus families identified 9 genes that are shared by all of these viruses and 22 genes that are shared between the majority of the virus families (Iver *et al*., 2001). This and subsequent comparisons indicate that all NCLDV families descended from a common ancestor which was a nucleocytoplasmic virus with an

icosahedral capsid, and encoded complex systems for DNA replication and transcription (Iver *et al*., 2006).

1.2.2 Virus morphology

The virus particles exhibit a complex structure with several concentric layers and are approximately 200 nm in diameter (Andres *et al.*, 1998; Carrascosa *et al.*, 1984). The viral core consists of a DNA containing nucleoid surrounded by a layer of core protein to form a shell (Carrascosa *et al.*, 1984**).** The core is wrapped in a single lipid bilayer thought to be derived from the endoplasmic reticulum (ER), on which an outer icosahedral capsid is assembled (Hawes *et al*, 2008; Andres *et al.*, 1998**).** Extracellular virons usually have an outer envelope, gained by budding through the plasma membrane of infected cells (Breese, 1966; Carrascosa *et al.*, 1984) (Figure 1.1). A diagram of the virus structure and electron micrographs of the virus particle are shown in Figure 1.1.

1.2.3 Genome

The viral genome consists of a single linear molecule of DNA, which is approximately 170-182 kbp in length, varying between isolates, with inverted terminal repeats and covalently closed hairpin-loops at each end (Gonzalez *et al.*, 1986; Sogo *et al.*, 1984). The complete genome sequence of several ASFV isolates has been determined and these are available on the website www.virology.ca. The genomes are predicted to encode between 151 and 167 ORFs, which are read from both DNA strands across the length of the genome (Chapman *et al.*, 2008; Yanez *et al.*, 1995). The genome organisation map of the Malawi LIL20/1 isolate, a virulent field isolate of ASFV, is shown in Figure 1.2 (Dixon & Chapman, 2008). The genome consists of a central region, which is conserved in length, with variable length regions at either end. The variable regions encode a number of multigene families (MGF) which vary considerably in number between virus isolates (Dixon & Wilkinson, 1988). The functional significance of these genes is not fully understood, but they are thought to play a role in determining host range and

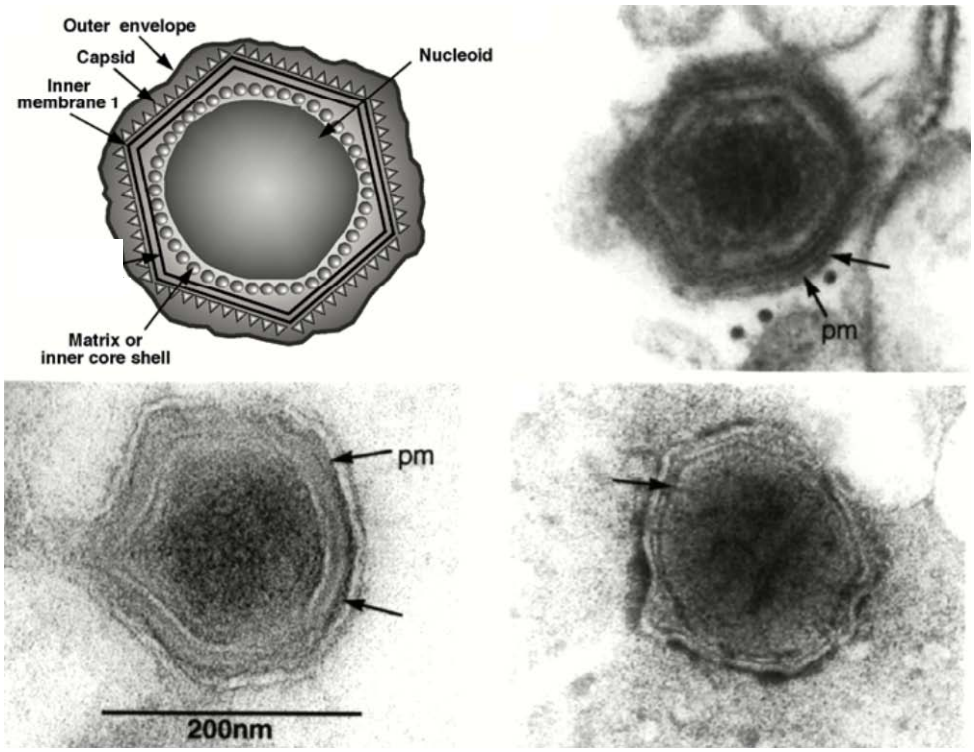

Figure 1.1 African swine fever virus morphology.
(Top left) Diagram of a viron section with lipid membranes, capsid and nucleoprotein core visualised of ASFV particle. (Top right) Thin section, (Bottom left) cryo-section and (Bottom right) a negative contrast electron micrograph of ASFV particles. The arrow indicated the membrane components of the virus; pm=plasma membrane. (EMs were provided by Dr S. Brookes, IAH Pirbright). The bar represents 200nm. Diagram courtesy of Dr L. Dixon (Dixon 2003).

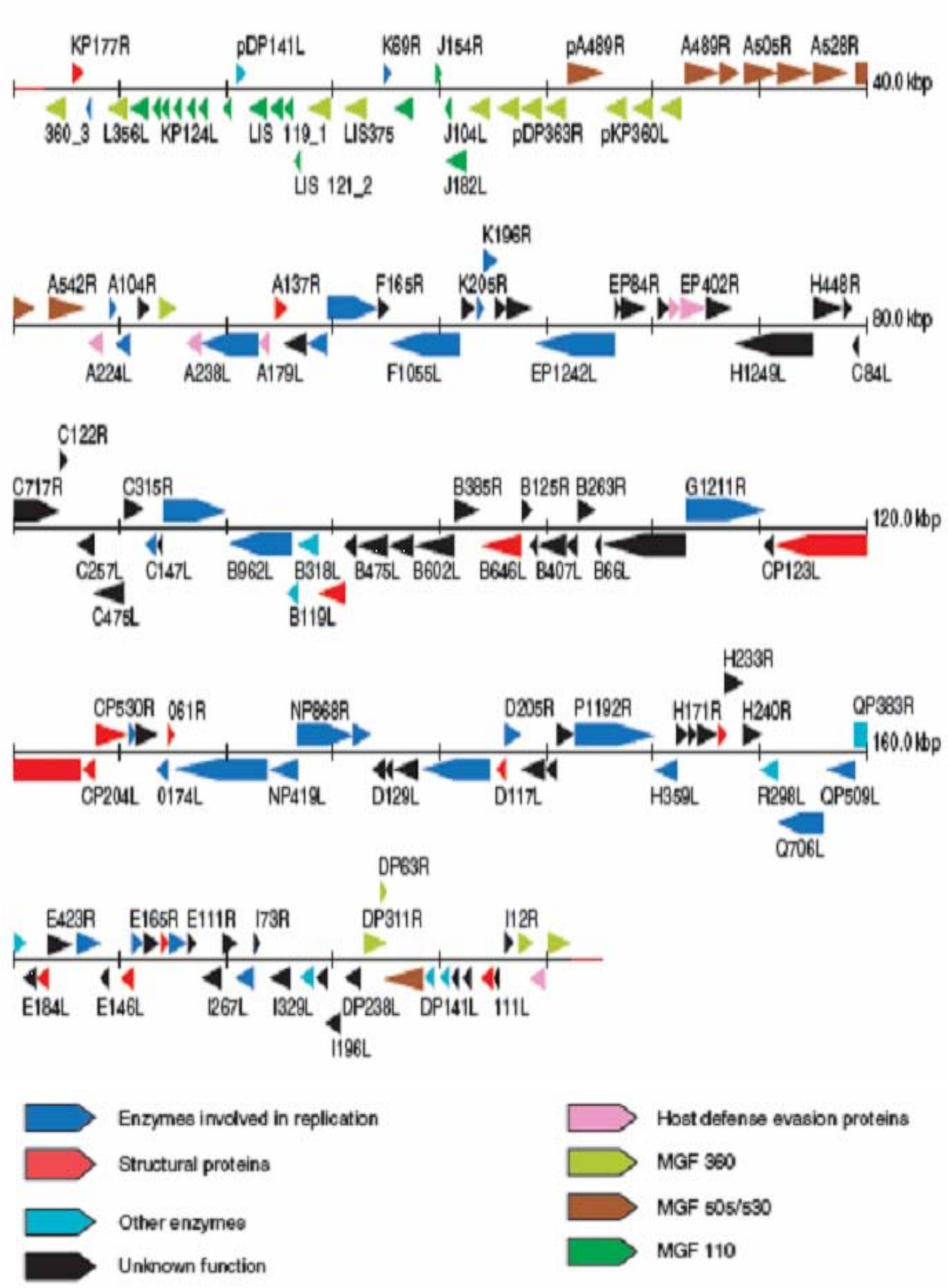

Figure 1.2 Genome map of the ASFV strain Malawi Lil-20-1. The orientations of the arrows denote the direction in which the open reading frame is read. Diagram provided by Dr. Linda Dixon (Dixon 2008).

virulence (Zsak *et al.*, 2001). Deletion of 6 copies of MGF 360 and 2 of MGF 505/530 has been shown to affect viral growth in macrophage cell cultures and virulence in pigs. These MGF family members have been also been implicated in modulating the host IFN response (Afonso *et al.*, 2004; Neilan *et al.*, 2002; Zsak *et al.*, 2001). MGF 360 genes have also been shown to affect virus replication and generalization of infection in *Ornithodoros porcinus* ticks (Burrage *et al.*, 2004).

A comparison between the genomic sequences of non-pathogenic and pathogenic ASFV isolates has identified 109 non-duplicated open reading frames (ORFs) that are conserved between all 10 of the available ASFV genomes. These ORFs encoded proteins which include enzymes involved in nucleotide metabolism, DNA replication and repair, mRNA transcription and processing, enzymes involved in post-translational momodification of proteins, structural proteins and proteins involved in evading the host defence system (Chapman *et al.*, 2008) (see Table 1.1). Although the MGF family members vary between isolates some copies are conserved between isolates, indicating selective pressure to retain these genes.

1.2.4 Virus proteins

The virion contains approximately 50 proteins. These include structural proteins and enzymes and factors necessary for early mRNA transcription and processing. The enzymes packaged include RNA polymerase, poly A polymerase, guanyl transferase, a protein kinase, two nucleoside tri-phosphydrolases, an acid phosphatase and a deoxyribonuclease active on single stranded DNA (Tables 1.1) (Dixon, 2003; Salas, 1999). The A224L inhibitor of apoptosis (IAP) homolog protein is also packaged within the virion core. The genes encoding 15 viron structural proteins have been identified: p72, p30, p12, p17, p22, p54 (J13L), p49, j18L, 5JR, and 6 core proteins derived form 2 polyprotein precursor molecules, pp220 and pp62 (Dixon, 2005; Salas, 1999). p150, p37, p34 and p14 are derived from pp220 (Andres *et al.*, 1997; Simon-Mateo *et al.*, 1997) and p35 and p15 are derived from pp62. The proteolytic processing of these

Table 1.1 Functions of ASFV encoded proteins

Nucleotide metabolism, transcription, replication and repair	Gene Name (BA71V isolate)	Predicted Protein size
Thymidylate kinase	A240L	27.8
Thymidine kinase	K196R	22.4
dUTPase*	E165R	18.3
Ribonucleotide reductase (small subunit)	F334L	39.8
Ribonucleotide reductase (large subunit)	F778R	87.5
DNA polymerase β	G1211R	139.8
DNA topoisomerase type II*	P1192R	135.5
Proliferating cell nuclear antigen (PCNA) like	E301R	35.3
DNA polymerase family X *	O174L	20.3
DNA ligase*	NP419L	48.2
Putative DNA primase	C962R	111.2
AP endonuclease class II*	E296R	33.5
RNA polymerase subunit 2	EP1242L	139.9
RNA polymerase subunit 6	C147L	16.7
RNA polymerase subunit 1	NP1450L	163.7
RNA polymerase subunit 3	H359L	41.3
RNA polymerase subunit 5	D205R	23.7
RNA polymerase subunit 10	CP80R	8
TFIIB like	C315R	31.5
Helicase superfamily II	A859L	27.8
Helicase superfamily II similar to origin binding protein	F1055L	123.9
Helicase superfamily II	B962L	109.6
Helicase superfamily II VV D6/D11 like involved in transcription termination	D1133L	129.3
Helicase superfamily II VV D5 like	Q706L	80.4
Helicase superfamily II VV A18 like	QP509L	58.1
Transcription factor SII	I243L	28.6
Guanyl transferase*	NP868R	29.9
Poly A polymerase large subunit	C475L	54.7
FTS J like methyl transferase domain	EP424R	49.3
ERCC4 nuclease domain	EP364R	40.9
Lambda-like exonuclease	D345L	39.4
VV A2L like transcription factor	B385R	38.5
VV A7L like transcription factor	G1340L	134
VV VLTF2 like late transcription factor, FCS like fnger	B175L	17.5
VV D5 like ATPase involved in replication	C962R	96.2
Other enzymes with unknown roles		
Prenyl transferase*	B318L	35.9
Serine protein kinase*	R298L	35.1
Ubiquitin conjugating enzyme*	I215L	24.7
Nudix hydrolase*	D250R	29.9
Host cell interactions		
IAP apoptosis inhibitor*	A224L	26.6
Bcl 2 apoptosis inhibitor*	A179L	21.1
IkB homolog and inhibitor of calcineurin phosphatase*	A238L (5EL)	28.2
C type lectin like*	EP153R	18.0

Continued on next page

Table 1.1 –continued

CD2 like. Causes haemadsorbtion to infected cells*	EP402R (CD2v)	45.3
Similar to HSV ICP34.5 neurovirulence factor	DP71L	8.5
Nif S like PLP dependent transferase	QP383R	42.5
Mn dependent superoxide dismutase	C129R	12.9
Structural proteins and proteins involved in morphogenesis		
P22 Transmembrane domain.	KP177R	20.2
A104R Histone-like structural protein.HF-like DNA binding protein	A104R	11.5
P11.5	A137R	21.1
P10	A78R	8.4
P72 Major capsid protein. Involved in virus entry	B646L	73.2
B438L Required for formation of vertices in icosahedral capsid.	B438L	49.3
B602L Chaperone. Involved in folding of p72 capsid protein. Not incorporated into virus particles.	B602L	45.3
B119L ERV 1 like. Involved in redox metabolism* Not incorporated into virus particles	B119L	14.4
Sumo 1 like protease. Involved in polyprotein cleavage	S273R	31.6
P220 Polyprotein precursor of p150, p37, p14, p34 core shell components. Required for packaging of nucleoprotein core.	CP2475L	281.5
P30 Phosphoprotein. Involved in virus entry.	CP204L	23.6
P60 Polyprotein precursor of p35 and p15. Present in core shell.	CP530R	60.5
P12 Attachment protein involved in virus entry. Transmembrane domain.	O61R	6.7
P17 Transmembrane domain.	D117L	13.1
J5R Transmembrane domain.	H108R	12.5
P54 Binds to LC8 chain of dynein, involved in virus entry. Transmembrane domain. Required for recruitment of membranes to virus factories.	E183L	19.9
J18L Transmembrane domain. VV J5 like membrane protein	E199L	22.0
E248R Possible component of redox pathway required disulfide bond formation. Structural protein.	E248R	24.8
A151R Contains CXXC motif similar to that in thioredoxins. Binds to E248R protein. Possble component of redox pathway.	A151R	15.1
P14.5 DNA binding. Required for movement of virions to plasma membrane	E120R	13.6
XP124L Multigene family 110 member. Contains KDEL ER retrieval sequence and transmembrane domain. Involved in modification of ER in preparation for virus assembly.	XP124L	10.6

Table 1.1. Courtesy of Dr Linda Dixon and adapted from Dixon, 2005.

polyproteins is catalyzed by the viral protease pS273R, which is also located in the core shell and is related to the Sumo-like family of proteases (Alejo *et al.*, 2003). Proteins involved in virus entry include p12, p30, p54 and also the major capsid protein p72. Other proteins present in the capsid include 3 DNA binding proteins and pE120R which associates with p72 and is essential for virus transport from assembly sites to the plasma membrane (Rodriguez *et al.*, 2004).

1.2.5 ASFV replication

ASFV replicates mainly in cells derived from the monocyte/macrophage lineage and exhibits a predominantly cytoplasmic replication cycle. A diagram of the replication cycle of ASFV is shown in Figure 1.3. Virus attachment to porcine macrophages may be mediated by porcine CD163 (Sanchez-Torres *et al.*, 2003). Expression of CD163 on porcine monocytes and macrophages has been shown to correlate with permissiveness to ASFV infection and monoclonal antibodies against CD163 were able to inhibit ASFV infection and virus binding to alveolar macrophage in a dose dependent manner. Entry occurs *via* receptor-mediated endocytosis, and is energy and temperature dependent (Valdeira *et al.*, 1998; Valdeira & Geraldes, 1985). Following internalisation, the viral envelope fuses with that of endosomes at an acidic pH releasing the viral core to the cytoplasm of the host cell (Valdeira *et al.*, 1998). The virus initiates gene expression immediately following entry into the cytoplasm, using enzymes and factors packaged into the virus core. Viral gene transcription does not require the host RNA polymerase and is dependent on the viral RNA polymerase and specific virus-encoded transcription factors. The temporal expression of ASFV genes is strongly regulated and four temporal classes of ASFV genes have been described: early, immediate-early, intermediate and late. The expression of early and immediate-early genes begins immediately after infection. Early gene expression can continue throughout infection; however a sub-class of early genes (immediate-early) are silenced before the onset of virus DNA replication (Almazan *et al.*, 1992). Intermediate gene expression is detected 4 to 6 hours postinfection, and coincides with the maximum expression of early genes. The

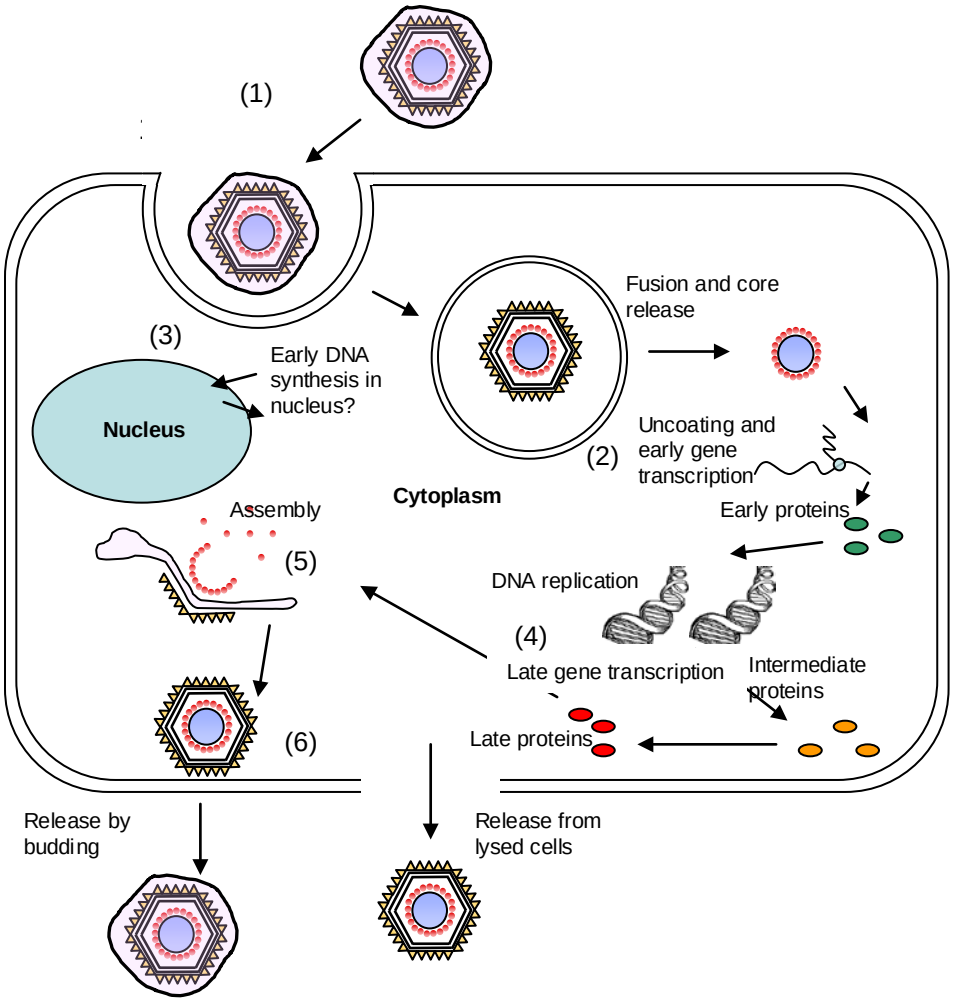

Figure 1.3 African Swine Fever virus replication cycle. 1. ASFV binds to receptors on target cells and enters cells by receptor mediated endocytosis . This is followed by low pH-mediated fusion of the viral membrane with the endosomal/lysosomal membrane. 2. Early mRNA synthesis begins in the cytoplasm immediately following virus entry using enzymes and factors that are packaged in the virion. 3. a) An early stage of DNA synthesis takes in the nucleus b) followed by the synthesis and formation of mature DNA in the cytoplasm from about 6 hours post infection, 4. Late gene expression is dependent on onset of DNA replication. Late mRNAs encode structural proteins and enzymes needed for early stages of next round of infection. 5. Virus assembly takes place in cytoplasmic factory areas and involves wrapping of the nucleoprotein core in a membrane layer on which the virus capsid is formed. 6.Progeny virus are transported via microtubules to the cell membrane where they exit by budding through membrane or cell lysis. Diagram courtesy of Dr. Gavin Bowick, Institute for Animal Health.

expression levels of intermediate genes decrease as late mRNA synthesis increases. Late genes are expressed after the initiation of DNA synthesis (Rodriguez *et al.*, 1996). This temporal expression of genes suggests that ASFV genes are expressed in a cascade model, similar to that described for vaccinia virus, with factors required for transcription of one class of genes synthesised during the previous temporal stage (Moss, 2001).

Newly synthesised viral DNA is found in the nucleus and cytoplasm in the early stages of DNA replication, and is found only in the cytoplasm at later stages (Garcia-Beato *et al.*, 1992; Rojo *et al.*, 1999). This may indicate the involvement of cellular nuclear factors in the early stages of viral DNA synthesis. Smaller DNA fragments are synthesised in the nucleus, with larger genome length fragments found in the cytoplasm at later time points. Pulse-chase experiments are consistent with the hypothesis that these nuclear fragments are precursors of the mature cross-linked viral DNA found in the cytoplasm (Rojo *et al.*, 1999). However it is not clear if the nuclear stage of DNA replication is essential. Replication of the full length ASFV genome takes place in virus factory areas via head-to-head concatemers, as has been described for poxvirus genome replication (Gonzalez *et al.*, 1986; Sogo *et al.*, 1984). Following resolution of these concatameric forms into unit length genomes, the complete genomes are then packaged into virus particles (Brookes *et al.*, 1996). Virus morphogenesis takes place in virus factories that are located in discrete perinuclear foci, that are located next to the microtubule organising center (Heath *et al.*, 2001). The microtubule network is required for maintenance of virus factories. The virus factories resemble aggresomes, which are formed in cells in response to misfolded proteins (Heath *et al.*, 2001). Following assembly mature virus particles are transported from the virus factories along microtubules to the cell surface (Jouvenet *et al.*, 2004) and are released by budding from the plasma membrane from projections that resemble filopodia (Jouvenet *et al.*, 2006).

1.3 Pathogenesis of ASFV

The clinical symptoms of ASF vary considerably between the virus isolate and host species. In domestic pigs the disease is characterised into 4 forms: peracute, acute, subacute and chronic (Boinas *et al.*, 2004; Hess, 1981; Wardley *et al.*, 1983). The clinical symptoms associated with these forms are presented in Tables 1.2. Symptoms range from 100 % mortality within a few days of infection before clinical signs are detected (peracute), to chronic infections where pigs exhibit few signs of illness. Pigs infected with moderately virulent isolates of ASFV can recover from infection, but remain persistently infected, providing a potential reservoir of virus in domestic herds. Virus has been isolated from the lymph nodes of recovered animals up to 48 days post-infection (Oura *et al.*, 1998) and viral DNA has been detected in peripheral blood mononuclear leukocytes (PBML) at greater than 500 days post-infection by a PCR assay (Carrillo *et al.*, 1994). In its most

Table 1.2 Clinical effects of ASF

Clinical symptoms are presented 5-15 days after infection, and can include one or more of the following forms of disease. Adapted from www.pighealth.com/ASF.htm#Clinical.

Classification	Clinical Symptoms
Peracute	Pigs are suddenly found dead, or close to death.
Acute	Pigs exhibit fever, loss of appetite and inactivity. Red or blue skin discolouration may be present on the chest or abdomen, tips of ears or distal limbs. Diarrhoea, vomiting, coughing, breathing difficulty and abortion may also occur. Almost 100% of pigs with these symptoms will die within 7 days.
Subacute	Affected pigs show mild symptoms, with intermittent fever for up to one month, followed by recovery in most cases. Mortality ranges from 30-70% and pregnant sows may abort. Recovered animals can still excrete virus for up to six week following infection.
Chronic	Pigs show few clinical signs with the exception of occasional bouts of fever, reduced growth stunting and emaciation. Patches of necrotic skin, may be present and chronically infected animals are vulnerable to secondary infection, pneumonia and lameness. Mortality is less than 30%.

acute form ASF is characterised by multiple haemorrhages, lymphopenia associated with intense destruction of lymphoid tissue and disseminated intravascular coagulation, leading to death within a few days as a result of shock.

The ability of ASFV to infect and replicate in cells of the monocyte/macrophage lineage is considered to play a critical role in the pathogenesis of this disease. ASFV has been reported to infect other cell types, including endothelial cells, fibroblasts and reticular cells (Carrasco *et al.*, 1997; Gomez-Villamandos *et al.*, 1997). However, infection of these cells is limited to the late stages of infection after the characteristic symptoms of ASFV have been observed and therefore is not thought to play a central role in disease pathology.

Immunocytochemistry on infected tissues from domestic pigs infected with Malawi, a highly pathogenic isolate of ASFV, exhibited extensive apoptosis of uninfected lymphocytes in association with ASFV infected macrophages in the lymphoid tissue (Oura *et al.*, 1998)**.** The mechanisms involved in ASFV-induced lymphocyte apoptosis have not been defined, but are thought to include the release of proinflammatory cytokines, such as TNF-α and IL-1β from infected monocytes/macrophages. Salguero et al (2002, 2005) demonstrated an increase in the serum levels of TNF-α and IL-1β which was shown to coincide with lymphocyte apoptosis. These studies also showed an increase in the immunohistochemical detection of macrophages expressing TNF-α, IL-1 and IL-6 in proximity to lymphocytes undergoing apoptosis (Salguero *et al.*, 2002; Salguero *et al.*, 2005).

The removal of positive cell survival signals has also been proposed as an indirect mechanism involved in B cell apoptosis. T cell apoptosis has been shown to precede that of B cells in pigs infected with Malawi (Oura *et al.*, 1998). One study investigating the effect of ASFV on B cells in pigs infected with the Malawi isolate Lilongwe 20/1, demonstrated that the CD40 ligand (CD154), a cell survival signal expressed by T-cells, was able to rescue B cells from ASFV infected pigs from apoptosis. The hypothesis

suggested by the authors is that B cells are activated during ASFV infection and would normally receive survival signals from CD154 expressed on T cells. However, due to the drastic depletion of T cells, which occurs early during ASFV infection, these survival signals may not be delivered to rescue the B cells from apoptosis (Takamatsu *et al.*, 1999).

Factors from ASFV infected macrophages have also been associated with increased vascular permeability and the stimulation of adjacent endothelial cells, leading to haemorrhage (Carrasco *et al.*, 1997)**.** An increase in the levels of TNF-α has been shown to coincide with ASFV disease pathology (Carrasco *et al.*, 2002; Gomez del Moral *et al.*, 1999; Salguero *et al.*, 2002)**,** and is thought to make a significant contribution to some of the major clinical manifestations of acute ASF. In addition to providing signals involved in the induction of apoptosis, TNF-α induces vasodilation, an increase in vascular permeability and activation of the vascular endothelium (Mantovani, 1997)**.** These contribute to damage to the vascular endothelial cells and result in haemorrhage.

The pathogenesis of ASFV shares several similarities with other viral haemorrhagic fevers, including Ebola and Marburg viruses. These viruses also primarily infect cells of the mononuclear phagocytotic system but spread to other cell types as the disease progresses. Infected monocytes release cytokines and chemokines which can indirectly lead to the destruction of endothelial cells (Feldmann *et al.*, 1996; Stroher *et al.*, 2001) and induce apoptosis of uninfected lymphocytes (Geisbert *et al.*, 2000). Virus infected macrophages, in combination with the cytotoxic properties of the virus's surface glycoproteins (Feldmann *et al.*, 1999) are considered to be the main pathological determinants of these diseases.

1.4 Host Immune response to ASFV infection

At present there is no vaccine available against ASFV. Homologous protective immunity against ASFV infection has been demonstrated in pigs that survive infection

with moderately virulent or attenuated variants of ASFV are protected against closely related but not more distantly related isolates (Boinas *et al.*, 2004; Hamdy & Dardiri, 1984; Leitao *et al.*, 2001). The exact mechanism of protective immunity is not fully understood. Antibody-mediated immune mechanisms have been shown to play a role in protection. An antibody-mediated reduction of infectivity of virulent ASFV isolates in Vero cells and swine macrophages has been demonstrated *in vitro* in the presence of ASFV hyperimmune serum (Ruiz Gonzalvo *et al.*, 1986a; Ruiz Gonzalvo *et al.*, 1986b) and passive antibody transfer delayed onset of symptoms and reduced mortality in infected pigs treated with anti-ASF immunoglobulin (Ig) (Wardley *et al.*, 1985). The effectiveness of antibodies against the virus proteins p30, p54 and p72 in inhibiting virus attachment and entry has been demonstrated (Gomez-Puertas & Escribano, 1997; Gomez-Puertas *et al.*, 1996). In one report partial protection of pigs was demonstrated using a mixture of recombinant proteins p30 and p54 (Barderas *et al.*, 2001). However in another study immunisation with these recombinant proteins was shown to induce some neutralising activity but failed to protect pigs from viral challenge and merely delayed the onset of clinical symptoms by two days (Neilan *et al.*, 2004). It is therefore likely that ASF antibody-mediated protection is complex and requires responses to several different viral proteins.

Components of the cell mediated immune response have also been shown to play a significant role in protective immunity to ASFV. Cytotoxic T lymphocytes specific for ASFV infected macrophages have been identified in pigs infected with the non-lethal ASFV isolate (NHVP68) (Martins *et al.*, 1993). In addition, diminished protection against OUR/T88/1 isolate was observed following depletion of CD8+ cells from pigs vaccinated with the non-pathogenic ASFV isolate OURT88/3 (Oura *et al.*, 2005). Natural killer cell activity has also been associated with protection following infection with (NHVP68) (Leitao *et al.*, 2001). Overall the host mechanisms involved in the protective immune response are complex and evidence suggests they include both cellular and serological components.

1.5 Modulation of macrophage function by ASFV infection

Macrophages are key cells involved in activating and co-ordinating the innate and adaptive immune response to infection. The ability of ASFV to infect and replicate in macrophages is thought to play a critical role in ASFV disease pathology. ASFV infection has a direct effect on host macrophage function *in vitro*. Antibody mediated phagocytosis, chemiluminesence and chemotaxis are all modulated in ASFV-infected macrophages (Martins *et al.*, 1987)**.** Whittall et al (1997) demonstrated inhibition of TNF-α and IL-1β transcription and protein expression in primary macrophage cells infected in *vitro* with Malawi, a virulent isolate of ASFV. Powell et al (1996) also demonstrated the inhibition of TNF-α, IL-8 and interferon (IFN)-α gene transcription in macrophages infected with this isolate. In both studies the inhibition was limited to pro-inflammatory cytokines, as transforming growth factor (TGF)-β, a pleuripotic cytokine with anti-inflammatory properties was expressed throughout ASFV infection. The inhibition of TNF-α production in these studies contrasts with a more recent study investigating the effect of E75 (a virulent isolate of ASFV) on TNF-α expression during infection (Gomez del Moral *et al.*, 1999)**.** This study demonstrated the induction of TNF-α mRNA and TNF-α protein, in infected macrophages and cell supernatants respectively, following ASFV infection in *vitro*. This discrepancy between results could be due to inherent differences between the ability of different ASFV isolates to modulate the expression of TNF-α. This suggests that the ability of ASFV to modulate the expression of TNF-α alone may not be responsible for the disease pathogenesis as both Malawi and E-75 are virulent isolates causing high levels of mortality.

ASFV has also been shown to inhibit the ability of macrophages to respond to stimulation with IFN-γ (Whittall & Parkhouse, 1997)**.** IFN-γ and IFN-α have been shown to inhibit ASFV replication in porcine monocytes and alveolar macrophages (Esparza *et al.*, 1988) and have also been shown to cure Vero cells from lytic and persistent infection with ASFV (Paez *et al.*, 1990). Therefore the ability of ASFV to inhibit the expression of IFN-α in infected macrophages (Powell *et al.*, 1996), in

addition to suppressing the response of infected cells to IFN-γ activation could play an important role in the ability of ASFV to replicate and in host macrophages.

1.6 Viral immune evasion

Viruses are obligate intracellular parasites dependent on the host cell for survival. This coexistence between viruses and their hosts exerts an evolutionary pressure on both organisms, leading to the development of a complex anti-viral host immune response and the evolution of numerous viral strategies to counteract it.

Immune evasion strategies vary greatly between individual viruses however in general viruses with a large coding capacity, such as large DNA viruses, tend to produce a wide array of proteins with specific immune-evasion functions. These proteins can include viral homologues of host genes. For example several poxviruses and herpesviruses encode homologues of cytokines (virokines) and cytokine receptors (viroceptors) (Johnsen *et al*., 2003). Virokines include the herpesvirus cytokine homologues vIL-6 and vIL-17 and the poxvirus vIL-18 binding protein(vIL-18BP). vIL-18BP functions in the same was as it's mammalian homologue binding to host IL-18 and inhibiting it's action. IL-18 is a potent inducer of IFN γ, therefore inhibition of IL-18 indirectly regulates IFN action. In addition many poxvirus also produce viral mimics of both IFN α/β and IFN γ receptors (IFN-Rs). These proteins are secreted from virus infected cells where they bind with high affinity to IFNs. This effectively decreases the amount of IFN available to interact with host IFN-Rs (Johnson *et al*., 2003). The similarity between these genes and the host counterpart suggests that they have been 'stolen' from the host and modified for the benefit of the virus. Herpesviruses also have an additional capacity to hide from the host's immune system by their ability to establish latency. (Vossen *et al*., 2002). In contrast to large DNA viruses, viruses with small genomes, common among many RNA viruses, are constrained by their coding capacity. These viruses often encode multifunctional proteins which carry out immune-evasion functions and functions essential for virus replication. For example the Flavivirus nonstructural protein

(NS1), described below, is an essential gene which functions as a cofactor for viral RNA replication and also inhibits complement activation by a separate mechanism (Chung et al., 2006).

1.6.1 Viral mechanisms to evade host defence

Viral immune evasion strategies cover all aspects of the host response to infection, including the humoral immune response, the cellular immune response and immune effector functions such as cytokines and apoptosis. Some specific examples of inhibition of the humoral and cellular immune response are described below. Examples of ASFV strategies to counteract immune effector functions are discussed in section 1.7.

Inhibition of the humoral Immune response

Antigenic drift is an important strategy for avoiding immune detection by neutralising antibody. Due to the low fidelity of RNA-polymerases, RNA viruses such as picornaviruses, and retroviruses are constantly subject to random mutations leading to changes in their envelope proteins and the selection of variants with different antigenic properties. In addition, RNA viruses with segmented genomes such as Influenza can exhibit both antigenic drift, resulting in small mutations due to errors in transcription and antigenic shift, a major alteration which occurs when RNA segments from different viruses recombine.

The complement system is also a target for virus subversion. Activation of the complement system can lead to neutralization of cell-free viruses, phagocytosis of C3b-coated viral particles, lysis of virus-infected cells, and generation of inflammatory and specific immune responses. Therefore many viruses have developed mechanisms to counteract it. Several large DNA viruses encode viral homologues of complement regulatory proteins which block complement activation. vaccinia, cowpox and variola members of the poxvirus family all encode complement homologues (Bernet *et al*.,

2007). In contrast the West Nile virus nonstructural protein NS1 has no similarity to cellular counterparts. This protein binds to the regulatory protein factor H and promotes the fI-mediated cleavage of C3b. In addition cell surface-associated NS1 attenuates the deposition of C3b and C5b–9 membrane attack complexes (Chung *et al*., 2006). Other viruses such as HIV and human cytomegalovirus (HCMV), 'borrow' host cellular factors involved in complement control such as CD59 and incorporate them into the viral envelope. There by protecting the virions from complement lysis (Favoreel *et al*., 2003).

Inhibition of cell-mediated immune responses

The cellular immune response to infection plays an important role in host defence. CD8+ cytotoxic T lymphocytes (CTLs) and natural killer (NK) cells, in particular, play a critical role in the destruction of virus infected cells. In general, CD8+ CTLs recognize antigenic peptides in the complex with major histocompatibility complex (MHC) class I molecules. Therefore many viruses have developed strategies to interfere with the activation of CTLs cells by blocking MHC class 1 antigen processing and presentation. For example the HCMV protein unique short 6 (US6) inhibits the loading of viral peptides into MHC class 1 complexes by blocking the transporter associated with antigen processing (TAP-1) protein function. TAP is a transmembrane protein that delivers cytosolic peptides into the endoplasmic reticulum (ER) (Hewitt *et al*., 2001). The adenovirus protein E3/19K prevents expression of newly synthesized MHC molecules by inhibition of ER export (Windheim *et al*., 2004).

Down regulation of MHC class 1 molecules has the potential to make virus infected cells vulnerable to natural killer (NK) cell recognition. Therefore some viruses have additional strategies to counteract this effect. Molluscum contagiosum virus (MCV) has been shown to encode an an MHC I homologue, MC080R which binds to b2-microglobin a sub-unit of the MHC class molecule (Johnston *et al*., 2003). HCMV has been shown to encode several genes capable of suppressing NK cell recognition. These

include UL16, UL18, UL141 and UL142. UL16, UL142 act together with a HCMV microRNA (miR-UL112) to suppress the presentation of ligands on the cells surface for the NK cell activating receptor NKG2D. UL18 acts as a MHC-I homologue and UL141 acts post-translationally to suppress cell surface expression of CD155 a NK cell activating receptor (Wilkinson *et al*., 2008).

MHC class II molecules are also a target for virus subversion. These molecules present antigen to CD4+ T cells. CD4+ T cells regulate the induction of CTLs, antibodies and memory T cells. For example HMCV protein US3 causes the rapid retrotranslocation of MHC class II proteins from the ER, followed by their proteasome-mediated degradation (Hedge *et al.,* 2002).

1.6 ASFV proteins involved in immune evasion

The ability of ASFV to modulate macrophage function and to persist in its natural hosts and in domestic pigs, which recover from infection with less virulent isolates, indicates that this virus has effective mechanisms for evading the host immune system and avoiding viral clearance. Several ASFV proteins involved in modulating the host's defence response to infection have been identified. These include proteins involved in inhibiting apoptosis, cell adhesion proteins and proteins which interfere with host macrophage signalling pathways to inhibit the transcriptional activation of immune response genes (Dixon *et al.*, 2004). ASFV strategies involved in evading the immune response to infection are represented in Figure 1.4 and individual proteins are discussed in more detail below.

1.6.1 ASFV and Apoptosis

Apoptosis is the process whereby cells undergo systematic programmed cell death in response to a wide variety of stimuli, and is an important cellular strategy to limit virus

replication and reduce virus spread. Apoptosis is observed both in ASFV infected macrophages and bystander non-infected lymphocytes (Oura *et al.*, 1998). In ASFV infected Vero cells apoptosis was shown to be triggered at early time points after virus internalization, before early ASFV protein synthesis. However, the onset of apoptosis is only observed at late times (between 16 and 18 hours post-infection) following ASFV infection (Carrascosa *et al.*, 2002; Hernaez *et al.*, 2006). At this time point progeny virions have been produced and induction of apoptosis is therefore unlikely to limit replication and the spread of progeny virus. This suggests that although the process of infection triggers apoptosis the virus must have mechanisms which delay the onset of apoptosis until later in infection. This is likely to be a tightly regulated process, where the action on cellular apoptotic proteins is balanced by the expression of viral anti-apoptotic genes.

Mammals have two distinct apoptosis signalling pathways: one initiated by members of the TNF receptor family, known as death receptors and the other initiated by cell stress and is regulated by pro- and anti-apoptotic members of the Bc1-2 protein family members. Bcl-2 protein is the prototypical member of the anti-apoptotic members of the Bc1-2 family and interacts with pro-apoptotic members to preserve mitochondrial integrity (Petros *et al.*, 2004). Pro-apoptotic members of this family function by inactivating the protective function of the pro-survival members of the Bcl-2 family and by activating the Bax/Bax-like pro-apoptotic family members. These pro-apoptotic family members permeabilise the mitochondrial membrane leading to the release of cytochrome c and subsequent activation of caspases (Bouillet & Strasser, 2002). Caspases, a family of cell death proteases, exist as inactive precursor molecules which require proteolytic cleavage for activation. Once activated, the effector caspases are responsible for the proteolytic cleavage of a broad spectrum of cellular targets, leading ultimately to cell death. The known cellular substrates include structural components (such as actin and nuclear lamin), regulatory proteins (such as DNA-dependent protein kinase) and other proapoptotic proteins and caspases (Shi, 2002).

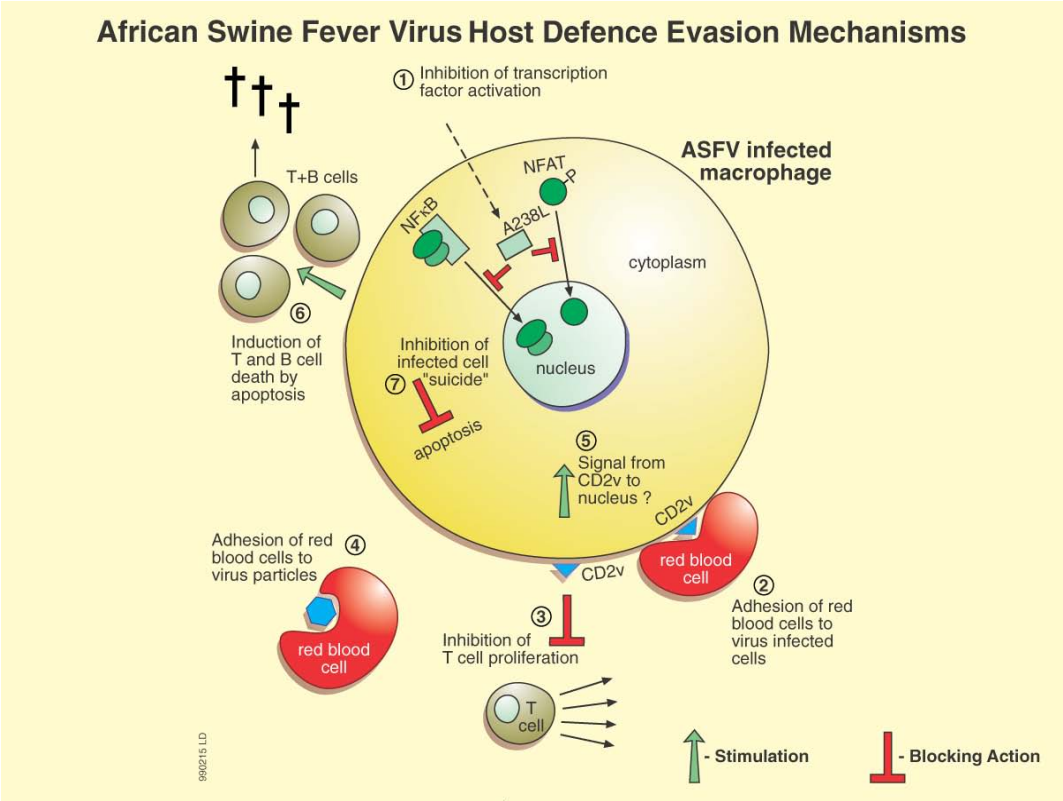

Figure 1.4 Mechanisms that the African swine fever virus uses to evade the hosts immune defence. 1. The virus encoded A238L protein inhibits activity of NF-KB directly and NFAT indirectly via inhibition of calcineurin activity. Hence this protein can inhibit the expression of a wide range of immunomodulatory proteins in macrophage whose expression depends on these factors. 2. CD2v protein encoded by the virus is expressed on the surface of infected cells and causes red blood cells to adhere to their surface, camouflaging them from the immune system. 4. CD2v is also present on extracellular virus particles, which adhere to red blood cells, facilitating dissemination of ASFV in infected animals. 3. Expression of CD2v in infected macrophage also interferes with the ability of T cells to divide, and 5 may send signals to the nucleus by interaction between its cytoplasmic tail and host cell signalling pathways. 6. Virus infection causes apoptosis in neighbouring T and B cells, thus reducing populations of these important immune cells. 7. The virus also encodes proteins which inhibits apoptosis of the host cell, thereby promoting virus replication. Courtesy of Dr. Linda Dixon (Dixon, Abrams et al. 2000).

ASFV encodes three proteins which have been shown to inhibit apoptosis in infected cells; A224L, A179L and EP153R. These proteins are expressed at different times during the ASFV replication cycle and target different components of the cellular apoptosis machinery. A179L, is a viral Bcl-2 homologue which is expressed throughout ASFV infection and is essential for virus replication (Brun *et al.*, 1996; Neilan *et al.*, 1993). This protein has been shown to inhibit the apoptotic activity of porcine BID, a member of the core Bc1-2 apoptotic machinery, which acts in the death receptor apoptosis pathway downstream of caspase 8 (Galindo *et al.*, 2008). A224L, an IAP homologue, is expressed late in ASF infection and has been shown to inhibit the proteolytic processing of caspase-3 and also interacts with the proteolytic fragment of this protein inhibiting it activity (Chacon *et al.*, 1995; Nogal *et al.*, 2001). This protein is thought to play a role in controlling the survival of the infected cell during virus morphogenesis. EP153R has been demonstrated to inhibit apoptosis, possibly by inhibiting the transactivating activity of p53 (Hurtado *et al.*, 2004).

The ability of ASFV to induce apoptosis in bystander immune cells could also be an effective strategy to limit the immune response to infection.

1.6.2 CD2v: an ASFV cell adhesion protein

The CD2v protein, encoded by the EP402R gene, is a transmembrane protein which is expressed on the surface of ASFV infected cells and also in the external membrane of extracellular virus. This protein encodes an extracellular domain, which exhibits significant similarity to the T-cell adhesion molecule CD2 (Borca *et al.*, 1994; Rodriguez *et al.*, 1993)**.** CD2v is transcribed in the late stages of ASFV replication and is responsible for the haemoadsorbtion of swine erythrocytes to virally infected cells and extracellular virus particles (Borca *et al.*, 1994; Rodriguez *et al.*, 1993)**.** The expression of another ASFV protein, EP153R, which resembles a C-type lectin, has been shown to enhance the interaction between CD2v and red blood cells. The heamadsorbtion of erythrocytes to extracellular virus is responsible for the predominantly erythrocyte

associated viremia exhibited in pigs infected with heamadsorbing isolates of ASFV and this facilitates dissemination of the virus around the host (Borca *et al*., 1998)**.** CD2v is non-essential for virus replication in primary porcine macrophage cell cultures, and deletion of the gene does not reduce mortality of virulent isolates for pigs (Borca *et al.*, 1998)**.** However, pigs infected with CD2v deletion mutants of ASFV exhibited a delay in the spread of virus infection to the lymph nodes, a delay in vireamia and also reduced viral titres in the blood (Borca *et al.*, 1998).

CD2v is also required for the inhibition of mitogen-dependent lymphocyte proliferation of swine peripheral blood mononuclear cells *in vitro.* The mechanism of inhibition is not known (Borca *et al*., 1998)**.** ASFV does not infect lymphocytes indicating that this effect is mediated through factors on the surface or secreted from ASFV infected cells. The similarity in structure and function of CD2v to the T-cell adhesion molecule CD2 and requirement of CD2v expression to suppress the proliferation of lymphocytes, suggests that its plays an important role in evading the host immune system.

1.6.3 Modulation of host gene transcription by ASFV

Regulation of host macrophage gene transcription appears to be an important strategy used by ASFV to modulate the hosts' immune response. A238L is an important protein involved in the modulation of host macrophage signalling pathways and is described below. Other ASFV proteins with the potential to regulate gene transcription include j4R, and the ASFV ubiquitin conjugating (UBCv) enzyme. j4R has been demonstrated to bind to the the host α-NAC protein (Goatley *et al.*, 2002). α-NAC can act as a transcriptional co-activator potentiating transcription dependent on c-Jun (Moreau et al.1998). The transcription factor c-Jun is activated in response to cell stress and is involved in the transcription of many immunomodulatory genes (Foletta *et al.*, 1998). Therefore j4R could regulate c-Jun dependent gene transcription through interaction with α-NAC. UBCv, encoded by the I215L gene has been shown to bind to the host nuclear protein SMCy which is involved in transcription regulation (Bulimo 2000). In

addition, deletion of members of multigene families 360 and 530 has been shown to increase production of type I IFN and activation of IFN induced genes in infected macrophages. This suggests that these genes may have a role in inhibiting transcription of type I IFN genes although this remains to be demonstrated (Afonso *et al.*, 2004).

1.6.3.1 A238L

The A238L protein varies between 238 and 239 amino acids in length and is highly conserved between different ASFV field isolates (Neilan *et al.*, 1997), indicating that it has an essential role in the survival of ASFV in its natural hosts. The protein is predicted to encode 4 ankyrin repeat domains, located in the central region of the protein. Ankyrin repeats are structural motifs involved in protein-protein interactions (Yanez *et al.*, 1995). Database comparisons with annotated proteins demonstrated that A238L (also known as 5EL) was significantly similar to the cellular inhibitor of NF-κB (IκB-α) protein, suggesting that it may function as a viral IκB-α homologue (Yanez *et al.*, 1995). At the amino acid level A238L exhibits 20 % identity and 40 % similarity to porcine inhibitor of NF-κB (IκB-α) (Figure 1.5)(Revilla *et al.*, 1998). This sequence similarity is limited to the ankyrin repeat domains and does not extend to the amino or carboxyl- terminus of A238L. Expression of A238L in porcine and monkey kidney cells has been shown to inhibit the expression of an NF-κB-dependent luciferase reporter gene and also inhibits binding of NF-kB to oligonucleotides containing its DNA binding site. AP-1 dependent gene expression and DNA binding were not inhibited, indicating that this action was specific to NF-κB and that A238L acts a functional homologue of IκB-α (Powell *et al.*, 1996; Revilla *et al.*, 1998; Tait *et al.*, 2000). The NF-κB family of transcription factors is involved in regulating the expression of a diverse range of genes involved in the immune response, including proinflammatory cytokines and chemokines, anti-apoptotic genes such as IAP proteins and Bcl-2, acute phase proteins and adhesion molecules (Ghosh *et*

al., 1998)**.** Therefore, through inhibition of NF-κB, A238L has the potential to play a significant role in counteracting the host's immune response to ASFV infection.

A238L has also been shown to bind to and inhibit the activity of the cellular calcium/calmodulin regulated phosphatase, calcineurin (CaN) (Miskin *et al.*, 1998). This phosphatase was previously known as protein phosphatase 2B but has been renamed protein phosphatase 3C or PP3C. This work also demonstrated that A238L was capable

of inhibiting the activation of the CaN regulated transcription factor Nuclear Factor of Activated T Cells (NFAT). Calcineurin and NFAT, regulate the expression of a large number of inducible genes encoding cytokines and cell-surface receptors that are essential for a productive immune response (Rao *et al.*, 1997).

Surprisingly, despite the potential ability of A238L to inhibit the expression of a wide range of host immunomodulatory genes during ASFV infection, deletion of the A238L gene does not reduce virus replication in primary porcine macrophages or established cell lines and deletion of the A238L gene does not reduce viral virulence in domestic swine (Neilan *et al.*, 1997)**.** This observation has been supported in a recent study examining the infection of pigs with the highly virulent ASFV E-70 isolate, compared to an E-70 A238L deletion mutant. No significant differences were observed in the clinical signs or pathology between both groups. However, peripheral blood monocyte cultures (PBMC) from pigs inoculated with the virus deleted in A238L showed elevated levels of TNF-α and IL- 1 mRNA compared to those from the parental E-70 isolate. This demonstrates that A238L does inhibit proinflammatory cytokine expression in *vivo*. Upregulation of transcription of these proinflammatory cytokine genes was not observed in the PBMC of animals inoculated with parental E-70 isolate, even though apoptosis of bystander lymphocytes and haemorrhages were evident. Possibly this disease pathology may be caused by secretion of these cytokines by bystander non-infected monocytes or macrophages (Salguero *et al.*, 2008) or may be induced by other factors from infected macrophages. A238L may have an important role in viral persistence in its natural hosts

(a)

(b)

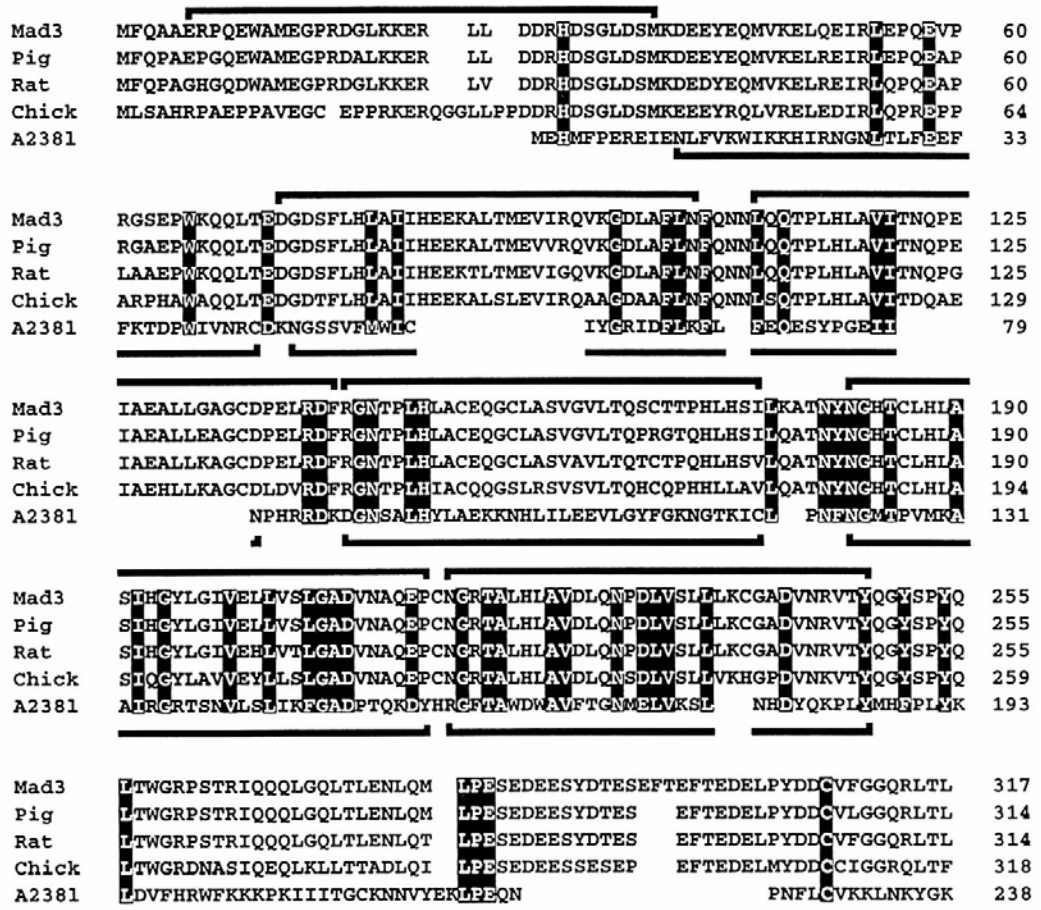

Figure 1.5 Schematic representation of A238L. Panel (A) represents the A238L protein which is 238 aa in length. A238L is predicted to encode four ankrin repeat domains (Ank) (represented by red boxes). A238L also contains a CaN binding motif located at the C-terminus and depicted in red (Misken et al 2000). Diagram is not to scale. Panel (B) Homology of A238L to IκBα proteins.The amino acid sequence of A238L was compared to the IκBα sequences from several mammalian species: Mad3, human; Pig, porcine and Rat. The black lines above the sequence show the positions of the ankrin repeats in IκBα and the black lines below the sequence represent putative Ankrin repeat motifs identified within the A238L protein (Yanz et al 1995). Adapted form Revilla Y et al.(1998).

or recovered pigs rather that being directly responsible for viral virulence in domestic swine. Considering the important role of NF-κB and NFAT in regulating the expression of immune response genes, it is also possible that A238L exhibits functional redundancy with other ASFV proteins that can compensate for the loss of A238L.

A238L is expressed throughout infection as two molecular mass forms of 28 kDa and 32 kDa (Tait *et al.*, 2000). Both forms of A238L can be expressed from cDNA in uninfected cells, indicating that the difference between these forms is due to post-translation modification. However, the nature of this modification has not yet been determined (Tait *et al.*, 2000).

A238L contains 4 ankyrin repeat domains located in the central region of the protein (Figure 1.5). These domains are a common motif found in a large number of functionally diverse proteins including proteins involved in cell cycle control, transcriptional regulation, innate immunity and apoptosis. They are most common in eukaryotes, but have been found in a small number of prokaryotes and viruses. The presence of these domains in prokaryotes and viruses is thought to be the result of horizontal gene transfer (Bork *et al.*, 1993). Ankyrin repeats are characterized as 30-33 amino acid residues which consist of two alpha helices separated by beta hairpin loops. Several ankyrin repeat motifs are usually present within any individual protein where they combine to produce a stacked structure unit which acts to present critical residues on the proteins surface and promote protein-protein interaction (Li *et al.*, 2006). Ankyrin repeat proteins do not recognise specific sequences and interacting residues are discontinuously dispersed throughout the protein. The repeats act as structural motifs providing protein stability and promoting specific binding. A238L was originally proposed as an IkBα homologue based on the similarity between the ankyrin repeat domains of these proteins (Yanez *et al.*, 1995). Therefore considering the known function of these repeats it could be that the similarity between these proteins is confined to the conserved structure of ankrin repeat domains and not specific interacting residues.

Thus A238L may not function by the same mechanism as IkBα to inhibit NF-κB mediated gene transcription.

1.6.3.1.1 NF-κB

The NF-κB family of transcription factors consists of 5 members: RelA/p65, p50, p52, c-rel and rel-B. These proteins are characterised by the presence of a REL homology domain (RHD) that consists of a DNA binding domain, dimerisation domain and a Nuclear Localisation Signal (NLS). These proteins associate as homo- or heterodimers which bind to κB sites within promoters/enhancers of target genes and regulate transcription through the recruitment of coactivators and corepressors. NF-κB proteins are classified into 2 groups based on the properties of their carboxy-terminal regions. Class one proteins (p65, c-REL and REL-B), contain transactivation domains (TAD) within the carboxy-terminal regions, which interact with components of the basal transcriptional apparatus and also the transcriptional co-activators, p300 and cyclic-AMP-response element (CREB) binding protein (CBP) (Chen & Greene, 2004). Class two proteins, p50 and p52, are synthesised as the precursor proteins p105 and p100 respectively. p105 and p100 contain a series of ankyrin repeat domains in their carboxy-terminal regions which can associate with NF-κB within the cell and act as IκB proteins. p50 and p52 contain no TAD, and therefore p50 and p52 homodimers can act as repressors to NF-κB specifc gene transcription (Ghosh *et al.*, 1998).

Heterodimers composed of p50 and p65 are the most common cellular form of NF-κB. The p50-p65 heterodimer is predominantly regulated through its sub-cellular localisation. In resting cells, NF-κB is associated with an inhibitory molecule IκB-α, which binds to NF-κB in such a way as to mask the NLS on the p65 sub-unit, but leaves the NLS on p50 partially exposed (Baeuerle, 1998). This leads to the continual shuttling of the NF-κB complex between the cytoplasm and nucleus and results in a predominantly cytoplasmic localisation in resting cells (Carlotti *et al.*, 2000). Activation of the IκB kinase complex, which can occur by a range of different stimuli including

lipopolysaccharide (LPS), TNF-α and IL-2, results is the phosphorylation of IκB-α at two conserved serine residues in the C-terminus (ser-32 and ser-36). This leads to the polyubiquitination of IκB-α and its subsequent degradation by the 26s proteasome (Karin & Ben-Neriah, 2000). Degradation of IκB-α exposes the NLS on p65 enhancing the nuclear translocation of NF-kB (Figure 1.6). One of the target genes of NF-κB transcription is IkB-α. Newly synthesised IκB-α proteins enter the nucleus to bind to and remove NF-κB from gene promoters and export the complex to the cytoplasm mediated by nuclear export signals on IκB-α. This auto-regulatory loop leads to shut-off of NF-κB induced genes.

The transcriptional activity of p65 is also regulated through post-translation modifications; phosphorylation and acetylation. P65 is phosphorylated at several different sites within both the RHD and TAD, by several different kinases including protein kinase A (PKA) and the mitogen and stress-activated kinase-1 (MSK 1) (Chen & Greene, 2004; Zhong *et al.*, 2002; Zhong *et al.*, 1998). Phosphorylation of p65 has been shown to regulate the DNA binding and oligomerization of p65 and also the recruitment of various transcriptional co-activators such as p300 and CBP. Interaction of p300/CBP with p65 leads to its acetylation and this enhances binding of p65 to DNA and impairs its assembly with IkB-α (Chen *et al.*, 2001b; Chen *et al.*, 2002).

The molecular mechanism by which A238L inhibits NF-κB gene transcription has not been resolved. The addition of recombinant A238L to the nuclear extracts of Vero cells was shown to inhibit the binding of NF-κB complexes to κB DNA sequences, as identified using electrophoretic mobility shift assays (EMSA), of the DNA protein complex formed. Supershift assays with specific antibodies against p65 and p50 (Revilla *et al.*, 1998) demonstrated that A238L inhibited formation of complexes between p50-p65 and DNA. A238L has also been shown to co-precipitate with p65 from extracts from cells either transfected with a plasmid expressing A238L, or infected with ASFV (Powell *et al.*, 1996; Revilla *et al.*, 1998), suggesting that A238L is present in cells in

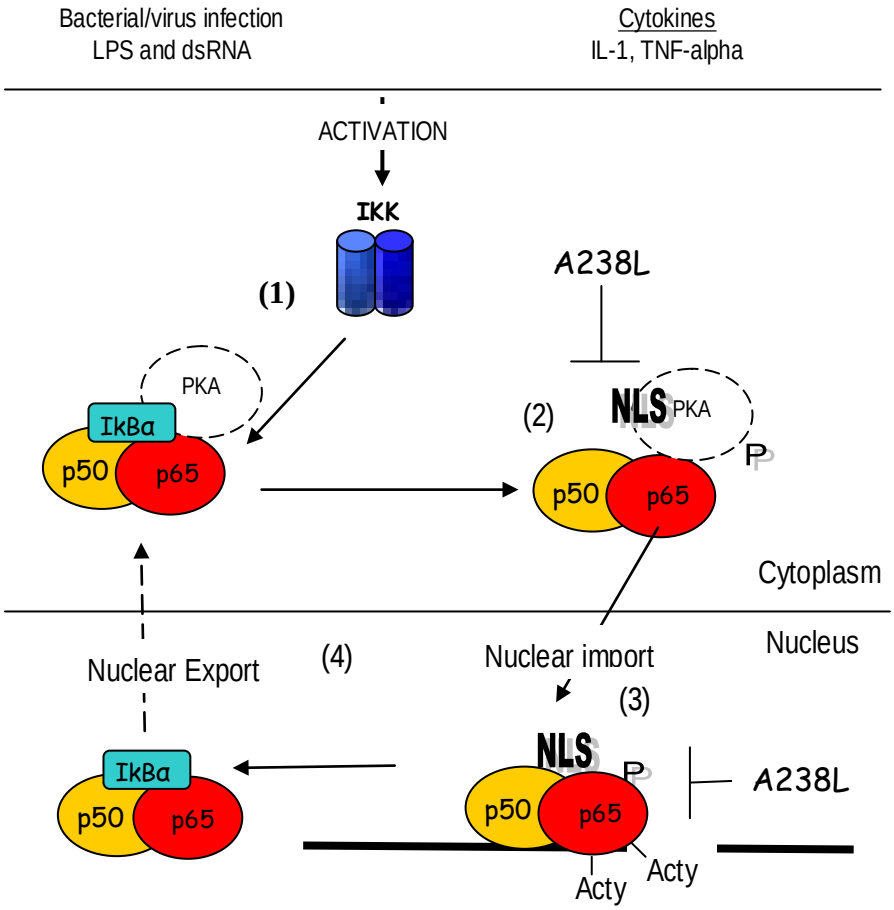

Figure 1.6 Schematic diagram of the NF- κB activation pathway. In resting cells the NF-κB :IκBα complex is predominantly located in the cytoplasm in a complex with several other cellular proteins including Phosphatase Kinase A (PKA), which is inhibited through its interaction with IκBα. Cell activation leads to the activation of the IKB Kinase complex (IKK). Activated IKK phosphorolates IκBα at two conserved Serine residues (1), leading to polyubiquitination of IκBα and its subsequent degredation via the 26s proteasome. Degradation of IκBα exposes a NLS on p65 leading to the nuclear import of NF-kB, and also induces the activation of PKA which phosphorolates p65 at serine-276 (2). Once in the nucleus phosphorolated NF-κB associates with CBP/p300 transcriptional co-activators. Acelylation of p65 by p300 and CBP acetytransferrases enhances p65 DNA binding and impairs assembly I κ Bα assembly (3). De-acetylation of p65 by the histone de-acetylase 3(HDAC3) regulates NF- κB gene transcription by promoting IKBα binding and nuclear export. Adapted from Ghosh 1997, Chen 2002, Chen 2001 and Zhong 1998). A238L binds directly to the p65 sub-unit of NF-κB (Tait, Reid et al. 2000) and is thought to inhibit NF-κB activity by either masking the NLS on p65 (thus preventing nuclear translocation of NF-κB) or disrupting NF-κB binding to its κ B binding site once NF-κB is in the nucleus.

complex with NF-κB p50-p65 heterodimers. The p32 kDa form of A238L has been shown to preferentially co-precipitate with the p65 sub-unit of NF-κB in virus infected cells (Tait *et al.*, 2000)**.** This interaction was reduced by the inhibition of IκB-α proteasomal degradation suggesting that A238L cannot displace IκB-α from preformed NF-κB/IκB-α complexes, but interacts with NF-κB following IκB-α degradation. These results suggest that A238L may act by inhibiting the binding of the p65-p50 NF-κB heterodimer to kB binding sites and that post-translational modification of A238L may regulate this activity. Unlike IκB-α, A238L is not degraded in activated cells (Tait *et al.*, 2000) and therefore is thought to provide a mechanism for the prolonged inhibition of NF-κB gene transcription during ASFV infection.

1.6.3.1.2 Calcineurin

Calcineurin (CaN) is a serine/threonine protein phosphatase that is directly regulated by calcium and calmodulin. CaN is activated by the release of calcium within the cell, which triggers the binding of calmodulin to CaN. This induces a conformational change in CaN, displacing the autoinhibitory domain of this protein from its catalytic active site (Rao *et al.*, 1997)**.** The immunosuppressive drugs cyclosporin A (CsA) and FK506 bind to and inhibit CaN phosphatase activity in a complex with the immunophilin proteins cyclophilin A (CypA) and FKBP12, respectively (Schreiber & Crabtree, 1992). The crystal structure of the FK506-FKBP12 complex bound to CaN has been solved, and this indicates that this complex blocks access to the CaN active site (Kissinger *et al.*, 1995; Stoddard & Flick, 1996).

CaN modulates the phosphorylation state of several proteins involved in signal transduction. BAD, a pro-apoptotic member of the Bcl-2 family is a direct substrate of CaN, and CaN is involved in promoting Ca^{+2} induced apoptosis through the de-phosphorolation of this protein (Wang *et al.*, 1999). CaN also dephosphorylates two cellular transcription factors: Elk-1, a transcription factor activated by mitogen activated protein kinases (MAPK), and NFAT.

NFAT proteins are found in many different cell types and play a central role in the transcription of cytokine genes and other genes involved in the immune response (Crabtree & Olson, 2002; Rao *et al.*, 1997). 5 NFAT family members have been identified and four of these (NFAT1-4) are regulated through dephosphorylation by CaN. In resting cells NFAT is present in the cytoplasm in a hyperphosphorylated form. An increase in intracellular calcium levels leads to activation of CaN and this results in the dephosphorylation of NFAT. This exposes a NLS on NFAT and also enhances its DNA binding affinity. Translocation of NFAT to the nucleus results in binding to specific DNA sequences (Figure 1.7) (Rao *et al.*, 1997). Within the nucleus NFAT proteins bind co-operatively with activator protein (AP)-1 transcription factor, which consist of c-Fos - c-Jun heterodimers, to induce the expression of many genes involved in the immune response. The AP-1 complex is formed in cells where both c-Fos and c-Jun have been activated, through stimulation of the Ca^{+2} and PKC/Ras pathways respectively (Karin, 1995). In the absence of PKC/Ras activation, NFAT has the capability of initiating gene transcription in an AP-1 independent manner (Macian *et al.*, 2000). NFAT can be phosphorylated by protein kinases within the nucleus resulting in its export to the cytoplasm and switching off of NFAT-dependent gene transcription.

A238L has been shown to bind to and inhibit the activity of CaN through interaction with the CaN catalytic subunit (Miskin *et al.*, 2000; Miskin *et al.*, 1998). This activity has been mapped to an 82 amino acid region based in the c-terminus of A238L (Abrams *et al.*, 2008). This region also contains a PxIxITxC/S motif, which is required for binding of A238L to CaN. This motif closely resembles those in substrate proteins of CaN, including NFAT (Aramburu *et al.*, 1998; Aramburu *et al.*, 1999; Miskin *et al.*, 2000b). NFAT 2 cDNA has been isolated from porcine macrophages and A238L has been shown to inhibit NFAT dependent gene expression. The suggestion was that A238L may inhibit NFAT-regulated gene transcription through inhibition of CaN phosphatase activity, thus preventing the dephosphorylation and the subsequent nuclear translocation of NFAT (Miskin *et al.*, 1998). However, a direct effect on the phosphorylation status and nuclear localisation of NFAT, mediated by A238L was not

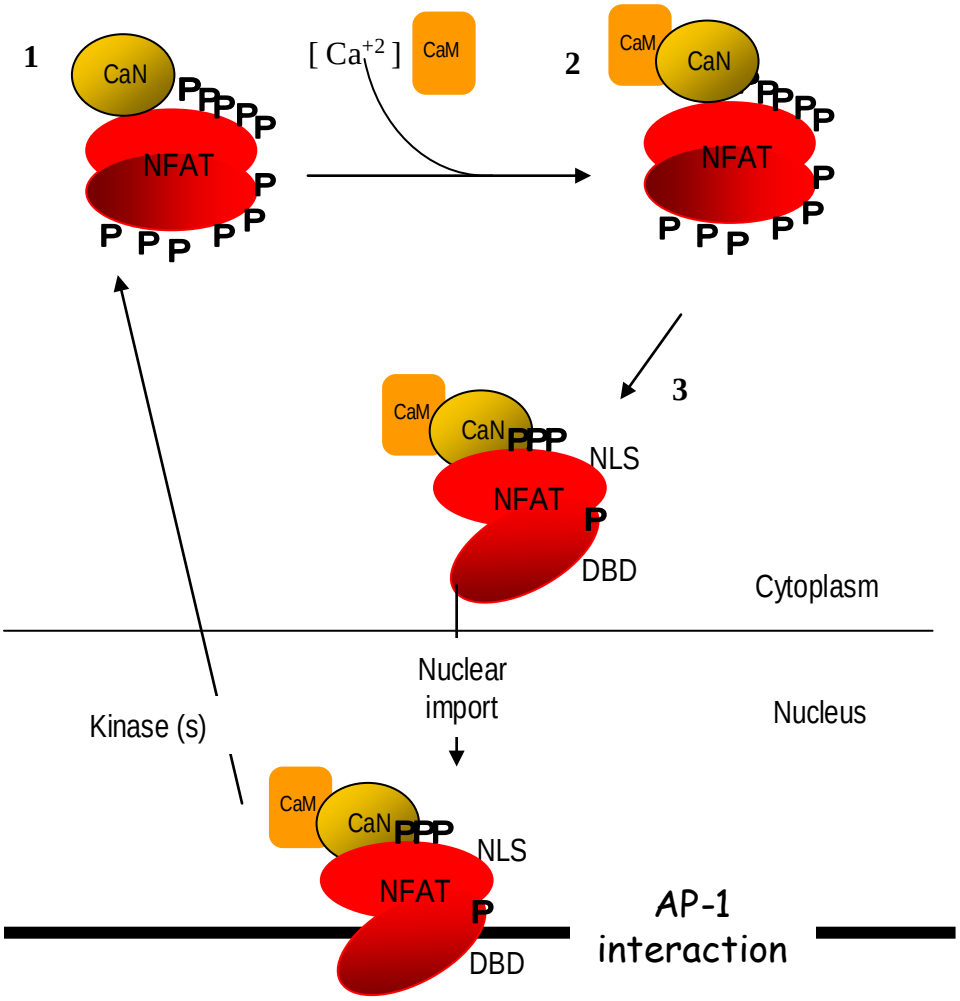

Figure 1.7 Schematic diagram of NFAT proteins activation.1) NFAT in association with Calcineurin (CaN) is held in the cytoplasm of resting cells. 2) Ca+2 release within the cell, following cell activation, triggers calmodulin to bind to Calcineurin. This activates calcineurin by inducing a conformational change in the enzyme to expose its catalytic site. CaN activity can be inhibited by the immunosupressive drug cyclosporin A (CsA), which in complex with cyclophilin A (CyA), binds to CaN inhibiting its activity. A238L also binds to CaN inhibiting its activity. 3) Activated calcinurin dephosphorolates NFAT. This induces a conformational change in NFAT exposing a Nuclear localisation Signal (NLS) and residues within the DNA binding Domain (DBD) that associate with NFATs complementary DNA binding site. This results in nuclear import of NFAT, where NFAT is involved in initiating gene transcription. Gene transcription can occur independently or in association with members of the AP-1 family of transcription activators. Rephosphorylation of NFAT proteins returns them to their original state in the cytoplasm. Adapted from Rao et al 1997.

demonstrated in this work. Through inhibition of CaN, A238L has the potential to regulate the activity of other cellular proteins dependent on CaN activity, such as BAD and Elk-1. This raises the possibility that A238L could function as an anti-apoptotic protein, inhibiting Ca^{+2} induced apoptosis or alternatively could act to promote gene transcription through Elk-1.

Recent work published during the course of this study has shown that A238L inhibits the expression of the Cyclooxygenase-2 gene (COX-2) through an NFAT dependent transcriptional transactivation pathway (Granja *et al.*, 2004b). COX-2 is transiently expressed following cell stimulation and is the key enzyme involved in prostaglandin synthesis. Prostaglandins are important mediators of inflammation. This study demonstrated that A238L did not prevent the nuclear translocation of NFAT in virus infected cells and that inhibition of Cox-2 gene expression did not involve inhibition of the binding between NFAT and its specific DNA sequences in the Cox-2 gene promoter. However, NFAT-mediated transactivation was strongly inhibited, suggesting that A238L may act through an alternatively mechanism to inhibit NFAT dependent gene transcription (Granja *et al.*, 2004b). Subsequent studies have demonstrated that A238L is able to inhibit the expression of TNF-α and iNOS through a mechanism that involves the transcriptional co-activators p300/CBP, presenting an additional mechanism of A238L action (Granja *et al.*, 2006a; Granja *et al.*, 2006b). This work is discussed in more detail in Chapters 5 and 7.

1.7 Project Aims

A238L is predicted to have a significant effect on the expression of host macrophage immune response genes. Previous work on A238L has demonstrated that this protein has the potential to interact with and inhibit the activity of several cellular proteins involved in signal transduction. However the exact mechanism of A238L action and the overall effect on host macrophage gene transcription is not known. Previous work on A238L

has been limited to investigating the effect of A238L on specific cell signalling pathways and/or the expression of individual host genes, and several potential effects of A238L, mediated through inhibition of CaN have not been investigated.

1.7.1 Investigation of the effect of A238L protein on host macrophage gene transcription

The first aim of this study was to examine the global effect of A238L on host macrophage gene transcription using a porcine microarray. Using this approach transcripts for thousands of genes can be examined at one time, providing a global overview of the effect of A238L on host macrophage gene transcription. Microarrays have already provided valuable insights into previously unknown mechanisms of how viruses modify the expression of cellular genes to counteract the host immune response to infection and/or promote the expression of cellular genes required for viral replication. For example, gene expression profiling of cells expressing the HIV Nef protein, demonstrated that this protein induces a transcriptional program similar to anti-CD3 activated T-cells. Many of the proteins up-regulated by Nef have been shown to be involved in enhancing HIV replication (Simmons *et al.*, 2001). Analysis of changes in host gene transcription induced by Herpes simplex virus, showed that expression of early virus genes can suppress the host cells antiviral responses to viral penetration (Mossman *et al.*, 2001).

It was expected that this approach would provide a more comprehensive view into how A238L functions to modulate macrophage gene transcription and identify new targets for A238L. This information will contributed to a greater understanding into the functional significance of A238L expression during ASFV infection.

1.7.2 Investigation of the subcellular localisation of A238L.

Previous work has demonstrated that A238L is present in both the nucleus and cytoplasm of ASFV infected cells and has indicated that A238L could function within either/or both of these compartments. However the mechanism of A238L action is not fully understood. One study suggested that A238L may inhibit NF-κB by retaining it in the cytoplasm (Tait 2000), whereas another study suggested A238L acted in the nucleus to prevent NF-κB binding to κB binding sites (Revilla *et al*., 1998). The activity of many proteins can be regulated through the control of their subcellular localisation. For example both NF-κB and NFAT transcriptional activity is partially regulated through the retention of these proteins in the cytoplasm of resting cells (Ghosh & Karin, 2002; Rao *et al.*, 1997) . The second aim of this study was to investigate the nuclear/cytoplasmic shuttling of A238L to gain better understanding into the mechanism of A238L action.

Chapter 2

Materials and methods

2.1 Suppliers

Unless otherwise stated all chemicals were obtained from Sigma Aldrich and enzymes and reagents were purchased from Promega UK.

2.2 Bacteria Strains

Escherichia coli XL-1 Blue strain *(recA1 / endA1 / gurA96 / gurA96 / thi-1 / hsdR17 / supE44 / relA1 / La* [F' *pro AB lacI*^{q} *ZΔ M15 Tn10 (tet*^{r}*)*]*)* was obtained from Stratagene.

2.3 Reagents

2.3.1 Antibodies and antibody detection reagents

Antibodies and secondary antibody detection reagents are listed in Table 2.1. Supplier information and reagent concentrations for western blot (WB) and immuno-fluorescence (IF) are provided.

2.3.2 Primers

Sequences of the primers used in this study are given in Table 2.2. Primers, Pc*Nco*I, Pc*Hind*III, TriExUp, and ORF1629 were manually selected directly from available sequence information. The remaining primers were designed using the Primer3 program (http://www.genome.wi.mit.edu/genome_software /other/ prime3). Primers were supplied by MWG Operon.

Table 2.1 Antibodies and secondary antibody detection reagents

Antibody/reagent	**Supplier**	**Concentration for Western Blotting**	**Concentration for Immunofluorescence**
Mouse Anti Pk-Tag (SV5-Pk)	Serotec	2 μg/ml	20 μg/ml
α-tubulin (B-7) sc-5286 mouse monoclonal	Santa Cruz Biotechnology	0.2 μg/ml	N/A
NF-kb p65 sc-372 rabbit polyclonal	Santa Cruz Biotechnology	0.2 μg/ml	2 μg/ml
C18, anti-p30 mouse monoclonal (hybridoma supernatant)	IAH (Afonso et al 1992)	NA	1/10
Anti-pE120R polyclonal rabbit serum	IAH (Jouvenet et al. 2004)	N/A	1/500 dilution
ProteinA – ab7456	Abcam	2 μg/ml	N/A
AlexaFlur ® 488 goat anti-mouse polyclonal	Molecular Probes	N/A	10 μg/ml
AlexaFlur ® 568 goat anti-rabbit polyclonal	Molecular Probes	N/A	10 μg/ml
4H3, anti-vp72 mouse monoclonal (hybridoma supernatant)	IAH (Cobbold et al. 1996)	N/A	1/5 dilution

Table 2.2 Primer sequences.

Primer	Forward	Reverse	Annealing Temperature
Pc*Nco*I/ Pc*Hind*III	5’ tagtaacggccgccagtg 3’	5’ cctctagatgcaagcttgagcgg 3’	60 ^{o}C
TriExUp/ ORF1629	5’ gttattgtgctgtctcatcat 3’	5’ tgcaccatcgctttctaacg 3’	55 ^{o}C
AMCF-1	5’ atgacttccaaactggctg 3’	5’ gtacaaccttctgcaccc 3’	55 ^{o}C
TNFα	5’ cccagaaggaagagtttccag 3’	5’ cagcaaagtccagatagtcgg 3’	55 ^{o}C
IL-8	5’ tttctgcagctctctgtgagg 3’	5’ ctgctgttgttgttgcttctc 3’	55^{o}C
β-actin	5’ ggacttcgagcaggagatgg 3’	5’ gcaccgtgttggcgtagagg 3’	55^{o}C
IL-6	5’ ttcacctctccggacaaaac 3’	5’ tctgccagtacctccttgct 3’	55^{o}C
IkBζ	5’ tctggaactcattcgcctct 3’	5’tcaaccgatactgcaagctg 3’	55^{o}C
Cox-2	5' ttcaaatgagattgtgggaaattggt 3'	5'agatcatctctgcctgagtatctt 3'	55^{o}C

2.4 Cell culture and ASFV infection

2.4.1 Cell cultures

An immortalised porcine alveolar monocyte cell line (IPAM), was obtained from Dr H. M. Weingartl (Weingartl *et al.*, 2002a). IPAM cells were maintained in RPMI cell culture medium supplemented with 5 % bovine foetal calf serum (FCS), 5 µg/ml Gentamycin (Gibco Invitrogen) and 1 x Non Essential Amino Acids (Gibco invitrogen). Primary alveolar macrophages (PAM) were harvested from normal, out-bred pigs, by lung lavage and maintained in RPMI supplemented with 10 % fetal calf serum (FCS). *Spodoptera frugiperda* (Sf9, ATCC® CRL-1711), fall armyworm insect cells, were maintained at 28 ^{o}C in SF900 II medium containg 2 % FCS. *Cercopithecus aethiops* (Vero, ATCC® CCL-81), African green monkey kidney cells, were maintained in Dulbecco's Modified Eagle's Medium (DMEM) containing 25 mM HEPES and supplemented with 2 mM glutamine and 5 % FCS. Unless stated otherwise the cells were maintained at 37 ^{o}C with 5 % CO_2 and culture media was supplemented with Penicillin (100 µg/ml), Streptomycin (100 µg/ml), and Fungizone (2.5 µg/ml).

2.5 Viruses and cell culture

2.5.1 Virus isolates

Initial virus stocks were obtained from Dr. Charles Abrams, IAH. BA71V is an attenuated, tissue culture-adapted strain which has been described previously (Enjuanes *et al.*, 1976) SV5Gal and vIKGAL are recombinant viruses derived from BA71V (Miskin *et al.*, 1998). SV5GAL has a Pk epitope tag from SV5 virus inserted at the N-terminus of the A238L gene and vIKGAL is a deletion mutant from which the A238L gene has been removed and replaced with a reporter cassette expressing β-galactosidase.

2.5.2 Production of virus stocks.

Vero cells, at 80-90 % confluence, were incubated in serum free medium containing ASFV at a multiplicity of infection (m.o.i) of 5. After 1 hr, at 37 ^{o}C, the medium was removed and replaced with medium containing 2 % FCS. 3 days following infection, the cells were scraped into the culture medium, sonicated twice for 5 seconds using a cup horn sonicator and then centrifuged at 2000 g for 20 min to remove cell debris. The supernatant, containing ASFV, was stored at 4 ^{o}C for up to 6 months or at -70 ^{o}C for long term storage.

2.5.3 Virus titration

96 well plates containing Vero cells at 80-90 % confluence were infected in triplicate with 10 fold serial dilutions of ASFV supernatant. The cells were incubated at 37 ^{o}C for 16 hrs, washed twice with PBS and then fixed in ice cold methanol for 20 min. After washing with PBS, the cells were blocked in blocking buffer consisting of PBS containing 3 % (w/v) Bovine Serum Albumin. Hybridoma supernatant containing the 4H3 mouse monoclonal (anti-vp72) was diluted 1/5 in blocking buffer and 50 µl was added to each well. Following incubation, the plate was washed three times with PBS and then incubated with AlexaFlur ® 488 goat anti-mouse polyclonal diluted in blocking buffer. All incubation steps took place at room temperature and lasted for 20 min. The plate was then washed three times with PBS and ASFV-infected cells were detected using an inverted fluorescent microscope. Wells containing infected cells were scored as positive and the $TCID_{50}$ calculated (Reed & Muench, 1938).

2.6 DNA Manipulation Techniques

2.6.1 Polymerase chain reaction (PCR) amplification of DNA

Unless stated otherwise, PCR reactions were carried out using the TripleMaster®PCR reagents (Eppendorf). Reaction mixtures of 50 µl contained HighFidelity Buffer with Mg^{2} (x1), 10 pMol of each primer, dNTPs (200 µM), triple master DNA polymerase (1

unit), and 50-100 ng of DNA. Thermal cycling was carried out using an Eppendorf Mastercycler. The PCR program consisted of 95 ^{o}C for 2 min, 30 cycles of 96 ^{o}C for 1 min, optimised primer annealing temperature for 45 secs, 72 ^{o}C for 1 min followed by a final elongation step of 72^{o}C for 5 min. Samples were held at 4 ^{o}C prior to use. Primer annealing conditions are shown in Table 2.2.

2.6.2 Agarose gel electrophoresis

DNA samples were mixed with DNA loading buffer (Biogene), loaded onto an 1 % agarose/TAE gel containing ethidium bromide (0.3 ug/ml), and separated at 100 v for 1 hr in TAE buffer. DNA fragments were detected by a GeneDoc gel viewer (BioRad) and imaged using Quantity One-4.1.0 software (BioRad). The size of the DNA fragments was estimated by their relative mobility compared to a 1 kbp or 100 bp molecular weight ladder (Biogene).

2.6.3 DNA purification

Restriction enzyme digested DNA fragments and PCR products were purified using a GFX PCR DNA and Gel Band Purification Kit (Amersham Biosciences). Manufacturer's guidelines were followed. PCR products or DNA in solution were mixed thoroughly with 500 µl of capture buffer and added to a GFX column. DNA fragments separated using agarose gel electrophoresis were excised from the gel, mixed with 10 µl of capture buffer for every 10 mg of agraose gel and incubated at 60^{o}C for 5 - 10 min until the agarose had completely dissolved. The solution was then loaded onto a GFX column. From then on both types of sample were centrifuged, washed once with GFX wash buffer and then eluted from the GFX column in 50 µl of H_20. All centrifugation steps were at 12,000 g for 1 min.

2.6.4 Restriction enzyme digestion

Restriction enzyme digestions were carried out in a volume of 20 µl per 1 µg of DNA using cuts all enzyme buffer (CAB) containing 5 units of each restriction enzyme (Promega). Reactions were incubated at 37 ^{o}C for 2 hrs. The required product was separated by agarose gel electrophoresis and then purified by gel extraction.

2.6.6 Formation of blunt-ends using the Klenow fragment of DNA polymerase 1

DNA polymerase 1 Klenow fragment (Promega) has 5'→ 3' polymerase and 3'→ 5' exonuclease activities. To generate blunt-ended fragments from restriction enzyme digestion products containing 5' protruding ends, 1 unit of Klenow fragment and 40 µM of dNTPs were added to the restriction enzyme reaction mix after the digestion had been completed. The reaction was carried out at room temperature for 10 min. Enzyme activity was stopped by heating the mixture at 75 ^{o}C for 10 min.

2.6.7 Dephosphorylation

To prevent re-ligation of linearised vector DNA with compatible ends, calf intestinal alkaline phosphatase (CIP) (Promega) was used to remove the 5'-phosphate groups from the vector 5'-termini. Reaction mixtures containing 0.01 units of CIP and ~1 µg of DNA were incubated at 37 ^{o}C for 30 min in 1 x CIP buffer (Promega). Following the addition of another 0.01 units of CIP the reaction was incubated for a further 30 min and then stopped by the addition of 300 µl of CIP stop buffer.

2.6.8 Ligations

50 ng of vector was incubated with a 16 ng of insert in a 10 µl reaction volume of 1 x T4 ligase buffer (Promega) containing T4 ligase (3 Weiss units)(Promega). The reaction mix was incubated overnight at 16 ^{o}C.

2.6.9 Preparation of plasmid DNA

2.6.9.1 Preparation of competent *Escherichia coli*

All incubation steps took place at 37 ^{o}C with constant shaking unless otherwise stated. *E. coli* cultures were streaked onto luria broth (LB) agar plates and incubated overnight, without shaking, to obtain individual colonies. The next day 10 ml of LB medium was inoculated with 2-3 individual colonies and incubated overnight. 2-3 mls of this culture was used to inoculate 100 mls of LB medium in a 500 ml conical flask. The culture was incubated until it reached an OD_{600} of 0.3-0.5, placed on ice for 15 min and then centrifuged at 10,000 g to harvest the cells. The cells were re-suspended in 33 ml of ice cold RF1, incubated on ice for 15 min, pelleted at 10,000 g and then re-suspended in 8 mls of ice-cold RF2. The solution was then incubated on ice for 15 min, dispensed into pre-chilled 1.5 ml microfuge tubes (Eppendorf), flash-frozen in liquid nitrogen and immediately stored at –70 ^{o}C.

2.6.9.2 Transformation of *E.coli*

Competent XL-Blue cells (stored at –70 ^{o}C) were rapidly defrosted, and dispensed into 40 µl volumes which were stored on ice. 1 µl of ligation mixture was added to individual aliquots. After 30 min incubation, on ice, the cells were heat-shocked at 42 ^{o}C for 45 secs and immediately placed back on ice for a minimum of 2 min. The aliquots were then made up to a final volume of 500 µl using antibiotic free LB broth and incubated at 37 ^{o}C with constant shaking for 1 hr. To isolate transformed colonies, 100 µl of transformed XL1-blue culture was spread on LB agar plates supplement with ampicillin

(100 µg/ml) and incubated over night at 37 ^{o}C. Single colonies were selected for further analysis.

2.6.9.3 Small scale preparation of plasmid DNA

Plasmid DNA was purified using a GenElute™ Plasmid Miniprep Kit. The procedure was carried out following the manufacturer's guidelines. All centrifugation steps were carried out at 12,000 g for 1 min unless stated otherwise. Single colonies were inoculated into 10 mls of LB broth supplemented with ampicillin (100 µg/ml) and incubated overnight at 37 ^{o}C with constant agitation. 1.5 mls of culture was centrifuged to harvest cells. Following re-suspension of the cells in 200 µl of resuspension solution, the cells were lysed by the addition of 200 µl of lysis solution. Genomic DNA and cell debris was precipitated by the addition of 350 µl of neutralisation solution and removed by centrifugation. The supernatant was transferred to a GenElute Miniprep binding column for plasmid purification. Following centrifugation, the column was washed once with 750µl of wash solution and the flow-through discarded. The column was then centrifuged again to remove excess ethanol and the plasmid DNA eluted in 50 µl of dd$H_2$0. The plasmid DNA was stored at –20 ^{o}C until use.

2.6.9.4 Large scale preparation of plasmid DNA

Plasmid DNA was isolated using alkaline-SDS lysis followed by purification using a CsCl-ethidium bromide density gradient. 200 ml of LB broth supplemented with ampicillin (100 µg/ml) was inoculated with a single bacterial colony and incubated over night at 37 ^{o}C with constant shaking. Cells were harvested by centrifugation at 6,000 g for 10 min, re-suspended in 10 mls of Solution 1 containing 2 mg/ml of lysozyme and incubated at room temperature for 5 min. 20 ml of freshly prepared solution 2 was added and the tube placed on ice. After 10 min incubation 15 ml of solution 3 was added and the solution incubated for a further 20 min on ice. Cell debris and chromosomal DNA

was pelleted by centrifugation at 7,000 g for 30 min at 4 ^{o}C and the supernatant, containing the plasmid DNA, transferred to a new tube. The plasmid DNA was precipitated by the addition of an equal volume of isopropanol and, after 20 min incubation on ice, the pellet was collected by centrifugation at 8,000 g for 10 min. The pellet was washed once in 70 % ethanol, re-suspended in 8 ml of TE buffer and mixed with 8 g of CsCl and 200 ul of ethidium bromide solution at 10 mg/ml. The solution was transferred to a Quick-Seal™ 16 x 76 mm Beckman centrifuge tube, which was sealed, and then centrifuged at 55 K overnight in a Beckman Type 70.1 Ti rotor, using a Beckman Ultracentrifuge, to create a CsCl density gradient. The band of closed circular DNA was removed using a syringe and the ethidium bromide extracted by repeatedly mixing the sample in an equal volume of water saturated n-butanol. This was continued until the organic phase became colourless. The aqueous phase was removed, made up to 10 ml in TE buffer and diluted at a ratio of 1:3 in ethanol to precipitate the DNA. The DNA was pelleted using centrifugation at 3,000 g for 15 min, washed once in 70 % ethanol and then re-suspended in 250 µl of H_2O. Plasmid DNA was stored at –20 ^{o}C until use.

2.6.9.5 Quantification of DNA

The DNA concentration in samples was estimated using an Ultrospec 2100 pro UV/visible Spectrophotometer. One OD_{260} unit represents 50 µg/ml of DNA.

2.6.9.6 Sequencing DNA

Plasmid DNA was sequenced on the Beckman Coulter CEQ 8000 Genetic Analysis System using the CEQ DTCS Quick Start Kit 608120 (Beckman Coulter) following manufactures guidelines. 350 fmol of plasmid DNA combined with 3.2 pmol of primer was used for each sequencing reaction. This was added to 8 µl of DTCS quick start Master Mix (diluted at a 1:1 ratio in Dilution Buffer supplied with the kit) and made up

to a total volume of 20 µl with dd H_2O. The template was heated at 96 ^oC for 20 secs, followed by 50 ^oC for 20 secs and 60 ^oC for 4 min, this was repeated for 30 cycles and the samples held at 4 ^oC. Following amplification, the reaction was stopped by the addition of 5 µl of Stop Solution/Glycogen mixture which consisted of 2 µl of 3 M sodium acetate (pH 5.2), 2 µl of 100mM Na2-EDTA (pH 8.0) and 1 µl of 20 mg/ml of glycogen. 60 µl of 95 % cold ethanol (stored at – 20 ^oC) was then added and the sample centrifuged at 13,000 g for 15 min at 4 ^oC. The resulting pellet was then washed twice with 200 µl of 70 % cold ethanol (stored at – 20 ^oC) and the pellet left to air dry at 37 ^oC for 10 min. The sample was then resuspended in 40 µl of Sample Loading Solution (Beckman), loaded onto the sample plate (PN 609801), overlaid with mineral oil and then processed by the Beckman Coulter CEQ 8000 Genetic Analysis System.

2.7 RNA manipulation techniques

2.7.1 DEPC treated water

0.1% diethylpyrocarbonate (DEPC) was added to ddH_20 and mixed overnight at room temperature. The solution was then autoclaved for 20 min to inactivate residual DEPC.

2.7.2 Isolation of total RNA from mammalian cells

Total RNA was extracted using TRI REAGENT™ (Sigma), following manufacturer's guidelines. All consumables used for this procedure were certified RNase free. Monolayer cultures of IPAM cells were washed once with PBS and then lysed by the addition of 1 ml of TRI REAGENT™ . The cell lysate was transferred to a 2 ml microfuge tube and incubated at room temperature for 5 min. Following the addition of 200 µl of chloroform, the sample was vortexed for 15 seconds, allowed to settle for 10 min at room temperature and then centrifuged at 12,000 g for 15 min at 4 ^oC to separate the mixture into an organic phase and an aqueous phase (containing RNA). The aqueous

phase was transferred to a fresh tube, mixed with 0.5 ml of isopropanol and incubated at room temperature for 10 min. Precipitated RNA was pelleted at 12,000 g for 10 min at 4 ^{o}C. The pellet was washed once in 75 % ethanol and then re-suspended in 0.1 % DEPC treated H_2O.

2.7.3 Quantification of RNA

The concentration of RNA in samples was estimated using either an Ultrospec 2100 pro UV/visible Spectrophotometer or the Nanodrop ND-1000 spectrophotometer (Agilent). One OD_{260} unit represents 40 µg/ml of RNA.

2.7.4 RT-PCR

Unless otherwise stated, RT-PCR reactions were carried out using SuperScript^{TM} III First-Strand Synthesis System for RT-PCR (Invitrogen). Manufacturer's guidelines were followed. Briefly, 0.5 - 5 µg of RNA was added to 5 µM oligo$(dT)_{20}$ and 1 mM dNTP's and made up in a total volume of 10 µl, in DEPC-treated water. This was incubated at 65 ^{o}C for 5 min, placed on ice for a minimum of 1 minute, and then added to 10 µl of cDNA synthesis mix (1 x RT buffer, 5 mM $MgCl_2$, 10 mM DTT, RNaseOUT^{TM} (40U) and SuperScript^{TM} III RT (200 U). Samples were incubated at 50 ^{o}C for 50 min and the reactions terminated by heating at 85 ^{o}C for 5 min. After cooling on ice, RNase H (2 U) was added and samples incubated at 37 ^{o}C for 20 min. The resulting cDNA was either used immediately for PCR or stored at – 20 ^{o}C.

2.7.5 Analysis of RNA integrity

The size distribution of RNA fragments within total RNA and aaRNA samples was assessed using the Agilent 2100 bioanalyzer with an RNA 6000 LabChip kit. This procedure was carried out according to manufacturers' guidelines. Briefly, Agilent RNA 6000 nano chips were prepared by the addition of 9 µl of gel-dye mix into specifically

marked wells. Prior to loading, the RNA samples and the RNA 600 Nano marker were heat denatured at 70 ^{o}C for 2 min and then stored on ice until use. 1 µl of RNA 600 Nano marker was added into a well marked with a ladder symbol and 1 µl of each of the test samples were loaded into the sample wells. Empty sample wells were loaded with 1 µl of double distilled H_20 (ddH_20). The chip was then vortexed for 60 seconds at 2000 rpm using an IKA vortex mixer and loaded immediately onto the Agilent 2100 bioanalyzer for analysis. The resulting electropherograms of the RNA ladder and of each sample tested was compared against standard manufacture sample profiles to assess the quality of the RNA.

2.7.7 RNA amplification

Messenger RNA was amplified from total RNA samples using an Amino Allyl MessageAmp^{TM} II aRNA Amplification Kit (Ambion). Manufacturer's guidelines were followed. Briefly, 1 µg of total RNA and 1 µl of T7 Oligo (dT) Primer in a total volume of 12 µl was incubated at 70 ^{o}C for 10 min and then placed on ice. 8 µl of Reverse Transcription master mix was then added and the samples incubated at 42 ^{o}C for 2 hrs and then placed on ice. Following the addition of 80 µl of Second Strand Master Mix, the samples were incubated at 16 ^{o}C for 2 hrs. 250 µl of cDNA binding buffer was added to each sample and the samples were then loaded onto cDNA Filter cartridges. Following one wash with 500 µl of Wash buffer the cDNA was eluted into 2 x 9 µl of Nuclease-free water. 26 µl of In Vitro Transcription (IVT) Master Mix (containing 1:1 ratio of UTP to amino allyl UTP) was then added to the purified cDNA, mixed, and the samples were incubated for 14 hrs at 37 ^{o}C. 60 µl of Nuclease-free Water was then added to each sample to stop the IVT reaction. The resulting aminoallyl-amplified RNA (aRNA) was purified using aRNA filter cartridges. This involved combining the IVT reaction mixtures with 350 µl of aRNA Binding Buffer followed by the addition of 250 µl of 100 % ethanol to each sample. Each sample was then loaded onto an aRNA cartridge, centrifuged and washed with 650 µl of Wash Buffer. aRNA was eluted in 100 µl of Nuclease-free water at 50 ^{o}C and then stored at -20 ^{o}C until use. Prior to labelling

the quality of the aaRNA was assessed using the Agilent 2100 bioanalyzer. Unless otherwise stated all centrifuge steps took place at 10,000 g for 1 min at 4 ^{o}C.

2.7.8 Coupling CyeDye to aRNA

aRNA was labelled using an Amersham CyDye (Cy3/Cy5) kit (RPN5661). Manufacturer's guidelines were followed. 8 µl of aRNA was used in each dye coupling reaction. Where appropriate the aRNA sample was reduced to a volume of ~ 5 µl by spin drying before re-suspension in 0.1 M sodium bicarbonate buffer (pH 8.7) to a final volume of 40 µl. This sample was then added directly into a single tube of either Cy 3 or Cy 5 reactive dye, mixed thoroughly using a pipette and then incubated at room temperature for 90 min in the dark. 15 µl of 4 M hydroxylamine was then added to the reaction and the reaction incubated for a further 15 min.

2.7.9 Purification of CyDye labelled aaRNA

Cy3 and Cy5 labelled aaRNA was purified using the reagents provided in the Amino Allyl MessageAmp^{TM} II aRNA Amplification Kit (Ambion). This procedure was carried out following manufacture guidelines. Cy3 or Cy5 labelled aaRNA was mixed with 140 µl of aRNA binding buffer 100 µl of 100 % ethanol was then added, mixed three times with a pipette and the sample was placed immediately onto an aRNA Filter Cartridge. Following centrifugation the cartridge was washed once with 500 µl of Wash Buffer and then eluted into two times 10 µl of Nuclease-free water at 50 ^{o}C. The purified labeled RNA was then stored at -80 ^{o}C in the dark. All centrifugation steps took place at 10,000 g for 1 min at 4 ^{o}C. Final RNA concentration and dye incorporation rates were measured using the Nanodrop ND-1000 spectrophotometer (Agilent). Dye incorporation rates were calculated using the dye incorporation calculator on the Ambion website (www.ambion.com/tools/dye) using the formula shown in Figure 2.1.

$$\frac{\text{\# dye molecules}}{\text{1000 nt}} = \frac{A_{dye}}{A_{260}} \times \frac{9010\ \text{cm}^{-1}\,\text{M}^{-1}}{\text{dye extinction coefficient}} \times 1000$$

Dye	Absorbance maximum	Extinction coefficient*
Cy3	550 nm	150,000
Cy5	650 nm	250,000

* Extinction coefficient (ε) at λ_{max} in $cm^{-1}M^{-1}$

Figure 2.1 Method to calculate Cy3 and Cy5 dye incorporation rates into aaRNA.

A dye incorporation rate of 30 – 60 dye molecules per 1000 nt was required for microarray analysis.

2.7.10 Porcine Oligonucleotide Microarray slides

Microarray slides were produced in house by printing the Array-Ready Oligo Sets™ for the Pig Genome, version 1.0 and the Pig Genome Oligo extension Set, Version 1.0 (Operon) onto Nexterion® Slide HiSens E (SCHOTT). This procedure was carried out by Dr Charles Abrams, IAH, Pirbright, Surrey. An additional set of 360 oligonucleotides specific for genes present on the Pig 3K Immune cDNA (Zhang *et al.*, 2006b), but not identified within the Operon Oligonucleotide sets were also produced by Operon and included on this array.

2.7.11 Microarray Hybridisation

Microarray hybridisations were carried out following Nexterion® Slide HiSens E (SCHOTT) manufactures guidelines. Prior to hybridisation the microarray slides were washed in 0.1 % Triton X-100 for 5 min, followed by two washes in 1mM HCL solution for 2 min, with a final wash in 100 mM KCL for 1 min. The slides were then rinsed in

dd H_20 for 1 min and immediately placed in Nexterion® Blocking Solution for 15 min at 50 ^oC. After a final rinse in ddH_20 for 1 min the slides were dried by centrifugation at 200 g for 5 min and used immediately for hybridisation. Hybridisations were carried out using the HS400Pro automated hybridisation chamber (Tecan). The hybridisation programme involved an initial 30 second prime with pre-hybridisation buffer, followed by sample injection and denaturisation at 95 ^oC for 3 min and hybridisation for 12 hrs at 60 ^oC . The slides were washed with Wash 1 solution at 25 ^oC, followed by wash 2 solution at 23 ^oC and finally at 23 ^oC with wash 3 solution. All washing steps consisted of 1 min constant flow followed by 45 s static. The slides were then dried within the hybridisation chambers and stored at room temperature in the dark. Pre-hybridisation and Wash solutions were filtered and degassed by sonication for 30 min before use in the hybridisation chamber. Hybridisation samples consisted of 2 µg of each test and control labelled aRNA combined together and suspended in Nexterion® hybridisation buffer to a total volume of 130 µl, with a minimum composition of 90 % (v/v) buffer. Slides were scanned using a GenePix 4000B instrument (Molecular probes) and the raw data captured using GenePix Pro6.0 software.

2.7.12 Microarray sample processing

Total RNA samples were isolated and analysed using a spectrophotometer at both 260 and 280 nm to test the purity of the sample and quantify the yield. All of the samples tested exhibited a ratio of A_{260} to A_{280} between 1.7 and 2.1 indicating they were free from DNA and protein contamination. The integrity of the samples was also examined using an Agilent 2100 bioanalyser to produce a size distribution profile of the RNA sample and to compare the ratio of 28S to 18S ribosomal RNA. The size distribution profiles of three representative samples can be seen in Figure 2.2. The traces demonstrate that nearly equal amounts of 28S and 18S rRNA are present within the samples, indicating a small degree of degradation has occurred. This is typical of standard RNA preparations and was considered to be within acceptable limits for further analysis, according to the manufacturers guidelines (Agilent). All of the test and control

RNA samples analyzed exhibited similar traces and were therefore suitable for further analysis.

To expand the amount of RNA harvested and produce enough RNA for the microarray hybridizations, mRNAs from all of the RNA samples, including the common reference, were amplified using an Amino Allyl MessageAmp^{TM} II aRNA Amplification Kit (Ambion). mRNA within the sample was reverse transcribed using an oligo(dT) primer encoding a T7 promoter, to produce cDNA. Following a second strand synthesis and clean up, the cDNA was amplified, in the presence of 5-(3-aminoallyl)-UTP, by *in vitro* transcription with T7 RNA polymerase. This resulted in the generation of many thousands of antisense RNA (aRNA) copies of each mRNA, containing modified uracil bases to facilitate labeling. Following amplification the aRNA size distribution profiles of the samples were evaluated using an Agilent bioanalyzer to ensure successful and representative amplification of the RNA sample. Traces of three representative samples can be seen in Figure 2.2. The samples tested exhibited traces consistent with the manufacturer's guidelines; a distribution of sizes between 250 to 5500 bases with most of the aRNA between 1000 to 1500 bases (Agilent).

Amplified aRNA was labeled using Amersham CyDye (Cy3/Cy5) kit. Cy3 or Cy5 reactive dyes were chemically coupled to aaUTP present in the aRNA. Following purification, aRNA yield and dye incorporation rate was determined using a spectrophotometer. Dye incorporation rates of 30-60 (one label every 30 to 60 nt) as required were obtained in all samples to ensure adequate signal for downstream microarray analysis. Equal quantities of test and control samples, labeled with either Cy3 or Cy5 were combined and co-hybridised onto the Operon *Sus scrofa* (pig) v1.0 and *Sus scrofa* (pig) extension Oligo^{TM} microarray (Operon). Hybridisatations were carried out using an automated hybridization station to minimise variability between slides. Two hybridisations were carried out for each comparison, with the dye assignments reversed in the second hybridisation to account for labeling bias between dyes. Images of the hybridised arrays were obtained by laser confocal scanning.

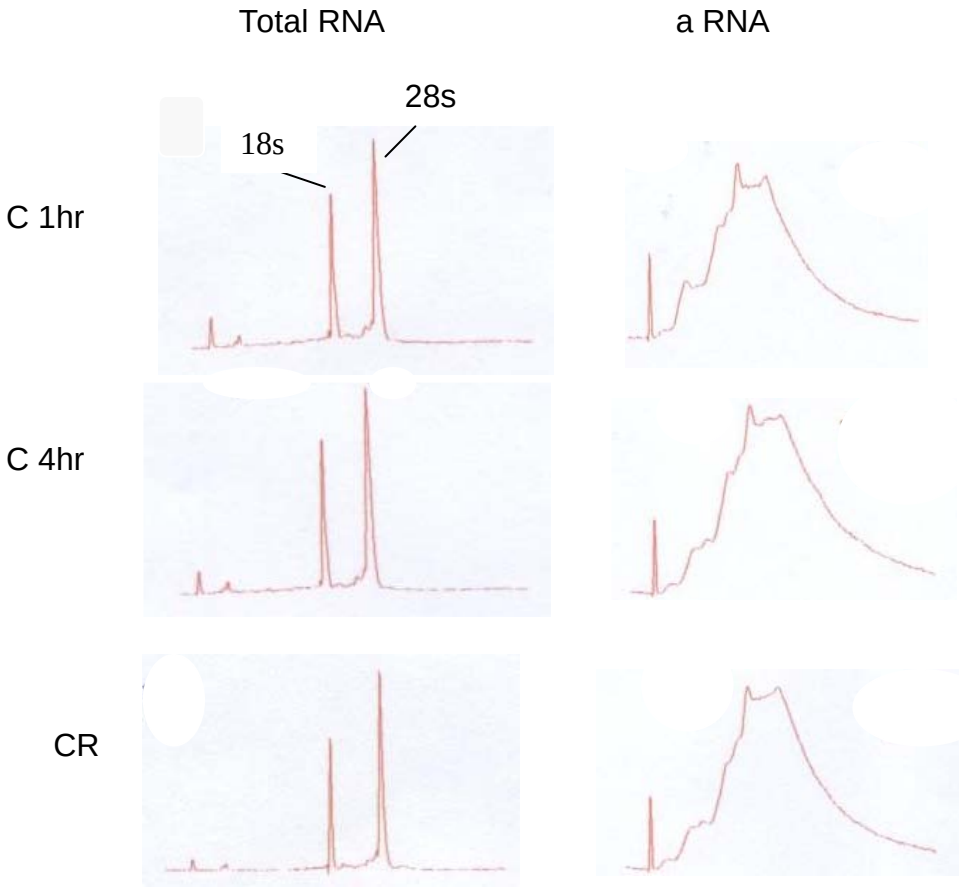

Figure 2.2 **Bioanalyzer images of IPAM RNA preparations before and after RNA amplification**. Fluorescent labelled total RNA and aaUTP modified amplified RNA samples were analysed on an Agilent bioanalyser 2100 using the RNA 600 marker and Nano LabChip Kit. The graphs show the bioanalyzer electropherogram from two RNA samples isolated from Baculovirus treated and LPS, PMA and ionomycin stimulated IPAM cells (S) at 1 and 4 hrs following stimulation and a common reference, untreated IPAM RNA. The samples show the size distribution profile of the RNA samples both before (total RNA) and after amplification (aRNA. The vertical axis represents fluorescence and the horizontal line represents the migration time (s). The graphs represent samples both before and after RNA amplification.

2.7.12 Microarray data analysis.

Raw data files were processed using BlueFuse for microarrays version 3.3 to extract feature information and remove background noise and artifacts. Processed data files were then analyzed using software tools from the TM4: microarray software suite. Microarray Data Analysis System (MIDAS) was used to normalize the data sets both within slides (locally weighted scatterplot smoothing (Lowess)) and between slides (SD regularization). This was followed by dye swap consistency checking to account for labeling bias between dyes. Multiexperiment Veiwer (MeV) was used to filter out poor quality data and identify differentially regulated mRNA using Significant Analysis of Microarrays (SAM) analysis (Tusher v.G, Chu 20001). SAM identifies genes with statistically significant changes in expression by assimilating a set of gene-specific t-tests. Each gene is assigned a score on the basis of its change in gene expression relative to the standard deviation of repeated measurements for that gene. Genes with scores greater than a threshold are deemed potentially significant. This method has the advantage over typical parametric t-tests in that it also calculates the number of these potentially significant genes which have been identified by chance - the False Discovery Rate (FDR). To estimate the FDR, nonsense genes are identified by analysing permutations of the measurements.

Annoatated gene lists were analyzed using the Database for Annotation, Visualisation and Intergrated Discovery (DAVID) 2008 (Dennis *et al.*, 2003) to identify significantly enriched terms associated with biological processes and signaling networks. DAVID is a large integrated knowledge base linking information from most of the common genomic bioinformatics resources including: National Center for Biotechnology Information (NCBI), SWISS-PROT, gene ontonlogy (GO) and Kyoto Encyclopedia of Genes and genomes (KEGG). DAVID therefore provides access to a diverse array of functional and sequence annotation. The platform provides a range of functional annotation tools which allow query based access to the database. These tools provide batch annotation of up-

loaded gene lists and the identification of significant biological themes within these lists. Genbank accession numbers from annotated gene lists were uploaded onto DAVID and compared against a default Human background of 30,000 genes. EASE, a modified Fischer's exact P-value was used to determine the probability that gene-enrichment for a specific annotation was not due to chance alone (Hosack *et al.*, 2003).

2.8 Protein Expression and Analysis

2.8.1 Mammalian Cell transfection

Mammalian cells were transfected using Lipofectamine™ 2000 (Invitrogen). Manufacturer's guidelines were followed. Mammalian cells at 90 – 95 % confluence were washed once in PBS and overlayed with transfection reagent. The transfection reagent was prepared following the manufacturer's guidelines: Lipofectamine™ 2000 was diluted in an appropriate amount of Opti-MEM® I Reduced Serum Medium, incubated for 5 min at room temperature and then combined with plasmid DNA which was also prepared in Opti-MEM® I Reduced Serum Medium. The reaction mixture was incubated for a further 20 min at room temperature. After 4 hrs at 37 ^{o}C, 5 % CO_2, the transfection reagent was replaced with antibiotic free culture medium and the cells incubated for a further 16 hrs unless otherwise stated.

2.8.2 Gel electrophoresis of proteins using SDS polyacrylamide gel electrophoresis (SDS-PAGE)

Cell monolayers were detached by trypsinisation, collected by centrifugation at 15000 g for 5 min and then washed twice in ice cold PBS. The cells were then solubilised in cell lysis buffer at 4 ^{o}C for 5 min, vortexed briefly and then centrifuged at 12,000 g for 10 min to pellet insoluble cell debris. The supernatant was transferred to a clean tube, diluted in 5 x SDS-PAGE sample loading buffer and heated at 90 ^{o}C for 5 min to

denature the protein sample. Proteins were resolved at 100 v on polyacrylamide gels with a 4 % polyacrylamide stacking gel.

2.8.3 Western Blotting

Proteins resolved using SDS-PAGE were transferred onto Hybond-C extra nitro-cellulose membrane (Amersham Biosciences) using a transfer cassette submerged in transfer buffer for 1 hr at 100 v. The system was cooled using a pre-frozen cooling block. Following protein transfer the membrane was incubated in blocking buffer for 1 hr, washed once in PBST for 15 min, and then incubated with primary antibody (Table 1) diluted in blocking buffer. After 1 hr the membrane was washed twice in PBST for 15 min, incubated with horse radish peroxidase (HRP) conjugated Protein A (Abcam) diluted in blocking buffer for 45 min, washed twice in PBST and once in PBS for 10 min. All incubation steps took place at room temperature with gentle agitation. To detect bound antibodies, the membrane was incubated in freshly prepared ECL reagent for 1 min, placed in a cassette and exposed to Kodak MX1 film for variable time periods. The film was developed using a X-ograph Imaging System Compact X-4 machine.

2.8.4 Indirect Immunofluorescence Microscopy

Cell monolayers were grown on 22 x 22 mm glass cover slips in 35 mm wells. Following cell transfection and a subsequent incubation period the cells were fixed for 1 hr in PBSe containing 4 % paraformaldehyde. The cover slips were washed once in PBSe, incubated in 1 % Triton x-100 PBSe for 15 min to permeablise the cytoplasmic and nuclear cell membranes and then washed again in PBSe. The cells were initially incubated in 5 % BSA/PBSe for 30 min to inhibit non-specific antibody binding and then incubated for a further 1 hr with primary antibody diluted in 0.5%BSA/PBSe. Excess antibody was removed by washing the cells three times in PBSe for 5 min, and secondary antibody diluted in 0.5 % BSA/PBSe was applied. After 1 hr the coverslips were washed three times in PBSe for 5 min, dipped into ddH_2O and then mounted onto

glass slides, cell-side down, using VectaShield mounting medium with Dapi (Vector Laboratories). The edges of the cover slips were sealed using nail varnish to prevent desiccation. The cells were visualized using a Leica TCS SP2 confocal laser scanning microscope. Data was collected sequentially to prevent cross-talk between detection channels and was analysed using LCS (Leica Confocal Software). The images shown are representative of three independent experiments.

2.9 Recombinant Baculovirus

2.9.1 Production of recombinant baculovirus

35 mm wells of a 6-well plate were seeded with 9 x 10^5, mid-log culture, SF9 cells in 2 mls of SF900 II S medium. After cell attachment, at 28 ^oC for a minimum of 1 hr, the cells were washed once in antibiotic free SF900-II S medium and then overlayed with 1 ml of transfection reagent. The transfection reagent was prepared following manufacturers guidelines: 0.5 μg of linearised baculovirus DNA , 1 μg of transfer vector and 6 μl of CELLFECTIN® were diluted in antibiotic free SF900-II S, incubated for 30 min at room temperature and then made up to a final volume of 1 ml using antibiotic free SF900-II S. Following incubation at 28 ^oC for 5 hrs the transfection reagent was replaced with 2 mls of antibiotic free SF900-II S. Cell medium, containing recombinant baculovirus, was harvested 72 hrs post-transfection, centrifuged at 500 g for 5 min to remove cell debris and then stored at 4 ^oC for further analysis.

2.9.2 Amplification and concentration of baculovirus stocks

A 200 ml suspension of SF9 cells, at a concentration of 2 x 10^6 cells/ml, was inoculated with recombinant baculovirus at a multiplicity of infection (MOI) of 0.1, incubated at 28 ^oC, with constant agitation for 48 hrs, and then centrifuged at 500 g for 5 min to remove cell debris. To concentrate the virus, 33 mls of virus containing supernatant was loaded

into each of six Beckman SW28 tubes and underlayed with 3 mls of 25 % sucrose (w/w) in 5 mM NaCl, 10 mM EDTA. Following centrifugation at 80,000 g for 75 min at 4 ^{o}C, the supernatant was discarded. The resulting virus pellet was resuspended in 2 mls of PBS, filtered through a 0.2 μm filter and stored at 4 ^{o}C until use.

2.9.3 Baculovirus DNA purification from cultured cells

Baculovirus DNA was purify from cell culture supernatants using a GFX™ Genomic Blood DNA and Cell Culture DNA purification kit (Amersham Biosciences). The procedure was carried out following manufacturer guidelines. All centrifugation steps were at 12,000 g for 1 min unless stated otherwise. 100 μl of cell supernatant was incubated in 500 μl of extraction solution for 5 min at room temperature, loaded onto a GFX column, centrifuged and the flow-through discarded. The GFX column contains a glass fibre matrix that binds DNA at high salt concentrations, which are present in extraction solution. The matrix bound DNA was washed once with 500 μl of Extraction solution and once with Wash solution to remove contaminants. The column was then centrifuged at standard speed for a further 2 min to dry the column. Baculovirus DNA was eluted in 200 μl of ddH_20 at 70 ^{o}C following 1 min incubation at room temperature.

2.9.4 Baculovirus plaque assays

SF9 cell monlayers at 20-30 % confluence (approximately 2.5 x 10^5 cells per 35 mm well) were inoculated with sequential dilutions of recombinant baculovirus. Following 1 hr incubation at room temperature the inoculum was removed and replaced with 3 mls of SF900-II S containing 1 % low melting temperature agarose. The agar overlay was maintained at 40 ^{o}C prior to addition to the SF9 cell monolayers. Once the overlay had set, the SF9 cells were incubated at 28 ^{o}C for 14 days or until visible plaques could be detected. Each dilution was tested in duplicate and the procedure was repeated on 3 separate occasions. The virus titre was estimated from the virus dilution which produced

between 10-50 plaques. The average number of plaques counted was calculated and multiplied by the dilution factor to produce the final virus titre.

2.10 Buffers and solutions

2.10.1 DNA manipulation techniques

Agarose Gel Loading Buffer**:** 3.73 mM Bromophenol blue and 1.17 M Sucrose.

CIAP stop buffer**:** Tris-HCL (pH 7.5) 10 mM, EDTA (pH 7.5) 1 mM, NaCl 200 mM and SDS 0.5 %.

Cuts All Buffer (CAB): 200 mM Tris-HCl (pH 7.5), 70 mM $MgCl_2$, 1000 mM KCl and 20 mM β-mecaptoethanol.

Luria Broth (LB): 1 % Tryptone, 0.5 % Yeast extract and 1 % NaCl.

LB Agar: 1.5 % Agar in LB

PBST**:** 0.05 % Tween 20 in PBS

RF1: RbCl 1.21 % w/v, MnCl2.4H2O 0.99 % w/v, KC2H3O2 0.29 % w/v, CaCl2.2H2O 0.29 % w/v and 15 % glycerol made to a pH 5.8 with 10 M NaCL.

RF2: MOPS 0.21 % w/v, RbCl 0.12 % w/v, CaCl2.2H2O 1.1 % w/v and glycerol 15 % w/v at pH 6.8

Solution 1: 50 mM glucose, 25 mM Tris-HCl (pH 8.0) and 10 mM EDTA (pH 8.0).

Solution 2**:** 0.2 M NaOH and 1 % (w/v) SDS.

Solution 3: 3 M KCl_2H3O_2 and 11.5 % (v/v)Acetic acid.

TAE (50X): 2M Tris, 5.7% v/v Acetic Acid and 50 mM EDTA at pH7.7

TE buffer: 10 mM Tris-HCl (pH 8.0) and 1 mM EDTA (pH 7.7).

2.10.2 Protein Expression and Analysis

Cell Lysis Buffer : 500 mM NaCl, 50 mM Tris-HCl (pH 7.5), 5 mM EDTA (pH 7.5), 0.05 % IGEPAL NP-40 and 1ug/ml small protease inhibitors (Pierce).

IF Blocking solution: PBSe containing 5% BSA.

ECL reagent**:** 22 µl of Reagent A (p-coumaric acid; 90 mM in DMSO) combined with 50 µl of Reagent B (Luminol; 250 mM in DMSO), dissolved in 10 mls of 0.1 M Tris-HCL (pH 8.5) and 3 mM H_2O_2.

PBSe: 138 mM NaCl, 2.70 mM KCl, 1.47 mM KH_2PO_4 and 9.67 mM Na_2HPO_4.

PBS**:** 138 mM NaCl, 2.70 mM KCl, 0.49 mM $MgCl_2.6H_2O$, 1.47 mM KH_2PO_4, 9.67 mM Na_2HPO_4 and 6.80 mM $CaCl_2.2H_2O$.

WB Blocking solution: dried low-fat skimmed milk 5 % in PBS.

SDS-PAGE resolving gel (10 %) : 40% stock acrylamide solution [acrylamide:N,N -methylene bisacrylamide, 37.5:1] 25% (v/v), 0.4 M Tris-HCl pH 8.8, 0.1% (w/v) SDS, 0.2% (v/v) ammonium persulphate and TEMED (N,N,N',N'-Tetramethylethylenediamine) 0.1% (v/v).

SDS-PAGE stacking gel (4 %): 40% stock acrylamide 10% (v/v), Tris-HCl pH 6.8 100mM, SDS 0.1% (w/v), ammonium persulphate 0.2% (w/v) and TEMED 0.1% (v/v).

Protein gel resolving buffer: 15.4 % (w/v) Glycine, 3 % (w/v) Tris and 0.5 % (w/v) SDS.

Protein gel sample buffer (3x): 3 % (w/v) SDS, 3 % (v/v) β-mecaptoethanol, 20 % (v/v) Glycerol and 0.001 % (w/v) Bromophenol Blue.

Transfer Buffer: 25 mM Tris, 190 mM Glycine and 20 % (v/v) Methanol.

2.10.3 Cell culture

RMPI S: RMPI 1640 (sigma), 100 µg/ml penicillin, 100 µg/ml Streptomycin, 2.5 µg/ml Fungizone, 5 µg/ml Gentamycin, 1:100 Non Essential Amino acids (Gibco) and 10 % (v/v) FCS.

SF900-II S: SF900 II (sigma), 100 µg/ml Penicillin, 100 µg/ml Streptomycin, 2.5 µg/ml Fungizone, and 10 % (v/v) FCS.

2.9.4 Microarray hybridisation buffers

20 x SSC: 3 M NaCl and 0.3 M sodium citrate buffer (pH 7.0)

Pre-hybridisation buffer: 3 x SSC containing 0.1 % SDS

Sodium citrate buffer: 3.0 M NaCl and 0.3 M sodium citrate made up to pH 7.0 with 10 M NaOH.

Wash 1: 2x SCC containing 0.2 % SDS

Wash 2: 2x SCC

Wash 3: 0.2x SSC

Chapter 3

Development of an A238L gene expression and delivery system suitable for porcine alveolar macrophage cells

3.1 Introduction

The aim of this project was to investigate the individual effect of the ASFV protein A238L on host cell gene transcription using a porcine microarray. To achieve this it was necessary to develop a gene expression system capable of expressing A238L under the control of a mammalian cell active promoter and then to deliver this gene to a high proportion of the target cells with minimal disruption to normal cell function.

One approach to ensure that a high proportion of the target cells are expressing the target gene would be to generate a cell line stably expressing A238L under the control of an inducible promoter, such as the tetracycline inducible promoter (T-Rex, Invitrogen). However, this approach is only suitable for an immortalized cell line. A transient gene delivery system offers a more flexible approach with the potential to mediate gene delivery to a range of both primary and immortalized cells.

3.1.1 A238L gene expression

Previous work carried out at the IAH has shown that A238L protein expression levels are low and often undetectable when transcribed under the control of the nuclear polymerase II promoter present in pcDNA3. However, A238L is expressed efficiently from a T7 RNA polymerase promoter when transfected into cells infected with Vaccinia virus (MVA-T7) expressing T7 RNA polymerase(Miskin *et al.*, 2000b; Tait *et al.*, 2000).

ASFV replicates in the cytoplasm of infected cells using its own transcriptional apparatus. Therefore, unlike mammalian genes and viruses that replicate in the nucleus of infected cells, ASFV gene transcripts are unlikely to be optimized for transcriptional processing and the nuclear export of newly synthesized mRNA in mammalian cells. Thus, low levels of A238L protein expression produced using pcDNA3 could be due to the poor post-transcriptional processing and export of A238L mRNA and the retention of pre-processed A238L mRNA in the nucleus of transfected cells. Previous research has shown that the addition of cis-acting regulatory modules, such as splice sites and viral RNA regulatory elements, can significantly improve the expression of intronless genes from plasmid or viral vectors (Schambach *et al.*, 2000); Callendrat et al 2007). Schambach *et al* investigated the ability of three different RNA modules to enhance the expression of intronless genes from reteroviral gene transfer vectors. The modules tested were: splice signals (SS), used to create an intron in the 5' untranslated region of the test gene; a constitutive RNA transport element (CTE), found in D-type retroviruses; and a post-transcriptional regulatory element present in the woodchuck hepatitis virus (WPRE), which enhances post transcriptional processing and nuclear export of mRNA. Both the CTE and WPRE interact directly with cellular factors in the nucleus and do not require additional viral proteins to function (Gruter *et al.*, 1998; Zufferey *et al.*, 1999). The results from these studies demonstrated that the function and potential synergy of the RNA elements investigated was dependent on the characteristics of the individual gene tested. Overall the WPRE demonstrated the most uniform and strongest capability to promote transgene expression. This was particularly apparent in the expression of two genes (enhanced green fluorescent protein (EGFP) and human multidrug resistance-1(MDR1)). These genes were selected due to the ability of their transcripts to be processed in the absence of introns but only at low, sub-optimal levels. These characteristics are similar to those exhibited by A238L when expressed under the control of the nuclear polymerase II promoter present in pcDNA3. Therefore the ability of the WPRE to improve A238L gene expression was investigated.

3.1.2 A238L gene delivery

To obtain results representative of the effect of A238L on individual host cell gene transcription, and reduce background noise from cells not expressing A238L, a high level of transfection efficiency is required. Porcine cells derived from the monocyte/macrophage cell lineage are the main target cells for ASFV infection *in vivo* and therefore offer the most biologically relevant system for examining the effect of A238L on host cell gene expression. Primary porcine alveolar macrophage (PPAM) obtained by lung lavage from domestic pigs are used for the culture and scientific investigation of ASFV field isolates *in vitro*. These cells are extremely difficult to transfect using conventional methods and work in our laboratory has shown that PPAM's typically exhibit a transfection efficiency of less than 1 % using standard cationic lipid reagents such as lipofectamine^{TM} 2000 (Invitrogen) (Lynnette Goatley personal communication). In addition the quality, composition and activation status of isolated cells is variable between animals, introducing a significant amount of variability between biological replicates. As a potential alternative to PPAM a continuous clonal porcine monomyeloid cell line derived from alveolar macrophage, has been obtained from Dr Weingartl (Weingartl *et al.*, 2002b). This cell line has been shown to support the replication of ASFV. Compared to primary macrophages this cell line offers an unlimited quantity of RNA with minimal variability between cultures due to its clonal origin. Higher levels of transfection (approximately 40%) were achieved using lipofectamine^{TM} 2000 in these cells, compared to primary macrophages, however the number of un-transfected bystander cells still exceeds those expressing the target protein. Therefore a gene delivery system capable of achieving high levels of transfection in both primary and immortalised porcine alveolar macrophage cells was required.

Defective virus vectors are capable of delivering genes to target cells but unable to initiate a productive infection. Several of these have been shown to achieve high levels of transfection efficiency in primary mammalian cells. Baculoviruses naturally replicate in insect cells, but also have the ability to enter mammalian cells by a mechanism

involving clathrin-mediated endocytosis (Long *et al.*, 2006). Recombinant baculoviruses, which have been modified to contain mammalian cell active promoters, have several advantages over other mammalian virus vectors. These include their inability to produce a productive infection in mammalian cells, their apparent lack of cytotoxicity, ability to target many different cell types, and safety features relative to mammalian virus-based transduction systems (Kost *et al.*, 2005). Recombinant baculoviruses have previously been successfully used to deliver genes to both immortalised and primary porcine cells, with a transfection efficiency of 90-100 % achieved in a porcine kidney cell line. No visible cytopathic effect could be detected in porcine kidney cells inoculated with this virus (Kost & Condreay, 2002). Therefore the ability of recombinant baculovirus to deliver ASFV genes to porcine alveolar macrophage cells was investigated.

3.2 Results

3.2.1 Cloning of the Woodchuck hepatitis postranscriptional regulatory element into an A238L expression vector.

To test if the WPRE could enhance the expression level of A238L, this element was cloned into the plasmid pcDNA3-SV5A238L to produce pcDNA3-SV5A238L-WPRE. PcDNA3-SV5A238L encodes the A238L protein fused to an N-terminal, 14 amino acid Pkepitope tagdownstream of the CMV immediate early promoter. The Pk epitope is derived from the paramyxovirus, Simian Virus 5 (SV5) proteins P and V. No antibodies specific to A238L are available in our laboratory therefore this tag allows the detection of A238L using PK epitope specific antibodies. Pervious work has shown thatthis tag does not interfere with the biological function of A238L (Miskin *et al.*, 1998). To generate pcDNA3-SV5A238L-WPRE a 600 nucleotide cassette containing the WPRE was digested from pHR'CMV-GFP (Zufferey *et al.*, 1999) at *Eco*R I sites either side of the WPRE element. The resulting 5' overhangs were end-filled using the Klenow fragment of DNA polymerase I in the presence of excess dNTP's. The WPRE was then gel purified and ligated into pcDNA3-SV5A238L at an *Eco*R V site located in the 3'

untranslated region of A238L, between the stop codon of A238L and a polypurine tract present in pcDNA3 (Figure 3.1)**.** WPRE is sense dependent and therefore its insertion in the correct orientation was confirmed (Zufferey *et al.*, 1999). Since sequence analysis of the WPRE identified a unique *Nco* I restriction site at nucleotides 413 - 419, restriction mapping of pcDNA3-SV5A238L-WPRE with *Nco* I was used to confirm the presence of the WPRE and determine its orientation (Figure 3.2).

3.2.2 Analysis of the effect of WPRE on A238L expression

The effect of the WPRE on SV5-A238L gene expression was initially examined using Western blotting (WB). IPAM cells were transfected in parallel with pcDNA3, pcDNA3-SV5A238L or pcDNA3-SV5A238L-WPRE. At 16 hrs post-transfection cell lysates were harvested, resolved using SDS-PAGE and then blotted onto a nitrocellulose membrane. The membrane was probed for the presence of SV5-A238L using anti-Pk tag antibodies, which were detected using HRP conjugated protein A. A band migrating at approximately 30 kDa, corresponding to SV5A238L, was detected in cell lysates transfected with pcDNA3-SV5A238L and pcDNA3-SV5A238L-WPRE. No band was detected in cell lysates transfected with pcDNA3 alone. A parallel blot probed with antibodies against α-tubulin was used to confirm that relative levels of protein loaded between samples were similar. From Figure 3.3 (a) it can be seen that cell lysates transfected with pcDNA3-SV5A238L-WPRE contained higher levels of SV5-A238L than cell lysates transfected with pcDNA3-SV5A238L. This suggests that the WPRE can enhance the level of A238L expression using the pcDNA3-SV5-A238L expression vector, in IPAM cells. To confirm if this overall increase in the level of A238L gene expression was due to the direct effect of the WPRE within individual cells and not due to the more efficient transfection of pcDNA3-SV5A238L-WPRE compared to pcDNA3-SV5A238L, transfected cells were examined by Immuno-Fluorescence (IF) followed by confocal microscopy. IPAM cells were transfected using the conditions described above. At 16 hrs post-transfection the cells were fixed, permeabilised and stained with an antibody specific to the Pk tag followed by a fluorescently labeled secondary antibody.

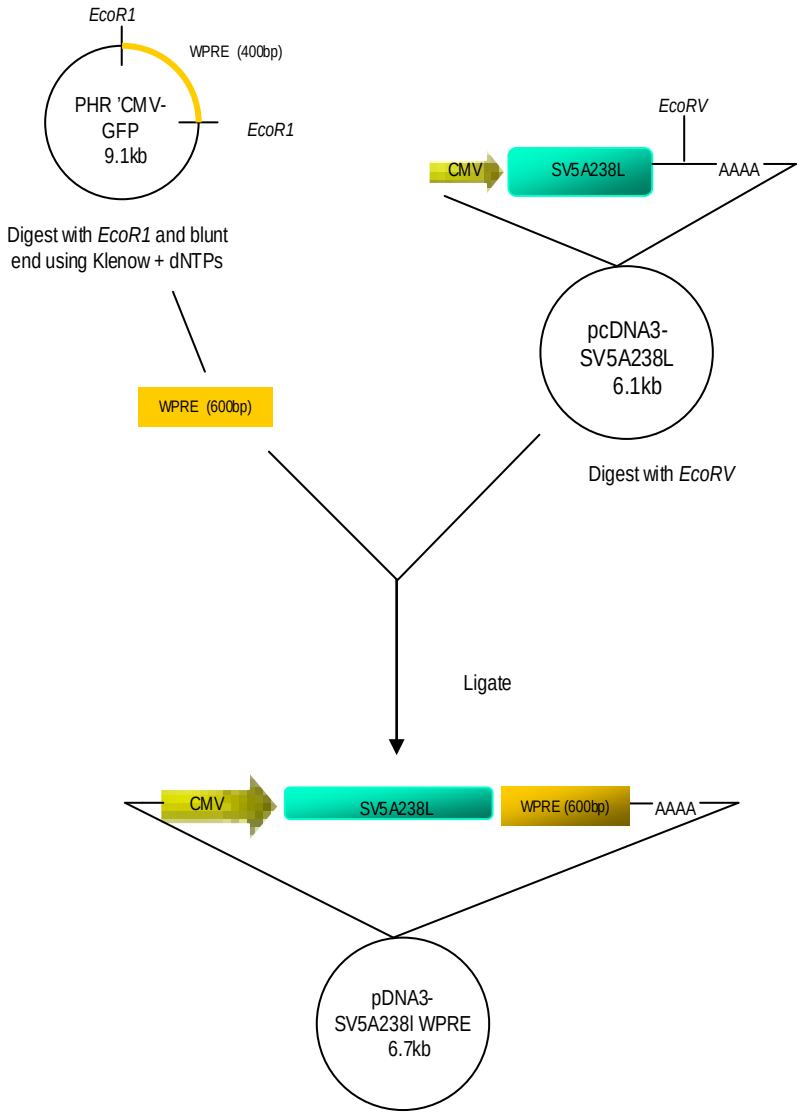

Figure. 3.1 Illustration of the cloning strategy to clone WPRE into pcDNA3-SV5A238L. A 600bp WPRE cassette was digested from PHR'CMV-GFP using *Eco* RI. 5' overhangs were then end filled using the Klenow fragment of E.coli DNA polymerase 1, in the presence of excess dNTPs. The resulting blunt-ended WPRE fragment was then ligated into pcDNA3-SV5A238L at an *Eco*R V site located between the stop codon of A238L and a polypurine tract present in pcDNA3.

DNA was stained with DAPI to detect the cell nuclei. Images were produced at the same brightness and gain to allow comparison between the relative levels of SV5-A238L expression. The transfection efficiency between pcDNA3-SV5A238L and pcDNA3-SV5A238L-WPRE transfected cells was comparable at approximatley 8%. No pcDNA3 transfected cells could be detected using the anti-Pk tag antibody demonstrating that this antibody is specific to SV5-A238L expressed in IPAM cells (data not shown). SV5-A238L staining exhibits a diffuse pattern throughout both the cytoplasm and nucleus of transfected cells (see Figure 3.3 (b)). Staining of SV5-A238L was higher in cells transfected with pcDNA3-SV5A238L-WPRE compared to cells transfected with pcDNA3-SV5A238L. This increase in SV5-A238L expression was limited to within individual cells and not due to an increase in the overall number of cells transfected, supporting the predicted function of the WPRE, in enhancing post-transcriptional processing of mRNA in cells (Zufferey *et al.*, 1999)**.** Together, these results demonstrate that the addition of the WPRE to pcDNA3-SV5A238L can enhance A238L gene expression to a level that is readily detectable by WB and IF and therefore suitable for future experiments.

3.2.3 Generation of recombinant baculovirus for A238L gene delivery

Following the optimisation of A238L gene expression through the addition of the WPRE, two separate recombinant baculoviruses were produced to investigate the effect of A238L on host macrophage gene expression: a test virus encoding the A238L gene and the second, not containing the A238L gene, to act as a negative control. *Autographa californica nucleopolyhedrovirus* (AcNPV) were selected as an appropriate baculovirus virus vector, since previous work with these viruses has shown they are capable of mediating gene transfer to a wide range of mammalian cell lines with minimal cytopathic effect (Shoji *et al.*, 1997).

AcNPV recombinant baculoviruses were produced using a system which relies on homologous recombination between baculovirus DNA (encoded on the bacmid,

(a)

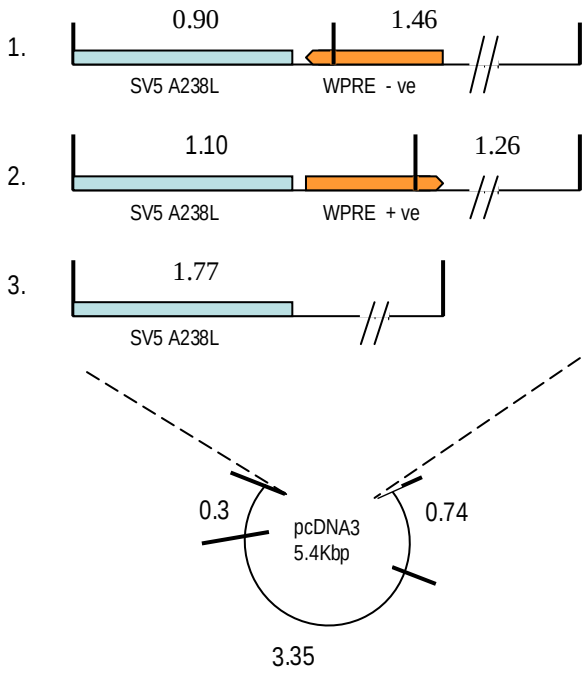

(b)

Plasmid	1	2	3
Restriction fragments	5	5	4
Size (kbp)	3.35	3.35	3.35
	1.46	1.26	1.77
	0.90	1.10	0.74
	0.74	0.74	0.3
	0.3	0.3	

(c)

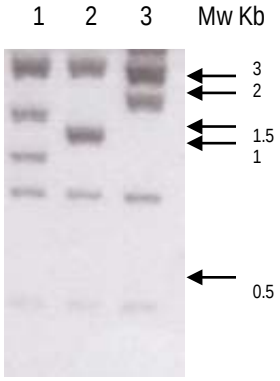

Figure 3.2 *Nco*I restriction enzyme site maps of plasmids pcDNA3-SV5A238L, pcDNA3-SV5A238L-WPRE (-) and pcDNA3-SV5A238L-WPRE(+ve). Panel A shows the expected maps of *Nco*1 sites on SV5A238L-WPRE (-)(1), pcDNA3-SV5A238L-WPRE(+ve) (2) and pcDNA3-SV5A238L (3). Solid lines indicate the positions of *NcoI* restriction sites and the numbers represent the number of nucleotide base pairs between each restriction site (restriction maps are not drawn to scale). The predicted size and number of DNA fragments produced by each plasmid following digestion with *Nco*1 is shown in Panel B.Panel C shows 1% agrose gel electrophoresis of *Nco*I digests of the above plasmids. The positions of the molecular weight markers, run in parallel, are indicated. Lane 1 shows a digest of pcDNA3-SV5A238L-WPRE (-), Lane 2 of pcDNA3-SV5A238L-WPRE(+ve) and lane 3 pcDNA3-SV5A238L. Lane 2 appears to shows only 4 fragments instead of the predicted 5 as the 1.26 and 1.10 Kbp fragment are not clearly resolved.

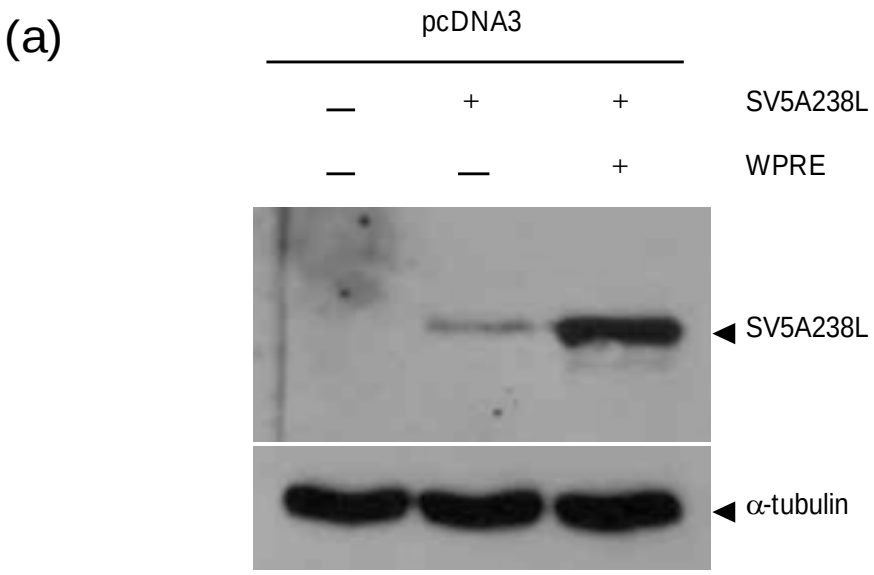

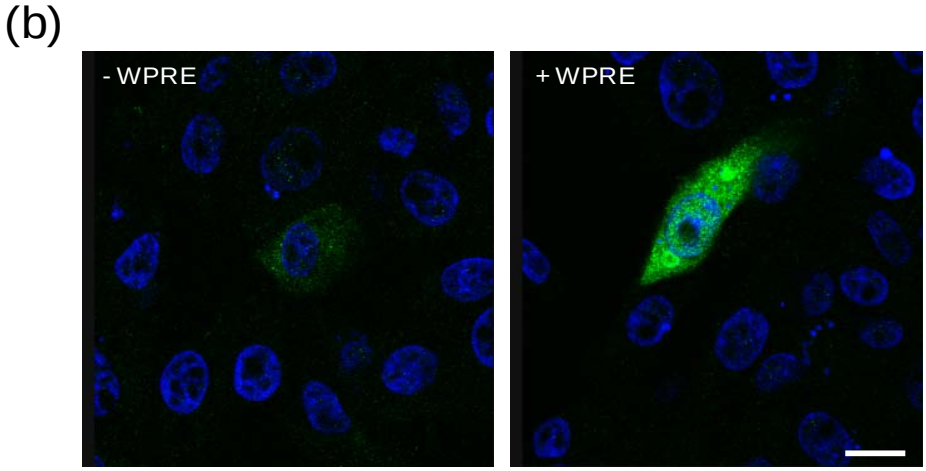

Figure 3.3 The WPRE increases A238L gene expression in IPAM cells. Panel A. Western blot analysis of IPAM cells transfected with either pcDNA3 (as a negative control), pcDNA3-SV5A238L or pcDNA3-SV5A238L-WPRE. Cell lysates were harvested at 16 hrs post-transfection. SV5-A238L was detected using an anti-PK mouse monoclonal antibody (Serotec). α-tubulin is shown as a loading control. Panel B. Images of IPAM cells transfected with either pcDNA3-SV5A238L or pcDNA3-SV5A238L-WPRE. Cells were fixed and stained 16 hrs following transfection. SV5-A238L is shown in green and cell nuclei are blue. Images were taken sequentially, at the same brightness and gain using confocal microscopy and then merged. Bar, 10 μm. Images shown in panel A and B are representative of 3 independent experiments.

Bac10:KO_{1629}) and a suitable transfer vector containing the target gene flanked by baculovirus DNA (Zhao *et al.*, 2003). The polyhedrin gene, which is flanked by ORF603 and ORF1629, was used as the locus of recombination. ORF603 encodes a 21 kDa non-essential protein and ORF 1629 encodes the 61 kDa viral capsid-associated protein which is essential for baculovirus replication (Possee *et al.*, 1991; Valdeira *et al.*, 1998). Bac10:KO_{1629} has been specifically modified to encode a truncated, non-functional ORF 1629. Viral DNA prepared from this knockout virus fails to initiate an infection unless rescued by recombination with a baculovirus transfer vector containing a complete, functional ORF 1629. This approach ensures that any baculovirus progeny produced must result from a successful recombination event and therefore eliminates the need for subsequent virus selection and the purification of recombinants (Figure 3.4)**.** Bac10:KO_{1629} also contains a unique *Bsu*361 restriction enzyme site allowing linearisation of the DNA prior to co-transfection. This facilitates recombination, as linear DNA is recombined more efficiently than circular DNA (Kitts & Possee, 1993).

3.2.4 Construction of transfer plasmids for the production of test and control recombinant baculovirus

pTriEx1.1 (Novagen) was selected as a suitable transfer vector to generate control and test recombinant baculovirus. This plasmid contains both a late p10 baculovirus promoter and CAG promoter, allowing expression of the target gene in both insect and mammalian cells respectively. pTriEx1.1 also contains a 256bp intron. Introns have been reported to enhance mRNA processing and export in eukaryotic cells (Nott *et al.*, 2003). The mammalian cell active promoter CAG is a composite promoter consisting of a CMV enhancer element fused to the chicken β-actin promoter. Previous work has shown that this promoter can successfully drive luciferase gene expression in a porcine kidney cell line (CPK) following baculovirus-mediated gene transfer (Shoji *et al.*, 1997).

To produce test recombinant baculovirus expressing A238L, the SV5A238L-WPRE expression cassette was cloned into pTriEx1.1 to produce pTriEx1.1-SV5A238L-WPRE.

To generate pTriEx1.1-SV5A238L-WPRE a 756 bp fragment containing SV5A238L was amplified from pcDNA3-SV5A238L by PCR, using the primers Pc*Nco* and Pc*Hind*, which contain *Nco* I and *Hind* III restriction sites respectively. Following digestion with *Nco* I and *Hind* III the PCR fragment was gel purified and ligated into *Nco* I and *Hind* III digested TriEx1.1 to produce pTriEx1.1-SV5A238L. A 600 bp WPRE cassette was then digested from pHR'CMV-GFP using *Eco*R I and, following gel purification, ligated into TriEx1.1-SV5A238L at a unique *Eco*R I site downstream of the SV5A238L coding sequence to produce TriEx1.1-SV5A238L-WPRE. To confirm the correct orientation of the WPRE, TriEx1.1-SV5A238L-WPRE was digested with *Nco* I and then analysed using agarose gel electrophoresis (Figure 3.5). The insert in the selected plasmid was then sequenced to confirm it was as expected.

To ensure that SV5-A238L could be expressed under the control of the CAG promoter in porcine macrophages, cells were transfected with TriEx1.1-SV5A238L-WPRE and examined for the expression of SV5-A238L. Expression levels of SV5-A238L were compared between the vectors TriEx1.1 and pcDNA3, both with and without the WPRE. IPAM cells were transfected with either pcDNA3-SV5A238L, pcDNA3-SV5A238L-WPRE, pTriEx1.1-SV5A238L or pTriEx1.1-Sv5A238L-WPRE. Cells transfected with pcDNA3 and TriEx1.1 were used as negative controls. At 16 hours post-transfection the cells were examined for the presence of SV5-A238L using western blotting and immunofluorescent confocal microscopy. Western blot analysis of the cell lysates using anti-Pk tag antibodies showed that SV5-A238L migrated as a 28 kDa molecular weight protein in all the cell lysates with the exception of the controls (Figure 3.6). Levels of SV5-A238L expressed in cells transfected with the TriEx1.1 vector (both with and without the WPRE) consistently showed higher levels of expression than in cells transfected with the pcDNA3 vector. This could be due to the CAG promoter being more active than the CMV promoter in IPAM cells and/or the presence of the intron enhancing SV5A238L mRNA processing. Consistent with previous results, the WPRE caused an increase in gene expression when SV5-A238L was expressed using pcDNA3. The WPRE also increased the level of SV5-A238L expression using the TriEx1.1

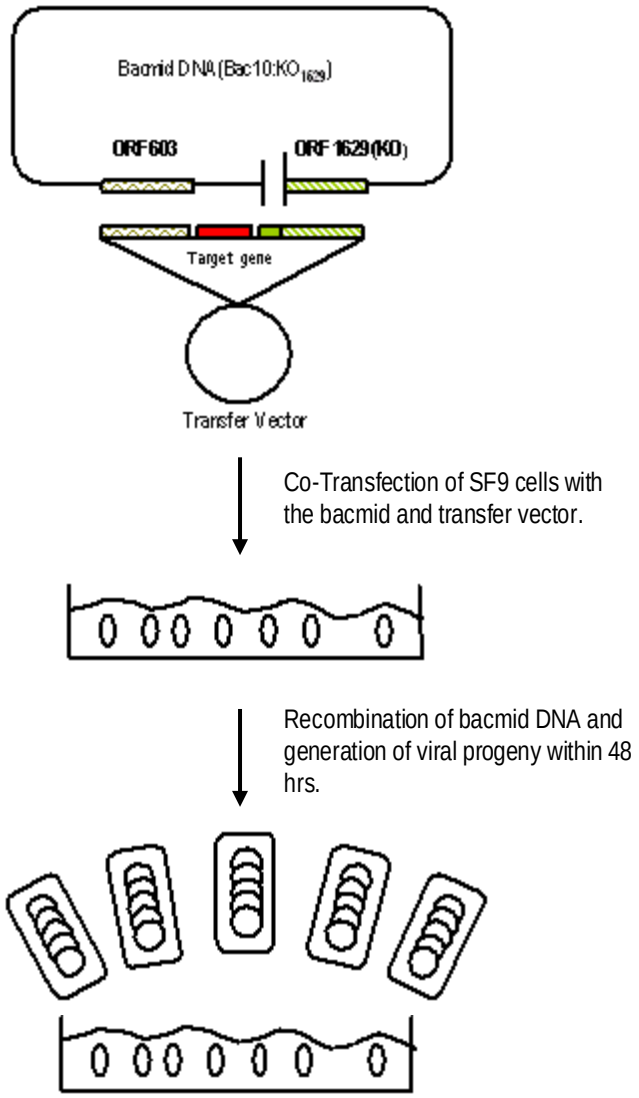

Figure 3.4 A schematic representaion of the generation of recombinant baculovirus using Bac10:KO1629. SF9 insect cells are transfected with linearised Bac10:KO1629 (which encodes a non-viable baculovirus genome, containing lethal deletion in ORF1629) and a transfer vector containing the target gene flanked by the baculovirus sequences to ORF603 and ORF1629. Homologous recombination between Bac10:KO1629 and the transfer vector repairs the lethal deletion in ORF1629 producing an infectious baculovirus DNA containing the target gene. Recombinant baculovirus encoding the target gene are then produced.

expression vector, although the results were much less pronounced than those seen for pcDNA3. These results demonstrate that higher levels of SV5-A238L are expressed from the plasmid pTriEx1.1 containing the WPRE compared to the plasmid pcDNA3, and this is therefore a suitable transfer vector for the production of recombinant baculovirus.

A transfer vector encoding the WPRE in the absence of the A238L gene was also produced to generate control baculovirus. To achieve this the WPRE element was digested from pHR'CMV-GFP using *Eco* RI and, ligated into TriEx1.1 at an unique *Eco* RI site located in the multiple cloning region of TriEx1.1, to produce TriEx1.1-WPRE. To confirm the presence of the 600 bp WPRE, TriEx1.1-WPRE was digested with *Eco* RI and then analyzed using agarose gel electrophoresis. Selected plasmids were then sequences to confirm the correct orientation of the WPRE.

3.2.3 Production of recombinant baculoviruses

To produce recombinant baculovirus, SF9 insect cells were co-transfected (using Cellfectin™) with linearised Bac10:KO_{1629} and either pTriEx1.1-SV5A238L-WPRE or pTriEx1.1-WPRE to produce both test and control recombinant baculoviruses. Cells were also transfected with Bac10:KO_{1629} alone to act as a negative control. Following incubation at 28 ^{o}C for 72 hrs, cell supernatants were harvested, centrifuged to remove cell debris and then tested for the presence of viable baculovirus using a plaque assay. Plaques were detected from supernatants isolated from cells co-transfected with Bac10:KO_{1629} / pTriEx1.1-SV5A238L-WPRE and Bac10:KO_{1629} /pTriEx1.1-WPRE. No plaques were detected from cell lysates transfected with Bac10:KO_{1629} alone, indicating that the viruses isolated from the other samples were the result of a successful recombination. Test (Bac-SV5A238L) and control (Bac-WPRE) baculovirus were then amplified and purified for further investigation.

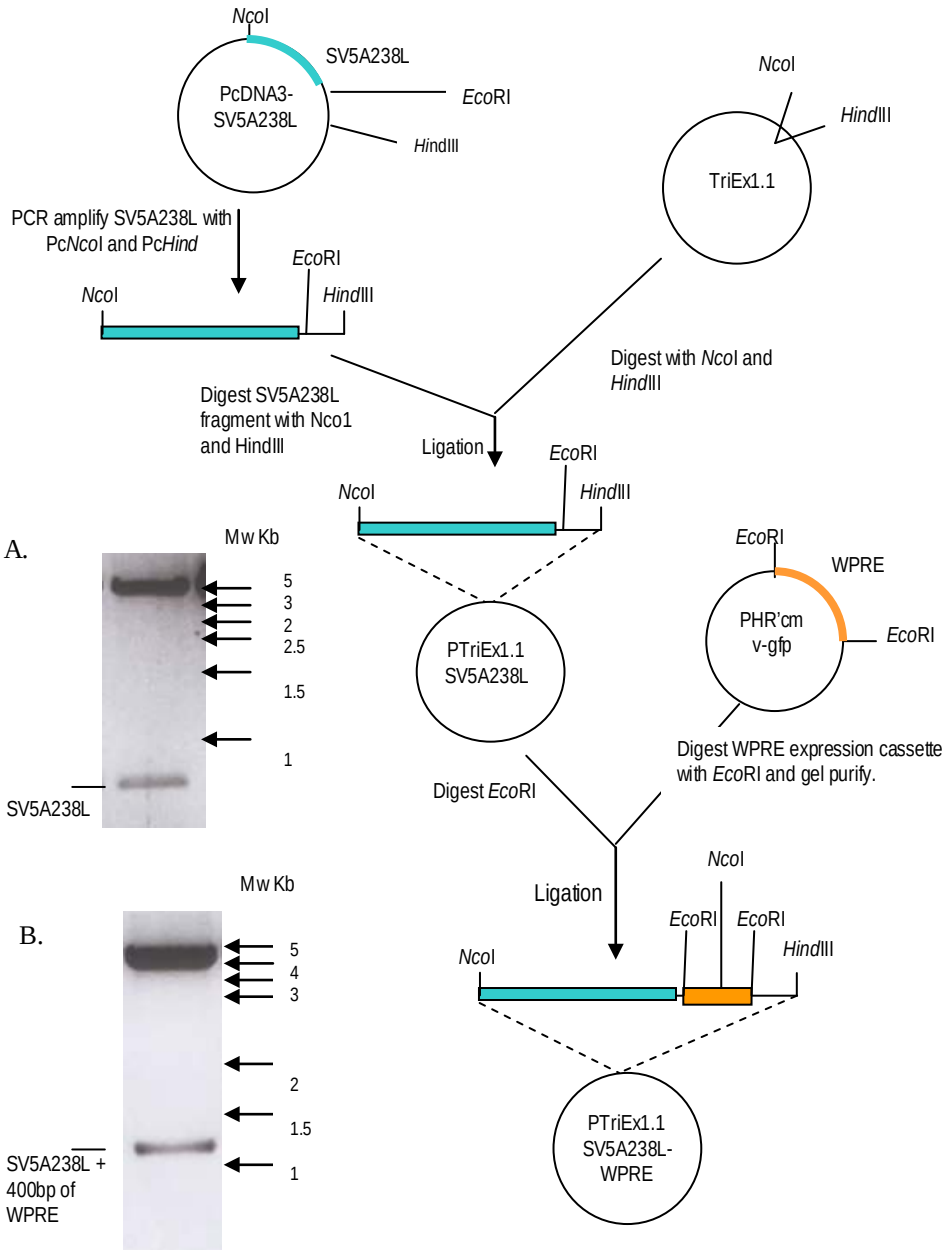

Figure 3.5 Cloning SV5-A238L-WPRE into the transfer vector TriEx1.1
A 756 bp fragment containing SV5A238L (blue) was PCR amplified from pcDNA3-SV5A238L using the primers Pc*Nco I* and Pc*Hind*, which contain *Nco* I and *Hind* III restriction sites respectively. TriEx1.1 and the PCR product were then restriction digested with *Nco*I and *Hind*III and ligated together to produce TriEx1.1-SV5A238L. TriEx1.1-SV5A238L digested with *Nco* 1 and *Eco*R I is shown (A). A 600bp WPRE (yellow) cassette was digested from pHR'CMV-GFP using *Eco*RI and ligated into TriEx1.1-SV5A238L to produce TriEx1.1-SV5A238L-WPRE. TriEx1.1-SV5A238L-WPRE was restriction digested with *Nco* I to confirm the correct orientation of WPRE (B).

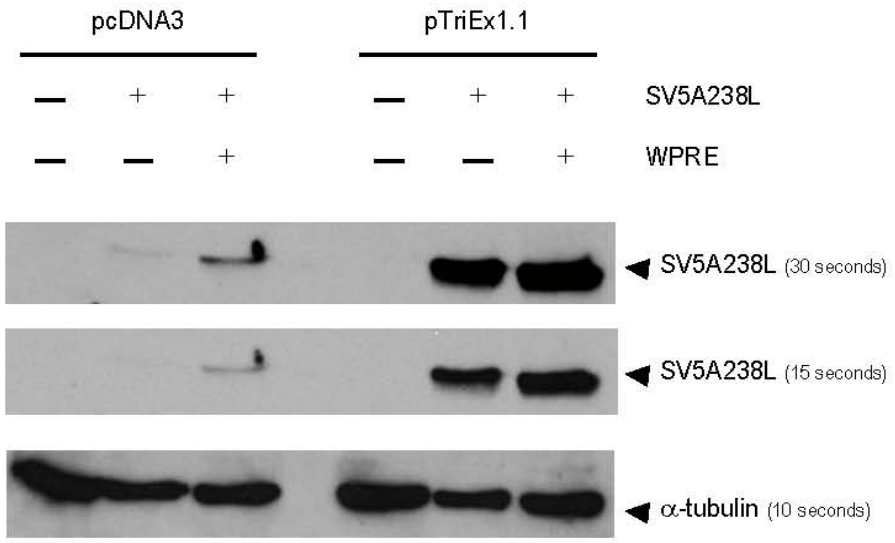

Figure 3.6 High levels of SV5A238L protein expression were achieved using the transfer vector pTriEx1.1 in combination with the WPRE. IPAM cells were transfected with either pcDNA3 or pTriEx1.1 encoding SV5-A238L or SV5A238L-WPRE. The presence or absence of SV5A238L and the WPRE is indicated by a cross (+) or line (-) respectively. Cell lysates were harvested at 16 hrs post transfection and examined by western blot. SV5A238L was detected using an anti-PK mouse monoclonal antibody (Serotec). Two separate images of the SV5A238L blot are show and represent different lengths of film exposure to the ECL reagent. The time of exposure is indicated. α-tubulin is shown as a loading control. Each procedure was repeated on 3 separate occasions and the images presented are representative of these results.

To confirm the presence of the SV5A238L-WPRE expression cassette in Bac-SV5A238L and the WPRE in Bac-WPRE, baculovirus DNA from these recombinant viruses was purified and then fragments containing the inserted sequences were amplified by PCR using the primers TriExUP (Novagen) and pORF1629. TriExUP is specific for the transfer vector pTriEx1.1 and is located upstream of the p10 promtor region and pORF1629 is located within ORF1629. Together theses primers flank the target insertion sequences. From Figure 3.7 it can be seen that PCR amplification of the baculovirus DNA from both Bac-SV5A238L and Bac-WPRE produced products of the correct size, approximately 2.7 Kbp and 1.8 Kbp respectively. This result confirms the presence of the target DNA sequences in the recombinant viruses.

3.2.5 Susceptibility of porcine cells to baculovirus-mediated gene transduction

To investigate the ability of Bac-SV5A238L to mediate gene transfer to porcine macrophage cells, the expression of SV5-A238L was examined in both an immortalised porcine alveolar macrophage cell line (IPAMs) and primary porcine alveolar macrophage (PPAM) by western blotting. Previous work using porcine kidney cells demonstrated that a m.o.i. of 10 to 100 was required to obtain high levels of gene transfection using recombinant baculovirus (Shoji *et al.*, 1997). Therefore, cultures of IPAM cells and PPAM were treated with either Bac-SV5A238L at an m.o.i. of both 10 and 50, Bac-WPRE at an m.o.i. of 50 or mock-infected at 37 ^{o}C in serum free medium. One hour following treatment the cell supernatant was removed along with excess virus and replaced with standard culture medium. Cell lysates from IPAM and PPAM cells were harvested at 24 and 48 hrs, respectively, following virus treatment, and analysed by western blotting. From Figure 3.8 it can be seen that SV5-A238L could be detected in cell lysates from both IPAMs and PPAM treated with Bac-SV5A238L. No bands were detected in cell lysates treated with the control baculovirus, Bac-WPRE, indicating that the the anti-Pk antibody was specific for SV5-A238L in this experiment and does not cross react with baculovirus proteins. In IPAM cells the SV5-A238L band present in cells treated at an m.o.i. of 50 appeared to be slightly more intense than the band

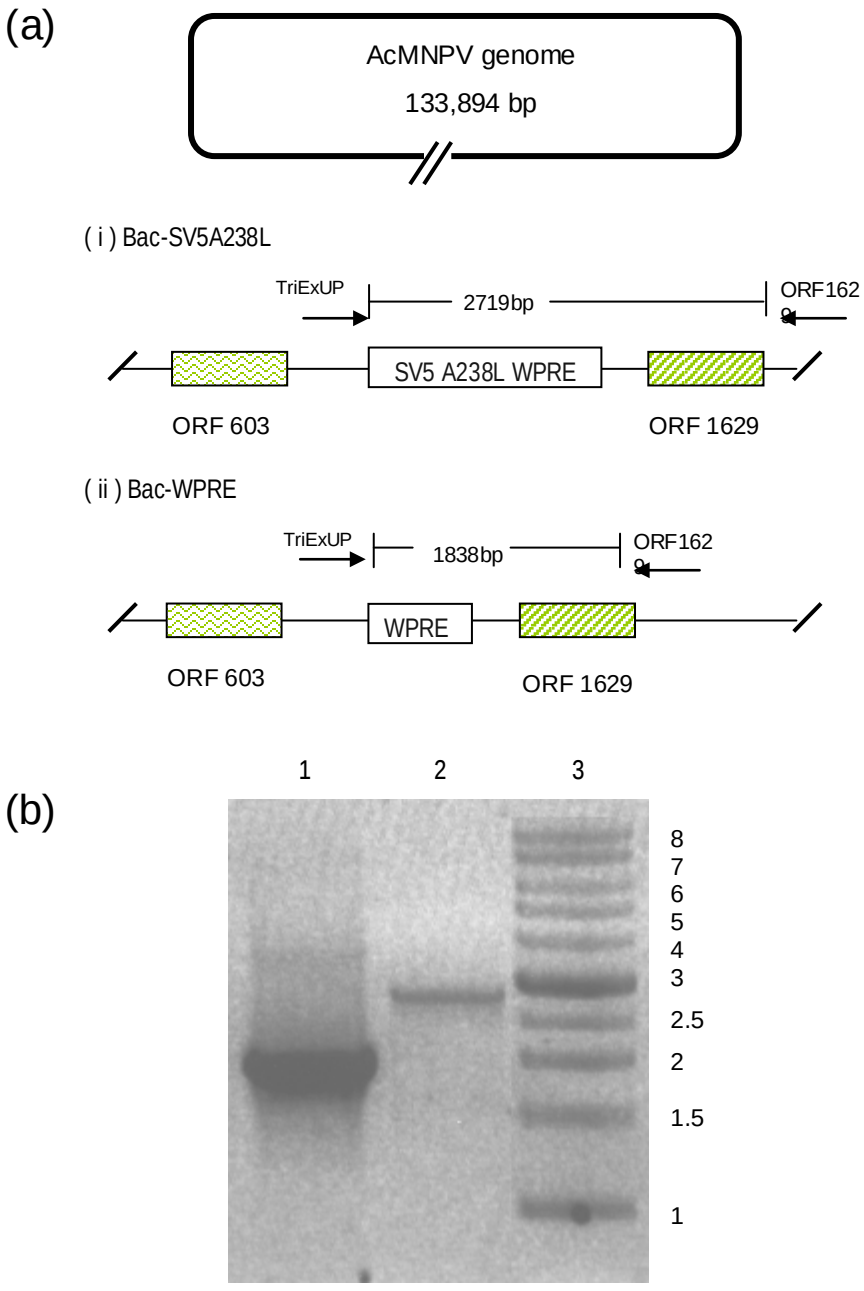

Figure 3.7 PCR analysis of recombinant baculovirus DNA. Panel A. Comparative maps of the baculovirus genome at the site of recombination are shown for Bac-SV5A238LWPRE (i) and Bac-WPRE (ii). The position and direction of the primers TriExUp and ORF1629 are indicated by the presence of an an arrow below the primers name. Panel B. PCR products produced from Bac-WPRE (lane 1) and Bac-SV5A238L DNA (Lane 2) using the primers TriExUp and ORF1629. DNA markers with their molecular mass (in Kbp) are shown in Lane 3.

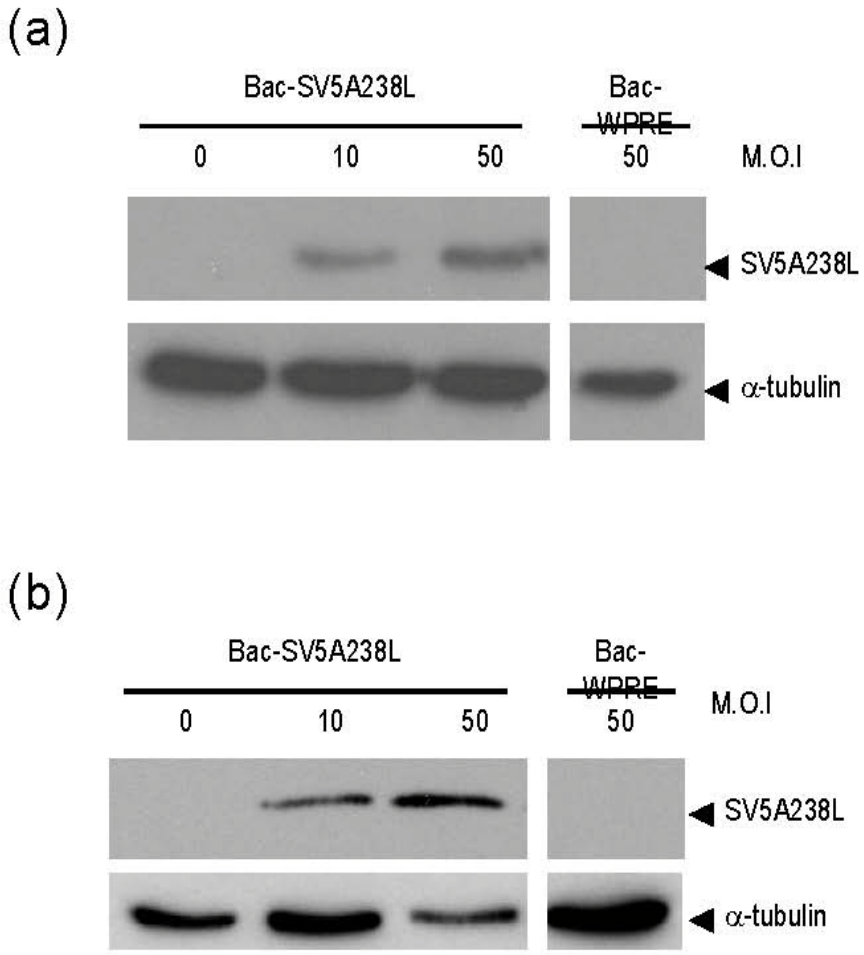

Figure 3.8 Immortalised and primary porcine alveolar macrophage cells are susceptible to gene transfer by recombinant baculovirus. IPAM cells (Panel A) and primary porcine alveolar macrophage (Panel B) were treated with either Bac-SV5A238L or Bac-WPRE at the indicated m.o.i. IPAM's and primary porcine alveolar macrophages were harvested at 16 and 24hrs post-infection respectively. Cell lysates were then analysed by western blot. α-tubulin is shown as a loading control

detected in cell lysates treated at an m.o.i.of 10. The results for PPAM were similar, although less pronounced. Higher levels of SV5-A238L protein expression associated with an m.o.i. of 50 probably indicate a higher rate of gene delivery at this m.o.i..

3.2.6 Transfection efficiency of baculovirus-mediated gene transduction to porcine cells

To investigate the efficiency of baculovirus-mediated gene transfer, IPAM cells were inoculated with Bac-SV5A238L at an m.o.i of 0, 10, 50 and 100 in duplicate. 16 hrs following inoculation the cells were fixed, permeabilised and stained for the presence of SV5-A238L using indirect immunofluorescence. Cells were imaged using confocal microscopy. 3 independent experiments were carried out. Visual inspection of the cells by light microscopy prior to fixation identified no difference in the morphology between mock-treated cells and Bac-SV5A238L treated cells; no cytopathic effect (CPE) was detected in either case. For each replicate in each experiment, 100 cells were counted and the percentage of cells expressing SV5-A238L calculated. Figure 3.9 represents the combined results from 3 independent experiments. From this Figure it can be seen that the proportion of cells expressing SV5-A238L increased in a dose-dependent manner with increasing m.o.i.. High levels of gene transfer of approximately 90 and 85 % were achieved at m.o.i.s of 50 and 100, dropping slightly to approximately 70 % at an m.o.i. of 10. The absence of any visual CPE and high level of transfection efficiency at high m.o.i.s is consistent with previous work investigating baculovirus-mediated gene transfer to mammalian cells (Shoji *et al.*, 1997) and supports the use of this virus vector for gene delivery to porcine macrophage cells. Unfortunately it was not possible to calculate the transfection efficiency of Bac-Sv5A238L to PPAM, due to high levels of background fluorescence observed in mock-inoculated cells.

3.2.7 Comparison of SV5-A238L gene expression between ASFV infected and baculovirus inoculated cells.

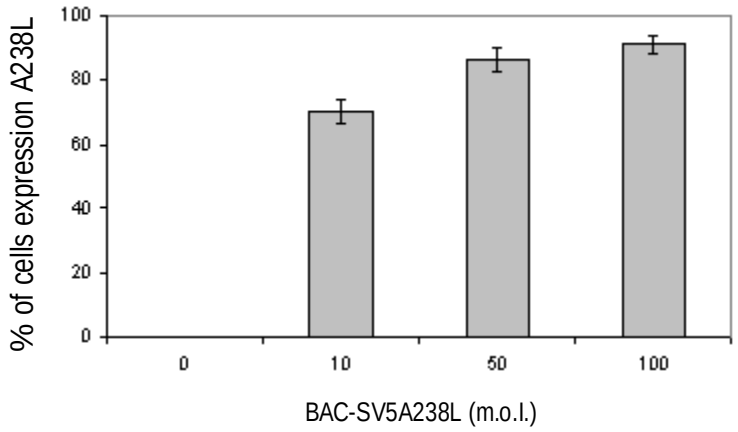

Figure 3.9 Recombinant baculovirus show a high level of transfection efficiency in IPAM cells. IPAM cells were treated with BAC-SV5A238L at the indicated m.o.i.. 16 hrs following treatment the cells were fixed and stained for SV5A238L using an anti-PK antibody followed by an Alexa-488 conjugated goat anti-mouse IgG secondary antibody. The cells were then examined by confocal microscopy and the percent of cells expressing SV5A238L calculated. Data presented is the mean (+/- S.D) of duplicate samples repeated on three separate occasions.

To provide an indication of relative levels of A238L gene expression between cells infected with ASFV or inoculated with Bac-SV5A238L, expression levels were compared between Vero cells infected with a recombinant ASFV which contains a Pk-tagged A238L gene (SV5GaL) (Miskin *et al.*, 1998) and Bac-SV5A238L inoculated IPAM cells using indirect immunofluorescence microscopy. Using this approach it was possible to compare SV5-A238L gene expression within individual cells, rather than the total level of gene expression within the cell population, therefore taking into account differences in infection efficiencies between SV5GaL and Bac-SV5A238L. It was not possible to directly compare levels of A238L gene expression within the same cell line as SV5GaL does not infect IPAM cells. At 16 hrs post-infection cells were fixed and stained for the presence of SV5A238L. Cells infected with ASFV were also stained with rabbit polycolonal antibodies against the late viral protein pE120R (Jouvenet *et al.*, 2004) to identify infected cells. Images were taken at the same brightness and gain to allow comparison between relative expression levels (Figure 3.10). The level of SV5-A238L detected in Vero cells infected with SV5-Gal was extremely low and only just above background level. In contrast images taken of IPAM cells inoculated with Bac-SV5A238L, were considerably brighter indicating a much higher level of gene expression within these cells. This result indicates that A238L gene expression is higher in Bac-SV5A238L transfected cells compared to endogenous level produced in SV5GaL infected cells.

3.3 Discussion

The aim of this chapter was to develop a gene expression and delivery system to produce detectable levels of A238L protein at a high rate of transfection efficiency in porcine alveolar macrophage cells and in a porcine macrophage cell line. This was achieved through the addition of the cis-acting WPRE element into the 3' UTR of the A238L gene, followed by the incorporation of this modified A238L gene into a recombinant baculovirus virus vector.

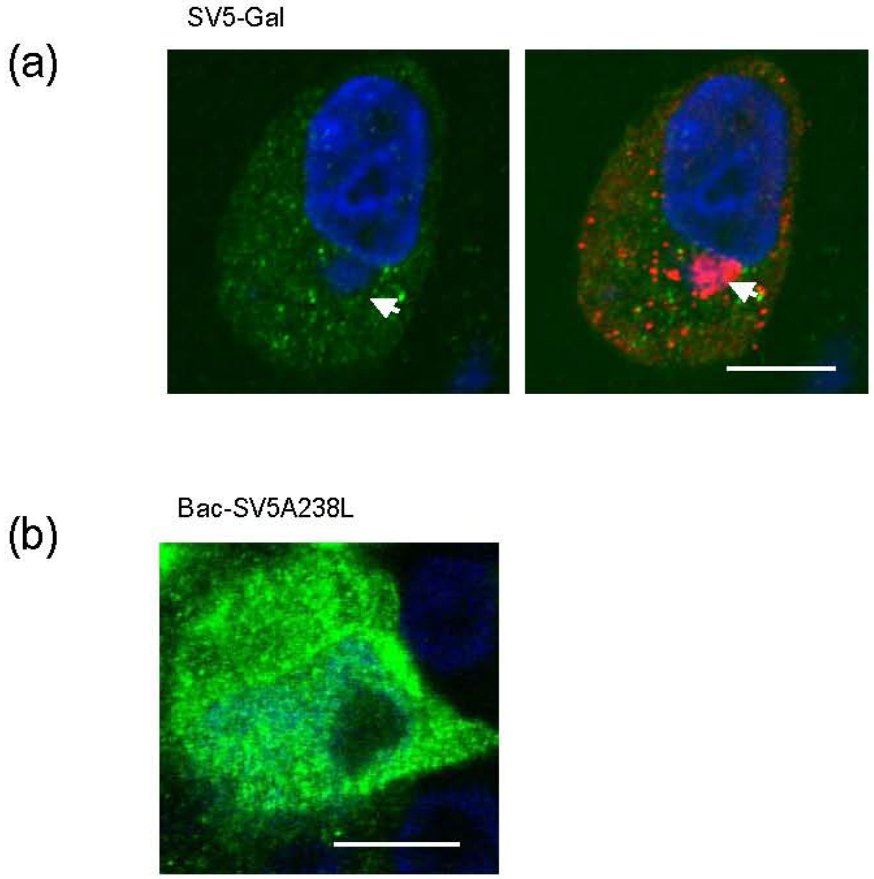

Figure 3.10 SV5-A238L is over expressed using baculovirus mediated gene expression compared to the expression levels in ASFV infected cells. Vero cells (Panel A) with and IPAM cells (Panel B) were infected with SV5-Gal and Bac-SV5A238L, respectively. 16 hrs following infection the cells were fixed and stained. SV5-A238L is shown in green and viral and cellular DNA are blue. ASFV infected Vero cells were also stained for pE120R(red) a late ASFV structural protein. Images shown were collected sequentially using confocal microscopy and then merged. The arrow indicates an ASFV virus factory. Scale bars, 10 µm.

3.1 A238L gene delivery

The WPRE is a viral RNA element which is being increasingly used to enhance the expression of intronless genes which exhibit low levels of gene expression using conventional DNA expression vectors (Callendret *et al.*, 2007; Garg *et al.*, 2004). This element consists of three cis-acting regulatory elements, which are responsible for enhancing the post-transcriptional processing of mRNA and mediating its nuclear export in a CRM-1 dependent and independent manner (Popa *et al.*, 2002; Zufferey *et al.*, 1999). This leads to increased levels of mRNA available for translation and greater protein production. The results presented in this chapter show that the addition of the WPRE to the 3' untranslated region of A238L increased the levels of A238L expressed in transfected cells using the expression vector pcDNA3. This suggests that the expression of A238L, using a mammalian system, is dependent on the efficient nuclear processing and export of A238L mRNA.

Interestingly higher levels of A238L expression were achieved using the pTriEx1.1 expression vector, both with and without the WPRE, than with pcDNA3 encoding A238L and the WPRE. Both of these plasmids utilise RNA polymerase II promoters, however pcDNA3 contains the CMV-IE promoter and pTriEx1.1 contains a hybrid promoter consisting of a CMV immediate early enhancer fused to the chicken β-actin promoter (CAG). pTriEx1.1 also contains a 258 bp intron. Both the CAG promoter and the intron could have contributed to the high levels of A238L gene expression achieved using pTriEx1.1 alone. Composite CMV-IE and B-actin promoters have been shown to drive higher levels of gene expression than the wild type CMV-IE promoter in several other studies (Niwa *et al.*, 1991; Sawicki *et al.*, 1998).

Intron-containing genes can exhibit dramatically different expression profiles, compared to the same gene with the intron removed, when expressed in mammalian systems (Buchman & Berg, 1988). Introns and the act of their removal by the spliceosome can effect gene expression at many levels, including transcription,

polyadenylation, mRNA export, translation efficiency and the rate of mRNA decay (Le Hir *et al.*, 2003). Thus introns and the WPRE have similar roles, in that they can both facilitate mRNA processing and nuclear export. Previous work has shown that the WPRE can compensate for the lack of an intron in the expression of β-globulin using a retroviral vector (Schambach *et al.*, 2000). Thus there may be considerable overlap in function between these elements. It is, therefore, highly likely that the presence of an intron within pTriEx1.1 contributed, in part, to the high level of A238L expression achieved using the pTriEx1.1 expression vector in the absence of the WPRE.

Expression of A238L using pTriEx1.1 was further enhanced by the addition of the WPRE, indicating an additive effect between the WPRE and intron. Synergy between introns and the WPRE has been reported in several studies, where the WPRE has been demonstrated to enhance the expression of both spliced mRNA and unspliced mRNA (Callendret *et al.*, 2007; Popa *et al.*, 2002; Schambach *et al.*, 2000; Zufferey *et al.*, 1999). WPRE RNA and spliced mRNAs use different factors for nuclear export, CRM-1 and TAP respectively, which could explain the ability of these two elements to act in synergy to enhance the level of A238L expression (Stewart, 2007).

Overall the TriEx1.1 expression vector containing the WPRE was considered to be most suitable for the generation of recombinant baculovirus as this plasmid produced the highest levels of A238L gene expression. In addition, recombinant baculovirus containing the target gene under the control of the CAG promoter have been shown previously to achieve gene transfer and expression in porcine cells (Shoji *et al.*, 1997).

3.3.2 A238L gene transfer

Several reports have shown that baculoviruses are useful tools for gene delivery into a number of mammalian cell lines, including porcine kidney cells (Kost & Condreay, 2002). The A238L gene cloned in the pTriEx1.1 vector with the WPRE was used to construct a recombinant baculovirus and the ability of this virus to delivery foreign

genes into immortalised and primary porcine alveolar macrophage cells was tested. Western blot analysis of lysates from cells inoculated with this recombinant baculovirus demonstrated efficient transduction of primary porcine alveolar macrophages and IPAM cells, an observation which has not previously been published. High levels of cell transfection of approximately 85 % and 90 % were observed in the immortalised cell line following inoculation with m.o.i.s of 50 and 100 respectively. These results are consistent with another study demonstrating that baculovirus can deliver genes to 90-100 % of cells at an m.o.i of 100 (Shoji *et al.*, 1997). This study also observed no visible CPE in cells inoculated with bacuovirus, even at m.o.i.s of 100, a result which is consistent with our findings. Unfortunately, it was not possible to obtain an exact measure of the transfection efficiency of the recombinant baculovirus in PPAM. However, it was not considered necessary to pursue these experiments further because the IPAM immortalised porcine alveolar macrophage cell line was selected for the future microarray experiments instead. Use of this cell line should produce more reproducible and statistically significant results by reducing the variability likely from using primary cells.

The level of A238L protein expressed in IPAM immortalised porcine cells transduced with the recombinant baculovirus was higher than in Vero cells infected with the BA71V ASFV isolate. However, for the purpose of this study, high levels A238L expression were preferable as the experimental approach was to produce excess A238L in order to characterise the full range of potential functions of this protein

3.3.3 Conclusion

The data presented in this chapter provide a valuable insight into the possible mechanisms responsible for low levels of A238L expression produced using the expression vector pcDNA3. The results demonstrated that RNA elements involved in the postranscriptional processing and export of mRNA are a key requirement for the expression of A238L using mammalian systems. These observations offer a useful

approach for optimising the expression of other ASFV genes which exhibit low levels of expression using similar systems.

In addition, this chapter also presents a novel approach for the delivery of ASFV genes to both primary and immortalised porcine macrophage cells which has the advantage of achieving a high rate of transfection with virtual absence of cytotoxicity in mammalian cells.

Chapter 4

Optimisation of the microarray experimental design

4.1 Introduction

One of the main aims of this thesis was to investigate the overall effect of A238L on host macrophage gene transcription by using a porcine microarray. Microarray experiments are costly and time consuming to perform and this limits the number of experimental conditions that can be examined. Therefore it was necessary to optimise and carefully select the experimental conditions prior to carrying out the analysis.

A238L is predicted to inhibit gene expression associated with activated immunological signal transduction pathways as discussed previously. This protein has been shown to inhibit the transcriptional activation of several genes involved in the host immune response to infection, including COX-2, TNF-α, inducible nitric oxide synthases (iNOS) and IL-8 (Granja *et al.*, 2004b; Granja *et al.*, 2006d; Powell *et al.*, 1996). Although the exact mechanism of this inhibition has not been fully established, previous work has shown that A238L inhibits the activity of three cellular proteins which are key regulators of signal transduction and gene transcription. These proteins are: the cellular transcription factor NF-κB; calcineurin (CaN) a serine/threonine protein phosphatase and the transcriptional co-activator p300/CBP (Granja *et al.*, 2006d; Miskin *et al.*, 1998; Powell *et al.*, 1996; Revilla *et al.*, 1998). The plan was to investigate the effect of A238L on host gene transcription in IPAM cells which had been treated with lipopolysaccharide (LPS), phorbol 12-myristate 13-acetate (PMA) and ionomycin, compounds which activate signalling pathways involving these transcriptional regulators. LPS activates several intracellular pathways via Toll-like receptor 4 including the IκB kinase (IKK)-NF-κB pathway and three mitogen-activated protein kinase (MAPK) pathways: extracellular signal-regulated kinases (ERK) 1 and 2, c-Jun N-terminal kinase (JNK) and p38 (Guha & Mackman, 2001). PMA activates Protein Kinase C and ionomycin is a calcium ionophore which increases intracellular levels of calcium, resulting in activation

of CaN. Together PMA and ionomycin mimic antigenic stimulation of leukocytes resulting in the transcription of NFAT dependent cytokine and immune response genes (Acuto & Cantrell, 2000; Rao *et al.*, 1997).

Regulation of gene expression is a dynamic process and gene expression profiles can change significantly over short periods of time in response to stimulation. Therefore, selection of the most appropriate conditions and time points to carry out microarray analysis following cell activation is an important consideration in order to produce informative data and biologically relevant results. The use of immortalised cell lines and artificial gene delivery systems (described in chapter 3) to infer the possible functions of A238L in host macrophages has both advantages and disadvantages. It is possible that IPAM cells may behave in an unpredicted manner in response to artificial gene delivery and stimulation. Therefore as a preliminary experiment it would be useful to gain a general overview of the activation state and gene expression profiles produced in IPAM cells without stimulation as well as in response to the experimental conditions alone. This would allow a more complete interpretation of how A238L may act within this system to alter gene expression. There were two main objectives for the experiments described in this chapter. The first objective was to optimise the microarray experimental design. This included the selection of an appropriate time point following A238L gene delivery to stimulate the cells and the selection of appropriate time points following stimulation to analyse gene transcription using microarrays. The second objective was to characterise the effect of baculovirus gene delivery followed by cell stimulation on resting IPAM cells in the absence of A238L gene expression.

4.2 Results

4.2.1 Optimisation of the microarray experimental design.

4.2.1.1 Expression of A238L in baculovirus transfected cell lines.

The previous chapter describes the development of a recombinant baculovirus vector capable of transferring the A238L gene to an immortalised porcine alveolar macrophage cell line, IPAM, at a high level of transfection efficiency. To determine the amount of

A238L protein present in IPAM cells following gene delivery using the baculovirus vector, Bac-SV5A238L, a time course experiment was carried out. IPAM cells were treated with Bac-SV5A238L at an m.o.i. of 50. At various time points post-infection cells lysates were harvested, separated using SDS/PAGE and then blotted onto a nitrocellulose membrane. The membrane was then probed for the presence of SV5-A238L using anti-Pk antibodies and these were detected using HRP conjugated protein A. The blot was then stripped and re-probed with antibodies against α - tubulin to confirm that comparable levels of protein were loaded in each sample.

From Figure 4.1 it can be seen that SV5A238L was detected at a low level from as early as 4 hrs post-infection with Bac-SV5A238L. By 12 hrs post-infection relatively strong levels of SV5A238L could be detected. Therefore 12 hours post Bac-SV5A238L mediated gene delivery was selected as an appropriate time point to stimulate IPAM cells with LPS, PMA and ionomycin.

4.2.1.2 Expression of immune response genes following LPS, PMA and ionomycin treatment of IPAM cells.

Following activation macrophages initiate a rapid transcriptional programme to modulate the hosts immune response. Proinflammatory response genes are activated immediately and these proteins can act to regulate subsequent gene expression. For example IkB-ζ , an immediate early (IE) LPS response gene has been shown to be expressed 30 min following LPS treatment of peritoneal macrophages and is essential for the expression of IL-6. Transcription of IL-6 follows IkB-ζ mRNA transcription by 60 min (Yamamoto *et al.*, 2004). A238L is expressed early during ASFV infection and the A238L protein can be detected as early as 2 hrs post-infection (Tait *et al.*, 2000). Therefore A238L has the potential to regulate host macrophage gene expression during the early phases of an ASFV initiated-macrophage response. Two

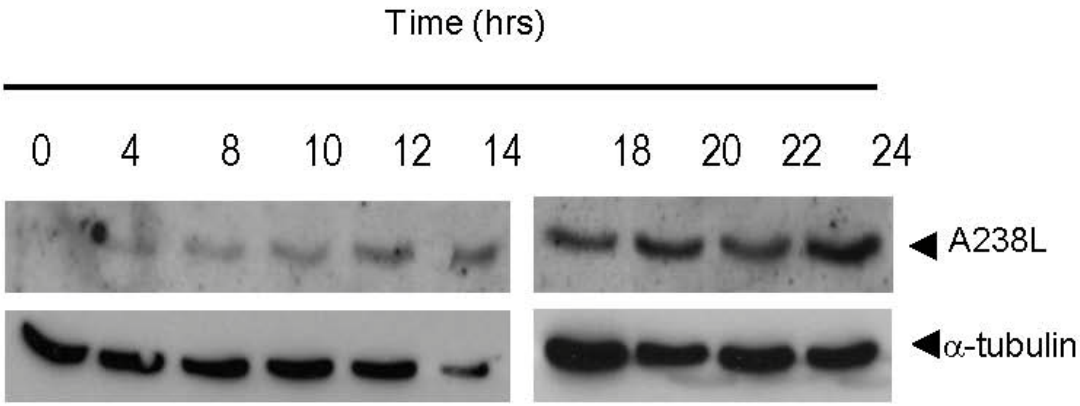

Figure 4.1 A238L is expressed in IPAM cells at early time points following Bac-SV5A238L transfection. IPAM cells were treated with Bac-SV5A238L at an m.o.i 50. Cell lysates were harvested at the indicated time points following infection and analysed by western blot. SV5A238L was detected using an anti-PK mouse monoclonal antibody (Serotec). α-tubulin is shown as a loading control.

early time points were selected, following IPAM activation, to investigate the effects of A238L on host gene transcription using microarray analysis. It was intended that the first time point would reflect changes in immediate gene expression, directly dependent on expression of A238L, and the second time point would reflect subsequent secondary changes in gene expression that occurred as a consequence of the expression of immediate early genes.

To select these time points total RNA was collect from PMA, LPS and ionomycin stimulated and mock-stimulated IPAM cells at 0, 15, 30, 60, 120, 240 min post-stimulation. Concentrations of PMA, LPS and ionomycin used have been reported previously (Miskin *et al.*, 2000a; Powell *et al.*, 1996). mRNA from both stimulated and mock-stimulated samples was reverse transcribed into cDNA using an oligonucleotide dT primer and the resulting cDNAs were then analyzed using semi-quantitative PCR to compare the relative levels of mRNA expression of selected genes between stimulated and mock-stimulated IPAM cells over time. Total RNA samples were treated with DNAse prior to reverse transcription to remove any DNA contamination. In addition, control samples, processed in the absence of reverse transcriptase enzyme, were analysed from selected samples to act as negative controls.

Genes selected for investigation were: TNF-α, IL-8, COX-2, which have previously been shown to be regulated by A238L expression (Granja *et al.*, 2004b; Powell *et al.*, 1996; Revilla *et al.*, 1998) ; IkB-ζ which is an immediate early LPS response gene and IL-6, which is a secondary LPS response gene dependent on IkB-ζ gene expression (Yamamoto *et al.*, 2004). IkB-ζ and IL-6 were selected as indicators for immediate and secondary phase gene transcription. β-actin was also examined as a housekeeping gene which is constituitively expressed.

From the results presented in Figure 4.2 it can be see that β-actin was present at similar levels in all of the samples tested, indicating equal RNA loading between samples. PCR products could be detected in both the mock-stimulated and stimulated IPAM cells for

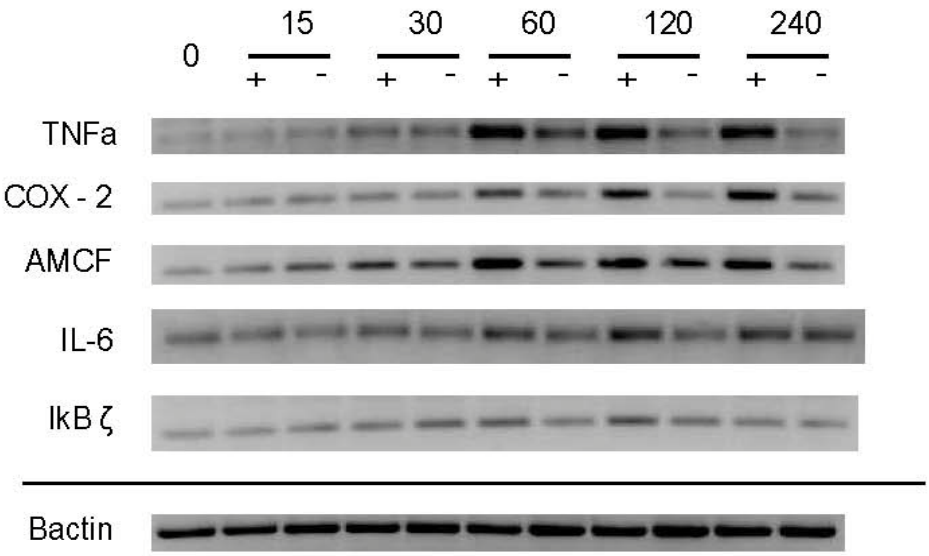

Figure 4.2 Expression profile of immune response genes over time following LPS, PMA and inomycin treatment of IPAM cells. IPAM cell were treated either with (+) or without (-) LPS (100 ng/ml), PMA (100 nM) and ionomycin (4 µm). Total RNA was isolated at 0, 15, 30, 60, 120 and 240 mins after treatment. TNFa, COX-2, AMCF, IL-6, IkB ζ and B-actin mRNA were semi-quantified using RT-PCR. TNFa, COX-2, AMCF, IL-6 and IkB ζ cDNA was amplified using gene specific primers for 15 cycles of PCR and B-actin was amplified for 10 cycles. All PCR products were below the saturation stage of amplification. DNA products were separated by electrophoresis on a 2 % agrose gel and visualised with ethidium bromide. Equal RNA was amplified for each sample as indicated by actin PCR shown below.

all of the samples tested, however relative levels of PCR-product varied between stimulated and mock-stimulated cells for a number of the genes tested.

TNF-α, COX-2 and IL-8 all showed an increase in the amount of mRNA detected in stimulated samples compared to mock-stimulated cells at 60, 120 and 240 minuets post-stimulation. The levels of IL-6 mRNA did appear slightly raised in stimulated samples compared to mock-stimulated controls at 60 and 120 minuets, returning to the level in mock-stimulated samples at 240 min. However, the difference was less pronounced than that seen for TNF-α, COX-2 and IL-8. No difference in the levels of IkB-ζ mRNA could be detected between stimulated and mock-stimulated samples for any of the time points tested using this assay. This was unexpected as previous work has demonstrated that IkBζ mRNA induction precedes and is required for induction of IL-6 expression (Yamamoto *et al.*, 2004).

Due to the small number of genes tested it is difficult to gain an accurate overview of the expression profile of IPAM cells in response to stimulation. However, the results clearly demonstrate that early/immediate gene expression associated with LPS/PMA and ionomycin stimulation can be detected from 60 minuets following treatment. All of the genes tested exhibited low levels of expression even in the absence of LPS, PMA and ionomycin treatment indicating that pathways associated with the expression of these genes may be constitutively activated in IPAM cells. No changes in the expression profile of the selected genes could be detected at 4 hrs compared to the other time points tested, which is undoubtedly due to the small number of genes examined. On the basis of these results and previously published data, which demonstrated a significant difference in the gene expression profile of whole blood leukocytes at 4 hrs post LPS stimulation compared to earlier time points (Boldrick *et al.*, 2002; Calvano *et al.*, 2005), 1 hr and 4 hr time points post LPS, PMA and ionomycin stimulation were selected for analysis in microarray experiments.

4.2.2 Microarray analysis of the effect of cell stimulation and baculovirus treatment on gene transcription profiles in IPAM cells

4.2.2.1 Microarray analysis

Two porcine microarrays were available for this study. A cDNA microarray containing 2,880 genes, known as Pig 3K Immune cDNA and an oligonucleotide array containing the Operon *Sus scrofa* (pig) v1.0 and *Sus scrofa* (pig) extension Array-Ready Oligo Sets^{TM}. The Pig 3K Immune cDNA is specifically targeted at investigating genes associated with the immune response (Zhang *et al.*, 2006b). The Operon *Sus scrofa* (pig) v1.0 and *Sus scrofa* (pig) extension Array-Ready Oligo Sets^{TM}, consists of 13,297, 70-mer oligonucleotides representing all known *Sus scrofa* gene sequences with a hit to human, mouse, or pig gene transcripts and a number of sequences containing a 3' expressed sequence Tag (EST) (Operon). Genes present on the Pig 3K Immune cDNA but not detected in the Operon oligonucleotide sets were also included on this array. The Operon array was selected for this investigation as it contained a larger and more diverse set of probes not restricted to a specific cellular response, and therefore more appropriate to investigate the global effect of A238L on host cell transcription.

To examine the effect of baculovirus treatment in combination with cell stimulation on untreated IPAM cells in the absence of A238L gene expression, gene expression profiles between cells treated with the control baculovirus vector (Bac-WPRE) and stimulated with LPS, PMA and Ionomycin (C) were compared directly against a reference pool of RNA collected from non-stimulated IPAM cells (CR) (Figure 4.3). This experiment was carried out in parallel with the experiment described in chapter 5. Three independent experiments were carried out. IPAM cells were treated with control baculovirus not expressing the A238L gene (Bac-WPRE) at an m.o.i. 50. 12 hours following baculovirus treatment the cells were stimulated with LPS, PMA and Ionomycin. At 1 and 4 hours post-stimulation total RNA was isolatedand mRNA was amplified to produce antisense RNA.

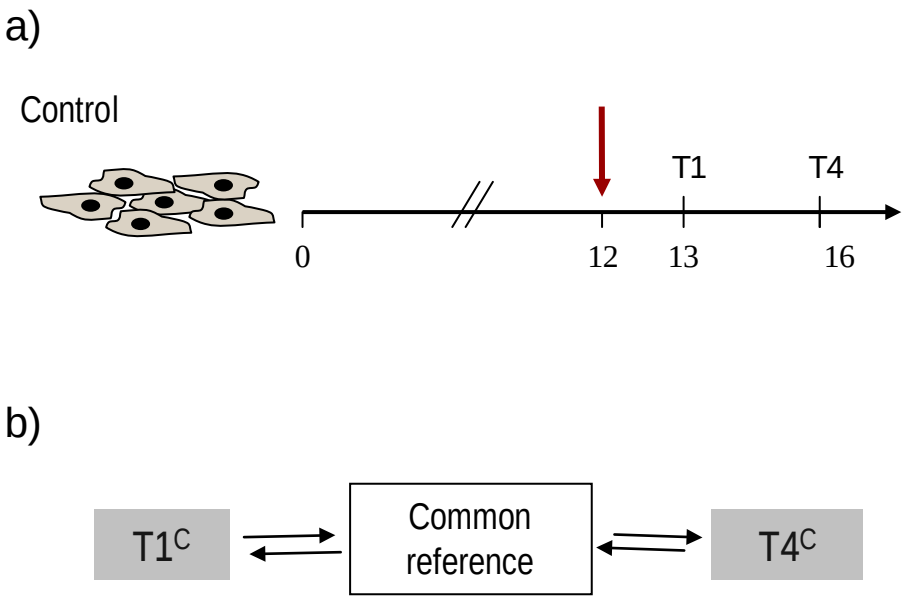

Figure 4.3 Schematic representation of the microarray experimental design used investigate the effect of baculovirus treatment, and LPS, PMA and ionomycin stimulated on untreated IPAM cells. Panel A) Experimental procedure: IPAM cells were infected with Bac-WPRE (control) at an moi 50. 12 hours following baculovirus treatment the cells were stimulated with LPS (100μg/ml), PMA (100 nM) and Ionomycin (4 μM). 1 hr (T1) and 4 hrs (T4) following stimulation total RNA was harvested, amplified and labeled with either Cy3 or Cy5 fluoresent dyes. The horizontal arrow represents the time line post baculovirus treatment. Panel B) Microarray experimental design. Control samples were compared indirectly against a common reference pool of un-stimulation IPAM RNA. Amplified mRNA from each sample and the common reference was labeled with either Cy3 or Cy5 fluoresent dyes. Each sample was then co-hybridised onto a separate porcine oligo arrays (operon) against the common reference sample in the opposite channel. Three biological replicates were carried out for each experimental condition, with a dye swap for each biological replicate.

Equal quantities of test and control samples, labeled with either Cy3 or Cy5 were combined and co-hybridised onto the Operon *Sus scrofa* (pig) v1.0 and *Sus scrofa* (pig) extension Oligo^{TM} microarray (Operon). Two hybridisations were carried out for each comparison, with the dye assignments reversed in the second hybridisation to account for labeling bias between dyes. Images of the hybridised arrays were obtained by laser confocal scanning. Raw image files were processed to extract feature information and remove background noise and artifacts using BlueFuse for microarrays software. Processed data files were then analysed using software tools from the TM4 microarray software suite; Microarray Data Analysis System (MIDAS) and Multiexperiment Veiwer (MeV) (Saeed *et al.,* 2006). Prior to statistical analysis the total data set was filtered to remove poor quality features. This resulted in a final data set from 10146 oligonucleotides out of an original total of 13657 unique oligonucleotides.

Significant Analysis of Microarrays (SAM) analysis was used to identify differentially regulated genes. This is a statistical method specifically adapted to analyse large amounts of data present in microarray data sets (Tusher *et al.,* 2001).

One and four hour data sets were analysed independently using a one class SAM analysis. The results from this analysis are presented in Figure 4.5 and 4.6. At 1 hr post-stimulation a total of 1277 (13%) unique oligonucleotides were identified as hybridising to RNAs that were significantly differentially regulated by baculovirus and LPS, PMA and ionomycin treatment, 11.12 of these oligonucleotides were estimated to be falsely significant (FDR 0.89%). 918 (9%) of these oligonucleotides hybridised to RNAs that were predicted to be significantly up-regulated and 359 (4%) oligonucleotides hybridised to RNAs that were predicted to be significantly down-regulated. Therefore at this time point a greater proportion of the oligonucleotides hybridised to RNAs that were significantly up-regulated. At 4hr post stimulation 797 (8%) oligonucleotides were identified as hybridising to RNAs that were significantly differentially regulated, 21 of these were estimated to be falsely significant (FDR 2.67%). 69 (1%) of these

oligonucleotides were shown to be hybridised to RNAs that were significantly up-regulated, the remaining 728 (7%) oligonucleotides were hybridised to RNAs that were significantly down-regulated. Therefore the majority of the oligonucleotides that were identified as hybridising to RNAs that were significantly differentially regulated at 4 hrs, hybridised to RNAs that were significantly down-regulated, in direct contrast to the results presented for the 1 hr time point. This indicates a suppression of differentially regulated gene transcription at 4 hrs post LPS, PMA and ionomycin treatment.

To examine the effect of baculovirus, LPS, PMA and ionomycin treatment on untreated IPAM cells, across both time points, the lists of oligonucleotides identified as differentially regulated by BacWPRE, LPS, PMA and ionomycin treatment (compared to untreated IPAM cells) at both 1 and 4 hrs were combined. This resulted in a final list of 1757 unique oligonucleotides that hybridised to differentially regulated RNAs at either or both 1 and 4 hrs post-stimulation. 952 (55 %) of these oligonucleotides hybridised to RNAs that were differentially regulated at 1 hr post-stimulation but not at 4 hrs, 306 (17 %) oligonucleotides intersected both time points and therefore hybridised to RNAs that were differentially regulated at both 1 and 4 hrs post-stimulation and 488 (27 %) oligonucleotides hybridised to RNAs differentially regulated at 4 hrs post-stimulation only. These results are represented as a Venn diagram in Figure 4.7. Individual oligonucleotides within each of these groups were then sorted into categories based on

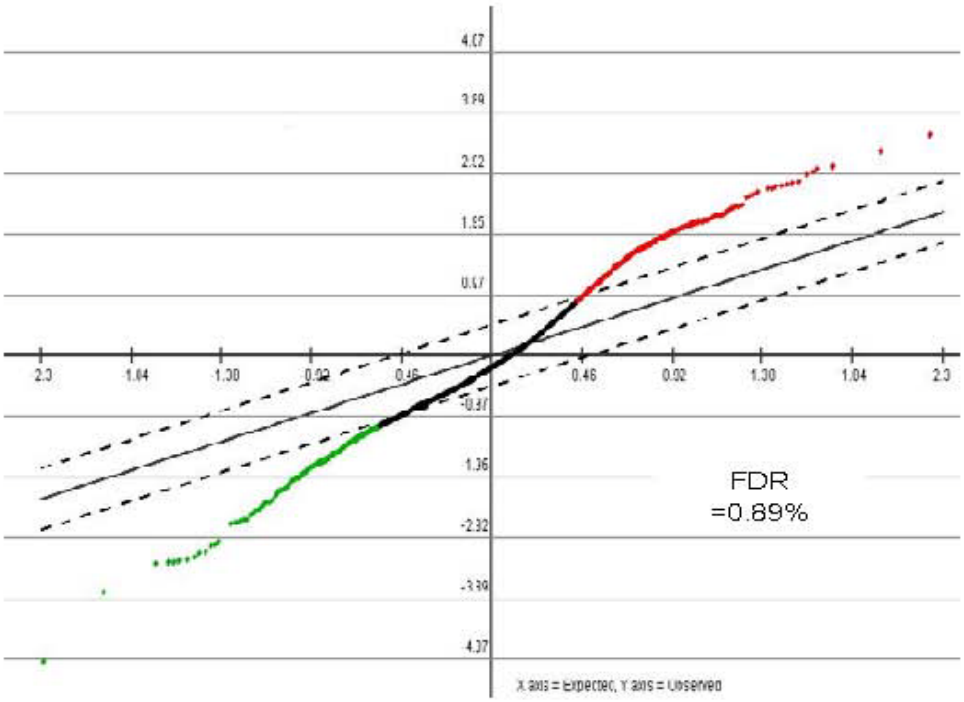

Positive Significant Genes	# of Positive Significant Genes: 918 % of Positive Significant Genes: 9%
Negative Significant Genes	# of Negative Significant Genes: 359 % of Negative Significant Genes: 4%
All Significant Genes	Total # of Significant Genes: 1277 % of Genes that are Significant: 13%
Non-Significant Genes	Total # of Non-Significant Genes: 8869 % of Genes that are Not Significant: 87%

Figure 4.5 Identification of genes significantly regulated by Bac-WPRE and LPS, PMA and ionomycin treatment at 1 hour post stimulation, using SAM. A scatter plot of the observed relative difference between control and test samples *d(i)* (Y axis), versus the expected relative difference *dE(i)*(X axis), calculated using a one class paired Significant Analysis of Microarrays (SAM) analysis. The solid line indicates the line for *d(i)= dE(i)*, where the observed relative difference is identical to the expected relative difference. The dotted lines are drawn at a distance of $\delta = 0.498$ from the solid line (the selected threshold for this analysis), values above (red) or below (green) this threshold are considered to be significantly regulated by A238L gene expression. The False Discovery Rate (FDR) based on $\delta = 0.498$, is presented on this graph and a summary of the results is shown below the scatter plot.

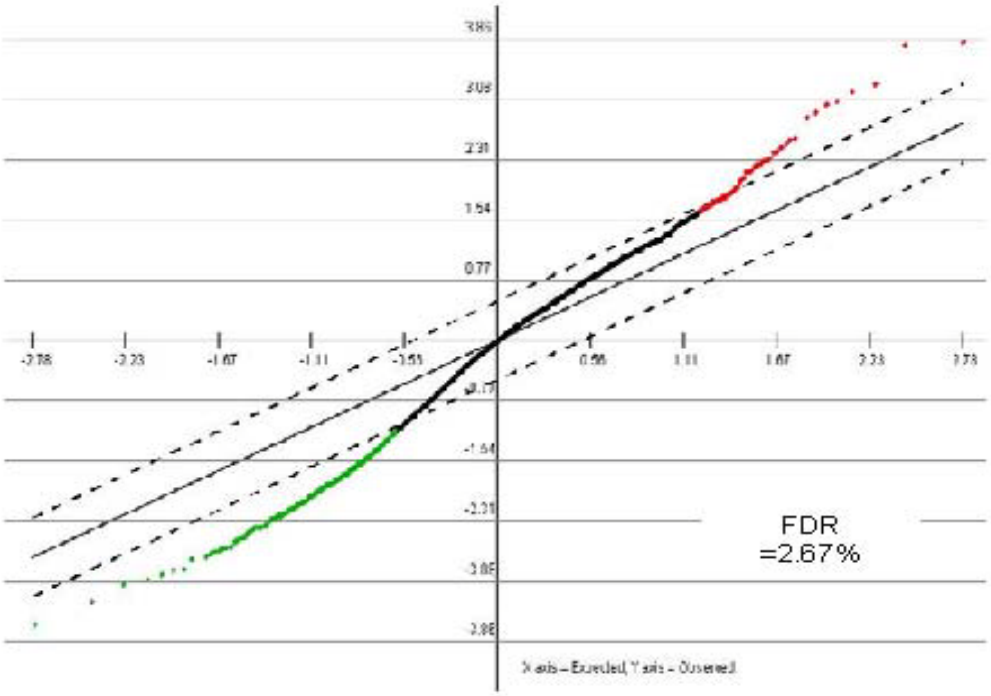

Positive Significant Genes	# of Positive Significant Genes: 69 % of Positive Significant Genes: 1%
Negative Significant Genes	# of Negative Significant Genes: 728 % of Negative Significant Genes: 7%
All Significant Genes	Total # of Significant Genes: 797 % of Genes that are Significant: 8%
Non-Significant Genes	Total # of Non-Significant Genes: 9349 % of Genes that are Not Significant: 92%

Figure 4.6 Identification of genes significantly regulated by Bac-WPRE and LPS, PMA and ionomycin treatment at 4 hours post stimulation, using SAM. A scatter plot of the observed relative difference between control and test samples *d(i)* (Y axis), versus the expected relative difference *dE(i)*(X axis), calculated using a one class paired Significant Analysis of Microarrays (SAM) analysis. The solid line indicates the line for *d(i)= dE(i)*, where the observed relative difference is identical to the expected relative difference. The dotted lines are drawn at a distance of $\delta = 0.498$ from the solid line (the selected threshold for this analysis), values above (red) or below (green) this threshold are considered to be significantly regulated by A238L gene expression. The False Discovery Rate (FDR) based on $\delta = 0.498$, is presented on this graph and a summary of the results is shown below the scatter plot.

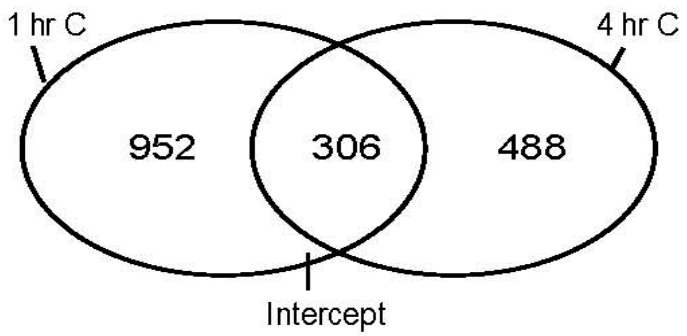

Figure 4.7 Venn diagram representing the relationship between oligonucleotides identified as differentialy regulated by baculovirus, LPS, PMA and ionomycin vs untreated IPAM cells at 1 and 4 hrs post stimulation. Group 1 (1hr C) represent all of the oligonucleotides differentially regulated at 1 hr. Group 2 (4 hrs C) represents all of the oligonucleotides differentially at 4 hrs. The intercept represents oligonucleotides common to both groups.

their regulation profiles. This resulted in the formation of a total of 8 separate clusters exhibiting different expression profiles. Graphical representation of the expression profiles of these clusters are presented in Figure 4.8. Cluster 1 contained 296 (16.8%) oligonucleotides that hybridised to RNAs that are significantly down-regulated at 1 hr post-stimulation returning to normal levels at 4 hrs post-stimulation. Cluster 2 contained 656 (37.5 %) oligonucleotides that hybridised to RNAs that were significantly up-regulated at 1 hr post stimulation but not significantly altered at 4 hrs post-stimulation. Cluster 3 contained 36 (2 %) oligonucleotides that hybridised to RNAs that were significantly down-regulated at 1 hr post -stimulation but up regulated at 4 hrs post-stimulation. Cluster 4 contained 23 (1.3 %) oligonucleotides that hybridised to RNAs that were significantly down-regulated at both 1 and 4 hrs post-stimulation. Cluster 5 contained 16 (1 %) oligonucleotides that hybridised to RNAs that were significantly up-regulated at both 1 and 4 hrs post-stimulation. Cluster 6 contained 239 (13.6 %) oligonucleotides that hybridised to RNAs that were significantly up-regulated at 1 hr post-stimulation but down-regulated at 4 hrs post stimulation. Cluster 7 contained 21 (1.2 %) oligonucleotides that hybridised to RNAs that are not significantly regulated at 1 hr post-stimulation but significantly up-regulated at 4 hr post-stimulation and Cluster 8 contained 467 (26.6 %) oligonucleotides that that are not significantly regulated at 1 hr post-stimulation but are significantly down-regulated at 4 hr post-stimulation.

Overall these results demonstrate that baculovirus treatment followed by LPS, PMA and inomycin stimulation leads to a profound and rapid effect on the gene expression profile of IPAM cells. The majority of oligonucleotides hybridised to RNAs that did not significantly alter during the conditions tested. The majority of the remaining oligonucleotides hybridised to differentially regulated RNAs that were significantly up-regulated at 1 hr post-stimulation and/or significantly down regulated at 4 hrs post stimulation, indicating that strong negative regulation of gene transcription occurs following the initial activation phase. A relatively small proportion of the oligonucleotides that hybridised to differentially regulated RNAs hybridised to RNAs that were differentially regulated at both time points (17 %). Significantly, the majority

of these oligonucleotides (13.6 %) hybridised to RNAs that were up-regulated at 1hr but down regulated at 4hrs post-stimulation, consistent with the overall expression profile exhibited by these cells.

4.2.2.2 Functional classification of differentially-regulated genes

Annotation was available for 1273 of the 1721 oligonucleotides which hybridised to differentially regulated RNAs. A number of genes were targeted by several different oligonucleotides, therefore, after editing to remove redundancy, a final list of 971 annotated genes was produced. A total gene list of differentially regulated genes along with their expression profiles can be found at Appendix 2.

Due to the large number of genes identified as differentially regulated by the test conditions, the gene lists were analyzed using the Database for Annotation, Visualisation and Intergrated Discovery (DAVID) 2008 (Dennis *et al.*, 2003) to identify significantly enriched terms associated with biological processes and signaling networks. Using this approach, Gene-GO term enrichment analysis and KEGG pathway analysis was used to identify and cluster functionally related genes according to their biological processes/molecular function and relevant signaling networks respectively. GO annotations, designated by the gene ontology consortium, provide a controlled vocabulary to describe the attributes of a gene product in any organism. This is based on the concept that a large proportion of the genes involved in core biological functions are shared by all eukaryotes. Genes are characterised using three structured vocabularies (or ontologies): molecular function, biological process and cellular component (Consortium, 2006; Harris *et al.*, 2004). KEGG PATHWAY is a knowledge base for the systematic analysis of gene functions linking genomic information with higher order functional information. It provides graphical information on cellular processes such as metabolism, signal transduction and the cell cycle (Kanehisa *et al.*, 2008).

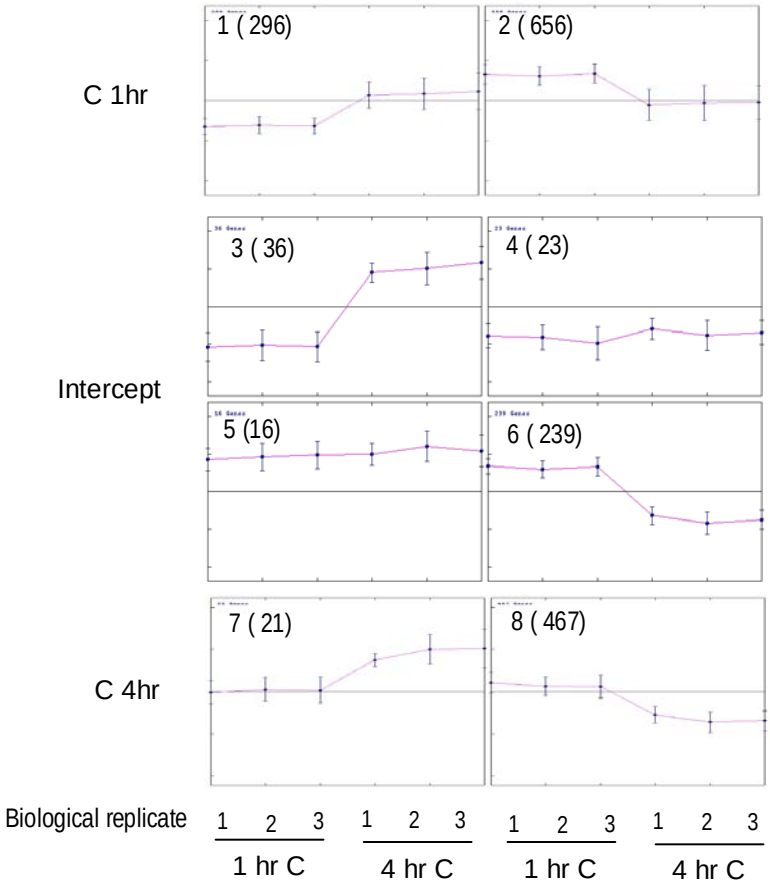

Figure 4.8 Overview of the expression profiles of oligos identified as hybridising to RNAs differential regulated by Bac-WPRE, PMA, LPS and ionomycin treatment. Expression graphs of individual clusters of oligos exhibiting different expression profiles. The number within each graph represents the cluster identifier followed by the number of oligos present within this cluster in brackets. The x-axis is centred (y=0) on the y axis and represents each biological replicate at 1 and 4 hrs post stimulation. The y axis represents the mean expression levels of all the oligos in the cluster (log2). Error bars represent the standard deviation of expression within the cluster.

A summary of the results obtained for Gene GO term enrichment analysis is presented in Table 4.1. From this Table it can be seen that similar biological themes were represented at both 1 and 4 hrs following LPS, PMA and ionomycin treatment. At 1 hr these themes were generally associated with up-regulated genes and at 4 hrs with down-regulated genes. A summary of genes associated with several of the major biological themes identified by GO term analysis, along with their expression profiles is presented in Table 4.2.

Macrophages are phagocytic cells that act through direct cell to cell contact or through the secretion of a wide array of immunoregulatory products. As a consequence of this, a considerable amount of energy is devoted to the synthesis and processing of proteins with immunomodulatory functions and the molecules involved in their production. Overall the most significantly enriched biological themes included; intracellular macromolecule transport; chromosomal organisation and biogenesis; intracellular signal transduction and genes associated with the regulation of cell proliferation and apoptosis. A considerable number of regulated genes were involved in protein biosynthesis, ranging from the manipulation of chromatin structure (to allow access of transcription factors) to the processing and movement of nanset polypeptide chains through the secretary pathway. Proteins involved in endocytosis, phagocytosis, cell adhesion and communication, and immune response genes were also enriched. This is consistent with the biological function of monocytic cells.

Immune response genes

A number of inflammatory response genes were identified as differentially regulated following baculovirus, LPS, PMA and ionomycin treatment and included chemokines, cytokines, cytokine receptors and interferon inducible proteins. These genes included granulocyte macrophage-colony stimulating factor (GM-CSF), IL-1α, IL-6, macrophage inflammatory protein MIP-2α and IL- 2 receptor, gamma (IL-2R γ) and interferon (alpha, beta and omega) receptor (IFNR1). IFN inducible genes included interferon-induced protein 44 and guanylate binding protein 2 (GBP-2).

GO: Biological response	1 hr C		4 hrs C	
	Up	Down	Up	Down
Intracellular transport	**37**	**23**	**6**	**56**
Intracellular protein transport	29	14		50
Protein nuclear transport	13			19
Secretary pathway	7	6		12
Endocytosis	12	4		3
Cytoskeleton-dependent transport	4	3		3
RNA transport	9		3	13
Chromosomal organisation and biogenesis	**31**	**5**		**32**
Chromatin and nucleosome assembly	24			26
Nucleotide biosynthesis process	**10**	**8**		**15**
Purine	4			8
RNA	3			6
Protein biosynthesis				
Amino acid synthesis	7			11
tRNA synthesis and metabolic process	5			5
Translation	21			26
Intracellular signalling cascades	**71**			**66**
Regulation of the cell cycle	**34**	**24**	**6**	**52**
Regulation of programmed cell death	22	4	6	30
Mitosis	9	5		11
Lipid biosynthetic process	**8**			
Membrane lipid biosynthesis	5	15		
Fatty acid metabolism		4		
Immune cell differentiation	**7**			**8**
Acute inflammatory response				**4**
Cell matrix adhesion	**7**			
Angiogenesis	**5**			**9**
Wound healing/blood coagulation	**3**			**3**
Regulation of cell migration	**5**			**8**
Cell projection morphogenesis	**2**		**5**	**7**

Table 4.1 Numbers of genes associated with significantly enriched biological themes in baculovirus treated IPAM cells at 1 and 4 hrs post LPS, PMA and ionomycin treatment. Go term enrichment analysis using DAVID functional annotation software (EASE Score p <=0.1) was used to identify biological enriched themes within annotated gene lists of differentially regulated genes at both 1 (1 hr S) and 4 hrs (4 hr S) post LPS, PMA and ionomycine treatment. The results represent the number of differential regulated genes associated with each biological term for the conditions listed. Results associated with up-regulated are in dark red and down regulated gene results are in black.

Table 4.2 Biological characterisation of selected genes regulated by baculovirus, LPS, PMA and ionomycin treatment

Accession	Description	1 hr (log_2 fold change)		4 hrs (log_2 fold change)	
Transcription and mRNA processing					
NM_015425	polymerase (RNA) I polypeptide A, 194kDa (POLR1A), mRNA	0.52	(0.48 , 0.57)	-0.85	(-1 , -0.71)
NM_018082	polymerase (RNA) III (DNA directed) polypeptide B (POLR3B), mRNA	0.45	(0.23 , 0.66)	-0.47	(-0.64 , -0.29)
NM_004229	cofactor required for Sp1 transcriptional activation, subunit 2, 150kDa (CRSP2), mRNA			-0.68	(-0.92 , -0.44)
NM_004380	CREB binding protein (Rubinstein-Taybi syndrome) (CREBBP), mRNA			-0.56	(-0.9 , -0.22)
NM_006079	Cbp/p300-interacting transactivator	0.99	(0.61 , 1.37)		
NM_006662	Snf2-related CBP activator protein (SRCAP), mRNA	-0.53	(-0.73 , -0.34)		
NM_003185	TAF4 RNA polymerase II, TATA box binding protein (TBP)-associated factor (TAF4)			-0.43	(-0.52 , -0.35)
NM_006044	histone deacetylase 6 (HDAC6), mRNA	1.01	(0.88 , 1.13)		
NM_016596	histone deacetylase 7A (HDAC7A), transcript variant 2, mRNA	0.68	(0.64 , 0.73)		
NM_014707	histone deacetylase 9 (HDAC9), transcript variant 3, mRNA	0.79	(0.57 , 1)		
NM_015885	pre-mRNA cleavage complex II protein Pcf11 (PCF11), mRNA	0.56	(0.27 , 0.84)		
NM_004768	splicing factor, arginine/serine-rich 11 (SFRS11), mRNA	0.42	(0.31 , 0.54)		
NM_014884	splicing factor, arginine/serine-rich 14 (SFRS14), mRNA			-0.66	(-1.03 , -0.29)
NM_006275	splicing factor, arginine/serine-rich 6 (SFRS6), mRNA	0.67	(0.56 , 0.78)		
NM_013291	cleavage and polyadenylation specific factor 1, 160kDa (CPSF1), mRNA	0.77	(0.53 , 1.01)		
Translation					
NM_001961	eukaryotic translation elongation factor 2 (EEF2), mRNA	0.47	(0.36 , 0.58)		
NM_004094	eukaryotic translation initiation factor 2, subunit 1 alpha, 35kDa (EIF2S1), mRNA	-0.55	(-0.65 , -0.46)		
NM_012199	eukaryotic translation initiation factor 2C, 1 (EIF2C1), mRNA	0.82	(0.49 , 1.16)		
NM_003758	eukaryotic translation initiation factor 3, subunit 1 alpha, 35kDa (EIF3S1), mRNA	0.43	(0.3 , 0.56)	-0.49	(-0.74 , -0.23)
NM_001568	eukaryotic translation initiation factor 3, subunit 6 48kDa (EIF3S6), mRNA	0.51	(0.32 , 0.69)		
NM_198244	eukaryotic translation initiation factor 4 gamma, 1 (EIF4G1), transcript variant 3, mRNA			-0.48	(-0.65 , -0.31)
NM_001418	eukaryotic translation initiation factor 4 gamma, 2 (EIF4G2), mRNA	0.73	(0.64 , 0.82)		
NM_003760	eukaryotic translation initiation factor 4 gamma, 3 (EIF4G3), mRNA	0.62	(0.4 , 0.83)	-0.65	(-1.2 , -0.1)

Continued on next page

Table 4.2 - continued

Accession	Description	1 hr (log_2 fold change)		4 hrs (log_2 fold change)	
NM_004846	eukaryotic translation initiation factor 4E member 2 (EIF4E2), mRNA	0.76	(0.44 , 1.07)	-0.65	(-1.16 , -0.14)
NM_001969	eukaryotic translation initiation factor 5 (EIF5), transcript variant 1, mRNA			-0.44	(-0.59 , -0.3)
NM_020117	leucyl-tRNA synthetase (LARS), mRNA	0.43	(0.33 , 0.53)	-0.48	(-0.7 , -0.27)
NM_006295	valyl-tRNA synthetase 2 (VARS2), mRNA	1.13	(0.86 , 1.4)	-1.14	(-1.6 , -0.69)
NM_001605	alanyl-tRNA synthetase (AARS), mRNA			-0.79	(-1 , -0.58)
Protein transport					
NM_002267	karyopherin alpha 3 (importin alpha 4) (KPNA3), mRNA	0.54	(0.06 , 1.02)	-0.51	(-0.69 , -0.33)
NM_024658	importin 4 (IPO4), mRNA	0.66	(0.5 , 0.82)		
NM_018085	importin 9 (IPO9), mRNA	0.64	(0.26 , 1.03)		
NM_018230	nucleoporin 133kDa (NUP133), mRNA	0.45	(0.31 , 0.6)		
NM_017921	nuclear protein localization 4 (NPL4), mRNA	-1.2	(-1.56 , -0.84)		
Secretary pathway					
NM_016128	coatomer protein complex, subunit gamma (COPG), mRNA			-0.62	(-0.96 , -0.28)
NM_006464	trans-golgi network protein 2 (TGOLN2), mRNA			-0.61	(-1.01 , -0.21)
NM_138619	golgi associated, gamma adaptin ear containing, ARF binding protein 3 (GGA3)	0.98	(0.57 , 1.39)	-1.08	(-1.51 , -0.64)
NM_007357	component of oligomeric golgi complex 2 (COG2), mRNA	-0.66	(-0.77 , -0.55)	0.84	(0.44 , 1.25)
NM_005194	CCAAT/enhancer binding protein (C/EBP), beta (CEBPB), mRNA	-0.59	(-0.96 , -0.22)	-0.58	(-0.67 , -0.5)
NM_016042	exosome component 3 (EXOSC3), transcript variant 1, mRNA	-0.53	(-0.63 , -0.43)		
NM_015219	exocyst complex component 7 (EXOC7), mRNA	-0.63	(-0.8 , -0.47)		
NM_006854	KDEL (Lys-Asp-Glu-Leu) endoplasmic reticulum protein retention receptor 2 (KDELR2)	-0.47	(-0.58 , -0.36)		
NM_004910	phosphatidylinositol transfer protein, membrane-associated 1 (PITPNM1), mRNA	1.06	(0.74 , 1.38)		
Endocytic pathway					
NM_014045	low density lipoprotein receptor-related protein 10 (LRP10), mRNA	0.49	(0.4 , 0.58)		
NM_014608	cytoplasmic FMR1 interacting protein 1 (CYFIP1), mRNA	0.7	(0.48 , 0.92)	-0.73	(-1.26 , -0.19)

Continued on next page

Table 4.2 - continued

Accession	Description	1 hr (log_2 fold change)		4 hrs (log_2 fold change)	
NM_024712	engulfment and cell motility 3 (ced-12 homolog, C. elegans) (ELMO3), mRNA	0.54	(0.22 , 0.85)		
NM_004945	dynamin 2 (DNM2), transcript variant 3, mRNA	0.43	(0.31 , 0.56)		
NM_033104	stonin 2 (STN2), mRNA	0.89	(0.55 , .24)		
Cell projection and morphogenesis					
NM_006614	cell adhesion molecule with homology to L1CAM (close homolog of L1) (CHL1), mRNA	0.72	(0.16 , 1.29)		
NM_002291	laminin, beta 1 (LAMB1), mRNA	0.77	(0.22 , 1.31)		
NM_000210	integrin, alpha 6 (ITGA6), mRNA			-0.53	(-0.82 , -0.24)
NM_030884	microtubule-associated protein 4 (MAP4), transcript variant 2, mRNA			-0.69	(-1.04 , -0.35)
NM_003980	microtubule-associated protein 7 (MAP7), mRNA	0.42	(0.31 , 0.53)		
NM_002373	microtubule-associated protein 1A (MAP1A), mRNA	-0.52	(-0.7 , -0.35)		
Cell adhesion / migration					
NM_001627	activated leukocyte cell adhesion molecule (ALCAM), mRNA	0.82	(0.66 , 0.98)		
NM_000210	integrin, alpha 6 (ITGA6), mRNA			-0.53	(-0.82 , -0.24)
NM_000201	intercellular adhesion molecule 1 (CD54), human rhinovirus receptor (ICAM1), mRNA			-0.5	(-0.58 , -0.42)
NM_000419	integrin, alpha 2b (antigen CD41B) (ITGA2B), mRNA			-0.85	(-1.21 , -0.5)
NM_002859	paxillin (PXN), mRNA			-0.6	(-0.97 , -0.23)
NM_002291	laminin, beta 1 (LAMB1), mRNA	0.77	(0.22 , 1.31)		
NM_002210	integrin, alpha V (vitronectin receptor, alpha polypeptide, antigen CD51) (ITGAV), mR	0.75	(0.49 , 1.01)		
NM_006614	cell adhesion molecule with homology to L1CAM (close homolog of L1) (CHL1), mRNA	0.72	(0.16 , 1.29)		
NM_001901	connective tissue growth factor (CTGF), mRNA	0.62	(0.44 , 0.81)		
NM_002291	laminin, beta 1 (LAMB1), mRNA	0.61	(0.39 , 0.82)		
NM_001305	claudin 4 (CLDN4), mRNA	-0.46	(-0.52 , -0.41)		
NM_002444	moesin (MSN), mRNA	0.46	(0.21 , 0.7)	-0.61	(-0.9 , -0.32)
NM_181351	neural cell adhesion molecule 1 (NCAM1), mRNA	0.44	(0.26 , 0.63)	-0.83	(-1.26 , -0.39)
NM_004162	RAB5A, member RAS oncogene family (RAB5A), mRNA	0.78	(0.69 , 0.86)		

Continued on next page

Table 4.2 - continued

Accession	Description	1 hr (log_2 fold change)		4 hrs (log_2 fold change)	
NM_000211	integrin, beta 2 (antigen CD18 (p95), lymphocyte function-associated antigen 1(ITGB2)	-0.71	(-1.35 , -0.07)		
Cell surface receptors					
NM_014452	tumor necrosis factor receptor superfamily, member 21 (TNFRSF21), mRNA	0.92	(0.66 , 1.18)		
NM_002447	macrophage stimulating 1 receptor (c-met-related tyrosine kinase) (MST1R), mRNA	0.82	(0.66 , 0.98)	-1.16	(-1.57 , -0.74)
NM_002856	poliovirus receptor-related 2 (herpesvirus entry mediator B) (PVRL2), mRNA	0.67	(0.48 , 0.85)		
NM_058172	anthrax toxin receptor 2 (ANTXR2), mRNA	0.56	(0.34 , 0.79)		
NM_002856	poliovirus receptor-related 2 (herpesvirus entry mediator B) (PVRL2), mRNA	0.4	(0.3 , 0.5)		
Coagulation/complement					
NM_003246	thrombospondin 1 (THBS1), mRNA	1.63	(1.19 , 2.07)		
NM_000014	alpha-2-macroglobulin (A2M), mRNA	1.34	(1.21 , 1.46)		
NM_000313	protein S (alpha) (PROS1), mRNA	0.51	(0.43 , 0.6)	0.71	(0.53 , 0.88)
NM_002659	plasminogen activator, urokinase receptor (PLAUR)	-0.71	(-0.81 , -0.61)	-0.52	(-0.7 , -0.34)
NM_000186	complement factor H (CFH), mRNA	0.69	(0.52 , 0.85)		
Immune response					
NM_004705	protein-kinase, interferon-inducible double stranded RNA dependent inhibitor, repress	0.53	(0.46 , 0.61)		
NM_006820	interferon-induced protein 44 (IFI44L), mRNA	0.92	(0.77 , 1.06)		
NM_004120	guanylate binding protein 2, interferon-inducible (GBP2), mRNA	0.53	(0.29 , 0.77)		
NM_000575	interleukin 1, alpha (IL1A), mRNA	-1.48	(-1.72 , -1.24)		
NM_000758	colony stimulating factor 2 (granulocyte-macrophage) (CSF2), mRNA	-1.21	(-1.57 , -0.86)	-1.11	(-1.37 , -0.85)
NM_000206	interleukin 2 receptor, gamma (IL2RG), mRNA	-0.52	(-0.75 , -0.29)		
NM_000629	interferon (alpha, beta and omega) receptor 1 (IFNAR1), mRNA	-0.53	(-0.78 , -0.27)		
NM_017801	chemokine-like factor super family 6 (CKLFSF6), mRNA			-0.4	(-0.45 , -0.36)
NM_005194	CCAAT/enhancer binding protein (C/EBP), beta (CEBPB), mRNA	-0.59	(-0.96 , -0.22)	-0.58	(-0.67 , -0.5)

Continued on next page

Table 4.2 - continued

Accession	Description	1 hr (log_2 fold change)		4 hrs (log_2 fold change)	
Apoptosis					
NM_206835	TNF receptor-associated factor 7 (TRAF7), transcript variant 2, mRNA			-0.66	(-0.95 , -0.37)
NM_006595	apoptosis inhibitor 5 (API5), mRNA			-0.52	(-0.7 , -0.34)
NM_016252	baculoviral IAP repeat-containing 6 (apollon) (BIRC6), mRNA			-0.77	(-1.01 , -0.52)
NM_004435	endonuclease G (ENDOG), nuclear gene encoding mitochondrial protein, mRNA	-0.58	(-0.62 , -0.54)		
NM_032991	caspase 3, apoptosis-related cysteine protease (CASP3), transcript variant beta, mRNA	-1.2	(-1.37 , -1.03)	1.74	(0.59 , 2.89)
Signal Transduction					
JAK/STAT					
NM_002227	Janus kinase 1 (a protein tyrosine kinase) (JAK1), mRNA	0.67	(0.47 , 0.86)		
NM_004157	protein kinase, cAMP-dependent, regulatory, type II, alpha (PRKAR2A), mRNA	0.58	(0.34 , 0.82)		
NM_139276	signal transducer and activator of transcription 3 (acute-phase response factor) (STA	0.49	(0.31 , 0.67)		
NM_000206	interleukin 2 receptor, gamma (IL2RG), mRNA	-0.52	(-0.75 , -0.29)		
NM_000629	interferon (alpha, beta and omega) receptor 1 (IFNAR1), mRNA	-0.53	(-0.78 , -0.27)		
PI3K/AKT					
NM_003629	phosphoinositide-3-kinase, regulatory subunit 3 (p55, gamma) (PIK3R3), mRNA	0.66	(0.35 , 0.97)		
NM_005027	phosphoinositide-3-kinase, regulatory subunit 2 (p85 beta) (PIK3R2), mRNA	0.44	(0.33 , 0.55)		
NM_005027	phosphoinositide-3-kinase, regulatory subunit 2 (p85 beta) (PIK3R2), mRNA	0.44	(0.33 , 0.55)		
NM_005163	AKT1	0.62	(0.57 , 0.66)	-1.01	(-1.34 , -0.69)
NF-kB					
NM_001556	inhibitor of kappa light polypeptide gene enhancer in B-cells, kinase beta (IKBKB)	0.81	(0.66 , 0.96)	-0.66	(-0.99 , -0.32)
NM_020529	nuclear factor of kappa light polypeptide gene enhancer in B-cells inhibitor, alpha (NFKBIA)	-1.04	(-1.14 , -0.94)	-0.76	(-0.91 , -0.6)
NM_003998	nuclear factor of kappa light polypeptide gene enhancer in B-cells 1 (p105) (NFKB1)	0.65	(0.5 , 0.8)	-0.53	(-0.71 , -0.34)

Continued on next page

Table 4.2 - continued

Accession	Description	1 hr (log_2 fold change)		4 hrs (log_2 fold change)	
NM_002502	nuclear factor of kappa light polypeptide gene enhancer in B-cells 2 (p52/p100) (NFKB2)			-1.1	(-1.55 , -0.64)
MAPK					
NM_139124	mitogen-activated protein kinase 8 interacting protein 2 (MAPK8IP2), transcript variant 3,	0.55	(0.39 , 0.72)	-0.47	(-0.61 , -0.33)
NM_002748	mitogen-activated protein kinase 6 (MAPK6), mRNA	0.86	(0.57 , 1.15)	-0.53	(-0.73 , -0.33)
BC003562	dual specificity phosphatase 6, mRNA	0.66	(0.5 , 0.81)	-0.54	(-0.85 , -0.22)
NM_022652	dual specificity phosphatase 6 (DUSP6), transcript variant 2, mRNA	1.11	(0.94 , 1.28)	-0.62	(-0.85 , -0.39)
NM_145110	mitogen-activated protein kinase kinase 3 (MAP2K3), transcript variant C, mRNA	0.57	(0.42 , 0.72)	-0.71	(-0.72 , -0.7)
NM_004579	mitogen-activated protein kinase kinase kinase kinase 2 (MAP4K2), mRNA	0.46	(0.19 , 0.74)		
NM_003684	MAP kinase interacting serine/threonine kinase 1 (MKNK1), mRNA	0.44	(0.34 , 0.53)		
NM_203351	mitogen-activated protein kinase kinase kinase 3 (MAP3K3), transcript variant 1, mRNA			-0.75	(-1.34 , -0.15)
NM_032960	mitogen-activated protein kinase-activated protein kinase 2 (MAPKAPK2)			-0.75	(-1.17 , -0.32)
NM_002228	c-jun (JUN), mRNA			-0.59	(-0.68 , -0.5)
NM_004417	dual specificity phosphatase 1 (DUSP1), mRNA			-0.58	(-0.62 , -0.55)
NM_002745	mitogen-activated protein kinase 1 (MAPK1), transcript variant 1, mRNA			-0.5	(-0.57 , -0.43)
NM_144729	dual specificity phosphatase 10 (DUSP10), transcript variant 3, mRNA	0.92	(0.59 , 1.24)		
NM_015675	growth arrest and DNA-damage-inducible, beta (GADD45B), mRNA	-0.78	(-0.81 , -0.75)		
NM_002467	c-myc, mRNA	0.81	(0.7 , 0.92)	-0.45	(-0.57 , -0.32)
Calcium signaling					
NM_002224	inositol 1,4,5-triphosphate receptor, type 3 (ITPR3), mRNA	1.26	(1.22 , 1.29)		
NM_005184	calmodulin 3 (phosphorylase kinase, delta) (CALM3), mRNA			-0.57	(-0.97 , -0.16)
NM_003688	calcium/calmodulin-dependent serine protein kinase (MAGUK family) (CASK), mRNA	0.83	(0.54 , 1.12)		
NM_000945	protein phosphatase 3 (formerly 2B), regulatory subunit B, 19kDa, (Calcineurin)	0.66	(0.52 , 0.81)		

Continued on next page

Table 4.2. IPAM cells treated with control baculovirus (Control), were stimulated with LPS (100μg/ml). PMA (100 nM) and Ionomycine (4 μM). Total RNA was harvested at both 1 and 4 hrs post stimulation. mRNA was then amplified and labelled with either Cy3 or Cy5 dyes. Samples from control treatment conditions were hybridised to separate arrays with a common reference sample in the second channel. Data sets were analysed using TIGR software and genes differentially regulated by A238L were identified using a using a two class paired Significant Analysis of Microarrays (SAM) analysis ($\delta = 0.498$). Selected annotated genes that are regulated by baculovirus, LPS, PMA and ionomycin treatment are presented in this table. The data presented is the log ratio of the experimental sample to the common reference. Mean values from 3 individual experiments are followed by the 95% confidence interval within brackets (logs are taken to base 2, so a value of 1 represents a 2-fold change in gene expression between the test and control sample). Accession No. are from the human gene bank.

A number of genes usually up regulated following either LPS or PMA/ionomycin treatment were not found in the final gene list (Appendix 2). These genes included TNF-α, IFN-α, IL-8 and IL-2. To determine if these genes were present on the porcine oligonucleotide array, the gene names were cross referenced with the Pig Genome Oligo Set and Extension V1.0 gene list. Oligonucleotide ID's, were available for TNF-α, IFN-α and IL-2, however no oligonucleotides specific for IL-8 could be detected. From the original data files it was found that all of the oligonucleotides specific to TNF-α had been eliminated prior to analysis due to poor quality data. Oligonucleotides specific for IFN-α and IL-2 were present in the final data set, however any changes in their expression levels were not considered to be statistically significant using SAM analysis.

Surprising IL-1α, GM-CSF, IL-2 Rγ and IFNR1 were all down-regulated at 1 hr following LPS, PMA and ionomycin treatment, whereas the IFN inducible genes were up-regulated. This may indicate the targeted inhibition of signalling pathways associated with the expression of these genes at 1 hr post-stimulation. The ccaat/enhancer binding protein C/EBP-β gene, an important transcriptional activator in the regulation of inflammatory response genes such as IL-6 and CD18 antigen, was also down-regulated at 1 hr following stimulation.

Signal transduction

Go-term and KEGG pathway enrichment analysis identified significant enrichment for genes associated with the Janus kinase/signal transducers and activators of transcription (JAK/STAT), Mitogen Activated Protein Kinase (MAPK) and NF-κB signalling pathways across both time points post-stimulation. The MAPK and NF-κB are directly activated by LPS (Guha & Mackman, 2001). The JAK-STAT signalling pathway regulates the cellular response to cytokines and growth factors and can be activated by immediate response genes, such as IFN-α and IL-1-α, which are expressed in response to LPS treatment.

Several differentially-regulated genes involved in signal transduction are common to a number of cellular pathways. For example, phosphatidylinositol 3-kinase (PI3K), AKT, IKKB, CaN, and NF-κB, in particular, are associated with T-cell receptor, B cell receptor and the Toll-like receptor signalling pathways. This highlights the complexity and the considerable cross-talk between signal transduction pathways within the cell.

GO term and KEGG pathway enrichment analysis did not detect a specific enrichment for genes associated with calcium signalling. However proteins regulated by NFAT, NF-κB and CREB, transcription factors activated by calcium mobilisation (Dolmetsch RE, et al., 1997) were present in the final gene list and a number of genes directly associated with calcium signalling were identified (Table 4.2). These include: Inositol 1,4,5-trisphosphate receptor type 3, a secondary messenger that mediates the release of intracellular calcium from the endoplasmic reticulum membrane; calmodulin 1, which is activated through calcium binding and mediates the control of a large number of enzymes; the calcium/calmodulin-dependent serine protein kinase 1(CASK 1) and CaN, both of which were up-regulated at 1 hr following baculovirus, LPS, PMA and ionomycin treatment.

MAPK pathway

Several proteins associated with the MAPK pathway were regulated by baculovirus, LPS, PMA and ionomycin treatment at both time points (Table 4.2). These included upstream activators: MAP2K3 which catalyses the phophorylation of p38; MAP3K2 which acts upstream of ERK and MAP3K3, which is involved in directly regulates the stress-activated protein kinase (SAPK) and extracellular signal-regulated protein kinase (ERK) pathways by activating SEK and MEK1/2 respectively. Down stream targets of the MAPK pathway are: c-jun, MAP kinase-activated protein kinase2 (MAPKAPK2) and MAPK interacting kinase 1(MKNK1). The c-jun transcription factor is activated by JNK. MAPKAPK2 is phosphorylated by p38 and is known to be involved in many cellular processes including stress and inflammatory responses and MAPK interacting kinase 1 is activated by p38 and ERK and may play a role in the response to

environmental stress. In addition genes encoding negative regulators of MAPK were also differentially regulated: dual specific phosphatases DUSP1, DUSP6 and DUSP10. These proteins de-phosphorylate activated MAPKs, thus suppresing their activity. DUSP1 and DUSP 6 specifically de-phosphorylate ERK and DUSP 10 de-phosphorylates p38 and JNK.

With the exception of growth arrest and DNA damage protein, GADD45 β, the majority of genes associated with this pathway were either up-regulated 1 hr following LPS, PMA and ionomycin and down regulated at 4 hrs, or down regulated at 4 hrs alone (Table 4.2). Many genes involved in the regulation of this pathway are auto-regulated and include transcription factors such as c-Jun and DUSPs. The results indicate a strong activation of this pathway 1 hr following treatment followed by a general suppression at 4 hrs.

NF-κB pathway

Differentially-regulated genes belonging to the NF-κB signal transduction pathway included: IκB kinase beta (IκBKβ) which is a component of the IκB kinase complex, p50/p105 and p52/100 which are members of the NF-κB family, and IκBα a cellular inhibitor of NF-κB. IκBKβ and p50/p 100 were up-regulated at 1 hr following stimulation and down-regulated at 4 hrs. p52/100 was down regulated at 4 hrs only and IκBα was down regulated at both 1 and 4 hrs. Similarly to the MAPK pathway, the transcription of a number genes involved in the NF-κB pathway are NF-κB dependent, these include IκBα, p50/p105 and p52/p100. Other NF-κB dependent genes include: IL-1α, GADD45 β, uPAR and GM-CSF and ICAM (HL Pahl, 1999). Interestingly the majority of these genes were found to be down-regulated at 1 hr following baculovirus, LPS, PMA and ionomycin treatment. This could indicate targeted suppression of genes associated with this pathway at 1 hr following treatment.

Overall GO term and KEGG pathway enrichment analysis of the annotated gene lists demonstrated that IPAM cells express proteins consistent with the physiological processes and immunological signalling pathways which are involved in the monocyte/macrophage activation response (Burke B, 2002). However the expression profile exhibited by these genes was not typical of LPS, PMA and ionomycin stimulated primary blood derived leukocytes (Bjorkbacka *et al.*, 2004; Boldrick *et al.*, 2002; Calvano *et al.*, 2005).

4.3 Discussion

Microarray experiments are expensive and time consuming to carry out, limiting the number of conditions that can be investigated in any one experiment. The aim of this chapter was to optimise the microarray experimental design and, in addition, characterise the effect of gene delivery using baculovirus and subsequent LPS, PMA and ionomycin stimulation on IPAM cell gene expression in the absence of A238L gene expression. This was a means to enhance interpretation of the effect of A238L on activated IPAM gene expression and also to asses the suitability of these cells for carrying out investigations into the effects of A238L on host gene transcription.

3.3.1 Optimisation of the microarray experimental design

Semi-quantitative RT-PCR was used to identify suitable time points, early in the pro-inflammatory signalling cascade, that would be suitable for microarray analysis. Using this approach a number of early immune response genes, TNF-α, IL-8 and COX-2 were shown to be induced 60 min following stimulation. This demonstrates that the IPAM cells respond to LPS, PMA and ionomycin stimulation. Notably all of the genes tested were expressed at background levels in un-treated IPAM cells, which suggests that signalling pathways associated with the expression of these genes are constitutively-activated in IPAM cells. Two additional LPS response genes were selected to represent early and second phase gene induction, IκB-ζ and IL-6 respectively. Other work has demonstrated that IκB-ζ is essential for IL-6 gene expression, thus IκB-ζ expression precedes that of IL-6 (Yamamoto *et al.*, 2004). However, this was not found to be the

case in IPAM cells. IL-6 gene expression appeared to be slightly raised in stimulated cells at 60 and 90 min post-treatment, however there was no observable increase in IκB-ζ mRNA, and this remained constant throughout the time course. Previous work has demonstrated that, although IκB-ζ is required for IL-6 gene expression, other factors are involved in IκB-ζ mediated gene transduction. IκB-ζ preferentially binds to the NF-κB p50 subunit (Yamazaki *et al.*, 2001) and investigations using NF-κB p50 deficient cells demonstrated that p50 is required for IκB-ζ induced gene expression (Motoyama *et al.*, 2005). As IκB-ζ appears to be constitutively expressed within IPAM cells and therefore available to participate in IL-6 induced gene expression, it could be that alteration in the cellular concentration and or subcellular localisation of NF-κB p50 is responsible for the observed increase in IL-6 mRNA as opposed to a direct increase in IκB-ζ mRNA.

Due to the small number of genes examined in this analysis it was not possible to detect a secondary change in the expression profile of IPAM cells for the time points tested (0-240 Minuets). However several studies examining the global effects of LPS and PMA/ionomycin have reported significant changes in gene expression profiles at 4 hrs post-stimulation compared to earlier time points supporting the selection of 1 and 4 hrs post-stimulation for microarray analysis (Bjorkbacka *et al.*, 2004; Boldrick *et al.*, 2002; Calvano *et al.*, 2005).

4.3.2 Microarray analysis of the effect of cell stimulation and baculovirus treatment on gene transcription profiles in IPAM cells

Microarray analysis of the gene expression profile of IPAM cells treated with baculovirus followed by LPS, PMA and ionomycin stimulation demonstrated both the up-regulation and repression of genes at both 1 and 4 hrs following stimulation. The overall trend within the data set demonstrated a significant up-regulation of genes at 1 hr post-stimulation followed by significant repression 4 hrs post-stimulation. The rapid suppression of gene expression as early as 4 hrs following LPS or PMA and ionomycin is not consistent with other studies investigating the effect of these compounds on host cell gene transcription (Boldrick *et al.*, 2002; Calvano *et al.*, 2005; Feske *et al.*, 2001;

Macian *et al.*, 2002). These studes did demonstrate some down-regulation of gene expression in response to endotoxin and PMA/ionomycin treatment at early time points post-treatment. However, this response is typically accompanied by a significant up-regulation of other genes, whose expression profiles peaked at 4-9 hrs returning to baseline by 24 hrs (Calvano *et al.*, 2005).

Functional analysis of the differentially regulated gene sets identified similar biological categories at both 1 and 4 hrs following LPS, PMA and ionomycin treatment. Many of these categories were typical of monocyte/macrophage function as phagocytic and active secretory cells, demonstrating that IPAM cells can respond appropriately to activation. Biological themes included proteins associated with phagocytosis and cell projection morphogenesis (indicative of pseudopodia formation), proteins involved in the secretary pathway, cell adhesion and migration molecules, immune response genes and genes involved in the coagulation and complement pathway. The majority of these categories were up regulated at 1 hr followed by down regulation at 4 hrs, indicating a generalised non-specific suppression of gene transcription in baculovirus treated cells at 4 hrs following LPS, PMA and ionomycin treatment.

Genes involved in signal transduction were also significantly enriched within the differentially-regulated gene list and included members of the MAPK, NF-κB and JAK/STAT pathways. MAPK and NF-κB signalling pathways are both activated through LPS treatment and many genes associated with these pathways are auto-regulated. These results indicate regulation of these pathways in the treated IPAM cells. The majority of MAPK genes were up-regulated at 1 hr and down-regulated at 4 hrs. JAK 1 and STAT3, components of the JAK/STAT pathway and a number of components of the calcium signalling pathway (CaN, CASK) were also up-regulated at 1 hr following treatment. In contrast transcription of several genes dependent on NF-κB, were down-regulated at 1 hr following stimulation including IκB-α, IL-1α, GADD45 β, uPAR, GM-CSF and ICAM (HL Pahl, 1999). This suggests targeted inhibition of genes associated with this pathway at 1 hr following cell stimulation.

Down-regulation of some immune response genes, in treated compared to un-treated IPAM cells, indicates that signalling pathways associated with the expression of these genes are constitutively activated in untreated IPAM cells. This result is consistent with the RT-PCR results presented in section 4.2.1.2, which showed background levels of TNF-α, IL-8, COX-2 and IL-6 in untreated, control IPAM cells.

Overall microarray analysis demonstrated that IPAM cells pre-treated with baculovirus demonstrated a marked increase in gene expression at 1 hr following stimulation with LPS, PMA and ionomycin, followed by a rapid generalised suppression of gene expression at 4 hrs following treatment. Functional analysis of annotated genes also suggested targeted inhibition of some NF-kB dependent genes at 1 hr following stimulation.

One possible explanation for this atypical response to LPS, PMA and ionomycin treatment could be due to pre-treatment of the cells with recombinant baculovirus. A number of studies have reported that treatment of mammalian cells with the live baculovirus can stimulate an antiviral effect in mammalian cells. Abe *et al.*, 2003, demonstrated that intranasal inoculation with the baculovirus *Autographa californica* nuclear polyhedrosis virus (AcNPV) induced a strong innate immune response in mice and that AcNPV conferred protection from a lethal challenge of influenza A and B virus. This study also demonstrated that baculovirus induced the secretion of the inflammatory cytokines TNF-α, IL-6 and IL-12 in RAW164.7 cells (a murine macrophage cell line). Gronowski et al also reported that AcNPV stimulated IFN production in both human and mouse cells *in vitro* and *in vivo* (Gronowski *et al.*, 1999). Prior exposure of cells to LPS induces a transient state of cellular hyporesponsiveness to subsequent LPS stimulation. This is known as endotoxin tolerance. This tolerance results in the selective suppression of many proinflammatory cytokines including TNF-α, IL-1β, IL-6 and IL-12 (Schade et al 1999). Therefore it could be that the failure to up-regulate the expression of proinflammatory cytokines, in addition to the rapid suppression of gene transcription 4

hrs following stimulation, is due to prior sensitisation of stimulated cells with baculovirus.

From the results presented in this chapter it is not clear what mechanisms are responsible for the partially unexpected expression profile exhibited by IPAM cells in response to baculovirus treatment and LPS, PMA and ionomycin stimulation. It is likely that both the mechanism of gene delivery combined with inherent properties of the IPAM cells contributed to this response. Nevertheless, the results presented in this chapter have allowed the selection of appropriate conditions for the microarray experimental design. Overall the genes differentially regulated in IPAM cells following baculovirus treatment and LPS, PMA and ionomycin stimulation were consistent with biological processes associated with macrophage activation, providing support for the use of these cells to investigate the effect of A238L. However some anomalies in the response of these cells to LPS, PMA and ionomycin were detected. Prior knowledge of these anomalies provide a distinct advantage in interpreting the effects of A238L within these cells.

In conclusion, the results presented in this chapter demonstrate that IPAM cells treated with baculovirus respond rapidly to LPS, PMA and ionomycine, with a significant change in gene expression at 1 hr following treatment. The nature of this response and expression profile of individual genes changed significantly between 1 and 4 hrs following LPS, PMA and ionomycine treatment. Comparison between these results and other work investigating the effect of LPS, PMA and ionomycine on primary and immortalised cells indicate that IPAM cells treated with baculovirus do not produce a typical expression profile in response to these compounds. This could be due to the effect of baculovirus treatement prior to stimulation, inherent properties of the IPAM cells or a combination of both. The lack of similarity between IPAM cells compared to primary monocytes suggests that the results obtained from baculovirus infected IPAM cells are not representive of the potential effect of A238L in primary porcine alveolar macrophage. Therfore although interpretation of the results presented in chapter 5 as a whole to obtain a greater understanding into the mechanism of A238L action is valid,

the effect of A238L on the expression of individual IPAM proteins may not be significant in primary porcine macrophage.

Chapter 5

Inhibition of host gene expression assessed by expression of the ASFV protein A238L in a macrophage cell line

5.1 Introduction

The previous chapter describes the optimization of the microarray experimental design to investigate the effect of A238L on host macrophage gene transcription at early time points following cell activation. In addition it describes the effect of the experimental conditions on IPAM cells alone in the absence of A238L gene expression.

The results presented in this chapter describe the effect of A238L on gene transcription in these cells, with the aim of providing a greater understanding of the mechanism of A238L action and also the potential functional significance of this action within host cells.

5.2 Results

5.2.1 Microarray data analysis

To examine the effect of A238L on gene transcription changes caused by LPS, PMA and ionomycin treatment of IPAM cells gene expression profiles were compared between stimulated cells treated either with baculovirus expressing A238L (BacSV5A238L) or control baculovirus (BacWPRE) not expressing the A238L gene using a porcine oligonucleotide micorarray (Operon). Two time points post-stimulation were examined and 3 independent experiments were carried out. Gene expression profiles were compared between stimulated IPAM cells treated with test and control baculovirus indirectly using a common reference sample. This reference RNA consisted of a pool of

RNA from control untreated IPAM cells. The design for this microarray experiment is shown in Figure 5.1. Using this approach it was possible to carry out additional analysis on the data set to investigate the effect of baculovirus treatment followed by LPS, PMA, and ionomycin on IPAM cells (presented in chapter 4). IPAM cells were treated with BacSV5A238L or BacWPRE at an m.o.i. 50. 12 hours following baculovirus treatment the cells were stimulation with LPS, PMA and ionomycin. Total RNA was harvested at 1 and 4 hours post-stimulation of cells for both the test and control samples. To expand the amount of RNA harvested and produce enough RNA sample material for all of the hybridizations the mRNAs from these samples and the common reference sample were amplified to produce antisense RNA. Amplified RNA was then labeled with either Cy3 or Cy5 dyes respectively and co-hybridised onto the porcine oligonucleotide arrays (Operon). A more detailed description of these procedures is presented in Chapter 2 (section 2.7). Two hybridisations were carried out for each comparison, with the dye assignments reversed in the second hybridisation to account for labeling bias between dyes. Images of the hybridised arrays were obtained by laser confocal scanning and TIGR sofware was then used to normalize the data sets and identify oligonucleotides which hybridised to differentially regulated RNAs. Prior to statistical analysis, the total data set was filtered to remove poor quality spots and this identified a final data set of 10146 unique oligonucleotides.

1 and 4 hr data sets were analyzed independently using a two class paired Significant Analysis of Microarrays (SAM) analysis ($\delta = 0.498$). The results from this analysis are presented in Figuress 5.2 and 5.3. At 1 hr post-stimulation a total of 214 (2 %) unique oligonucleotides were identified as hybridizing to RNAs that were significantly differentially regulated by A238L gene expression; 19.98 of these targets were estimated to be falsely significant (FDR 9.34 %). Only 2 of these targets hybridized to RNAs that were significantly up-regulated, the remaining 212 hybridised to RNAs that were significantly

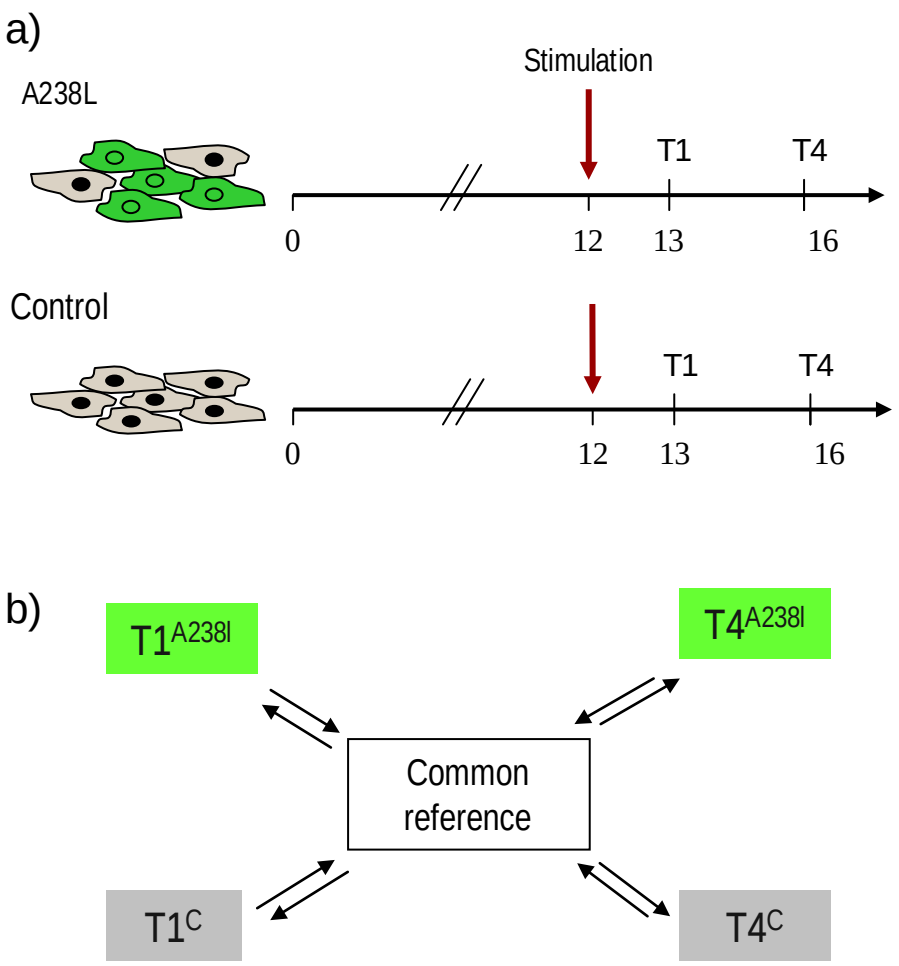

Figure 5.1 Schematic representation of the microarray experimental design used investigate the effect of A238L on stimulated IPAM cells. Panel A) Experimental procedure: IPAM cells were infected with Bac-SV5A238L (A238L) or Bac-WPRE (control) at an moi 50. 12 hours following baculovirus treatment the cells were stimulated with LPS (100μg/ml), PMA (100 nM) and Ionomycin (4 μM). 1 hr (T1) and 4 hrs (T4) following stimulation total RNA was harvested, amplified and labeled with either Cy3 or Cy5 fluoresent dyes. The horizontal arrow represents the time line post baculovirus treatment. Panel B) Microarray experimental design. Test and control samples were compared indirectly against a common reference pool of un-stimulation IPAM RNA. Amplified mRNA from each sample and the common reference was labeled with either Cy3 or Cy5 fluoresent dyes. Each sample was then co-hybridised onto a separate porcine oligo arrays (operon) against the common reference sample in the opposite channel. Three biological replicates were carried out for each experimental condition, with a dye swap for each biological replicate. This resulted in a total of 24 hybridisations.

down-regulated (see Figure 5.2). At 4hr post-stimulation 89 (1 %) of targets were identified as differentially regulated, 20.35 of these were estimated to be falsely significant (FDR 22.86 %) (Figure 5.3). All of these oligonucleotides were shown to hybridise to RNAs that were significantly down-regulated. It is notable that the number of genes identified as differentially regulated at 4 hrs is less than half the number at 1 hr. In addition, it is estimated that approximately 23 % of these genes may be falsely significant as opposed to only around 10 % at 1 hr post stimulation. It is therefore possible that the reduced number of genes identified as differentially regulated by A238L at 4 hrs is a result of high background present on the microarray slides at this time point, rather than of biological significance.

To examine the effect of A238L on baculovirus, LPS, PMA and ionomycin treated IPAM cells, across both time points, the lists of oligonucleotides identified as differentially regulated between BacA238L and BacWPRE treated IPAM cells at 1 and 4 hrs following LPS, PMA and ionomycin treatment were combined. This resulted in a final list of 294 unique oligonucleotides that hybridized to differentially regulated RNAs at either or both 1 and 4 hrs post-stimulation. 182 unique oligonucleotides hybridized to RNAs that were differentially regulated at 1 hr only, 25 to RNAs that were differentially regulated at both 1 and 4 hrs post-stimulation and 62 to RNAs that were differentially regulated at 4 hrs only. These results are presented as a Venn diagram in Figure 5.4. As stated previously, with the exception of 2 oligonucleotides which hybridized to differentially regulated RNAs at 1 hr post-stimulation, all of the remaining oligonucleotides hybridized to RNAs that were down-regulated in cells expressing A238L. Overall the number of oligonucleotides differentially regulated by A238L is relatively small, suggesting a specific targeted effect on host macrophage gene transcription, rather than generalized shut-off of host gene transcription. This is consistent with the predicted function of A238L as an inhibitor of transcription activation (Granja *et al.*, 2006a; Granja *et al.*, 2004a; Powell *et al.*, 1996).

a)

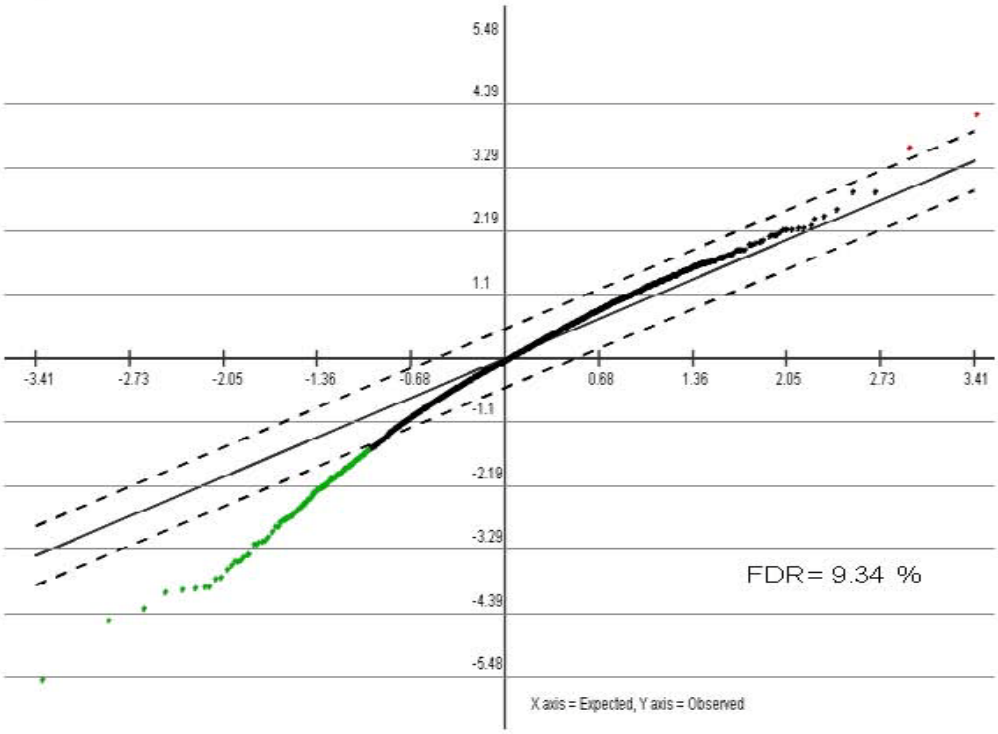

b)

	Number	Percent
Positive Significant genes	2	0
Negative Significant genes	212	2
All significant genes	214	2
Non-significant genes	9932	98

Figure 5.2 Identification of genes significantly regulated by A238L gene expression at 1 hour post stimulation, using SAM. Panel A shows a scatter plot of the observed relative difference between control and test samples *d(i)* (Y axis), versus the expected relative difference *dE(i)*(X axis), calculated using a two class paired Significant Analysis of Microarrays (SAM) analysis. The solid line indicates the line for *d(i)= dE(i)*, where the observed relative difference is identical to the expected relative difference. The dotted lines are drawn at a distance of $\delta = 0.498$ from the solid line (the selected threshold for this analysis), values above (red) or below (green) this threshold are considered to be significantly regulated by A238L gene expression. Up regulated oligonucleotides are shown in red and down regulated oligos are shown in green. The False Discovery Rate (FDR) based on $\delta = 0.498$, is presented on this graph. Panel B shows a summary of the results.

a)

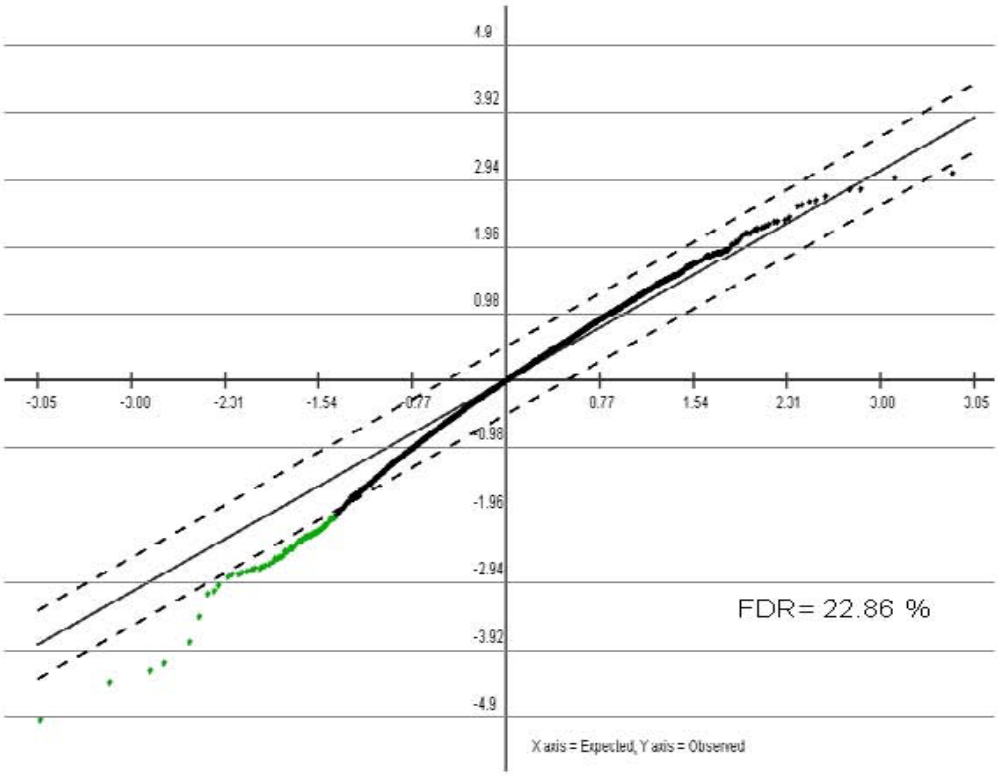

b)

	Number	Percent
Positive Significant genes	0	0
Negative Significant genes	89	1
All significant genes	89	1
Non-significant genes	10057	99

Figure 5.3 Identification of genes significantly regulated by A238L gene expression at 4 hour post stimulation, using SAM. Panel A shows a scatter plot of the observed relative difference between control and test samples *d(i)* (Y axis), versus the expected relative difference *dE(i)*(X axis), calculated using a two class paired Significant Analysis of Microarrays (SAM) analysis. The solid line indicates the line for *d(i)= dE(i),* where the observed relative difference is identical to the expected relative difference. The dotted lines are drawn at a distance of $\delta = 0.498$ from the solid line (the selected threshold for this analysis), values above or below this threshold are considered to be significantly regulated by A238L gene expression. Up regulated oligonucleotides are shown in red and down regulated oliogonucleotides are shown in green. The False Discovery Rate (FDR) based on $\delta = 0.498$, is presented on this graph. Panel B shows a summary of the results.

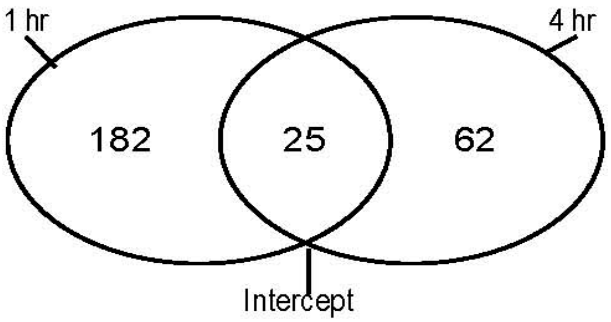

Figure 5.4 Venn diagram representing the relationship between oligonucleotides identified as differentially regulated between Bac-SV5A238L and Bac-WPRE , LPS, PMA and ionomycin treated IPAM cells at 1 and 4 hrs post stimulation. Group 1 (1hr) represent all of the oligonucleotides differentially regulated at 1 hr. Group 2 (4 hrs) represents all of the oligonucleotides differentially at 4 hrs. The intercept represents oligonucleotides common to both groups.

5.2.2 Functional classification of differentially-regulated genes

Annotation was available for 144 of the 294 oligonucleotides that hybridised to differentially regulated RNA. This annotation was obtained from the Pig Genome Oligo Set and Extension V1.0 gene list last updated in 2004 (OMAD Release: 04/13/04). All of the probes present in this array were designed from information present in The Institute of Genome Research (TIGR) Gene Index Database SsGI Release 5.0 (http://www.tigr.org/tdb/tgi/ssgi). The majority of the oligonucleotides were designed from sequences with a hit to a known human, mouse, or pig gene transcript (10,665 out of 13297). However a proportion of the genes (2632 out of 13297) were designed from tentative consensus sequences (TC's) which represented mRNA transcripts without homology to other known genes. Therefore, unlike similar mouse and human arrays, there is a significant lack of annotation available for many of the individual oligonucleotides spotted onto the porcine array. Annotation was available for less than half of the unique oligonucleotide ID's found to hybridise to RNAs differentially regulated by A238L, therefore many genes of interest were potentially excluded from the final data set. After editing to remove redundancy between genes targeted by a number of different oligonucleotides, a final list of 137 annotated genes was produced. This list included a large number of genes which have not previously been shown to be regulated by A238L expression.

Several genes, which have been shown previously to be down-regulated by A238L gene expression, were not identified as differentially-regulated in this analysis. These genes included TNF-α, IL-8, iNOS, COX-2 and IFN-α (Granja *et al.*, 2006a; Granja *et al.*, 2004a; Granja *et al.*, 2008a; Granja *et al.*, 2006c; Powell *et al.*, 1996). To determine if these genes were present on the porcine oligonucleotide array, the gene names were cross referenced with the Pig Genome Oligo Set and Extension V1.0 gene list. Oligonucleotide ID's, were available for TNF-α, IFN-α and iNOS, however no oligonucleotides specific for COX-2 and IL-8 could be detected. From the original data files it was found that all of the oligonucleotides specific to TNF-α had been eliminated

prior to analysis due to poor quality data. Oligos specific for IFN-α and iNOS were present in the final data set, and although down-regulation of these genes was observed in cells expressing A238L this was not found to be statistically significant using SAM analysis.

To assist in the functional characterization of genes identified as differentially- regulated by A238L, gene GO term enrichment analysis was used to highlight the most relevant biological classifications associated with this gene list (Harris *et al.*, 2004). The DAVID functional annotation tool was used to carry out this analysis and also to identify any clusters of genes common to cell signaling networks defined using KEGG pathways (Kanehisa *et al.*, 2008). A detailed description of these terms along with the DAVID software is presented in chapter 4. Using this approach several functionally-related classes of genes were identified. Genes not clustered using this method were manually placed into functionally related categories based on their GO-term annotation. The results from this analysis are presented in Tabless 5.1, 5.2, 5.3 and 5.4. Table 5.1 shows a summary of the main biological themes along with the number of genes associated with each category. Tables 5.2, 5.3 and 5.4 contain a list of the annotated genes down-regulated by A238L along with there expression profiles. These genes are clustered in Table 5.1 according to their most relevant biological category. Table 5.2 includes genes which were significantly regulated at 1 hr post-stimulation only. Table 5.3 includes genes that are regulated by A238L at both 1 and 4 hrs post-stimulation and Table 5. 4 shows genes down-regulated by A238L at 4 hrs only. From comparison of Tables 5.2, 5.3 and 5.4 with data presented in Chapter 4, it can be seen that a large proportion of genes regulated by A238L were not shown to be up or down-regulated by control baculovirus treatment and cell stimulation. Only 25 of the 137 annotated genes down regulated by A38L were significantly regulated in control baculovirus treated and stimulated cells. This demonstrates that the majority of genes regulated by A238L are constitutively expressed in unstimulated IPAM cells. Tables 5.2, 5.3 and 5. 4 also show that the relative difference in gene expression between test and control samples varied from Log_2 0.48 to Log_2 2.23, which is equivalent to a 1.4 – 4.7 fold change in gene

expression. This is similar to the range in expression level of differentially-regulated genes observed between un-stimulated and stimulated IPAM cells as shown in chapter 4.

Overall the majority of genes differentially regulated by A238L were those that are rapidly induced in response to stimulation or physiological stress (such as immune activation or DNA damage). From Table 5.1 it can be seen that the genes down-regulated by A238L cover a diverse range of biological categories. A significant number of genes down-regulated by A238L were associated with the immune response, response to stimulation and apoptosis. Proteins involved in intracellular signal transduction, transcription factors and cell surface/secreted proteins were also well represented. Other groups included genes involved in RNA processing, intracellular transport and amino acid metabolism.

Down-regulated immune response genes included the cytokines IL-1-α, GM-CSF, Monocyte chemotractant protein 1 (MCP 1), CD83 which is involved in antigen presentation, four acute phase genes involved in the coagulation cascade (urokinase plasminogen activator receptor (uPAR), alpha – 2-macroglobulin, coagulation factor II receptor-like 1 and protein S alpha) and nuclear localized factor 2 (NLF2). NLF2 belongs to a novel family of nuclear factors which are rapidly induced by pro-inflammatory cytokines (Warton *et al.*, 2004). Interferon-inducible genes associated with the JAK/STAT pathway were also identified: Interferon-induced protein 44-like (IFI44L), IFN regulatory factor 1, Interferon-induced protein with tetratricopeptide repeats 1 and PML-1. PML-1 is clustered with genes involved in apoptosis (Der *et al.*, 1998). None of these genes have previously been shown to be regulated by A238L gene expression. The expression profile of these genes and also the A238L regulated genes involved in apoptosis (disscused below) are presented in Table 5.5.

GO: Biological Response	Time post stimulation		
	1 hr	1+ 4 hrs	4hrs
Immune response genes	8	2	2
Apoptosis	6	-	-
Response to cell stimulus	6	-	-
Cell cycle	6	1	3
Intracellular signal transduction	9	3	9
Transcription factors/regulation	13	1	2
Cell surface/secreted proteins	9	2	-
Cell migration	2	2	-
RNA processing	5	-	-
Protein metabolism	3	-	-
Protein Transport	3	-	-
Transporter	3	-	3
Extracellular matrix	3	-	-
Cellular metabolism	-	-	3
Amino acid metabolism	-	-	3
Ubiquitination	-	-	1
Unknown	8	1	3

Table 5.1 Functional Classes of A238L down regulated genes. Go term enrichment analysis using DAVID functional annotation software was used to identify biological enriched themes within annotated gene list. Genes not clustered using this method were manually placed into categories based on their GO-term annotation. The results represent the number of differential regulated genes associated with each biological term for the conditions listed.

Table 5.2 Biological characterisation of genes regulated by A238L at 1 hour.

Accession no.	Description		1 hr (log_2 fold change) Control	1 hr (log_2 fold change) Test	Difference
A238L up regulated genes					
Extracellular matrix protein					
NM_080645	collagen, type XII, alpha 1 (COL12A1)		-0.78 (-1.14, -0.41)	0.26 (-0.14, 0.66)	-1.04
A238L down regulated genes					
Immune response genes					
177872	Alpha-2-macroglobulin		1.34 (1.21, 1.46)	0.60 (0.52, 0.68)	0.74
NM_006820	Interferon-induced protein 44-like (IFI44L)		0.92 (0.77, 1.06)	0.16 (-0.02, 0.34)	0.76
P09914	Interferon-induced protein with tetratricopeptide repeats 1	(NS)	0.01 (-0.47, 0.49)	-1.56 (-1.97, -1.15)	1.57
Q08353	I-kappa-B-alpha		-1.04 (-1.14, -0.94)	-2.07 (-2.47, -1.68)	1.03
Q29118	Granulocyte-macrophage colony-stimulating factor		-1.21 (-1.57, -0.86)	-2.00 (-2.37, -1.63)	0.79
P18430	Interleukin-1 alpha precursor		-0.57 (-1.86, 0.72)	-2.22 (-2.82, -1.61)	1.65
NM_001993	Homo sapiens coagulation factor III	(NS)	-0.42 (-0.60, -0.25)	-1.54 (-2.10, -0.98)	1.12
Q01151	CD83 antigen precursor		-0.47 (-0.98, 0.03)	-1.12 (-1.65, -0.59)	0.65
Response to stimulus					
NM_014685	Homocysteine-inducible, endoplasmic reticulum stress-inducible, ubiquitin-like domain member 1 (HERPUD1)	(NS)	0.75 (0.62, 0.89)	-0.7 (-1.20, -0.19)	0.82
NM_005347	Heat shock protein 72kDa		0.73 (0.60, 0.87)	-0.38 (-0.48, -0.29)	1.11
11559490	VDUP1	(NS)	-0.09 (-0.35, 0.16)	-0.61 (-0.93, -0.29)	0.52
P47974	TIS11 primary response gene	(NS)	0.28 (0.16, 0.40)	-0.56 (-0.77, -0.35)	0.84
13177685	Immediate early protein	(NS)	-0.40 (-0.72, -0.07)	-1.46 (-1.73, -1.19)	1.06
NM_001007595	Nuclear localized factor 2 (NLF2)	(NS)	-0.18 (-0.50, 0.14)	-1.23 (-1.55, -0.92)	1.05
Apoptosis					
NM_033240	Promyelocytic leukemia (PML)	(NS)	0.33 (-0.16, 0.82)	-0.75 (-0.93, -0.56)	1.08
BC031549	CDC-like kinase 1		0.90 (0.74, 1.07)	0.14 (-0.33, 0.62)	0.76
NM_002312	DNA ligase IV	(NS)	0.84 (0.65, 1.03)	0.26 (-0.25, 0.78)	0.58
O75293	Growth arrest and DNA-damage-inducible protein GADD45 beta		-0.78 (-0.81, -0.75)	-1.39 (-1.48, -1.30)	0.61
P24522	Growth arrest and DNA-damage-inducible protein GADD45 alpha	(NS)	-0.16 (-0.34, 0.01)	-0.89 (-1.19, -0.60)	0.73
NM_030952	SNF1-like kinase kinase (NUAK2)	(NS)	0.26 (0.03, 0.50)	-0.70 (-1.25, -0.15)	0.96
Cell cycle rgulation					
Q9UQL6	Histone deacetylase 5		0.61 (0.49, 0.74)	-0.08 (-0.66, 0.51)	0.69
NM_005611	Retinoblastoma-like 2 (p130)	(NS)	0.43 (0.13, 0.73)	-0.73 (-1.10, -0.36)	1.16
3075509	Serum-inducible kinase (Snk/Plk2)		0.59 (0.37, 0.81)	-0.05 (-0.24, 0.15)	0.64
P21274	Bone morphogenetic protein 2 precursor (BMP-2)		0.41 (0.27, 0.55)	-0.47 (-0.76, -0.17)	0.88
U14603	Protein-tyrosine phosphatase type IV		0.65 (0.18, 1.12)	-0.06 (-0.23, 0.11)	0.71

Continued on following page

Table 5.2 - continued

Accession	Description		1 hr (log_2 fold change)		Difference
			Control	Test	
A41236	Placental growth factor	(NS)	-0.06 (-0.61, 0.49)	-0.87 (-1.74, 0.00)	0.81
Intracellular signal transduction					
NM_018014	B-cell CLL/lymphoma 11A	(NS)	-0.01 (-0.09, 0.07)	-0.63 (-1.02, -0.24)	0.62
NM_001894	Casein kinase 1, epsilon	(NS)	-0.02 (-0.16, 0.13)	-0.68 (-1.07, -0.29)	0.66
AB125644	PKB/Akt-binding protein	(NS)	0.03 (-0.15, 0.21)	-0.46 (-0.61, -0.31)	0.49
P01121	Transforming protein RhoB (H6)	(NS)	0.17 (-0.12, 0.47)	-2.01 (-2.68, -1.35)	2.18
BC003562	Dual specificity phosphatase 6 (DUSP6)		0.49 (0.34, 0.65)	-0.36 (-0.69, -0.02)	0.85
BC006823	Protein phosphatase 2 (regulatory subunit B)	(NS)	0.30 (0.15, 0.45)	-0.26 (-0.43, -0.09)	0.56
NP_275869	Rho-kinase beta	(NS)	-0.11 (-0.40, 0.17)	-0.70 (-0.94, -0.45)	0.59
23386514	Ras SF1	(NS)	-0.18 (-0.24, -0.13)	-0.76 (-0.97, -0.54)	0.58
NM_018201	TBC1 domain family, member 13	(NS)	0.31 (0.28, 0.34)	-0.57 (-1.40, 0.27)	0.88
Transcription factors / transcription regulation					
NM_012446	Single-stranded DNA-binding protein 2	(NS)	0.18 (0.11, 0.26)	-0.36 (-0.56, -0.16)	0.54
O14896	Interferon regulatory factor 6 (IRF-6)	(NS)	0.00 (-0.07, 0.08)	-0.64 (-0.77, -0.51)	0.64
O18896	Transcription factor SOX-9	(NS)	-0.05 (-0.65, 0.55)	-1.10 (-2.31, 0.12)	1.05
Q01580	Heparin-binding EGF-like growth factor		-0.5 (-0.72, -0.27)	-1.43 (-1.67, -1.19)	0.93
M92844	Zinc finger transcriptional regulator (GOS24)	(NS)	-0.35 (-0.55, -0.14)	-1.40 (-1.74, -1.06)	1.05
P17275	Transcription factor jun-B	(NS)	-0.31 (-0.48, -0.14)	-1.22 (-1.71, -0.73)	0.91
NP_277037	POU domain region; homolog of mouse brn-3 (Oct-1)	(NS)	0.62 (0.24, 1.01)	-0.08 (-0.90, 0.74)	0.70
4581531	c-Fos protein		-0.59 (-1.10, -0.08)	-2.82 (-3.57, -2.06)	2.23
P56432	Proto-oncogene c-jun	(NS)	-0.23 (-0.59, 0.13)	-1.61 (-2.07, -1.15)	1.38
28798059	Interferon regulatory factor 1	(NS)	-0.11 (-0.39, 0.17)	-1.02 (-1.35, -0.70)	0.91
Q29031	c-myc	(NS)	0.81 (0.70, 0.92)	0.29 (0.21, 0.38)	0.52
AF454942	HMG-box transcription factor BBX	(NS)	0.23 (0.07, 0.39)	-0.36 (-0.86, 0.14)	0.59
NM_004089	TSC22 domain family, member 3	(NS)	0.29 (-0.06, 0.64)	-0.63 (-1.34, 0.08)	0.92
Cell surface/secreated proteins					
21954715	Matrix Gla protein	(NS?)	1.37 (1.10, 1.64)	0.52 (0.34, 0.70)	0.85
BC015028	Nephroblastoma overexpressed gene	(NS?)	1.15 (1.08, 1.22)	0.41 (0.23, 0.58)	0.74
1890128	Folate binding protein	(NS)	1.28 (0.91, 1.65)	0.48 (0.15, 0.81)	0.80
4097833	Connective tissue growth factor (CTGF)		0.62 (0.44, 0.81)	-0.53 (-0.75, -0.31)	1.15
O00622	CYR61 protein precursor	(NS)	-0.28 (-0.37, -0.18)	-1.60 (-1.86, -1.35)	1.32
904141	Protein S	(NS)	0.51 (0.43, 0.60)	-0.03 (-0.17, 0.11)	0.54
Q92692	CD112 antigen		0.67 (0.48, 0.85)	0.08 (-0.22, 0.38)	0.59
P17690	Beta-2-glycoprotein I precursor (Apolipoprotein H)		0.70 (0.52, 0.89)	0.01 (-0.15, 0.18)	0.69
Q99574	Neuroserpin precursor (Protease inhibitor 12)	(NS)	0.74 (0.42, 1.06)	0.26 (-0.13, 0.64)	0.48
Extracellular matrix protein					
NM_000093	collagen, type V, alpha 1 (COL5A1)	(NS)	0.45 (0.24, 0.65)	-0.24 (-0.47, 0.00)	0.69
NM_000055	Butyrylcholinesterase	(NS)	0.02 (-0.15, 0.18)	-0.53 (-0.89, -0.17)	0.55
NM_007037	ADAM metallopeptidase motif 8 (ADAMTS8)	(NS)	-0.17 (-0.90, 0.56)	-0.94 (-2.17, 0.29)	0.77

Continued on following page

Table 5.2 - continued

Accession	Description		1 hr (log_2 fold change) Control	Test	Difference
Cell migration					
NM_002356	Myristoylated alanine-rich C-kinase substrate		-0.69 (-0.84, -0.54)	-1.32 (-1.54, -1.09)	0.63
2467300	Phosphatidic acid phosphatase 2b	(NS)	0.38 (-0.39, 1.15)	-0.43 (-0.80, -0.06)	0.81
RNA processing					
NM_021133	Ribonuclease L (2',5'-oligoisoadenylate synthetase-dependent) (RNASEL)	(NS)	0.30 (0.11, 0.50)	-0.48 (-1.19, 0.22)	0.78
NM_001533	Heterogeneous nuclear ribonucleoprotein L (HNRPL)	(NS)	0.31 (0.14, 0.49)	-0.25 (-0.34, -0.17)	0.56
NM_020307	Cyclin L1 (CCNL1)	(NS)	0.18 (0.03, 0.33)	-0.51 (-0.77, -0.24)	0.69
O94913	Pre-mRNA cleavage complex II protein Pcf11	(NS)	0.22 (-0.10, 0.55)	-0.88 (-1.27, -0.48)	1.10
NM_018146	RNA methyltransferase like 1 (RNMTL1)	(NS)	0.26 (0.10, 0.42)	-0.37 (-0.54, -0.19)	0.63
Protein metabolism					
AY496012	Propionyl-coA carboxylase B (PCCB)	(NS)	-0.22 (-0.45, 0.01)	-0.93 (-1.55, -0.31)	0.71
JE0172	Ribonuclease T2	(NS)	0.39 (0.10, 0.68)	-0.23 (-0.66, 0.20)	0.62
S52084	Ribosomal protein L22	(NS)	0.32 (0.12, 0.52)	-0.24 (-0.36, -0.11)	0.56
Vesicle mediated / protein transport					
BC007458	Karyopherin alpha 4 (Import alpha 3)	(NS)	0.68 (0.30, 1.06)	0.12 (-0.22, 0.46)	0.56
11321325	Lin-7b	(NS)	0.13 (-0.65, 0.91)	-0.88 (-1.40, -0.35)	1.01
Q9NP90	Ras-related protein Rab-9B (Rab-9L)	(NS)	0.04 (-1.48, 1.57)	-0.75 (-2.73, 1.24)	0.79
Macromolecule transport					
NM_005502	ATP-binding cassette, sub-family A, member 1		0.54 (0.43, 0.65)	-0.23 (-0.42, -0.05)	0.77
Intracellular transport					
NM_144996	ADP-ribosylation factor-like 2 protein-like protein		0.55 (0.36, 0.74)	-0.05 (-0.38, 0.28)	0.60
Ion Transporter					
9501803	Potassium channel interacting protein 1	(NS)	0.17 (-0.09, 0.44)	-0.64 (-1.17, -0.11)	0.81
AJ619991	Small calcium-binding mitochondrial carrier 2	(NS)	-0.18 (-0.40, 0.03)	-0.95 (-1.04, -0.86)	0.77
Q96NB2	Sideroflexin 2	(NS)	0.67 (-0.68, 2.01)*	-0.78 (-1.37, -0.18)	1.45
Virus protein					
14530213	Gag protein[Porcine endogenous retrovirus M16]		0.46 (0.34, 0.65)	-0.17 (-0.33, -0.01)	0.63
Unknown function / Hypothetic proteins					
BC009624	Myeloid/lymphoid or mixed-lineage leukemia	(NS)	-0.11 (-0.54, 0.32)	-0.83 (-1.03, -0.63)	0.72
NM_017948	Nucleolar protein 8 (NOL8)	(NS)	0.20 (-0.11, 0.52)	-0.39 (-0.81, 0.04)	0.59
BC044777	Thioredoxin domain containing 13	(NS)	0.71 (0.32, 1.09)	0.19 (-0.10, 0.48)	0.52
15128489	Vascular endothelial cell specific protein	(NS)	0.57 (0.34, 0.80)	-0.34 (-0.91, 0.23)	0.91
DQ323403	Paternally expressed 10 (Peg10)		1.10 (0.82, 1.39)	0.50 (0.11, 0.90)	0.60
NM_030938	Transmembrane protein 49	(NS)	0.26 (0.20, 0.33)	-0.47 (-0.74, -0.21)	0.73
AF308819	Nuclear receptor-interacting factor	(NS)	0.29 (0.14, 0.43)	-0.20 (-0.40, 0.00)	0.49
P53804	Tetratricopeptide repeat protein 3	(NS)	0.55 (0.46, 0.64)	0.05 (-0.20, 0.29)	0.50

Table 5.2 IPAM cells treated with either recombinant baculovirus expressing the A238L gene (Test) or control baculovirus (Control), were stimulated with LPS (100μg/ml). PMA (100 nM) and Ionomycine (4 μM). Total RNA was harvested at both 1 and 4 hrs post stimulation. mRNA was then amplified and labelled with either Cy3 or Cy5 dyes. Samples from control and test treatment conditions were hybridised to separate arrays with a common reference sample in the second channel. Data sets were analysed using TIGR software and genes differentially regulated by A238L were identified using a using a two class paired Significant Analysis of Microarrays (SAM) analysis (δ = 0.498). Annotated genes that are regulated by A238L at one hour post stimulation only are presented in this Table. The data presented is the log ratio of the experimental sample to the common reference. Mean values from 3 individual experiments are followed by the 95% confidence interval within brackets. The difference between these two values is presented for both 1 and 4 hrs as a log ratio (logs are taken to base 2, so a value of 1 represents a 2-fold change in gene expression between the test and control sample). Genes that had not previously been shown to be significantly up or down regulated by treatment with LPS, PMA and ionomycine (Chapter 4, Tables 1, 2 and 3), are indicated by the presence of the letters NS (Not Stimulated) in brackets. Accession No. are taken from the Pig Genome Oligo Set and Extension V1.0 gene list (ref).

Table 5.3 Biological characterisation of genes regulated by A238L at both 1 and 4 hours post stimulation

Accession no.	Description		1 hr (log_2 fold change)			4 hrs (log_2 fold change)		Difference	
			Control	Test		Control	Test	1 hr	4 hrs
Immune response geans									
Q05588	Urokinase plasminogen activator surface receptor precursor (uPAR) (CD87 antigen)		-0.6 (-0.93, -0.3)	-1.59 (-2.19, -1.00)	(NS)	-0.19 (-1.08, 0.70)	-0.93 (-1.72, -0.13)	0.96	0.74
NM_001001861	Monocyte chemotractant protein 1 (MIP 1α)	(NS)	-0.5 (-0.95, -1.5)	-1.50 (-2.39, -0.61)	(NS)	-0.91 (-1.07, -0.75)	-2.06 (-2.37, -1.74)	1.03	1.15
P55085	Proteinase activated receptor 2 precursor (PAR-2) (Thrombin receptor- like 1) (Coagulation factor II receptor-like 1)	(NS)	-0.5 (-0.62, -0.3)	-1.06 (-1.29, -0.82)	(NS)	0.62 (0.50, 0.75)	-0.18 (-0.43, 0.06)	0.61	0.80
Cell cycle regulation									
P27049	BTG2 (NGF-inducible anti-proliferative protein)	(NS)	0.43 (0.23, 0.62)	-1.33 (-2.34, -0.31)	(NS)	0.37 (-0.25, 0.99)	-0.80 (-1.37, -0.24)	1.76	1.17
Intracellular signal transduction									
NM_003311	pleckstrin homology-like domain, family A, member 2 (PHLDA2), mRNA	(NS)	-0.3 (-0.45, -0.1)	-1.06 (-1.10, -1.02)		-0.53 (-0.66, -0.40)	-1.02 (-1.15, -0.89)	0.79	0.49
P28562	Dual specificity protein phosphatase 1(MKP-1)	(NS)	-0.4 (-0.57, -0.3)	-1.20 (-1.44, -0.97)	(NS)	0.50 (-0.04, 1.04)	-0.54 (-0.63, -0.46)	0.76	1.04
P17964	Ras-related protein RAP-2b	(NS)	0.18 (-0.19, 0.56)	-0.43 (-0.69, -0.17)	(NS)	0.04 (-0.20, 0.29)	-0.55 (-0.68, -0.43)	0.61	0.59
Transcription regulation									
BC035625	Early growth response 2	(NS)	-0.1 (-0.19, 0.09)	-1.70 (-2.06, -1.34)	(NS)	0.27 (-0.25, 0.80)	-0.57 (-0.91, -0.22)	1.65	0.84
Cell surface / secreated proteins									
A48149	Tumor-associated calcium signal transducer 2	(NS)	-0.1 (-0.18, -0.00)	-0.81 (-1.11, -0.52)	(NS)	0.40 (0.29, 0.50)	-0.71 (-0.85, -0.57)	0.70	1.11
Q92692	CD112 antigen		0.4 (0.30, 0.50)	-0.24 (-0.56, 0.07)	(NS)	0.24 (-0.18, 0.65)	-0.36 (-0.81, 0.09)	0.64	0.60
Cell motility / migration									
NM_152754	Semaphorin 3D precursor (SEMA3D)		0.79 (0.55, 1.03)	0.13 (-0.35, 0.60)	(NS)	0.30 (-0.01, 0.62)	-0.43 (-0.67, -0.18)	0.66	0.73
NM_004776	UDP-Gal:betaGlcNAc beta 1,4- galactosyltransferase, polypeptide 5 (B4GALT5)	(NS)	0.62 (0.36, 0.87)	0.05 (-0.22, 0.32)	(NS)	0.24 (-0.06, 0.54)	-0.48 (-0.69, -0.27)	0.57	0.72
Macromolecule metabolism									
Z14136	Spermidine/spermine N1-acetyltransferase	(NS)	0.38 (0.03, 0.72)	-0.80 (-1.10, -0.50)	(NS)	-0.48 (-0.76, -0.19)	-1.13 (-1.6, -0.66)	1.18	0.65
Hypothetical protein / Unknown function									
NM_019058	DNA-damage-inducible transcript 4	(NS)	-0.1 (-0.20, -0.00)	-0.85 (-1.07, -0.63)		-0.59 (-0.84, -0.34)	-1.33 (-1.71, -0.94)	0.74	0.74

Continued on following page

Table 5.3 IPAM cells treated with either recombinant baculovirus expressing the A238L gene (Test) or control baculovirus (Control), were stimulated with LPS (100μg/ml). PMA (100 nM) and Ionomycine (4 μM). Total RNA was harvested at both 1 and 4 hrs post stimulation. mRNA was then amplified and labelled with either Cy3 or Cy5 dyes. Samples from control and test treatment conditions were hybridised to separate arrays with a common reference sample in the second channel. Data sets were analysed using TIGR software and genes differentially regulated by A238L were identified using a using a two class paired Significant Analysis of Microarrays (SAM) analysis (δ = 0.498). Annotated genes that are regulated by A238L at both one and four hours post stimulation are presented in this table. The data presented is the log ratio of the experimental sample to the common reference. Mean values from 3 individual experiments are followed by the 95% confidence interval within brackets. The difference between these two values is presented for both 1 and 4 hrs as a log ratio (logs are taken to base 2, so a value of 1 represents a 2-fold change in gene expression between the test and control sample). Genes that had not previously been shown to be significantly up or down regulated by treatment with LPS, PMA and ionomycine (Chapter 4, tables 1, 2 and 3), are indicated by the presence of the letters NS (Not Stimulated) in brackets. Accession No.are taken from the Pig Genome Oligo Set and Extension V1.0 gene list (Operon).

Table 5.4 Biological characterisation of genes regulated by A238L at 4 hrs

Accession no.	Description		4 hrs (log_2 fold change) Control		4 hrs (log_2 fold change) Test		Difference
Immune response genes							
P25063	CD24 antigen		0.75	(0.60, 0.90)	0.16	(0.07, 0.24)	0.59
P10124	Secretory granule proteoglycan core protein precursor	(NS)	0.16	(-0.46, 0.78)	-0.67	(-1.02, -0.32)	0.83
Apoptosis							
14090240	Caspase-3	(NS)	1.74	(0.59, 2.89)	0.19	(-0.42, 0.80)	1.55
Q9NRA0	Sphingosine kinase 2(SK 2)	(NS)	0.46	(-0.34, 1.26)	-0.32	(-1.06, 0.42)	0.78
Cell cycle							
P31607	BTG1 protein (B-cell translocation gene 1 protein)	(NS)	0.76	(0.21, 1.31)	-0.12	(-0.46, 0.22)	0.88
P05979	Cyclooxygenase -1 (COX-1)	(NS)	0.48	(-0.69, 1.65)	-1.01	(-1.23, -0.78)	1.49
P05979	Prostaglandin-endoperoxide synthase 1 (PTGS1)	(NS)	-0.18	(-0.26, -0.10)	-0.80	(-0.97, -0.63)	0.62
Intracellular signal transduction							
NM_002660	Phospholipase C, gamma 1 (PLCG1)	(NS)	0.64	(0.08, 1.20)	0.08	(-0.51, 0.68)	0.56
NM_145185	Mitogen-activated protein kinase kinase 7 (MAP2K7)	(NS)	0.55	(-0.03, 1.13)	-0.43	(-1.08, 0.21)	0.98
NM_014976	Programmed cell death 11 (PDCD11)	(NS)	0.53	(0.03, 1.04)	-0.34	(-1.11, 0.44)	0.87
P39036	Alpha-S2 casein [Pig] {Sus scrofa}, complete	(NS)	0.47	(0.05, 0.89)	-1.01	(-2.67, 0.65)	1.48
9965905	synembryn	(NS)	0.77	(0.31, 1.22)	0.04	(-0.67, 0.76)	0.73
O75385	Serine/threonine-protein kinase ULK1	(NS)	0.11	(-0.13, 0.35)	-0.55	(-0.81, -0.29)	0.66
Q9Y6W6	Dual specificity protein phosphatase 10 (MKP-5)	(NS)	0.05	(-0.11, 0.20)	-1.28	(-2.17, -0.39)	1.33
O95999	B cell lymphoma/leukemia 10	(NS)	0.04	(-0.05, 0.13)	-0.51	(-0.58, -0.45)	0.55
6503078	B lymphocyte adapter protein BAM32	(NS)	-0.14	(-0.24, -0.05)	-0.84	(-1.01, -0.66)	0.70
Transcription regulation / Transcription factors							
BC008965	Transcription termination factor-I interacting protein 5	(NS)	0.14	(-0.46, 0.73)	-0.66	(-1.22, -0.09)	0.80
NM_020338	Zinc finger, MIZ-type containing 1 (hZimp10)		-0.63	(-0.86, -0.40)	-1.25	(-1.38, -1.12)	0.62
Extracellular matrix proteins							
AF069643	matrix metalloproteinase 13 precursor [Sus scrofa]	(NS)	0.13	(-0.87, 1.12)	-1.27	(-2.54, 0.00)	1.40
NM_214207	Matrix metallopeptidase 7	(NS)	0.64	(0.40, 0.88)	-0.40	(-1.02, 0.22)	1.04
P26022	Pentaxin-related protein PTX3 precursor (Tumor necrosis factor- inducible protein TSG-14).	(NS)	0.36	(-0.29, 1.01)	-0.37	(-1.08, 0.35)	0.73
Cellular metabolism							
2245376	Acetyltransferase	(NS)	0.69	(0.08, 1.30)	-0.14	(-0.70, 0.42)	0.83
O43175	D-3-phosphoglycerate dehydrogenase(3-PGDH)	(NS)	0.67	(0.40, 0.93)	-0.48	(-0.75, -0.21)	1.15
Y08134	ASM-like phosphodiesterase 3b	(NS)	0.41	(0.27, 0.55)	-0.17	(-0.31, -0.04)	0.58
Amino acid metabolism							
15281140	Arginase I	(NS)	-0.71	(-1.01, -0.40)	-1.41	(-1.99, -0.83)	0.70
BC012181	Furin (paired basic amino acid cleaving enzyme)	(NS)	0.79	(0.01,1.57)	-0.16	(-0.98, 0.66)	0.95
NM_022132	Methylcrotonyl-CoA carboxylase beta chain	(NS)	-0.05	(-0.24, 0.14)	-0.52	(-0.72, -0.32)	0.47
Protein ubiquination							
18700319	F-box domain Fbx25-containing protein	(NS)	0.40	(0.03, 0.76)	-0.50	(-0.93, -0.07)	0.90
Transporter activity							
BC049385	Solute carrier family 5 member 11	(NS)	0.75	(0.11, 1.39)	0.11	(-0.36, 0.59)	0.64

Continued on following page

Table 5. 4 - continued

Accession no.	Description	4 hrs (log_2 fold change)					Difference
			Control		Test		
Q28996	Steroidogenic acute regulatory protein (StAR)	(NS)	0.65	(-0.49, 1.78)	-0.55	(-1.48, 0.37)	1.20
AY027799	Ca2+ ATPase of fast twitch 1 skeletal muscle sarcoplasmic reticulum	(NS)	0.67	(0.15, 1.19)	-0.17	(-1.01, 0.66)	0.84
Macromolecule metabolism							
P79401	Cytochrome P450 3A29(CYPIIIA29)	(NS)	0.17	(0.03, 0.30)	-0.69	(-0.96, -0.41)	0.86
hypothetical protein / unknown function							
JC5964	Apoptosis inhibitor	(NS)	0.17	(-0.51, 0.86)	-0.63	(-0.90, -0.35)	0.80
NM_005656	Transmembrane protease, serine 2 (TMPRSS2)	(NS)	-0.77	(-1.79, 0.25)	-1.73	(-2.91, -0.56)	0.96
22137752	Calcium binding protein 39	(NS)	0.37	(-0.26, 0.99)	-0.38	(-1.08, 0.32)	0.75

IPAM cells treated with either recombinant baculovirus expressing the A238L gene (Test) or control baculovirus (Control) were stimulated with LPS (100μg/ml). PMA (100 nM) and Ionomycine (4 μM). Total RNA was harvested at both 1 and 4 hrs post stimulation. mRNA was then amplified and labelled with either Cy3 or Cy5 dyes. Samples from control and test treatment conditions were hybridised to separate arrays with a common reference sample in the second channel. Data sets were analysed using TIGR software and genes differentially regulated by A238L were identified using a using a two class paired Significant Analysis of Microarrays (SAM) analysis (δ = 0.498). Annotated genes that are regulated by A238L at four hours post stimulation only are presented in this table. The data presented is the log ratio of the experimental sample to the common reference. Mean values from 3 individual experiments are followed by the 95% confidence interval within brackets. The difference between these two values is presented for both 1 and 4 hrs as a log ratio (logs are taken to base 2, so a value of 1 represents a 2-fold change in gene expression between the test and control sample). Genes that had not previously been shown to be significantly up or down regulated by treatment with LPS, PMA and ionomycine (Chapter 4, tables 1, 2 and 3), are indicated by the presence of the letters NS (Not Stimulated) in brackets. Accession No. are taken from the Pig Genome Oligo Set and Extension V1.0 gene list (Operon).

Genes involved in mediating programmed cell death in response to cellular stress, including DNA damage, were also shown to be down-regulated by A238L. This group contained both pro and anti-apoptotic genes. GADD45beta, SNF1-like kinase kinase (NUAK2) and baculoviral IAP repeat-containing 3(BIRC3) are all NF-κB regulated anti-apoptotic proteins (Legembre *et al.*, 2004; Wang *et al.*, 1998; Zhang *et al.*, 2006a), whereas GADD45 alpha, Promyeloytic Leukemia (PML-1) and Caspase 3 are pro-apoptotic. Unlike A238L regulated anti-apoptotic genes, the regulation of these pro-apoptotic genes is associated with a number of different transcription factors. C-jun is one of the transcription factors involved in the transcriptional activation of GADD45 α, STAT 1 and IFR 1 are involved in transcriptional activation of caspase 3 expression and IFN regulatory factor 3 induces PML transcription (Chen *et al.*, 2001a; Earnshaw *et al.*, 1999; Kim *et al.*, 2007).

Proportionally (36/137) the largest number of genes regulated by A238L were involved in intracellular signal transduction and transcription (Table 5.1). These categories included a significant number of genes directly involved in regulating the NF-κB and the MAPK signaling cascade. The expression profile of selected genes belonging to these categories is presented in Table 5.6. These genes are disscussed in more detail below.

PML, IκB-α, Programmed cell death 11 protein and B cell lymphoma/leukemia 10 all target NF-κB regulated transcription. Programmed cell death 11 protein and Bcl10 both positively regulate the IKK leading to the phosphorylation and subsequent degradation of IκB-α, thereby allowing NF-κB to translocate to the nucleus and initiate gene transcription (Dennis *et al.*, 2003; Yeh *et al.*, 2006). In contrast IκB-α binds to and inhibits the activity of the p50/p65 NF-kB heterodimer retaining it in a predominantly cytoplasmic location. B cell lymphoma/leukemia 10 and IκB-α are both up-regulated by NF-κB, however Bcl10 requires additional modification to be functionally active (Carlotti *et al.*, 2000; Yeh *et al.*, 2006). IκB α provides a negative feedback mechanism

Table 5.5 Selected A238L regulated genes involved in the immune response and apoptosis

Accession no.	Description	1 hr (log_2 fold change)		4 hrs (log_2 fold change)		Difference	
		Control	Test	Control	Test	1 hr	4 hrs
Immune response genes							
Q29118	Granulocyte-macrophage colony-stimulating factor	-1.21 (-1.57, -0.86)	-2.00 (-2.37, -1.63)			0.79	
P18430	Interleukin-1 alpha precursor	-0.57 (-1.86, 0.72)	-2.22 (-2.82, -1.61)			1.65	
Q01151	CD83 antigen precursor	-0.47 (-0.98, 0.03)	-1.12 (-1.65, -0.59)			0.65	
NM_001007595	Nuclear localized factor 2 (NLF2)	-0.18 (-0.50, 0.14)	-1.23 (-1.55, -0.92)			1.05	
NM_001001861	Monocyte chemotractant protein 1 (MCP 1)	-0.5 (-0.95, -1.5)	-1.50 (-2.39, -0.61)	-0.91 (-1.07, -0.75)	-2.06 (-2.37, -1.74)	1.03	1.15
NM_006820	Interferon-induced protein 44-like (IFI44L)	0.92 (0.77, 1.06)	0.16 (-0.02, 0.34)			0.76	
P09914	Interferon-induced protein with tetratricopeptide repeats 1	0.01 (-0.47, 0.49)	-1.56 (-1.97, -1.15)			1.57	
28798059	Interferon regulatory factor 1	-0.11 (-0.39, 0.17)	-1.02 (-1.35, -0.70)			0.91	
Q05588	Urokinase plasminogen activator surface receptor (uPAR)	-0.6 (-0.93, -0.3)	-1.59 (-2.19, -1.00)	-0.19 (-1.08, 0.70)	-0.93 (-1.72, -0.13)	0.96	0.74
177872	Alpha-2-macroglobulin	1.34 (1.21, 1.46)	0.60 (0.52, 0.68)			0.74	
904141	Protein S	0.51 (0.43, 0.60)	-0.03 (-0.17, 0.11)			0.54	
P55085	Coagulation factor II receptor-like 1	-0.5 (-0.62, -0.3)	-1.06 (-1.29, -0.82)	0.62 (0.50, 0.75)	-0.18 (-0.43, 0.06)	0.61	0.80
Apoptosis							
NM_033240	Promyelocytic leukemia (PML)	0.33 (-0.16, 0.82)	-0.75 (-0.93, -0.56)			1.08	
O75293	GADD45 beta	-0.78 (-0.81, -0.75)	-1.39 (-1.48, -1.30)			0.61	
P24522	GADD45 alpha	-0.16 (-0.34, 0.01)	-0.89 (-1.19, -0.60)			0.73	
NM_030952	SNF1-like kinase kinase (NUAK2)	0.26 (0.03, 0.50)	-0.70 (-1.25, -0.15)			0.96	
14090240	Caspase-3			1.74 (0.59, 2.89)	0.19 (-0.42, 0.80)		1.55

Table 5.5 Differential gene expression between IPAM cells treated with either recombinant baculovirus expressing the A238L gene (Test) or control baculovirus not expressing A238L (Control) was analysed using a porcine oligonucleotide array. Samples were compared indirectly via a common reference. Test and control baculovirus treated IPAM cells were analysed at 1 and 4 hrs following LPS, PMA and ionomycine treatment. Genes differentially regulated by A238L were identified using a using a two class paired Significant Analysis of Microarrays (SAM) analysis ($\delta = 0.498$). The data presented is the log_2 ratio of the experimental sample to the common reference. Mean values from 3 individual experiments are followed by the 95% confidence interval within brackets. The difference between these two values is presented for both 1 and 4 hrs as a log_2 ratio.

for this pathway and prevents the uncontrolled transcription of NF-κB-regulated genes. Inhibition of NF-κB activation would be expected to result in down-regulation of genes that are activated by NF-κB. Other down-regulated genes involved in suppression of NF-κB mediated gene transcription are TSC22D3 (GILZ), a transcription factor regulator involved in the anti-inflammatory effects of IL-10 and glucocorticoids in macrophages and the pro-apoptotic protein PML. Both of these proteins have been shown to bind to the p65 subunit of NF-κB suppressing NF-κB -mediated gene transcription (Berrebi *et al.*, 2003; Wu *et al.*, 2003). PML is thought to induce apoptosis through repression of the NF-κB survival pathway, by direct interaction and inhibition of Rel A/p65. Unlike IκBα these proteins are not induced by NF-κB.

A significant number of genes involved in regulating the Mitogen Activated Protein Kinase (MAPK) signaling pathway were also differentially regulated by A238L as shown in Tablesss 5.2, 5.3 and 5.4. In addition to the GO-term analysis, KEGG pathway enrichment analysis also identified significant enrichment for genes associated with the MAPK signalling pathway. This pathway is involved in regulating cell cycle progression, differentiation and programmed cell death. The MAPK signaling pathway comprises of a 3 component protein cascade: MAP kinase, kinase, kinase (MAP3K), which phosphorylates and activates a dual specific protein kinase (MAP2K) which in turn activates a MAP Kinase. Once activated MAPKs phosphorylate numerous substrate proteins including transcription factors and phospholipases. Three major MAPK pathways that have been identified in mammals: MAPK/ERK, SAPK/JNK and p38/MAPK. A238L regulated genes are associated with the MAPK/ERK, SAPK/JNK and p38/MAPK pathways, all three of which are involved in transcriptional activation of genes involved in the innate immune response (Dong *et al.*, 2002). A238L regulated genes include activators, inhibitors and downstream targets of ERK, JNK and MAPK. Figure 5.5 represents a simplified overview of these three MAPK pathways and their interaction with proteins encoded by A238L down-regulated genes

Table 5.6 Selected A238L regulated genes involved in intracellular signal transduction and transcription

Accession no.	Description	1 hr (log_2 fold change)		4 hrs (log_2 fold change)		Difference	
		Control	Test	Control	Test	1 hr	4 hrs
Nf-kB regulated gene transcription							
NM_018014	B-cell CLL/lymphoma 11A	-0.01 (-0.09, 0.07)	-0.63 (-1.02, -0.24)			0.62	
NM_033240	Promyelocytic leukemia (PML)	0.33 (-0.16, 0.82)	-0.75 (-0.93, -0.56)			1.08	
Q08353	I-kappa-B-alpha	-1.04 (-1.14, -0.94)	-2.07 (-2.47, -1.68)			1.03	
NM_004089	TSC22 domain family, member 3	0.29 (-0.06, 0.64)	-0.63 (-1.34, 0.08)			0.92	
MAPK regulated gene transcription							
BC003562	Dual specificity phosphatase 6 (DUSP6)	0.49 (0.34, 0.65)	-0.36 (-0.69, -0.02)			0.85	
P17275	Transcription factor jun-B	-0.31 (-0.48, -0.14)	-1.22 (-1.71, -0.73)			0.91	
4581531	c-Fos protein	-0.59 (-1.10, -0.08)	-2.82 (-3.57, -2.06)			2.23	
P56432	Proto-oncogene c-jun	-0.23 (-0.59, 0.13)	-1.61 (-2.07, -1.15)			1.38	
Q29031	c-myc	0.81 (0.70, 0.92)	0.29 (0.21, 0.38)			0.52	
P28562	Dual specificity protein phosphatase 1(MKP-1)	-0.40 (-0.57, -0.3)	-1.20 (-1.44, -0.97)	0.50 (-0.04, 1.04)	-0.54 (-0.63, -0.46)	0.76	1.04
NM_145185	Mitogen-activated protein kinase kinase 7 (MAP2K7)			0.55 (-0.03, 1.13)	-0.43 (-1.08, 0.21)		0.98
NM_014976	Programmed cell death 11 (PDCD11)			0.53 (0.03, 1.04)	-0.34 (-1.11, 0.44)		0.87
Q9Y6W6	Dual specificity protein phosphatase 10 (MKP-5)			0.05 (-0.11, 0.20)	-1.28 (-2.17, -0.39)		1.33

Table 5.6 Differential gene expression between IPAM cells treated with either recombinant baculovirus expressing the A238L gene (Test) or control baculovirus not expressing A238L (Control) was analysed using a porcine oligonucleotide array. Samples were compared indirectly via a common reference. Test and control baculovirus treated IPAM cells were analysed at 1 and 4 hrs following LPS, PMA and ionomycine treatment. Differentially regulated by A238L were identified using a using a two class paired Significant Analysis of Microarrays (SAM) analysis ($\delta = 0.498$). The data presented is the log_2 ratio of the experimental sample to the common reference. Mean values from 3 individual experiments are followed by the 95% confidence interval within brackets. The difference between these two values is presented for both 1 and 4 hrs as a log_2 ratio.

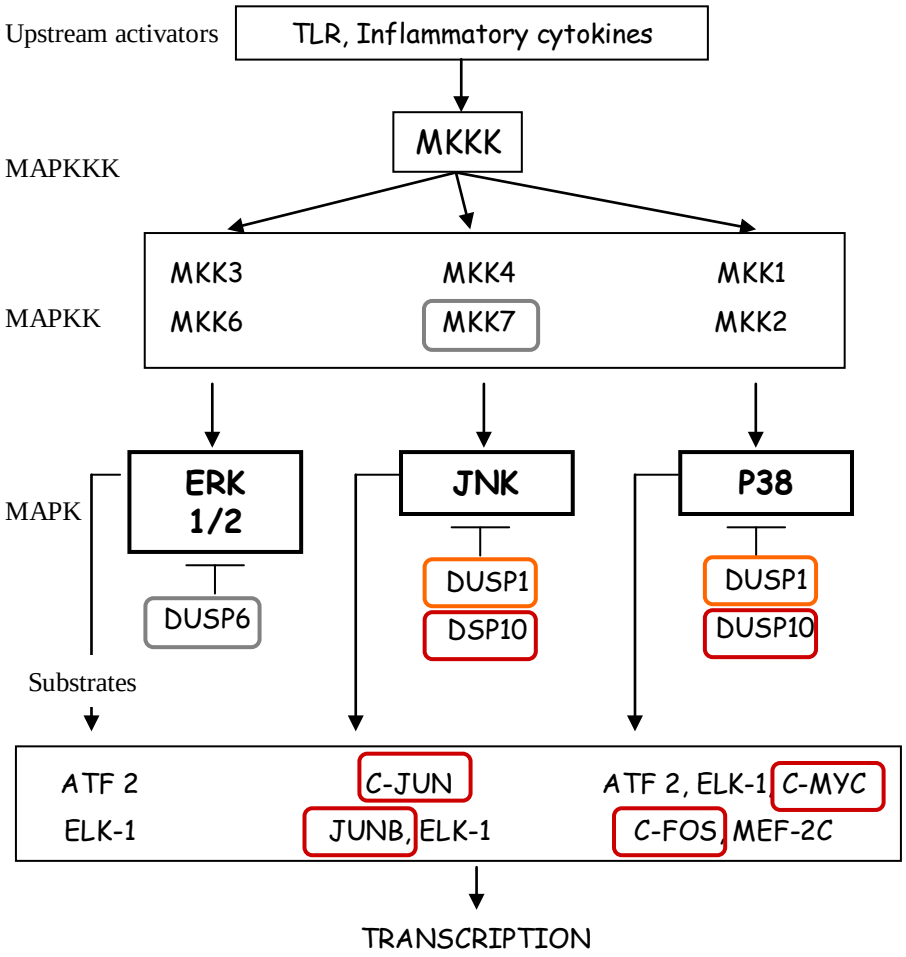

Figure 5.5 Schematic representation of the MAP Kinase signaling cascade This pathway consists of a 3 component protein cascade. Upstream activators, including ligation of the TLR and cytokine receptors, lead to the phophoralation and activation of MAP kinase, kinase, kinase (MAPKKK), which phosphorylates and activates a dual specific protein kinase (MAPKK) which in turn activates a MAP Kinase (MAPK). Once activated MAPK's phosphorylate numerous substrate proteins including transcription factors leading to gene transcription. 3 major MAPK pathways are represented: extracellular signal-regulated kinase (ERK), c-jun NH2-terminal kinase (JNK) and p38. These pathways are auto-regulated by dual-specific phosphatases (DUSP) which dephosphorylate and inactivated MAPK providing a critical negative feedback mechanism. Arrows represent direct interaction and activation of the target protein and blunt ended lines represent direct inhibition. A238L down regulated proteins are identified by coloured oblongs: genes down regulated at 1 hr only are red, 1 and 4 hrs are orange and genes down regulated at 4 hrs only are grey. Transcription of all of the A238L regulated genes is subject to auto-regulation of the MAPK signaling cascades. ATF 2, activating transcription factor 2; ELK 1, ets-like protein 1; MEF-2C, myocyte enhancer factor 2C. Adapted from Salojin et al 2007.

The activation of the mitogen-activated protein kinases, ERK, JNK and p38 is regulated through the reversible, dual phosphorylation of threonine and tyrosine residues within a conserved Thr-X-Tyr motif. The phosphorylation status of these enzymes is altered through the activity of Mitogen Activated Protein Kinase Kinases (MAP2K) and a family of dual-specificity tyrosine phosphatases (DUSP) (also known as MAPK phosphatases (MKP)). These enzymes activate and suppress the activity of MAPK signalling pathways respectively. The expression of three DUSP genes was down-regulated by A238L: DUSP1 (MKP-1), DUSP6 (MKP-3) and DUSP10 (MKP-5). These proteins are important negative-feedback regulators of MAPK signal transduction. DUSP6 gene transcription is dependent on ERK activation; following expression, DUSP6 dephosphorylates ERK inhibiting its activity (Ekerot *et al.*, 2008; Reffas & Schlegel, 2000). DUSP 10 binds to and inactivates p38 and SAPK/JNK and DUSP1 plays a critical role in the negative regulation of p38 MAPK and JNK in response to stress to promote cell survival (Wadgaonkar *et al.*, 2004; Wu & Bennett, 2005). DUSP 1 and DUSP10 gene expression is dependent on ATF 2, which is phosphorylated and activated by JNK (Teng *et al.*, 2007). The transcription factors AP1 and CREB have also been implicated in DUSP1 gene expression (Furst *et al.*, 2008). One activator of JNK, MAPKK7, was also down-regulated by A238L (Tournier *et al.*, 2001).

Several transcription factors which are activated by MAPK, and were shown to be down-regulated by A238L, are also subject to feedback regulation (c-Jun, c-fos and JunB). ERK activation leads to the rapid and transient induction of c-fos mRNA transcription by acting on the transcription factors constitutively bound to the c-fos promoter (Janknecht & Hunter, 1997). ERK then phosphorylates newly synthesised c-fos increasing its transcriptional activity (Murphy *et al.*, 2002). This dual mechanism of control is also involved in the control of c-jun by JNKs. The c-jun promoter contains several c-jun sites, therefore phosphorylation of c-jun by JNK enhances its transcriptional activity leading to an increase in its expression. c-jun is also involved in the transcription of GADD45α. This protein activates MKK4, an upstream kinase of JNK (Zhang *et al.*, 2006a). GADD45 beta and HSP72, also regulate MAPK signal

transduction, however these genes function by blocking JNK activity. GADD45 beta associates with the JNK N-terminal kinase MKK7, inhibiting its catalytic activity (Papa *et al.*, 2007) and HSP72 binds directly to JNK, blocking its activity, (Park *et al.*, 2001). HSP72 has also been implicated in suppressing ERK activation by protecting DUSP and suppressing MEK1/2 activity (Yaglom *et al.*, 2003)**.**

Nearly all of the biological categories described above contain genes with directly opposing function. In some cases the explanation for this is clear since down-regulation of activators of transcription is predicted to also down-regulate targets for these factors, including negative feedback regulators of these pathways. The ability of A238L to down-regulate so many genes with opposing functions is most likely to be the result of A238L targeting the activity of one or several common features involved in regulating the transcription of these genes.

Overall the regulation of genes suppressed by A238L was associated with several different signal transduction pathways and transcription factors. Genes induced by NF-κB, MAPK and JAK/STAT pathways are all present in Tablesss 5.2, 5.3 and 5.4. A large number of NF-κB dependent genes were present including IL-1α, GADD45 β, NF2, NUAK2, IκBα, coagulation factor 3 and uPAR (Monaco *et al.*, 2004; Warton *et al.*, 2004). NFAT dependent genes, regulated through CaN activation, were also identified within the gene lists and include MKP-1, GM-CSF and EGR-2 (Rao *et al.*, 1997). Several other transcription factors are involved in the transcription of genes down-regulated by A238L. These transcription factors are listed below with the A238L-regulated genes shown in brackets: STAT1 (IRF-1, caspase 3), CREB, (Heparin-binding EGF-like growth factor (HERPUD1), Cyr61, GADD45a, DUSP 1, JunB) (Abramovitch *et al.*, 2004), c-Jun (Alpha-2-macroglobulin, c-jun, GADD45a, DUSP 1 and DUSP 10), STAT 3 (Alpha-2-macroglobulin), ATF2 (DUSP1, DUSP 10) and IRF3 (PML). The transcription of many of the A238L regulated genes can be associated with more than one transcription factor. For example the expression of GM-CSF is dependent on cooperative binding between NFAT and the AP-1 heterodimer, Fos-Jun.

The ability of A238L to down-regulate NF-κB and NFAT dependent gene expression is not unexpected and has been described previously in Chapter 1. However the ability of A238L to regulate so many genes associated with such a diverse range of transcription factors has not previously been reported. Interestingly all of the transcription factors described above have been shown to interact with the transcriptional co-activators CBP/P300 (Garcia-Rodriguez & Rao, 1998; Janknecht & Hunter, 1996; Yoneyama *et al.*, 1998). This identifies a common link between these factors, and indicates that A238L may target CBP/P300 to inhibit gene transcription. This observation supports recent work demonstrating that A238L interacts with and inhibits CBP/P300 function (Granja *et al.*, 2006a; Granja *et al.*, 2008a; Granja *et al.*, 2006c).

5.3 Discussion

A238L is known to inhibit the activity of several cellular proteins involved in gene transcription including NF-κB, CaN and most recently, p300. Therefore A238L has the potential to effect the transcription of a large number of cellular genes. Previous work on A238L has been limited to investigating the effect of this protein on individual immune response genes and specific transcription factors. The aim of this chapter was to examine the global effect of A238L on host macrophage gene expression.

Differential gene expression between an immortalised porcine macrophage cell line expressing A238L and control cells was compared using a porcine oligonucleotide microarray. This microarray was produced using the Array-Ready Oligo Sets™ for the Pig Genome, version 1.0 and the Pig Genome Oligo extension Set, Version 1.0. An additional set of 360 oligonucleotides specific for genes present on the Pig 3K Immune cDNA (Zhang F et al 2006), but not identified within the Operon Oligonucleotide sets were also produced by Operon and included on this array. This array contains 13,657 oligonucleotides representing all currently known *Sus scrofa* gene sequences with a hit to human, mouse, or pig gene transcripts and a number of sequences containing a 3’

expressed sequence Tag (EST). Using this approach it was possible to investigate the effect of A238L in its natural host species and target cell type.

The results presented in this chapter demonstrated that A238L was a potent inhibitor of gene transcription, targeting many genes associated with the inducible response to cellular stress. A238L was shown to differentially regulate the expression of porcine mRNAs targeted by a total of 294 unique oligonucleotides over two time points following cell stimulation. Cells were treated with LPS, PMA and ionomycin to activate NF-κB, PKC and CaN dependent signalling pathways respectively. This data set translated to a final gene list of 132 unique annotated genes. A large proportion of these annotated genes were found to be inducible in response to cell stimulation, and a number of genes were associated with NF-κB, MAPK and NFAT transcription activation consistent with LPS, PMA and ionomycin treatment. However, surprisingly, comparisons between this data set and the results presented in chapter 4 demonstrated that the majority of genes regulated by A238L in IPAM cells were not found to be up-regulated by baculovirus, LPS, PMA and ionomycin treatment. This result indicates that genes associated with these pathways are constitutively activated in IPAM cells, and is consistent with other data presented in chapter 4 demonstrating the presence of NF-κB and NFAT regulated gene transcripts, TNF α, COX-2 and IL-8, in un-treated IPAM cells.

With the exception of two oligonucleotides, which were found to be up-regulated by A238L expression at 1 hr post-stimulation, all of the remaining 292 oligonucleotides were down-regulated. This result clearly demonstrates that A238L has a fundamental role in the suppression of host gene expression. Only one of the two oligonucleotides found to be up-regulated by A238L was annotated, and is predicted to be specific for the extra cellular matrix protein collegen, type Xii, alpha. Considering the relatively small number of oligonucleotides that hybridise to RNAs up-regulated by A238L, it is quite possible that the identification of these 2 oligonucleotides is due to statistical error since approximately 10 % of the oligonucleotides identified as being significantly regulated by

A238L at 1 hr post-stimulation are predicted to be falsely significant. Overall the number of oligonucleotides identified as differentially regulated between A238L expressing and control samples is relatively small number compared to the total number of oligonucleotides analysed (292 out of 10146), indicating that A238L does not mediate a general "switch–off" of host gene transcription but is targeted to a specific sub-set of genes. This is consistent with previous work on A238L which demonstrated that A238L specifically inhibits the expression of TNF-α and IFN-α gene transcripts, but not TGF-β suggesting a specific inhibition of target genes (Powell *et al.*, 1996). In addition, A238L has been shown to inhibit the transcriptional activity of NFAT and NF-κB reporter constructs, but not Sp-1 reporter constructs (Tait *et al.*, 2000)Granja *et al.*, 2008).

The majority of target oligonucleotides which hybridised to mRNAs differentially-regulated by A238L expression were transiently down-regulated at only one of the two time points examined. Only a relatively small group of 25 RNAs hybridising to unique oligonucleotide ID's were found to be regulated at both time points post-stimulation. Similarly, the results presented in chapter 4 (examining the effect of baculovirus treatment and cell stimulation on IPAM cells) also found that the majority of differentially-regulated genes were specific to either 1 or 4 hrs post-stimulation, reflecting the rapid ability of cells to adapt to environmental changes through altering their pattern of gene expression within the cell. Recent work carried out in our laboratory using a porcine cDNA to examine the effect of ASFV infection on primary host macrophage gene expression at both early and late times post infection, demonstrated marked differences in the regulation of host genes between these time points (Zhang *et al.*, 2006b).Together these results indicate that the inhibition of host macrophage gene transcription by A238L at different time points during ASFV infection is likely to be of different biological consequence.

The final gene list of 137 unique annotated genes regulated by A238L gene expression contained genes with a wide range of cellular functions. Biological characterization of

these genes indicated that a significant proportion of these genes were associated with the cells response to stimulation and/or physiological stress. Central themes included immune response genes, immediate early genes that response to growth factors and genes associated with regulating cell mediated cell death and progression through the cell cycle in response to physiological stress such as DNA damage. Genes involved in modulating intracellular signaling cascades were also common. Some were associated with regulating NF-kB activity. However the majority were associated with modulating the MAPK signaling cascades. MAPK signaling pathways are important mediators of transcriptional responses to extracellular signals and are involved in many cellular processes including growth, differentiation, apoptosis and the immune response. Most of the genes regulated by A238L are associated with ERK, JNK and p38 MAPK pathways. ERK is mainly activated by growth factors and hormones and is associated with cell proliferation and differentiation while JNK and p38 are activated by environmental stress and pro-inflammatory cytokines. JNK activation is associated with apoptosis (Baichwal & Baeuerle, 1997). Significantly ERK, JNK and p38 are all involved in regulating the innate immune response to infection (Dong *et al.*, 2002).The ability of A238L to regulate genes induced by the MAPK and the NF-κB pathway, which are both associated with regulating the inflammatory response, apoptosis and the cell cycle, could explain the high number of A238L down-regulated genes associated with these physiological processes.

Several of the genes regulated by A238L exhibited directly opposing biological functions. This was particularly apparent for A238L regulated genes involved in apoptosis and NF-κB and MAPK pathway regulation. The MAPK pathway is known to induce the expression of both negative and positive regulators of MAPK signal transduction leading to the auto-regulation of this pathway. Therefore this result is most likely to be due to A238L targeting the activity of one or several common features involved in the transcription of these genes rather than of biological significance. In addition, the experimental approach, which involved the over-expression of A238L in an attempt to identify all of the potential effects of A238L on host cell gene transcription

may also contribute to these results. It is probable that A238L exhibits a more specific effect during ASFV infection.

It was interesting to note, that all of the A238L regulated anti-apoptotic genes, GADD45 beta, SNF1-like kinase kinase (NUAK2) and baculoviral IAP repeat-containing 3 (BIRC3) are dependent on NF-κB mediated gene transcription (Legembre *et al.*, 2004; Wang *et al.*, 1998; Zhang *et al.*, 2005). NF-κB plays an important role inhibiting cell death through the expression of anti-apoptotic genes (Baichwal & Baeuerle, 1997). Indeed PML a pro-apoptotic gene, also regulated by A238L, induces apoptosis through the direct inhibition of NF-κB function. A238L is a known inhibitor of NF-κB mediated gene transcription, therefore the down-regulation of these anti-apoptotic genes could be predicted. ASFV encodes two proteins involved in inhibiting apoptosis: A224L and A179L. A224L is an IAP homologue that binds to and inhibits the activity of caspase 3 (Nogal *et al.*, 2001) and A179L is a viral Bcl-2 homologue which inhibits Bid induced apoptosis (Galindo *et al.*, 2008). Therefore it could be that in addition to inhibiting apoptosis induced through activation of the host immune response these proteins also function to counteract the pro-apoptotic effects of A238L. Interestingly, A238L also has the potential to inhibit apoptosis through inhibition of CaN. CaN dephosphorylates the pro-apoptotic Bcl-2 family protein BAD leading to its activation (Wang *et al.*, 1999). CaN inhibition by A238L could therefore inhibit apoptosis induced by BAD. Although viruses are required to inhibit apoptosis at early times during infection in order to replicate, at later times post-infection induction of apoptosis may possibly be an advantage for virus spread.

The results presented in this chapter demonstrate that A238L is able to suppress the expression of a large number of genes, regulated by wide range of transcription factors in addition to NFAT and NF-kB. All of the transcription factors identified interact with the transcription co-activator CBP/P300. In addition, recent work on A238L has proposed that A238L inhibits transcriptional activation mediated by NF-kB, NFAT and c-jun via a common mechanism involving the transcriptional co-activator CBP/P300

(Granja *et al.*, 2006a; Granja *et al.*, 2008a; Granja *et al.*, 2006c). Together these results provide strong evidence for the role of A238L as a potent inhibitor of gene expression which acts through CBP/P300 to regulate host macrophage gene expression.

Chapter 6

A238L is actively imported into the nucleus and exported by a CRM1 mediated pathway

6.1 Introduction

Previous work carried out in our laboratory has shown that the A238L protein fused to a 14 aa N-terminal Pk epitopetag is present in the both the nucleus and cytoplasm of infected cells at late times post-infection with ASFV (Bowick, 2004). In addition, recent work has demonstrated that A238L can be found in both the cytoplasm and nucleus of ASFV infected porcine alveolar macrophages and in Jurkat T cells stably expressing A238L (Granja *et al.*, 2006a). Together these data suggests that A238L may function within both the cytoplasm and nucleus of infected cells. However, a detailed study into the nuclear translocation of A238L has not been carried out.

The control of the subcellular localisation of proteins through regulation of their nuclear/cytoplamic transport can have a significant impact on protein function. Indeed many transcription factors, including NF-κB and NFAT are partially regulated through altering their subcellular localisation within the cell (Ghosh & Karin, 2002; Rao *et al.*, 1997). The aim of this chapter is to explore the mechanisms involved in the nuclear transport of A238L and to establish if A238L is retained in the nucleus or is actively exported from the nucleus.

6.2 Results

6.2.1 A238L is exported from the nucleus by a CRM-1 mediated pathway.

The active transport of molecules out of the nucleus typically involves interaction with carrier proteins, called exportins. CRM-1, also known as exportin-1, is a well

characterised nuclear export factor responsible for the export of numerous cellular and viral proteins. To investigate if A238L is exported from the nucleus *via* the CRM-1 pathway, the sub-cellular localisation of A238L was examined in the presence of Leptomycin B (LMB). LMB a specific inhibitor of the CRM-1 dependent nuclear export pathway and binds directly to CRM-1 inhibiting its interaction with target proteins (Kudo et al., 1998).

Levels of A238L expressed in Vero cells infected with the recombinant ASFV , Sv5GaL, which contains an SV5 Pk-tagged A238L gene (Miskin *et al.*, 1998) were low and difficult to detect using immunofluorescence microscopy (section 3.2.7). Therefore to produce detectable levels of A238L, Vero cells were transfected with a plasmid containing Pk-tagged A238L gene under the control of the A238L promoter (pFlanks-SV5A238L) and then infected with the ASFV isolate BA71V. This plasmid has been described previously (Miskin et al., 1998). At 3 hrs prior to fixation the cells were treated with LMB or were untreated, in either the presence or absence of PMA and LPS. Cells transfected with a plasmid containing Pk-tagged IκB-α were used as a positive control for LMB: IκB-α contains a CRM-1 dependent nuclear export signal and has previously been shown to accumulate exclusively in the nucleus in the presence of LMB (Huang et al., 2000). These cells were treated with PMA/LPS to activate NF-κB and enhance IκB-α nuclear import. Due to the predicted similarity between A238L and cellular IκB-α (Revilla *et al.*, 1998) the effect of PMA and LPS treatment on A238L was also examined. At 8 and 16 hrs post-infection the cells were fixed, permeabilised and stained with an antibody specific to the Pktag followed by a fluorescently labelled secondary antibody. Cells were then examined using confocal microscopy and the sub-cellular localisation of A238L determined.

As shown in Figure 6.1 (a), in cells stimulated with PMA/LPS, in the presence of LMB all of the IκB-α was present in the nucleus as expected. In the absence of LMB, although most of the IκB-α was in the nucleus, a small amount was present in the cytoplasm. This

is consistent with the nuclear export of IκB-α via the CRM-1 mediated pathway, and shows that the LMB is functionally active.

In ASFV infected cells expressing A238L under the control of its own promoter, A238L exhibited a distribution which could be characterised into three distinct patterns of sub-cellular localisation. These were either: preferentially nuclear, a uniform distribution throughout the cytoplasm and nucleus, or preferentially cytoplasmic (see Figure 6.1 (b)). One hundred cells were scored for the above three cellular distributions for each experimental condition and in three independent experiments. To avoid bias a number of slides were analyzed blind and the results were verified by an impartial research scientist. In the presence of LMB, at both 8 and 16 hrs post-infection, there was a significant increase in the number of cells exhibiting a predominantly nuclear localization compared to in the absence of LMB (approximately 50 % compared to less than 10 %) (Figure 6.2). This demonstrates that at least a proportion of the nuclear A238L is exported to the cytoplasm using the CRM-1 nuclear export pathway. In the cells treated with LMB, although A238L was predominantly present in the nucleus in more cells, nevertheless in approximately half of the cells treated with LMB A238L exhibited an even distribution of A238L throughout the nucleus and cytoplasm. Possibly a proportion of A238L is either not imported into the nucleus and remains in the cytoplasm, or if it is imported into the nucleus and it is then exported using a CRM-1 independent nuclear export pathway.

No difference was observed in the distribution of A238L in PMA and LPS treated cells compared to untreated cells. This result could indicate that, unlike IκB-α, the subcellular distribution of A238L is not dependent on NF-κB activation. However, this result is not conclusive as infection of cells with ASFV, even in the absence of LPS and PMA treatment, is likely to activate several cell signaling pathways including NF-κB (Powell *et al.*, 1996). The results from these experiments demonstrate that A238L is actively exported from the nucleus by a CRM-1 dependent pathway.

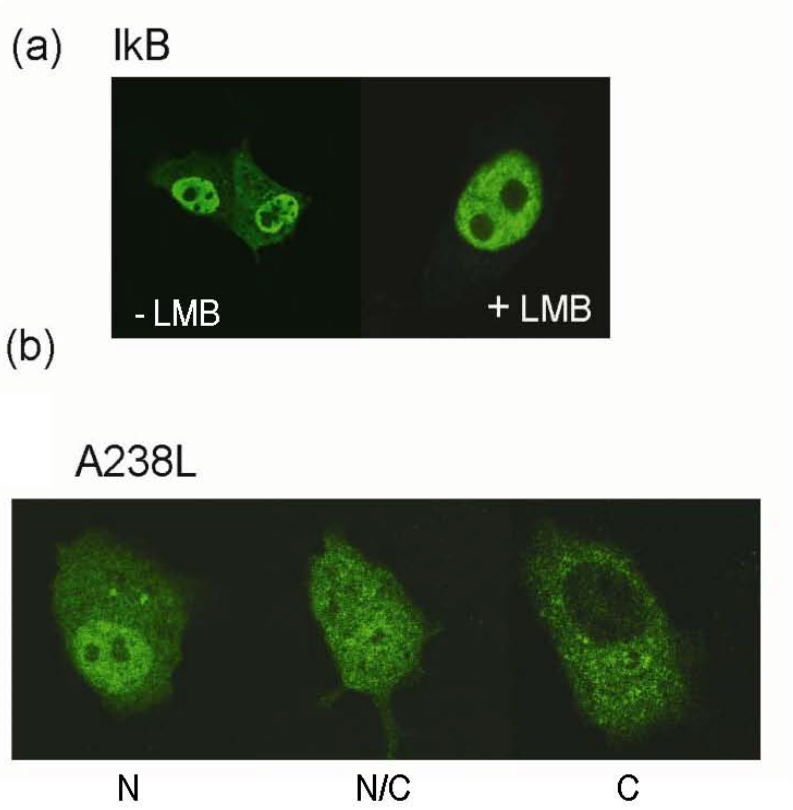

Figure 6.1. A238L is exported from the nucleus by a CRM1 mediated pathway. Panel (a) shows Vero cells which were transfected for 16 hrs with a plasmid expressing SV5-tagged IκB-α. 3 hrs prior to fixation the cells were treated with LPS (10 µg/ml) and PMA (100 nM) in the presence(+) or absence(-) of LMB (40nM). Panel (b) shows BA71V infected Vero cells expressing SV5-tagged A238L under the control of its own promoter. For both panels PK-tagged proteins, shown in green, were detected with anti-PK antibody (Sertoc). The sub-cellular localisation of PK-tagged A238L was characterised as either, preferentially nuclear (N), both nuclear and cytoplasmic (N/C) or preferentially cytoplasmic (C). Representative images are shown.

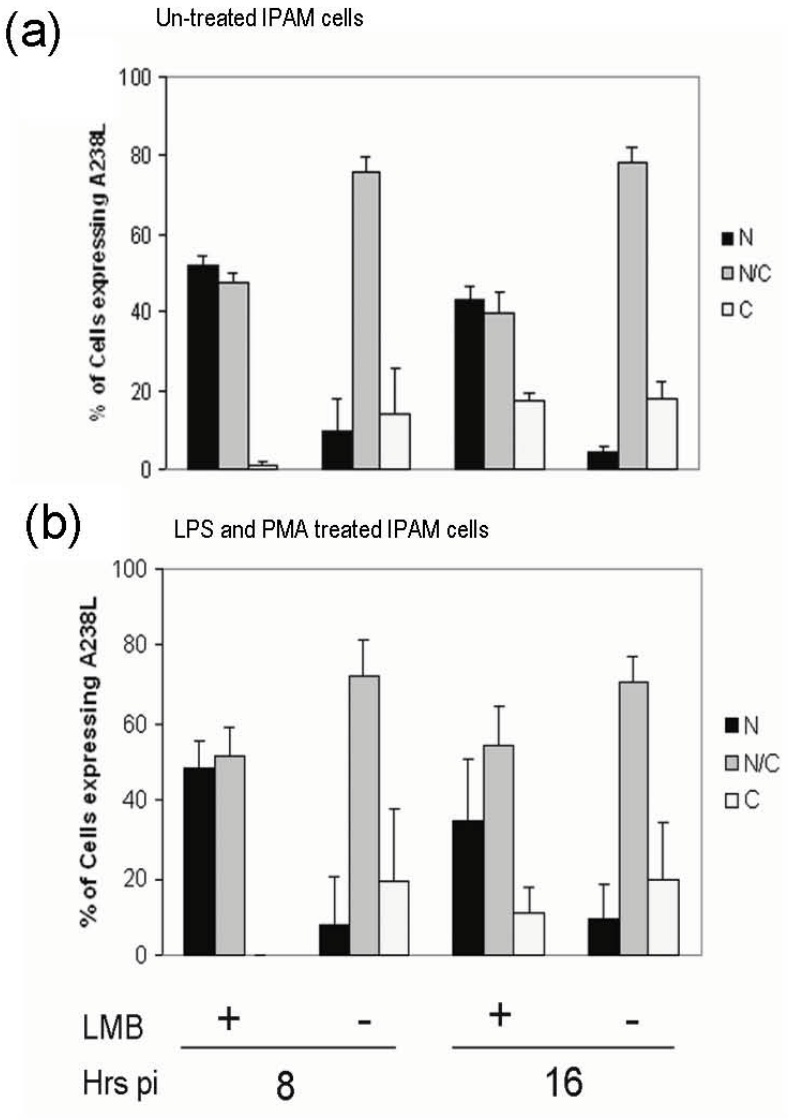

Figure 6.3 A238L is exported from the nucleus by a CRM1 mediated pathway. ASFV infected Vero cells expressing PK-tagged A238L under the control of it's promoter were treated with (a) or without (b) LPS (10 µg/ml) and PMA (100 nM) in the presence or absence of LMB (40nM). SV5-tagged A238L was detected by indirect immunofluorescence and imaged using confocal microscopy. The percent of cells exhibiting either N, N/C or C phenotype was determined for each condition tested. Panel (a) shows data collected from untreated cells and panel (b) shows data collected from cells treated with LPS and PMA. Data presented is the mean (+S.D) of three independent experiments.

6.2.2 Nuclear import of A238L occurs by an energy dependent process.

Following translation, proteins are imported into the nucleus through the nuclear pore complex. This process can occur by either active transport or passive diffusion. The diffusion exclusion limit of the nuclear pore complex is approximately 60 kDa, therefore passive diffusion of proteins can only occur if the molecular weight is below this limit. Since both forms of A238L are less than 60 kDa in size and could therefore enter the nucleus by diffusion, an additional experiment was carried out to determine if A238L is actively imported into the nucleus. This involved comparison of the sub-cellular localisation of A238L at 37 °C and 4 °C. At 4 °C all active transport processes are blocked, whereas the rate of diffusion is reduced but not inhibited. In addition, to determine if the nuclear pool of A238L resulted from import of existing cytoplasmic A238L or if new synthesis of A238L protein was required for transport into the nucleus, cells were also treated with cycloheximide to prevent de-novo protein synthesis. From Figure 6.3 it can be seen that in the majority of cells incubated at 4 ^{o}C, A238L was observed to be evenly distributed between the nucleus and cytoplasm, in both the presence and absence of LMB, demonstrating that A238L is able to passively diffuse between the cytoplasm and nucleus. However, when cells were incubated at 37 ^{o}C, the results were dramatically different: A238L exhibited a predominantly nuclear localisation in almost 50 % of the cells examined. This suggests that although passive diffusion may play a role in the nuclear accumulation of A238L, an additional active nuclear transport process is involved.

No significant difference in the distribution of A238L between cells treated with cycloheximide compared to untreated cells was detected (Figure 6.3). This demonstrates that new protein synthesis was not necessary for the nuclear accumulation of A238L and indicates that a pool of pre-existing cytoplasmic A238L is actively imported into the nucleus.

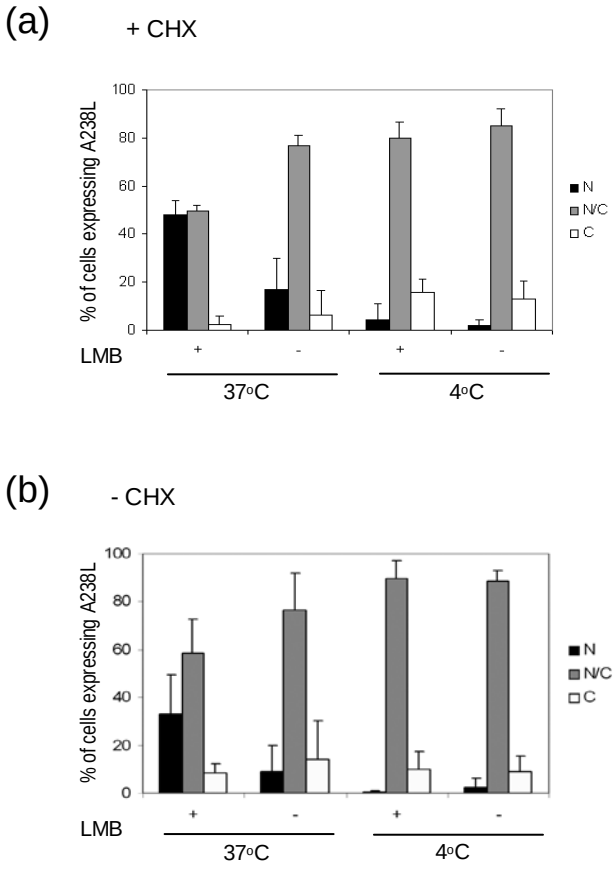

Figure 6.3 Movement of A238L is energy dependent. ASFV infected Vero cells expressing PK-tagged A238L under the control of it's promoter were treated with CHX (100 µg/ml) or were left untreated. 3 hrs prior to fixation the cells were treated with or without LMB (40 nM) and incubated at either 37°C or 4°C. PK-tagged A238L was detected by indirect immunofluorescence and imaged using confocal microscopy. The percent of cells exhibiting either N, N/C or C phenotype was determined for each condition tested. Data represents an average of 3 independent experiments (+ SD). Panel (a) shows data collected from cells treated with CHX and panel (b) shows data from untreated cells.

6.2.3 The role of putative nuclear localisation signals in A238L nuclear translocation

Most proteins that are actively transported between the nucleus and cytoplasm contain specific sequences required for interaction with the cellular import and export apparatus. Nuclear localization (NLS) signals typically consist of short mono or bi-partite stretches of amino acids that are highly enriched in basic residues. Typical nuclear export signals (NES) consist of short leucine rich motifs. Sequence analysis of A238L using PSORT (Horton, 2006), a computer program which predicts possible sub-cellular localisation motifs, identified two putative NLSs. These NLSs consist of a single short stretch of amino acids, highly enriched in basic residues. One of these (NLS-1) is located close to the N-terminus of A238L towards the C-terminal end of the first ankrin repeat domain and includes amino acids 80 to 86 (PHRRDKD). The second (NLS-2) includes amino acids 202 to 206, and is located close to the C-terminus within the PxIxITxC/S calcinurin binding domain. NLS-2 comprises of two short overlapping NLS sequences (KKKPK). Mapping these motifs onto a predicted structure of A238L, generated by Dr David Chapman, suggests that both NLS-1 and NLS-2 are located on exposed sites at the surface of the A238L protein and therefore have the potential to be to be functionally active (Figure 6.4). No typical nuclear export signals were identified using this program. This suggests that A238L may contain atypical CRM-1 nuclear export sites or is potentially exported in association with another protein.

To determine if the predicted nuclear localisation signals NLS1 and NLS2 were involved in the nuclear localisation of A238L, the sub-cellular localisation of A238L proteins containing mutations within either or both NLS1 and NLS2 was examined.

Plasmids expressing Pk-tagged A238L under the control of its own promoter and containing mutations within the CaN binding motif have been described previously

(a)

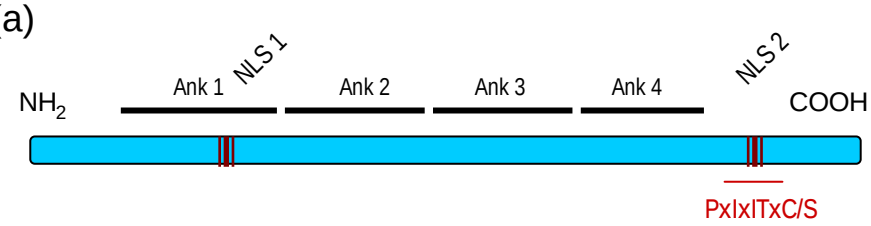

(b)

NLS 1 (aa 80 - 86)

PHRRDKD

NLS 2 (aa 202 - 206)

KKKPK

(c)

Figure 6.4 Schematic representation of A238L. Panel (A) represents the A238L protein which is 238 aa in length. A238L is predicted to encode four ankrin repeat domains (Ank) (represented by solid black bars) and two putative NLS, 1 and 2 (represented by three red stripes). A238L also contains a CaN binding motif located at the C-terminus and depicted in red. Diagram is not to scale. Panel (B) is the aa sequence of the predicted NLS1 and NLS2. Panel (C) is a 3 dimensional model of the predicted structure of the A238L protein based on it's similarity with IkBa. NLS1 and NLS2 are shown in yellow. This diagram is courtesy of Dr D. Chapman, Institute of Animal Health.

(Miskin *et al.*, 2000b). Due to the predicted location of NLS-2, within the CaN binding domain of A238L, some of these plasmids also contain mutations within the NLS-2. Plasmids W13-A238L and B19-A238L contain detrimental mutations within the predicted NLS-2. Plasmid W20-A238L contains a P to S mutation within NLS-2 however this is not predicted to disrupt NLS-2. W13-A238L and W20-A238L proteins do not bind to CaN whereas WT-A238L and B19-A238L proteins are CaN binding (Table 6.1).

A plasmid containing mutations within NLS-1 has also been produced previously (Chapman, unpublished). This plasmid (pcDNA3-A238L 84-88) encodes four valines at amino acid residues 84 to 88, instead of the wild type sequence, DKDG. Analysis of this mutant sequence using PSORT failed to identify the presence of a NLS at amino acids 80 to 86. Therefore the mutation of the amino acid residues 84, 85 and 86 within NLS 1 was considered to be sufficient to inactivate this NLS. To examine the effect of this mutation on the sub-celluar localisation of A238L in ASFV infected cells this mutant form of the A238L protein was cloned under the control of its own promoter and fused to the Pk epitope tag (pFlanks-WT-NLS-1).

To generate this plasmid the N-terminal 310 bp fragment of A238L 84-88 was amplified by PCR from pcDNA3-A238L 84-88, using forward and reverse primers containing an *Xho* I site and *EcoN* I site respectively. These sites are compatible with an *Xho* I site present at the start codon of A238L and an endogenous *EcoN* I restriction site present within the A238L gene. The resulting PCR product was then gel purified, digested with *Xho* I and *EcoN* I restriction enzymes, gel purified again and then ligated into compatible restriction sites on pFlanks-SV5A238L to generate pFlanks-WT-NLS-1. This cloning strategy is presented in Figure 6.5. To examine the effect of mutation of NLS-1 in conjunction with mutation of NLS-2 and/or the CaN binding domain, this cloning strategy was repeated to insert the 310 bp N-terminal fragment of A238L 84-88 into W13-A238L, W20-A238L and B19-A238L. The amino acid sequence of both NLS 1 and NLS 2 and the CaN binding properties of all of these plasmids are described in

A238L Construct	NLS 1 (aa 80 – 86)	NLS 2 (aa 202 – 206)	CaN Binding
WT A238L	P H R R D K D	K K K P K	Yes
W13	* * * * * * *	T T T S *	No
W20	* * * * * * *	* * * S *	No
B19	* * * * * * *	T T T * *	Yes
WT/NLS 1	* * * * V V V	* * * * *	Yes
W13/NLS 1	* * * * V V V	T T T S *	No
W20/NLS 1	* * * * V V V	* * * S *	No
B19/NLS 1	* * * * V V V	T T T * *	Yes

Table 6.1 Amino acid sequences of WT A238L and A238L constructs containing mutations within the putative nuclear localisation signals NLS 1 and NLS 2. Residues identical to the WT A238L sequence are identified by an asterix (*) and mutated residues are shown.

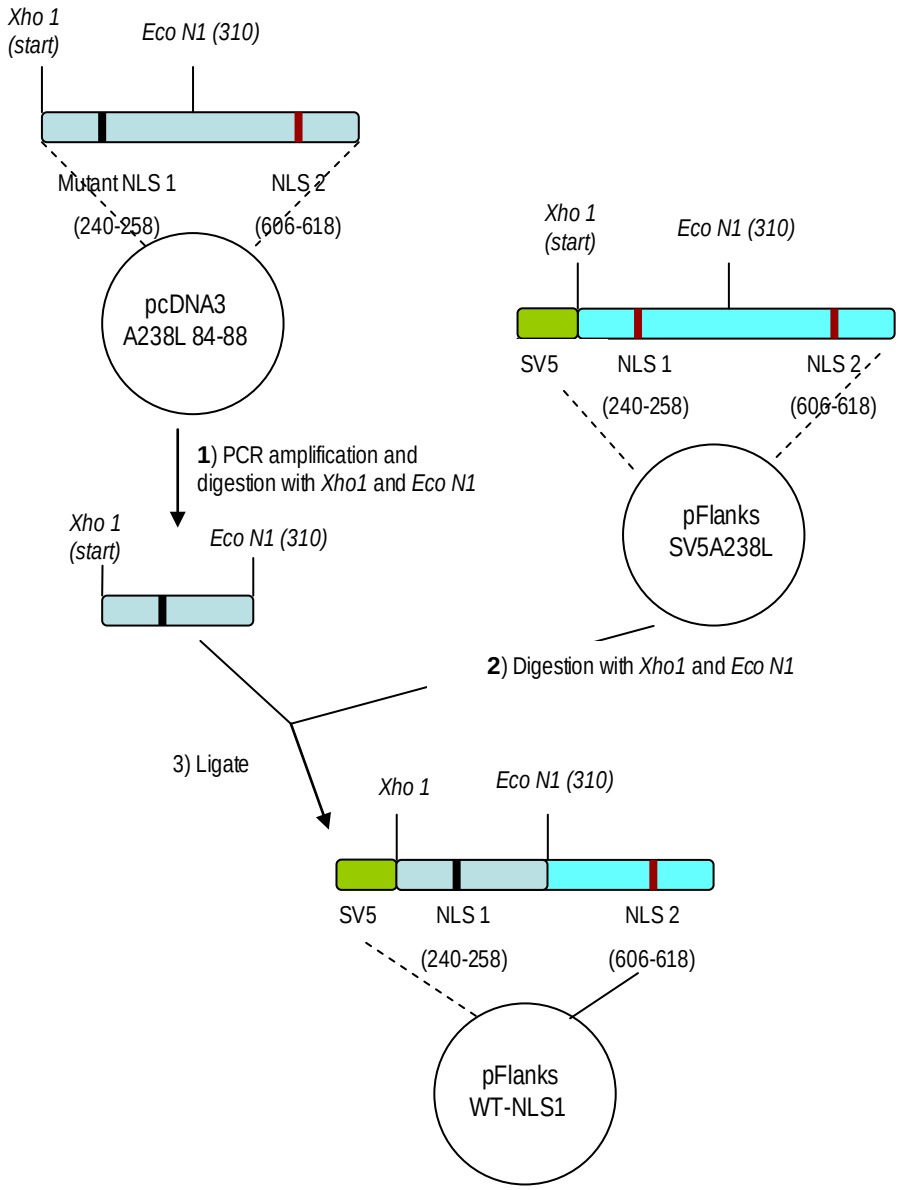

Figure. 6.5 Illustration of the cloning strategy to produce an A238L protein containing a non-functional NLS 1. PcDNA3-A238L 84-86 encodes an A238L protein which contains a mutated NLS 1.pFlanks-SV5A238L encodes an original A238L sequence fused to a pK tag at it's N-terminus. NLS are represented as vertical bars: red bars indicate a functional NLS and black bars represent a disrupted NLS. A238L is represented as a blue rectangle and the SV5 tag is in green. The position of restriction sites and the NLSs are shown along with their nucteotide postion indicated in brackets. To produce pFlanks WT-NLS1 a 310 nucleotide fragment containing the mutated NLS1 was PCR amplified from PcDNA3-A238L 84-86, digested with Xho1 and Eco N1 and then ligated into complementary restriction sites on pFlanks-SV5A238L.

Table 6.1. All the plasmids generated were sequenced to confirm the presence of the mutated bases.

To investigate the effect of these mutations on the subcellular localisation of A238L, ASFV infected Vero cells were transfected with plasmids expressing wild type or mutant A238L and examined at 16hrs post-infection by confocal microscopy. Observations were recorded in the presence or absence of LMB and this was added 3 hrs prior to fixation. The subcellular localisation of A238L was scored for 100 cells in three replicate experiments. The averages of these results for the plasmids tested are shown in Figure 6.6 and Figure 6.7. Figure 6.6 shows the effect of mutating NLS-2 on the subcellular distribution of A238L and Figure 6.7 shows the effects of mutating both NLS-1 and NLS-2.

The effect of disrupting NLS-2 alone was investigated first. NLS-2 is located within the A238L CaN binding motif. Therefore the effect inhibiting CaN binding to A238L was also investigated. The subcellular distribution of mutant A238Ls in Vero cells transfected with pflanks W13-A238L, W20-A238L and B19-A238L was compared to WT-A238L. As described previously, W13-A238L and B19-A238L are predicted to have a non-functional NLS-2 where as W20-A238L is predicted to encode a functional NLS-2. W13-A238L and W20-A238L are non-CaN binding and B19-A238L binds to CaN. All of these plasmids contain the wild type NLS-1 sequence. From Figure 6.6 it can be seen that both W13-A238L and B19-A238L showed a similar subcellular distribution to WT-A238L in both the absence and presence of LMB. This result demonstrates that disruption of the NLS 2 motif alone was not sufficient to alter the proportion of A238L which accumulates in the nucleus. This suggests that either a different or additional mechanism exists for nuclear import of A238L. Surprisingly cells transfected with a plasmid expressing the W20 protein, which has an intact NLS-2 but does not bind to CaN, showed a dramatic increase in the number of cells exhibiting a predominantly nuclear distribution compared to cells transfected with a plasmid expressing the wild type protein. The number of cells showing a predominantly nuclear

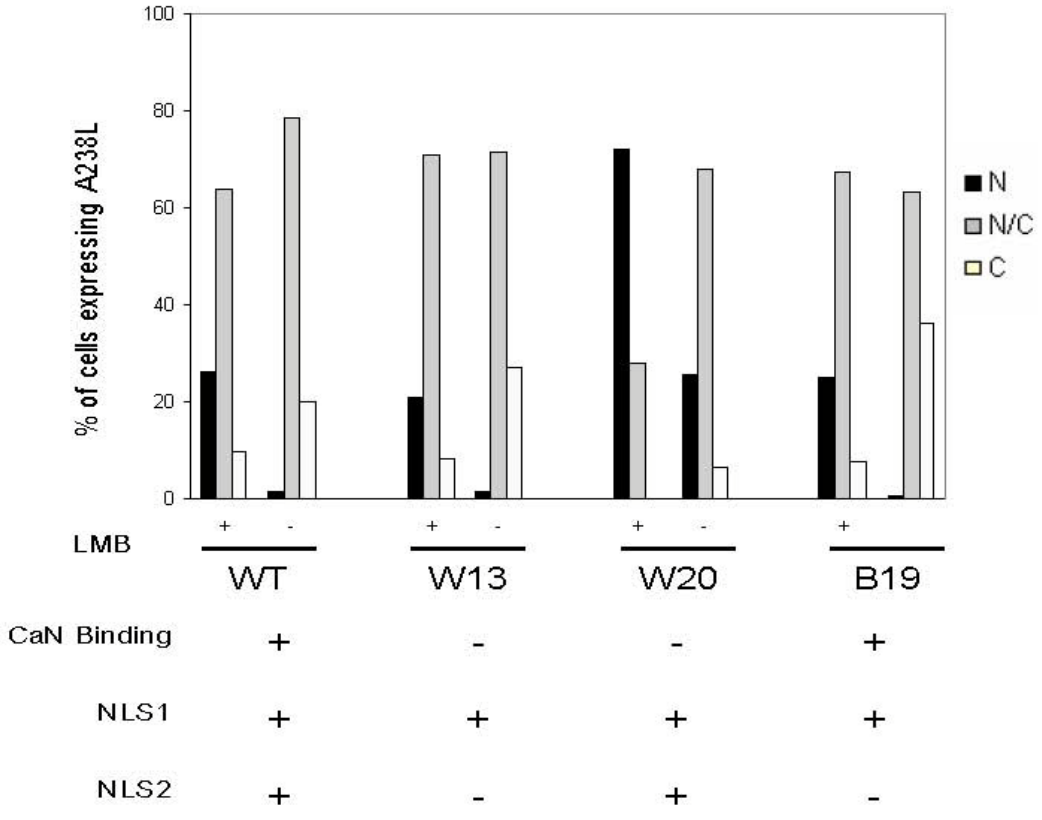

Figure 6.6 Mutation of NLS 2 does not effect its subcellular distribution of A238L. ASFV infected Vero cells expressing different versions of PK-tagged A238L under the control of it's promoter were treated with or without LMB (40 nM) 3 hrs prior to fixation. The cells were fixed at 16 hrs post infection and pk-tagged A238L was detected by indirect immunofluorescence. Cells were imaged using confocal microscopy. The percent of cells exhibiting N, N/C or C phenotype was determined for each A238L constructed tested and under each condition. Data represents an average of 3 independent experiments (+ SD). The properties of each plasmid tested are shown beneath the graph. A cross (+) represents a functional CaN binding site, NLS 1 and NLS 2 and a bar (-) represents non-functional motifs.

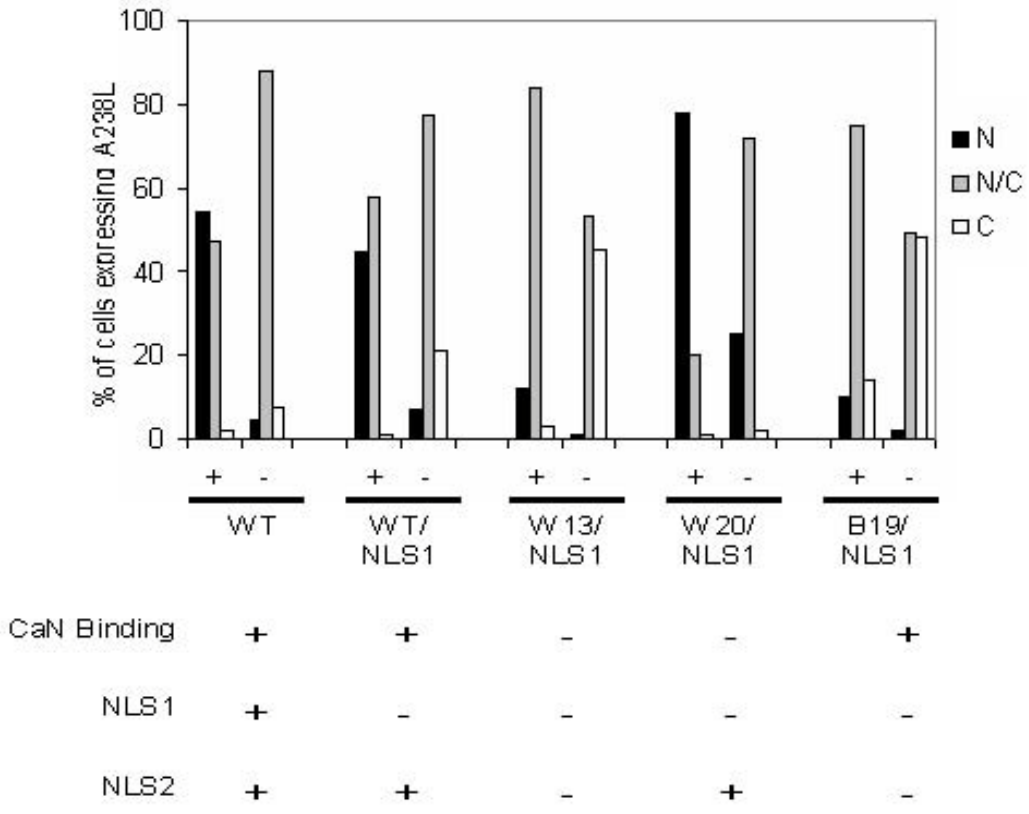

Figure 6.7 Mutation of both NLS1 and NLS2 reduces the nuclear accumulation of A238L. ASFV infected Vero cells expressing different versions of PK-tagged A238L under the control of it's promoter were treated with or without LMB (40 nM) 3 hrs prior to fixation. The cells were fixed at 16 hrs post infection and pk-tagged A238L was detected by indirect immunofluorescence. Cells were imaged using confocal microscopy. The percent of cells exhibiting N, N/C or C phenotype was determined for each A238L constructed tested and under each condition. Data represents an average of 3 independent experiments (+ SD). The properties of each plasmid tested are shown beneath the graph. A cross (+) represents a functional CaN binding site, NLS 1 and NLS 2 and a bar (-) represents non-functional motifs.

distribution, in the presence of LMB, increased from approximately 25 % for those transfected with WT-A238L compared to greater than 70 % for cells transfected with plasmid expressing W20-A238L. The number of cells showing a nuclear distribution was also significantly increased in the absence of LMB: from approximately 2 % for WT-A238L to approximately 30 % for W20-A238L. Since W20-A238L contains an intact NLS-2 sequence but does not bind to CaN, the data suggest that when A238L does not bind to CaN, significantly more A238L protein accumulates in the nucleus. A probable explanation for this result could be that the interaction between the WT-A238L and CaN masks NLS-2, and this may contribute to the retention of a proportion of A238L in the cytoplasm of cells.

The effect of mutating NLS-1 alone, and in combination with NLS-2, on the subcellular localisation of A238L was also examined. The subcellular localisation of A238L in the presence and absence of LMB was examined for 4 test plasmids which express mutant forms of the A238L protein (WT/NLS 1, W13/NLS 1, W20/NLS 1 and B19/NLS 1) and compared with WT A238L. All of the test plasmids contain a mutated NLS-1 motif. WT/NLS 1 and W20/NLS 1 contain a complete NLS2; WT/NLS1 binds CaN and W20/NLS 1 does not bind CaN. W13/NLS-1 and B19/NLS-1 both contain a mutated NLS-2; W13/NLS-1 is CaN binding and B19/NLS-1 does not bind CaN.

The results of this experiment are shown in Figure 6.7. WT/NLS-1 showed a similar subcellular distribution to WT-A238L, indicating that disruption of NLS 1 alone was not sufficient to alter the nuclear accumulation of A238L. Interestingly, disruption of NLS-1 also failed to affect the subcellular distribution of W20/NLS-1 which is also non-CaN binding, this plasmid showed a similar distribution to its parent W20 (see Figure 6.6). In both cases a significant increase was detected in the nuclear accumulation of these proteins compared to WT-A238L. In contrast to these results, plasmids W13/NLS-1 and B19/NLS-1, which contain mutations within both NLS 1 and NLS2, showed a dramatic decrease in the number of cells exhibiting a predominately nuclear distribution. In the presence of LMB, less than 15 % of the cells examined showed a predominately nuclear

distribution in cells transfected with either W13/NLS-1 or B19/NLS-1, compared to greater than 50 % for WT-A238L. In the absence of LMB, in cells transfected with these two plasmids a significantly higher proportion of cells exhibited a predominantly cytoplasmic distribution of A238L (approximately 50 %) compared to cells transfected with WT-A238L (<10 %). Therefore mutation of both of these putative NLS significantly reduced the nuclear accumulation of A238L. However, mutation of both NLS 1 and NLS 2 did not completely abolish the nuclear accumulation of A238L. Cells transfected with either W13/NLS-1 or B19/NLS-1 showed a difference in the number of cells exhibiting a nuclear and cytoplasmic distribution (N/C) between LMB treated (approximately 80 %) and untreated cells (< 60 %). These results suggest that, in addition to nuclear import mediated by NLS-1 and NLS-2, another mechanism may facilitate the nuclear localisation of A238L. It is possible that passive diffusion may contribute to the nuclear presence of A238, however this process is not effected by LMB treatment and therefore does not account for these results.

Taken together these results indicate that both NLS-1 and NLS-2 play a significant role in the nuclear localisation of A238L, and appear to act independently since loss of one NLS is compensated for by the presence of the other.

6.2.4 The cellular protein p65 is not involved in the nuclear export of A238L

No typical nuclear export signals (NES) were identified on the A238L protein using the PSORT prediction program. The possibility that A238L may be exported in conjunction with another cellular protein, the p65 subunit of NF-κB, was examined. P65 has been shown to contain a functional NES and is exported from the nucleus by a CRM-1 dependent pathway (Harhaj & Sun, 1999). In addition, A238L has previously been shown to co-precipitate with the p65 subunit of NF-κB demonstrating that the two proteins are in a complex together (Revilla *et al.*, 1998; Tait *et al.*, 2000). To investigate the effect of p65 on the cytoplasmic/nuclear shuttling of A238L, a mouse embryonic fibroblast (MEF) cell line, homozygous negative for the p65 subunit of NF-κB (p65 -/-)

was obtained from Professor Ron Hay at the University of St. Andrews. The unaltered original MEF cell line (p65 +/+) was also provided as a control.

MEF cells are not susceptible to infection with ASFV, therefore MEF p65 -/- and p65 +/+ cells were transfected with a plasmid expressing Pk-tagged A238L under the control of a mammalian cell active promoter. The cells were treated with or without LPS and PMA in the presence or absence of LMB 3 hrs prior to fixation. Cells transfected with Pk-tagged IkB-α and stimulated with LPS and PMA were used as a positive controls. Cells were fixed, permeabilized and stained with anti-Pk followed by a fluorescently labeled secondary antibody. At 16 hrs post-transfection the subcellular distribution of A238L was examined. Although the subcellular distribution of A238L did alter in response to LMB treatment, no difference could be detected between p65 -/- and control (p65 +/+) MEF (Figure 6.8). Treatment of cells with LPS and PMA, to activate NF-kB and induce the nuclear translocation of p65, also had no effect on the subcellular localization of A238L. These results show that p65 is not required for nuclear import or export of A238L. This suggests that A238L uses an alternative mechanism for nuclear export. From comparisons with Figure 6.2 and 6.3 it can be seen that A238L exhibits a different subcellular distribution profile in MEF p65 -/- and p65 +/+ cells compared to Vero cells. In MEF cells A238L exhibited a predominantly N/C and C distribution whereas in Vero cells the distribution was predominantly N and N/C with only a small proportion of cells exhibiting an exclusively cytoplasmic distribution. This could be due to difference in the efficiency or concentration of proteins associated with the nuclear import pathways between these cells.

6.2.5 Expression of A238L does not inhibit the nuclear translocation of p65.

NF-κB mediated gene expression can be regulated by several mechanisms including its subcellular localization within the cell. Previous work has suggested than A238L may inhibit NF-κB mediated gene transcription by retaining NF-κB in the cytoplasm of infected cells. This was based on an observation that A238L was found in complex with

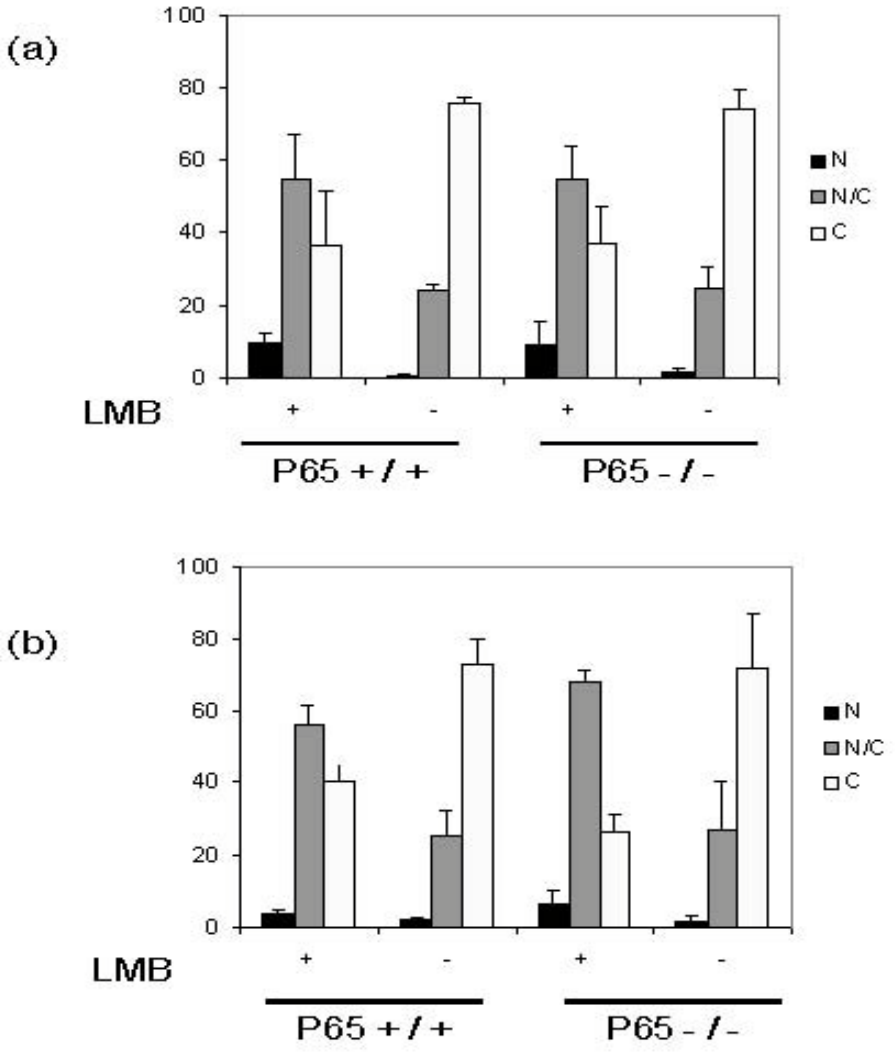

Figure 6.8 p65 is not involved the the movement of A238L into the nucleus. P65 +/+ MEF cells and p65 -/- cells were transfected with a plasmid expressing pk-tagged A238L under the control of a mammalian cell active promoter. 3 hrs prior to fixation the cells were treated with or without LMB (40 nM) in the presence or absence of LPS (10ug / ml) and PMA (100 nM). At 16 hrs post transfection the cells were fixed and pK-tagged A238L was detected by indirect immunofluorescence. Cells were imaged using confocal microscopy. The percent of cells exhibiting N, N/C or C phenotype was determined for each A238L constructed tested and under each condition. Data represents an average of 3 independent experiments (+ SD). Panel (a) shows data collected from untreated cells and panel (b) shows data from cells treated with LPS and PMA

the p65 sub-unit of NF-κB in cytoplasm of ASFV infected cell at 8 hrs post infection (Tait *et al*., 2000). These authors reported that A238L could not be detected in the nucleus at this time point post-infection (Tait et al., 2000) although other studies have detected A238L in the nucleus at early times (Bowick 2004, Silk *et al*., 2007). To investigate this possibility, the subcellular distribution and nuclear translocation of the p65 subunit of NF-κB was examined in ASFV infected cells using indirect immunofluorescence. Vero cells were infected with either the ASFV isolate BA71V, which expresses the wild type A238L protein, or a recombinant BA71V isolate from which the A238L gene has been deleted (vIKGAL) (Miskin et al 1998). 3 hrs prior to fixation the cells were treated with PMA/LPS in the presence or absence of LMB. PMA and LPS were used to enhance the nuclear translocation of NF-κB. Cells were fixed, permeabilized and stained at 8 hrs post-infection. Cells were treated with antibodies against endogenous p65 and an antibody specific for the ASFV early protein p30 (to identify ASFV infected cells). These antibodies were detected using Alexa 568-conjugated goat anti-rabbit IgG secondary antibody and Alexa 488-conjugated goat anti-mouse IgG respectively. Cells were then examined using confocal microscopy.

Figure 6.9 shows representative images of three independent experiments. ASFV infected cells were identified by staining for anti-p30 as detected by green staining, endogenous p65 was detected by an antibody specific for p65 and is shown as red staining and the nucleus and virus factories were detected by DAPI staining of DNA as shown in blue. P65 was detected in the nucleus of cells treated both in the presence and absence of LMB. As expected, treatment of cells with LMB resulted in an almost exclusive nuclear localisation of p65. In the absence of LMB an increase in the amount of cytoplasmic p65 was observed, demonstrating that p65 is exported from the nucleus to the cytoplasm by a CRM-1 mediated pathway. No difference could be seen in the amount of p65 in the nucleus of cells infected with either BA71V or ViKGal compared to uninfected cells. This suggests that nuclear translocation of p65 is not inhibited in cells infected with ASFV. Comparisons between cells infected with BA71V or vIKGal demonstrated that no difference could be observed between the cells infected with these

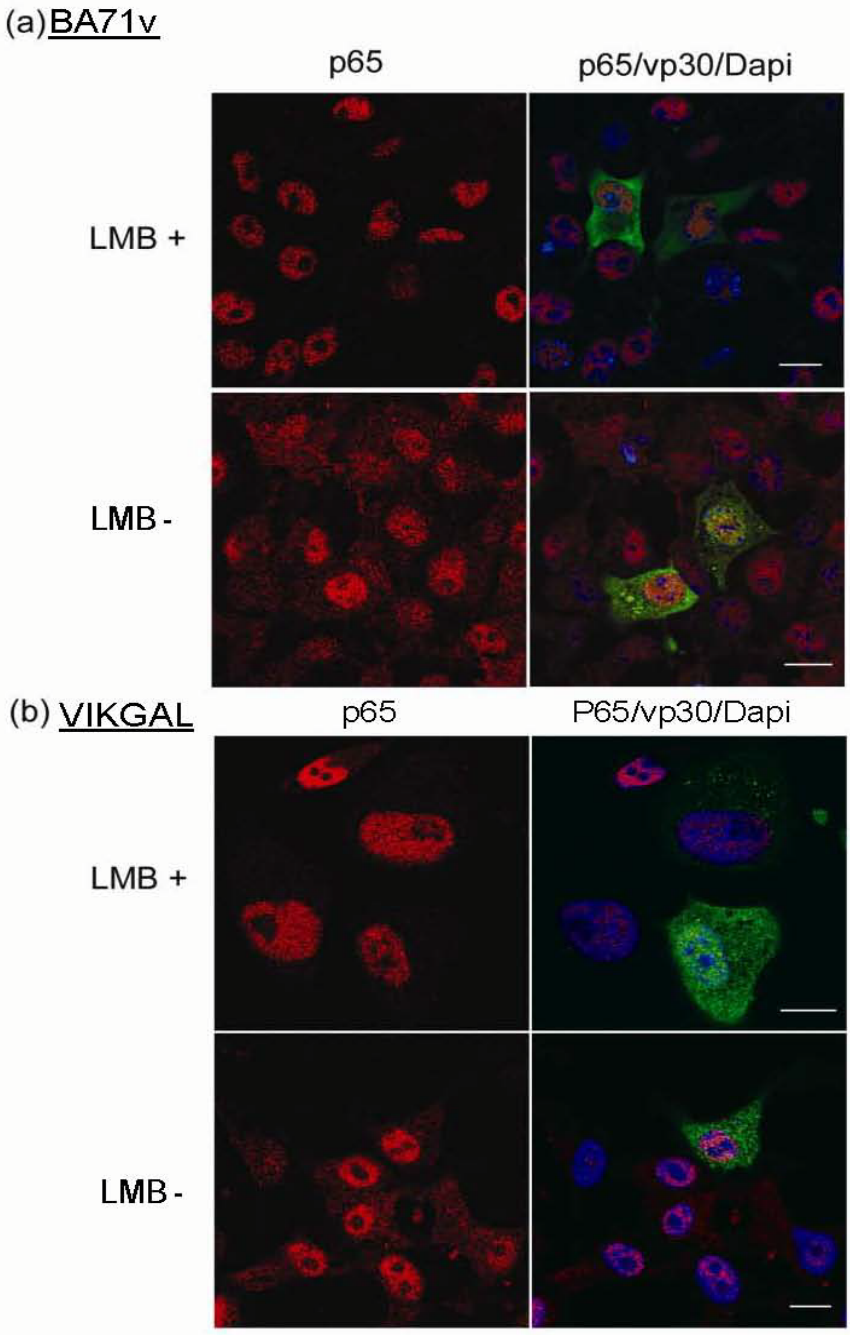

Figure 6.9 p65 nuclear import and export is not inhibited in ASF infected cells. Vero cells were fixed 8hrs after infection with either BA71V (a) or vIKGal isolates.I (b). 3 hrs prior to fixation the cells were stimulated with PMA (100 nM) and LPS(10 µg/ml) in the presence or absence of LMB. Cells were incubated with an antibody against cellular p65 (red signal) and with an antibody specific for the early viral protein p30 (green signal). DNA was labelled with DAPI (blue signal). Bar, 10 µm.

viruses, indicating that A238L does not alter the subcellular distribution of cellular p65 or inhibits the nuclear export of of this protein. These results suggest that A238L uses an alternative mechanism to inhibit NF-κB mediated gene expression.

6.3 Discussion

Previous work on A238L has shown that this protein can be detected in both the nucleus and cytoplasm of infected cells. However a detailed study of the movement of A238L within ASFV infected cells has not previously been carried out.

The data presented in this chapter shows that A238L is actively imported into the nucleus by an energy dependent process and is then exported utilising the CRM-1 pathway. LMB induced nuclear accumulation of A238L was insensitive to the protein synthesis inhibitor cycloheximide, demonstrating that new protein synthesis is not required for A238L nuclear import and that A238L is transported into the nucleus from a pre-existing cytoplasmic pool. Interestingly, even in the presence of LMB, A238L was not exclusively located in the nucleus and could be detected in the cytoplasm of infected cells. This suggests that either a proportion of A238L remains in the cytoplasm and is not imported into the nucleus (possibly through its interaction with CaN) or alternatively, that A238L can also be exported from the nucleus by a CRM-1 independent nuclear export pathway.

To identify possible sequences responsible for the nucleocytoplasmic shuttling of A238L, sequence analysis was performed. This analysis identified the presence of 2 classical NLS (NLS-1 and NLS-2). However no typical NES could be identified. Comparisons between the sub-cellular distributions of A238L mutants containing site-directed mutations within either NLS-1 or NLS-2 with WT-A238L, failed to identify differences in the nuclear import of A238L. However, mutation of both NLS- and NLS-2 together resulted in a significant reduction in the nuclear accumulation of A238L. This suggests that both of these sites are functional and exhibit redundancy, since mutation of

one site is compensated for by the presence of the other. Several proteins have been reported to contain multiple signals for nuclear import. These include the human immunodeficiency virus type 1 protein Vpr, the Adenovirus core protein pVII and the Epstein-Barr virus nuclear antigen 3A, the later has been shown to contain six functional localisation signals (Buck *et al.*, 2006; Sherman *et al.*, 2001; Wodrich *et al.*, 2006). It is not fully understood why proteins contain multiple NLS, however many of these proteins have multiple binding partners which could potentially mask one or several of the functional NLS. The presence of multiple, separate NLS would be an effective strategy to ensure that at least a proportion of the protein is targeted to the nucleus.

The presence of NLS-2 within the CaN binding site of A238L is consistent with this theory. If the CaN binding site in A238L is functional it is possible that binding of A238L to CaN, would mask NLS2 and possibly facilitate the retention of the A238L-CaN complex in the cytoplasm. If this is the case then a second NLS may be essential to ensure that an adequate proportion of A238L enters the nucleus either in complex with CaN or independently. Examination of the sub-cellular distribution of the A238L mutant W20-A238L, which is non-CaN binding, but has an intact NLS2, showed a large increase in the nuclear accumulation of A238L particularly in the presence of LMB. This would support the hypothesis that binding of A238L to CaN masks NLS-2 and could contribute to the retention of A238L in the cytoplasm of infected cells.

Interestingly mutation of both NLS-1 and NLS-2 did not completely prevent the nuclear translocation of A238L, suggesting that an additional mechanism could facilitate the movement of A238L to the nucleus. Due to the small molecular weight of A238L, passive diffusion could be responsible for the nuclear localisation of this protein. However, it is also possible that A238L may contain other, non-typical, NLS. A diverse range of sequences can act as NLS and new signals are continually identified. Thus producing a definitive list of consensus NLS is difficult. Indeed only two of the six NLS detected in the EBV protein, NA3A, were identified by the PSORT sequence analysis software (Buck et al., 2006). Ankyrin repeat domains (ARDs) have also been shown to

substitute for classical nuclear localisation signals in a number of other proteins, including IkB-α and Myxoma Nuclear Factor (MNF), a virulence factor encoded by myxoma virus (Camus-Bouclainville *et al.*, 2004; Sachdev *et al.*, 1998). A238L is predicted to contain four ARDs (Revilla *et al.*, 1998), which could potentially function as additional NLSs. To investigate this further it would be useful to construct a double EGFP-A238L fusion protein which is estimated to have a molecular weight of 88 kDa, well above the nuclear pore passive diffusion exclusion limit. Using this construct and others containing mutations within the predicted NLS-1 and NLS-2 it would be possible to prevent the passive diffusion of A238L into the nucleus of cells and establish if other non-typical NLS exist.

The nuclear accumulation of A238L in the presence of LMB clearly demonstrates that A238L is exported from the nucleus by a CRM-1 mediated mechanism. Although no typical NES were identified within A238L, it is possible that A238L contains non-classical NES or nucleo-cytoplasmic bidirectional signals. Another alternative is that A238L is exported from the nucleus in association with another protein using a 'piggyback' mechanism. This strategy is used by the Hepatitis B Virus X protein for nuclear import. The X protein interacts directly with IkB-α and this complex is imported into the nucleus. Import requires the presence of the second ARD of IkB-α which is involved in nuclear import of IkB-α following NF-κB activation (Weil et al., 1999). CaN is also transported in association with another cellular protein, NFAT (Shibasaki et al., 1996). A238L interacts with several cellular proteins. In particular, A238L has been suggested to bind to the p65 sub-unit of NF-κB (Tait et al., 2000), which contains a functional NES and exhibits CRM-1 dependent nuclear export (Harhaj & Sun, 1999), thereby raising the possibility that A238L could be exported in complex with p65. However, the results presented in this chapter failed to support this theory since no difference was detected in the subcellular distribution of A238L between wild type cells and a p65 homozygous negative cell line. This suggests that p65 does not contribute to nuclear export of A238L. This result does not exclude the possibility that another cellular protein may be involved in CRM-1 mediated nuclear export.

In the experiments carried out it was notable that treatment of cells with LMB did not result in the exclusive nuclear accumulation of A238L. One possible explanation for this is the involvement of an additional nuclear export pathway that is CRM-1 independent. Multiple nuclear export strategies have recently been reported for another ASFV protein, p37 (Eulalio et al., 2006). This protein contains three independent NES, two of which function via the CRM-1 pathway and one via a CRM-1 independent mechanism. Therefore, in addition to the presence of multiple NLS for nuclear import, A238L may also use multiple strategies for nuclear export.

NF-κB mediated gene transcription is regulated at by several mechanisms, which include altering the subcellular localisation NF-κB and also through post translation modification (Chen *et al.*, 2002; Ghosh & Karin, 2002). The phophoryalation and acetylation of p65 are particularly important in regulating NF-κB transcriptional activity within the nucleus. These modifications effect the ability of NF-κB to interact with transcriptional co-activators and also its cellular inhibitor protein IkB-α (Chen & Greene, 2004). IkB-α inhibits NF-κB through regulating its subcellular localisation. IkBα retains the p65-p50 NF-kB heterodimers in a predominantly cytoplasmic location preventing NF-kB from entering the nucleus and binding to its DNA binding site (Carlotti *et al.*, 2000). Considering A238L's homology with IκB-α and the ability of A238L to inhibit NF-κB mediated gene expression the effect of A238L on the subcellular localisation of p65 was explored. Comparisons between the subcellular distribution of endogenous p65 in infected and uninfected cells demonstrated that A238L did not alter the subcellular localisation of NF-κB and therefore does not function in a similar manner to IκB-α. This is consistent with previous work carried out in our laboratory which used Western blotting to demonstrate that A238L did not prevent the nuclear accumulation of the NF-κB p50 and p65 subunits in ASFV infected cells (Bowick, 2004). Together these results suggest that A238L uses an alternative mechanism to IκB-α and functions within the nucleus to inhibit NF-κB mediated gene transcription.

Presence of multiple NLS and the possibility that A238L uses more than one nuclear export pathway strongly suggests that nucleo-cytoplasmic shuttling of A238L is a key to the mechanism of action of this protein. However, the functional significance of the translocation of A238L between the cytoplasm and nucleus is still unclear. It could be that the ability of this protein to shuttle between the nucleus and cytoplasm is an essential strategy to ensure that adequate A238L is available in both the cytoplasm and nucleus to perform the multiple functions associated with this protein.

The data presented in this chapter support a model where by A238L functions both within the nucleus and cytoplasm and suggests that binding of CaN to A238L contributes to the cytoplasmic retention of A238L.

Chapter 7
Final Discussion

7.1 Introduction

The main aim of this thesis was to gain a greater understanding into the mechanism of A238L action and to better define the functional consequences of A238L expression within host cells. This was achieved through investigating the global effect of A238L expression on host macrophage gene expression and also through studies into the subcellular localisation of A238L.

7.2 Effect of A238L on host macrophage gene transcription

The global effect of A238L protein on host macrophage gene transcription was examined using a porcine oligonucleotide microarray. Oligonucleotidess present on this array were designed from gene clusters derived by sequencing of EST libraries from a wide range of porcine tissues and therefore cover target genes with a wide range of biological functions (Operon). Using this approach it was possible to investigate the effect of A238L expression in its target species by using a cell line derived from porcine macrophages, the main target cell of ASFV. To achieve this it was first necessary to develop an appropriate gene expression and delivery system suitable for use with porcine cells. The development and validation of this approach, which used baculovirus to deliver the A238L gene under control of a mammalian gene promoter, is described and discussed in detail in chapter 3 and 4. Using this approach the A238L gene was transiently expressed in 85 % of cells, thus increasing the chance of detecting its effect on host gene transcription.

Previous work has shown that A238L can inhibit NF-κB and NFAT regulated gene transcription (Miskin *et al.*, 1998; Powell *et al.*, 1996; Revilla *et al.*, 1998). These transcription factors are activated in response to cell stimulation. Therefore test cells

were treated with compounds which activate signalling pathways involving these transcriptional factors. These compounds were LPS, PMA and ionomycin. LPS activates NF-κB and the MAPK pathways (Guha & Mackman, 2001). Phorbol 12-myristate 13-acetate (PMA) activates Protein Kinase C and ionomycin is a calcium ionophore which increase intracellular levels of calcium, resulting in NFAT activation via CaN. Together PMA and ionomycin mimic antigenic stimulation of leukocytes resulting in the transcription of NFAT dependent cytokine and immune response genes (Acuto & Cantrell, 2000; Rao *et al.*, 1997).

The results presented in chapter 5 describe the effect of A238L on host cell gene transcription at 1 and 4 hrs following LPS, PMA and ionomycin treatment. These results demonstrated that A238L is a potent inhibitor of host cell gene transcription, down regulating the expression of porcine mRNA's targeted by a total of 292 oligonucleotides over both time points. In comparison only two oligonucleotides were found to hybridise to mRNA that were significantly up-regulated by A238L expression at 1 hr following stimulation. Due to the relatively small number of RNAs up-regulated across both time points it was assumed that the identification of these oligonucleotides was due to statistical error. Annotation was available for less than half of these oligonucleotides and resulted in a final gene list of 132 unique annotated genes. This highlights one of the disadvantages of using the porcine oligonucleotide array, as unlike similar mouse and human arrays, there is a significant lack of annotation available for many of the individual oligonucleotidess spotted onto the porcine array. Therefore many genes of interest were potentially excluded from the final data set.

Analysis of the functional classes of genes whose expression was down-regulated by A238L identified many genes which are inducible in response to cellular stress. The majority of these genes had not previously been shown to be regulated by A238L. Significantly, many of these genes were regulated through the NF-κB and MAPK pathways, key pathways involved in regulating the cells immune response to infection. NF-κB regulates the expression of pro-inflammatory cytokines, chemokines and acute

phase proteins that are involved in recruiting inflammatory cells to sites of infection (Ghosh *et al.*, 1998). MAPKs are involved in regulating many aspects of immune responses, from the initiation phase of innate immunity, the activation of adaptive immunity and cell death. In addition, a smaller number of genes were associated with the JAK/STAT pathway, which is involved in cytokine signal transduction including the IFN response (Dong *et al.*, 2002). This result demonstrates that A238L functions as a potent immunosuppressor protein by inhibiting the transcriptional activation of genes dependent on these pathways. Genes associated with MAPK pathway were particularly enriched. The ability of A238L to regulate genes associated with the MAPK and JAK/STAT pathway has not previously been reported.

Comparison between these results and the results presented in chapter 4, describing the effect of LPS, PMA and ionomycin treatment on IPAM cells alone, demonstrated that nearly all of the A238L regulated genes were not induced in response to stimulation but were constitutively expressed in resting IPAM cells. This suggests that pathways associated with the regulation of these genes are active in untreated IPAM cells. It is therefore possible that specific enrichment for genes associated with the NF-κB and MAPK pathway in cells expressing A238L is in part a consequence of the activation status of the IPAM cells.

Gene transcription is regulated at several levels and involves the simultaneous interaction of multiple different factors, including transcriptional activators, coactivators (also known as adaptors) and the basal transcriptional apparatus. Transcription factors bind directly to sequence specific DNA elements, whereas coactivators do not bind directly to DNA but interact with DNA binding proteins and can act to bridge interactions between transcription activators and basal factors. Proteins involved in modulating chromatin structure also play a significant role in the regulation of gene transcription by influencing the accessibility of DNA control elements to transcription factors (Ernst & Smale, 1995).

Early work on A238L, described in chapter 1, demonstrated that A238L was able to inhibit gene transcription dependent on the cellular transcription factors, NF-κB and NFAT (Miskin *et al.*, 1998; Powell *et al.*, 1996; Revilla *et al.*, 1998). This work proposed a model whereby A238L exhibited dual functionality inhibiting NF-κB and NFAT dependent gene expression by independent mechanisms. A238L was shown to co-precipitate with the p65 sub-unit of NF-κB and also prevent p50-p65 hetero-dimers, but not p50 homo-dimers, from binding to their DNA binding sites (Revilla *et al.*, 1998). This suggested that A238L interacts with p65, either directly or through interaction with another protein, to block binding of NF-κB to DNA. In a separate study the C-terminal 82 amino acids of A238L was shown to bind directly to CaN and inhibit CaN phophatase activity (Abrams *et al.*, 2008). CaN dependent pathways, including inhibition of NFAT mediated gene expression, are therefore inhibited (Miskin *et al.*, 1998). CaN acts to de-phosphorylate NFAT and this exposes nuclear localisation signals on NFAT resulting in its translocation into the nucleus. A238L was proposed to inhibit NFAT mediated gene transcription indirectly by inhibiting CaN-mediated dephosphorylation of NFAT therefore preventing its nuclear translocation. However, this work did not examine the subcellular localisation or phosphorylation status of NFAT in ASFV infected cells or in transfected cells expressing A238L and only proposed this model as a potential mechanism of action.

The results presented in Chapter 5 of this thesis demonstrate that A238L is able to inhibit gene transcription dependent on several transcription factors in addition to NF-κB and NFAT. All of the transcription factors identified interact with the transcription co-activator CBP/P300. This identifies a common link between these factors, and indicates that A238L may target CBP/P300 to inhibit gene transcription. This observation supports recent work demonstrating that A238L interacts with and inhibits CBP/P300 function (Granja *et al.*, 2006a; Granja *et al.*, 2008; Granja *et al.*, 2006b).In these studies A238L was shown not to prevent the nuclear translocation of NF-κB or NFAT, but inhibited NF-κB and NFAT dependent gene transcription through direct interaction and inhibition of the transcriptional coactivator CBP/P300. CBP and p300 are large nuclear

proteins which play a central role in the integration of multiple signaling events within the transcriptional apparatus, exerting their activity through several mechanisms (Chakravarti *et al.*, 1996; Chan & La Thangue, 2001; Janknecht & Hunter, 1996). These proteins do not bind directly to DNA but interact with a variety of sequence specific transcription activators including CREB/ATF, c-jun, c-Fos, NF-kB and NFAT, where they act as a scaffold protein, linking these transcription factors to the basal transcriptional apparatus. In addition they also have histone acetyltransferase (HAT) activity allowing them to influence chromatin structure and have been shown to acetylate a number of other cellular proteins including p53 and p65 altering their transcriptional activity . In an additional level of complexity the activity of CBP and p300 is also regulated through phosphorylation and auto-acetylation (Chan & La Thangue, 2001). Through these activities CBP and p300 play a central role in the regulation and integration of a multitude of signal transduction pathways, including the MAPK, NF-κB and JAK/STAT pathways (Janknecht & Hunter, 1996; Vo & Goodman, 2001).

CBP/p300 share extensive homology and have several conserved domains: including two separate transactivation domains located at the amino and carboxyl-terminal region and a central acetyl-transferase domain. A diagram of the arrangement of these domains, showing interactions with CBP/p300 binding proteins, is presented in Figure 7.1. The amino-terminal and carboxyl-terminal TADs can act independently and simultaneously with the transcriptional apparatus to regulated gene transcription (Swope *et al.*, 1996). A238L has been shown to specifically bind to the amino-terminal TAD of p300, preventing interaction between p300 and transcription factors regulated through this domain. However, transcription factors associated with the carboxy-terminal region, such as c-fos, are unaffected (Granja *et al.*, 2008b). This domain is essential for the transactivation of several transcription factors involved in the immune response including NF-kB-p65, STAT 3, IFR 3, NFAT and c-Jun (Garcia-Rodriguez & Rao, 1998; Janknecht & Hunter, 1996; Yoneyama *et al.*, 1998), providing support for the role of this protein in modulating the innate immune response. With the exception of ATF-2,

all of the transcription factors involved in the regulation of genes down-regulated by A238L were directly associated with the carboxyl-terminal transactivation domain of CBP/p300 providing additional and independent support for these results.

Interaction between p300 and A238L was also shown to inhibit the subsequent acetylation of the p65 subunit of NF-kB (Granja *et al.*, 2008b). Acetylation of RelA/p65 regulates NF-κB activity by enhancing its DNA binding activity and attenuating its interaction with IκBα (Chen *et al.*, 2002). Therefore this observation is consistent with previous work which demonstrated that A238L is able to prevent p50-p65 heterodimers, from binding to their DNA binding sites.

Granja et al (2008) also demonstrated that interaction between p300 and A238L did not affect the intrinsic HAT activity of p300, but blocked phosphorylation of a novel serine residue within the amino-terminus of p300 by PKC-θ. This inhibition prevented the autoacetylation of the amino-terminal TAD reducing the transactivation activity of this domain. The activity of CBP/p300 is regulated through post-translation modification, including phosphorylation, methylation and autoacetylation (Chawla *et al.*, 1998; Liu *et al.*, 1999; Stiehl *et al.*, 2007; Xu *et al.*, 2001). The post translation modification status of CBP/P300 has a direct effect on the HAT and transcriptional activities of this molecule and also alters the binding preference of this molecule for different transcription factors. For example, phosphorylation of CBP by IKKα at two serine residues within the carboxyl-terminal region of CBP, switches the binding preference of CBP from p53 to NF-κB (Huang *et al.*, 2007) and autoacetylation of p300 regulates complex formation with p53 (Stiehl *et al.*, 2007). Therefore it could be that by altering the acetylation status of p300, A238L acts as a molecular switch diverting CBP/ p300 activity away from transcription factors associated with the immune response (Granja *et al.*, 2008b).

a)

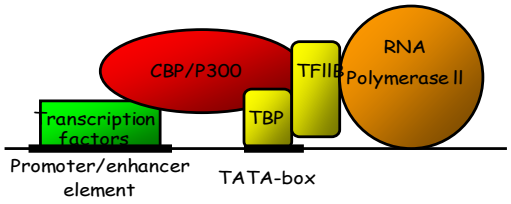

b)

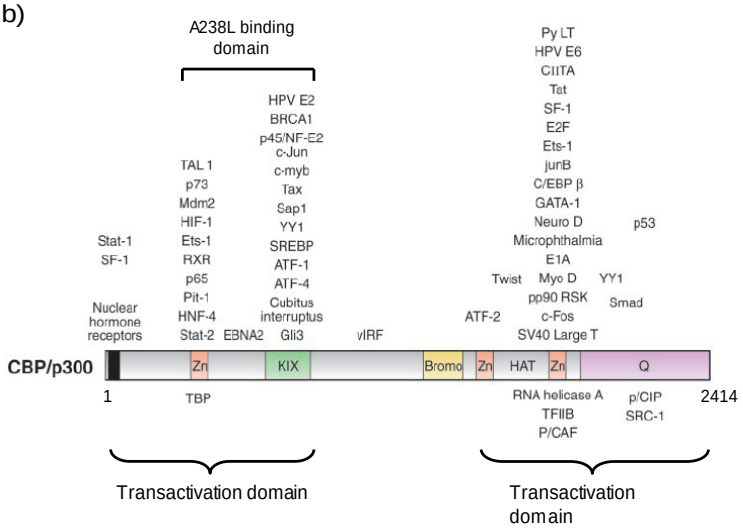

Figure 7.1 Organisation of CBP/p300 and it's interacting proteins.
Panel a) Model of CBP/p300 bridging between sequence specific transcription factors and components of the basal transcription machinery. TBP, TATA-box-binding protein; TF11B, transcription factor 11B.(Adapted from Janknecht R et al 1996 nature). Panel b) Schematic representation of CBP/p300 and its associated binding proteins. Transcriptional activators (top) and basal transcription factors and HATs (bottom). Functional domains are indicated: zinc fingers (Zn), CREB-binding domain (KIK), bromodomain (Bromo), HAT domain and glutamine-rich domain (Q)(adapted from Vo N J.et al 2001 and Granjer et al., 2008)

As yet the role of CaN inhibition by A238L within host cells has not been defined. As described above the evidence strongly suggests that A238L acts through the transcriptional coactivators CBP/p300 to inhibit gene transcription. However it is possible that inhibition of CaN by A238L could contribute to this mechanism. One study investigating the effect of A238L on COX-2 expression in a Junkat T-cell line (which was shown to be dependent on NFAT elements within the COX-2 promoter), demonstrated that A238L did not inhibit the nuclear translocation of NFAT or binding of NFAT to its DNA binding site. However, overexpression of a constitutively active version of CaN reversed A238L mediated inhibition of the expression of COX-2 (Granja *et al.*, 2004b). This suggests that inhibition of CaN by A238L is involved in the inhibition of COX-2 expression in these cells by an unknown mechanism. It could be that CaN is in some way involved in the activation of CBP/P300. Direct interaction between CaN and CBP/P300 has not been demonstrated. However CaN has been shown to act in synergy with protein kinase C to activate the IKKβ in both T lymphocytes and mouse peritoneal macrophages (Kim *et al.*, 2004; Trushin *et al.*, 1999). CaN has also been shown to preferentially synergise with PKC-θ in Jurkat T cells, together their signals converge on (or upstream of) Rac leading to potent JNK activation (Werlen *et al.*, 1998). The regulation of CBP/P300 is complex and involves multiple signalling pathways which result in the post translation modification of this protein. Therefore CaN could potentialy act at a point upstream in these signalling pathways indirectly affecting the activity of CBP/P300.

It is also possible that the ability of A238L to inhibit CaN activity has an alternative role, independent of regulation NFAT transcriptional activation. As described in chapter 1 CaN regulates the activity of several cellular proteins in addition to NFAT. These proteins include Elk-1 and BAD. CaN negatively regulates the activity of Elk-1, a transcription factor activated by mitogen activated protein kinases (MAPK) (Tian & Karin, 1999). Therefore inhibition of CaN could potential lead to an increase in Elk-1 dependent gene transcription; however no up-regulation of gene expression by A238L

was detected in this study. CaN is also responsible for activating the pro-apoptotic protein BAD (Wang *et al.*, 1999). Therefore it could be that A238L acts as an anti-apoptotic protein inhibiting calcium-induced apoptosis through CaN mediated dephosphorylation of BAD.

Many other viruses express proteins which modulate CBP/P300 function. These include several DNA virus oncoproteins such as the adenovirus E1A protein, the Simian virus 40 (SV40) large T antigen (TAg) and human papillomavirus E6 (Chakravarti *et al.*, 1999; Eckner *et al.*, 1996; Thomas & Chiang, 2005). CBP and P300 are important negative regulators of cell cycle progression, preventing premature exit from G1 phase to S phase (Rajabi *et al.*, 2005). Thus inhibition of CBP/P300 by these virus proteins promotes entry into S phase. This can promote virus replication by increasing supply of factors required for virus DNA replication. E1A directly represses the HAT activity of p300/CBP and blocks p53 acetylation (Chakravarti *et al.*, 1999). Simian virus Large T antigen alters the phosphorylation status of CBP/P300 and inhibits E2 transcription which is associated with a cysteine and histidine rich domain in the carboxy-terminus of CBP/P300 and E6 inhibits the p300-mediated acteylation of p53, inhibiting p53 dependent transcription (Eckner *et al.*, 1996; Thomas & Chiang, 2005). All of these proteins target the activation of carboxy-terminal interacting transcription factors, such as p53 or E2F, and can alter the HAT activity of P300/CBP promoting the malignant transformation of infected cells. In contrast to these viral oncogenic proteins, A238L has been shown to interact with the amino – terminal region of p300 consistent with an alternative role for this protein in regulating the host immune response. Retroviruses also express proteins which manipulate CPB/P300. The Tax protein from human T cell leukemia virus recruits CBP/P300 in conjunction with cellular CREB to conserved CRE-containing elements within the HTLV promoter. Together these proteins act as potent activators of viral transcription (Geiger *et al.*, 2008).

The results described in chapter 5 indicate the broad effect of A238L expression on host gene transcription. In this experiment A238L was over-expressed to indicate all of the

potential roles of this protein on host cell transcription. These results demonstrated that A238L can inhibit transcription of a diverse range of genes associated with several cellular processes. Studies in mice deficient in p300 or CBP have demonstrated that these molecules are in limiting supply within the cell and competition for CBP/P300 by different transcription factors can lead to negative interference between different signalling pathways (Janknecht & Hunter, 1999). Therefore it is probable that A238L exhibits a more specific effect during ASFV infection targeting a distinct subset of ASFV activated cellular genes. Future work comparing differential gene expression between A238L deletion mutant ASFV and wild type ASFV using the porcine microarray described in this study would help to resolve this question and could also provide an indication of functional redundancy between A238L and other ASFV genes. Considering the potential for A238L to exhibit different properties at different times during the ASFV infectious cycle, it would also be beneficial to look at differences in the host cell gene transcription at several different time points during ASFV infection.

7.3 Mechanisms involved in the subcellular localisation of A238L

The second aim of this thesis was to carry out further investigation into the mechanisms involved in the sub-cellular localisation of A238L to gain a better understanding of how this protein functions.

7.3.1 A238L is actively shuttled between the nucleus and cytoplasm

Previous work on A238L has demonstrated that this protein is present in both the nucleus and cytoplasm of ASFV infected cells (Bowick, 2004). Other work has also showed that A238L is present in the nucleus and cytoplasm of transiently transfected Vero cells and a human T-cell line expressing A238L (Granja *et al.*, 2004b; Granja *et al.*, 2006d). The results presented in chapter 6 demonstrated that A238L was located in both the nucleus and cytoplasm of ASFV infected cells and that a proportion of this cytoplasmic pool was actively imported into the nucleus and exported by the CRM-1 dependent pathway. This suggests that A238L consists of two populations within the

cell: molecules that are actively imported and exported from the nucleus and molecules that are retained in the cytoplasm. Previous work on A238L has shown that A238L consists of 2 molecular weight forms consisting of 32 kDa and 28 kDa (Tait *et al.*, 2000). Western blotting analysis of nuclear and cytoplasmic fraction of ASFV infected cell lysates demonstrated that both forms of A238L can be detected in the cytoplasm of infected cells throughout infection with the 32 kDa higher molecular mass form of A238L accumulating predominantly in the nucleus at later times post-infection (Bowick, 2004; Silk *et al.*, 2007). Treatment of infected cells with cytosine arabinoside, an inhibitor of ASFV DNA replication and late virus gene expression did not alter the cellular levels of A238L indicating that A238L is synthesised early during ASFV infection and that late gene expression is not required for the nuclear accumulation of A238L (Bowick, 2004).

The difference between the two forms of A238L has not been defined but is thought to be due to post-translational modification of A238L (Tait *et al.*, 2000). Possible explanations for accumulation of the 32 kDa form of A238L in the nucleus could be that the modification to the protein takes place in the nucleus or that this modification is required for nuclear translocation of the protein. Previous data has shown that A238L, co-localises and associates with CBP/P300 in the nucleus of both Vero cells and stimulated T-cells. Together this data could suggest that, particularly at late times post infection, the 32 kDa form of A238L preferentially functions within the nucleus to inhibit CBP/P300 action. It could be that this higher molecular mass 32 kDa form of A238L shuttles between the nucleus and cytoplasm, explaining the presence of both forms of A238L in the cytoplasm of infected cells.

Events responsible for the predominant nuclear accumulation of A238L at late time points post infection demonstrated by Bowick 2004 have not been established. The results presented in chapter 6 did not detect a significant difference between the subcellular distribution of A238L between 8 and 16 hrs post ASFV infection. However this work is not directly comparable to Bowick (2004). The approach used in chapter 6 involved transfecting cells with a plasmid expressing A238L under the control of its own

promoter and then infecting the cells with ASFV to activate gene transcription. This approach leads to the over expression of A238L in ASFV infected cells and was necessary to produce detectable levels of A238L for immunofluorescence analysis. Possibly over expression of A238L may lead to the presence of this protein in the nucleus at earlier time points during ASFV infection. The results presented in chapter 6 also demonstrated that A238L nuclear import and export was not dependent on cell pathways activated through PMA, LPS or ionomycin treatment in ASFV infected cells. This observation is inconsistent with recent work which demonstrated that A238L was localised preferentially in the cytoplasm of un-stimulated T cells and, after treatment with PMA/Ionomycin translocated to the nucleus (Granja *et al.*, 2008). A similar observation was demonstrated in Vero cells (Granja *et al.*, 2006b). Unlike the experiments carried out in chapter 6 these studies did not examine the subcellular localization of A238L in the presence of LMB, which blocks nuclear export of A238L. Bowick (2004) demonstrated that A238L predominantly accumulated in the nucleus at late times post-infection, however low levels of A238L could be detected within the nucleus from 3 hrs post-infection. Possibly A238L continually shuttles between the nucleus and cytoplasm in un-stimulated cells and is only retained in the nucleus following PMA/ionomycin treatment or ASFV activation of a cellular pathway at late times points following ASFV infection. Immunoprecipitation studies (Granja *et al.*, 2008), indicated that A238L preferentially interacts with p300 following PMA/ionomycin treatment. P300 activity is regulated through phosphorylation by many different kinases including PKC (Goodman & Smolik, 2000). PMA/ionomycin treatment leads to the activation of several PKC isotypes including PKC-θ. Therefore one possible explanation for these results could be that post-translational modification of p300 induced by PMA/ionomycin treatment or pathways activated by ASFV infection increases the binding efficiency between A238L and P300, leading to the nuclear retention of A238L.

Sequence analysis of A238L identified the presence of two putative nuclear localisation signals (NLS-1 and NLS-2). NLS-2 was located within the CaN docking motif. Both of

theses signals were found to be functionally active and exhibit functional redundancy. CaN is not thought to contain specific NLSs and instead is thought to shuttle into the nucleus in a complex with other proteins such as NFAT (Crabtree & Olson, 2002). Mutation of the A238L CaN motif alone in the presence of an intact NLS-2, resulted in a dramatic increase in the nuclear localisation of A238L. This suggests that binding of A238L to CaN masks NLS-2 contributing to the cytoplasmic retention of A238L. Therefore if it could be that if the higher molecular weight form interacts in the nucleus with CBP/P300, the lower 28 kDa form of A238L is held in the cytoplasm in complex with CaN. A representation of this model is presented in Figure 7.2.

A significant amount of further work is required to establish if this model is correct. As described above the difference between the two forms of A238L has not been established, but is thought to be due to post-translation modification (Tait *et al.*, 2000). CBP/P300 is known to acetylate several proteins including histones (Chan HM and La thang NB 2001). Therefore considering the interaction between A238L and CBP/P300 it is possible that this PTM could be due to acetylation. Two-dimensional gel electrophoresis (2DE) followed by Post-Source Decay Matrix-Assisted Laser Desorption/Ionization Mass Spectrometry (PSD-MALDI-MS) has recently revealed that the ASFV protein pE120R, essential for virus transport from assembly sites to plasma membranes, is acetylated at the N-terminal Ala residue during infection (Alfonso *et al.*, 2007). This approach could also be used to establish the nature and location of any PTM present on the A238L protein. This information could then be used to investigate the affinity of each form of A238L for p300 and CaN. Further investigation into the localization of CaN within ASFV infected and A238L transfected cells would also help to establish if the above model is correct.

7.4 Role of A238L during ASFV infection

Despite the ability of A238L to regulate the expression of many genes involved in the host's immune response, deletion of the A238L gene from ASFV field isolates does not

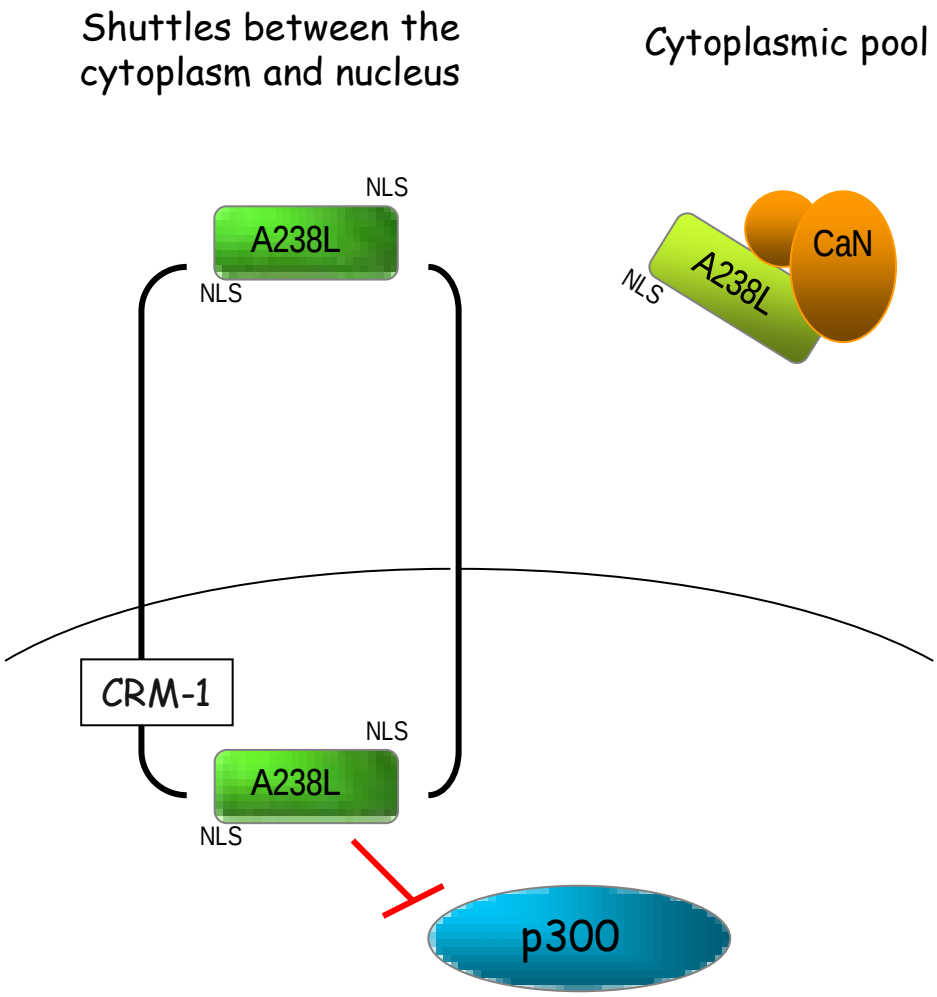

Figure 7.2 Schematic representation of the mechanism of A238L action.

A238L protein is proposed to consist of two populations: one set of molecules that are actively shuttling between the nucleus and cytoplasm and use CRM-1 mediated nuclear export and a second group that are retained in the cytoplasm through interaction with the cellular protein CaN. CaN is thought to mask a nuclear localisation signal (NLS) located within the CaN binding domain of A238L there by contributing to the cytoplasmic retention of A238L. Once in the nucleus A238L interacts with and inhibits gene transcription through direct binding and inhibition of the transcriptional co-activator CBP/P300. Experiments suggests that the 32 kDa form of A238L (dark green) shuttles between nucleus and cytoplasm and the 28 kDa form of A238L (light green) is located preferential in the cytoplasm. Experimental evidence providing support for this model is published in Granjer et 2008, Silk et al 2007, Abrams et al 2007 and Miskin et al 2000.

affect the pathogenesis of this disease or reduce ASFV replication in cell culture (Neilan *et al.*, 1997; Salguero *et al.*, 2008). A recent study comparing pathogenesis in pigs infected with a highly virulent isolate of ASFV (E-70) and an A238L E-70 deletion mutant demonstrated that TNF-α mRNA expression was enhanced in PBMC taken from pigs inoculated with the A238L deletion isolate compared to the wild type isolate. This indicates that A238L can inhibit pro-inflammatory gene expression *in vivo* in infected domestic pigs. However no significant differences in clinical symptoms and disease pathology were observed (Salguero *et al.*, 2008). Although this result seems surprising there are several possible explanations. First of all the effect of deleting A238L on secretion of proinflammatory cytokines has not been measured *in vivo*. Gene expression is regulated at several different levels and changes in transcription level may not lead to the same effect at the functional level. Other ASFV genes may also compensate for the loss of A238L to reduce proinflammatory gene expression.

It is also possible that A238L may have an essential role in the natural hosts of ASFV, warthogs and *Ornithodoros* ticks. The IKK, MAPK and JAK/STAT signalling pathways are ancient evolutionarily conserved pathways and have been identified in invertebrates (Arbouzova & Zeidler, 2006; Bantignies *et al.*, 2002; Govind, 1999; Sluss *et al.*, 1996). Functional homologues of CBP and CaN are also present in invertebrates (Bantignies *et al.*, 2002). It is therefore reasonable to propose that A238L may function in the tick vector. Therefore it would be interesting to investigate the replication and pathogenesis of A238L deletion mutants and wild type isolates in its tick vector, to establish the role of this protein in one of its natural hosts.

7.5 Summary

The results presented in this thesis provide compelling evidence for the role of A238L as a potent inhibitor of gene transcription through inhibition of the transcriptional co-activator CBP/P300 and demonstrates that A238L is able to suppress a number of immunological signalling pathways through this action.

The results also provide evidence that A238L functions within both the cytoplasm and nucleus of ASFV infected cells and suggest that a sub-population of A238L may be retained in the cytoplasm through interaction with CaN. These results combined with recent publications exploring the mechanism of A238L action (Abrams *et al.*, 2008; Granja *et al.*, 2008; Silk *et al.*, 2007) support a model where A238L acts within the cytoplasm of infected cells at early times post infection potentially inhibiting CaN, and is retained in the nucleus at late time points post infection to inhibit CBP/P300 action.

List of Abbreviations

AA	Amino acid
AcNPV	Autographa californica nucleopolyhedrovirus
AMCF	Aveolar macrophage chemotactic factor
AP-1	Activator protein-1
APC	Antigen presenting cells
ARD	Ankyrin repeat domains
aRNA	amplified RNA
ASF	African swine fever
ASFV	African swine fever virus
ATF	Activating transcription factor
BIRC3	Baculoviral IAP repeat-containing 3
BRCA1	Breast cancer 1,
BSA	Bovine serum albumin
C/EBP	CCAAT/enhancer-binding transcription factor
C/EBP-β	ccaat/enhancer binding protein
CAB	Cuts all enzyme buffer
CAB	Cuts all buffer
CaM	Calmodulin
CAM	Cell adhesion molecule
CaN	Calcineurin
CASK	Calcium/calmodulin-dependent serine protein kinase
CBP/P300	CREB binding protein
CD	Cluster Differentiation
cDNA	Complementary DNA
CIP	Calf intestinal alkaline phosphatase
p/CIP	CBPinteracting protein
CMV	Cytomegalovirus
COX	Cyclooxygenase
CPE	Cytopathic effect
CPK	Porcine kidney cell
CREB	Cyclic-AMP-response element
CRM	Chromosomal region maintenance
CsA	Cyclophilin A
CTE	Constitutive transport element
CypA	Cyclosporin A
DAVID	Database for Annotation, Visualisation and Intergrated Discovery

DBD	DNA binding domain
DEPC	Diethylpyrocarbonate
dH20	Deionised H20
DMEM	Dulbecco's Modified Eagle's Medium
DNA	Deoxyribonucleic acid
Dnase	Deoxyribonuclease
dNTPs	Deoxyribonucleotide triphosphate
DUSP	Dual specific phosphatases
EASE	Expression Analysis Systematic Explorer
EBNA	Epstein-Barr Virus Nuclear Antigen
EBV	Epstein-Barr virus
ECL	Enhanced chemiluminescence
EDTA	Ethylenediaminetetracetic acid
EDTA	Ethylenediaminetetra - acetic acid
EGFP	Enhanced green fluorescent protein
EM	Electron micrograph
ER	Endoplasmic reticulum
ERK	Extracellular signal-regulated kinases
EST	Expressed sequence tag
FCS	Foetal calf serum
FDR	False Discovery Rate
fmol	Femtomole
GADD45	Growth Arrest and DNA Damage
GATA	Globin transcription factor
GBP	Guanylate binding protein
GM-CSF	Granulocyte macrophage-colony stimulating factor
GO	Gene ontonlogy
HAT	Histone acetyl-transferase
HERPUD1	Heparin-binding EGF-like growth factor
HIF	Hypoxia-Inducible Factor
HIV	Human immunodeficiency virus
HNF	Hepatocyte Nuclear Factor
HPK	Hematopoietic progenitor kinase
HPV	Human papillomavirus
HRP	Horse radish peroxidase
HSP	Heat shock protein
HTLV	Human T cell leukemia virus
IAH	Institute for animal health
IAP	Inhibitor of apoptosis protein

IF	Immunofluorescence
IFN	Interferon
IFNR1	Interferon (alpha, beta and omega) receptor
IFR	IFN regulatory factor
Ig	Immunoglobulin
IKK	I Kappa B kinase
IL	Interleukin
iNOS	Inducible nitric oxide synthases
IPAM	Immortalised porcine alveolar monocyte cell line
IVT	In Vitro Transcription
IκB	Inhibitor of NF-κB protein
JAK	Janus kinase
JNK	Jun N-terminal Kinase
kbp	Kilobase pair
kDa	Kilodaltons
KEGG	Kyoto Encyclopedia of genes and genomes
L	Litre
LB	Luria broth
LCS	Leica Confocal Software
Lowess	Locally weighted scatterplot smoothing
LPS	Lipopolysaccharide
M	Molar
m.o.i	Multiplicity of infection
MAPK	Mitogen activated protein kinase
MAPKAPK	MAP kinase-activated protein kinase2
MARC	Meat Animal Research Centre
MCF	Macrophage Chemotactic Factor
MCS	Multiple cloning site
MDR1	Human multidrug resistance-1
MEF	Mouse embryonic fibroblasts
MeV	Multiexperiment Veiwer
mg	Milligram
MGF	Multigene families
MHC	Major histocompatability complex
MIDAS	Microarray Data Analysis System
MKNK	MAPK interacting kinase
MKP	MAPK phosphatases
ml	Millilitre
mM	Millimolar

MNF	Myxoma Nuclear Factor
MPMV	Mason-Pfizer Monkey Virus
mRNA	Messenger RNA
MSK 1	Mitogen and stress-activated kinase-1
NCBI	National Center for Biotechnology Information
NCFAD	The National Centre for Disease Control
NFAT	Nuclear Factor of Activated T Cells
NF-κB	Nuclear Factor-Kappa B
ng	Nanograms
NLF	Nuclear localized factor
NLS	Nuclear Localisation Signal
NS2	Non-structural protein
NUAK	SNF1-like kinase kinase
OD	Optical densisty
ORF	Open reading frame
P/CAF	p300/CBP Associated Factor
PAGE	Polyacrylamide gel electrophoresis
PBML	Peripheral blood mononuclear leukocytes
PBS	Phosphate buffered saline
PBSe	Calcium and magnesium free phosphate buffered saline
PCR	Polymerase chain reaction
PI3K	Phosphatidylinositol 3-kinase
PKA	Protein kinase A
PKC	Protein kinase C
PMA	Phorbol 12-myristate 13-acetate
PML-1	Promyeloytic Leukemia
PPAM	Primary porcine alveolar macrophage
PSD-MALDI-MS	Post-Source Decay Matrix-Assisted Laser Desorption/Ionization Mass Spectrometry
PTM	Post translation modification
RHD	REL homology domain
RNA	Ribonucleic acid
RPMI	Roswell Park Memorial Institute
RRE	Rev response element
RT	Reverse transcriptase
RXR	Retinoid X receptor
SAM	Significant Analysis of Microarrays
SAM	Significance analysis of *microarrays*
SDS	Sodium dodecyl sulphate

SF	Spodoptera frugiperda
SF	Steroidogenic factor
SH3	Src homology 3
SRC	Steroid-receptor coactivator
SRC	Steroid Receptor Co-Activator
SREBP	Sterol Regulatory Element Binding Protein
SS	Splice signals
STAT	Signal transducers and activators of transcription
SV	Simian virus
SWC	Porcine pan-myeloid cluster of differentiation
TAD	Transactivation domain
TAE	Tris-Acetate-EDTA
TAg	T antigen
TAP	Transport associated protein
TBP	TATAbinding protein
TCID	Tissue culture infective dose
TE	Tris-EDTA
TF	Transcription factor
TGF	Transforming growth factor
TIGR	The institute for Genomic Research
TLR	Toll-like receptor
TNF	Tumour necrosis factor
uPAR	Urokinase plasminogen activator receptor
UTP	Uracil triphosphate
UTR	Untranslated region
UV	Ultra violet
WB	Western blot
WPRE	Woodchuck hepatitis virus posttranscriptional regulatory element
µg	Micrograms
µl	Microlitre
- ve	Negative
%	Percent
+ ve	Positive

Appendix 1

Publications arising from this thesis

Journal of General Virology (2007), **88**, 411–419 DOI 10.1099/vir.0.82358-0

African swine fever virus A238L inhibitor of NF-κB and of calcineurin phosphatase is imported actively into the nucleus and exported by a CRM1-mediated pathway

Rhiannon N. Silk,† Gavin C. Bowick,† Charles C. Abrams and Linda K. Dixon

Institute for Animal Health, Pirbright Laboratory, Ash Road, Pirbright, Woking, Surrey GU24 0NF, UK

Correspondence
Linda K. Dixon
linda.dixon@bbsrc.ac.uk

Received 4 July 2006
Accepted 26 October 2006

This study examined nuclear and cytoplasmic shuttling of the African swine fever virus (ASFV) A238L protein, which is an inhibitor of NF-κB and of calcineurin phosphatase. The results showed that the protein was present in both the nucleus and the cytoplasm in ASFV-infected cells and that the higher molecular mass 32 kDa form of the A238L protein was the predominant nuclear form, which accumulated later in infection. In contrast, both the 28 and 32 kDa forms of the A238L protein were present in the cytoplasm. The A238L protein was actively imported into the nucleus and exported by a CRM1-mediated pathway, although a pool of the protein remained in the cytoplasm and did not enter the nucleus. By using a recombinant ASFV from which the A238L gene had been deleted, it was shown that expression of A238L did not inhibit nuclear import of the NF-κB p50 or p65 subunit and did not inhibit nuclear export of p65 by a CRM1-mediated pathway. The results were consistent with a model in which A238L functions within both the nucleus and the cytoplasm.

INTRODUCTION

African swine fever virus (ASFV) is a large cytoplasmic DNA virus that replicates primarily in macrophages *in vivo* and in macrophages and endothelial cells *in vitro*. ASFV causes an acute haemorrhagic fever in domestic pigs but inapparent infections in its natural hosts – warthogs, bushpigs and ticks of the species *Ornithodoros moubata* and *Ornithodoros erraticus*. In these hosts, and in domestic pigs, which recover from infection with less-virulent isolates, the virus can persist over long periods. The virus genome varies from about 170 to 192 kbp and encodes between 160 and 175 proteins. ASFV shares similarities in replication strategy with poxviruses but is classified in a separate family, the *Asfarviridae* (Dixon *et al.*, 2005). Estimates indicate that about 90 poxvirus proteins are required for virus replication in cells, suggesting that ASFV may require a similar number (Upton *et al.*, 2003). Other virus-encoded proteins include several with roles in evading host defence systems (Dixon *et al.*, 2004).

One of these, the A238L protein, functions by several different mechanisms to interfere with signalling pathways in infected macrophages. The first functions demonstrated for A238L were inhibition of NF-κB activation and inhibition of calcineurin phosphatase activity. As a consequence, calcineurin-activated pathways, such as activation of the NFAT (nuclear factor of activated T cells) transcription factor are inhibited. More recently A238L has been shown to inhibit TNF-α expression through a CREB-binding protein (CBP)/p300 transcriptional co-activators pathway (Granja *et al.*, 2004b; Miskin *et al.*, 1998, 2000; Powell *et al.*, 1996; Revilla *et al.*, 1998). By interfering with the activation of several different host factors, A238L is predicted to inhibit transcriptional activation of a broad spectrum of host response genes. So far, A238L expression has been shown to inhibit transcription of the COX-2 gene and production of prostaglandins and to inhibit transcriptional activation of the TNF-α gene. This could reduce the inflammatory response to ASFV and help prevent virus elimination (Granja *et al.*, 2006). Interestingly, deletion of the A238L gene from the genome of a virulent ASFV isolate did not reduce the virulence of the virus for domestic pigs (Neilan *et al.*, 1997), suggesting either that the pathways inhibited by A238L do not play a critical role in virus pathogenesis or that the virus encodes other complementary genes. which may compensate for the loss of A238L.

Mapping of the domain in the A238L protein required to bind to calcineurin has identified a 14 aa peptide located between residues 200 and 213, which binds with high affinity to calcineurin but does not inhibit its phosphatase activity. A

†These authors contributed equally to this work.

critical motif in this peptide, PxIxITxC/S, is similar to calcineurin-docking motifs in the NFAT substrate and other cellular inhibitors of calcineurin (Aubareda *et al.*, 2006; Martinez-Martinez & Redondo, 2004). A purified recombinant peptide containing the C-terminal 82 aa of A238L alone was sufficient to act as a potent inhibitor of calcineurin (C. C. Abrams, R. Silk, D. Chapman & L. K. Dixon *et al.*, unpublished results; Miskin *et al.*, 2000).

The A238L protein contains ankyrin repeats in the centre of the protein, which most closely resemble those in the IκBα protein, which acts as an inhibitor of NF-κB activation. This data suggests that, like IκB proteins, A238L may bind directly to NF-κB, inhibiting its activity. Further support for this model comes from experiments showing that expression of A238L inhibits NF-κB-dependent gene transcription and that A238L is co-precipitated from cell extracts with the p65 subunit of NF-κB (Revilla *et al.*, 1998). Moreover, addition of A238L recombinant protein to nuclear extracts from activated cells showed that A238L inhibited binding of p65/p50 NF-κB heterodimers to κB-binding sequences and displaced preformed complexes from these sequences. Together, these data suggest that A238L can act as a homologue of IκBα. However, a direct interaction between A238L and p65 has not been demonstrated and it remains possible that A238L acts by a different mechanism to inhibit NF-κB. It has also been shown that A238L is recruited into a complex with p65 only after signal-induced degradation of IκB, suggesting that A238L does not displace IκB from a complex with NF-κB but instead is incorporated into a complex after degradation of IκB (Tait *et al.*, 2000). Two different forms of the A238L protein have been detected with molecular masses of 28 and 32 kDa; these two forms are thought to result from post-translational modification, but the nature of the modification has not been defined. The 32 kDa form of A238L has been shown to co-precipitate with p65 (Tait *et al.*, 2000).

The IκB family of proteins consists of at least seven members (IκBα, IκBβ, IκBε, p105, p100, IκBζ and Bcl-3), which contain a central domain with five to seven ankyrin repeats. These act by several mechanisms to inhibit the activity of NF-κB (Hayden & Ghosh, 2004; Israel, 2000). The crystal structures of IκBα and IκBα bound to NF-κB p65/p50 heterodimers show that the ankyrin repeats of IκB make multiple contacts with NF-κB to block both the DNA-binding site and the nuclear localization signal (NLS) of p65 (Huxford *et al.*, 1998; Jacobs & Harrison, 1998; Malek *et al.*, 2001, 2003). However, the exposed NLS on the p50 subunit coupled with a nuclear export signal (NES) present on both IκBα and p65 result in constant nuclear–cytoplasmic shuttling of NF-κB/IκB complexes, although the steady-state localization is in the cytoplasm (Huang *et al.*, 2000; Johnson *et al.*, 1999). Signal-induced degradation of IκB alters the dynamics of this shuttling, leading to nuclear accumulation of NF-κB and activation of NF-κB-dependent gene transcription. Transcription of IκB genes is activated by NF-κB and this provides a negative feedback loop to regulate NF-κB activation. Newly synthesized IκB enters the nucleus forming a complex with NF-κB, which leads to its displacement from target DNA sequences and export from the nucleus (Huang & Miyamoto, 2001; Israel, 2000). Although previous data have suggested that A238L may function within the nucleus, one study showed that, at 8 h post-infection (p.i.), A238L was found exclusively in the cytoplasm in a complex with NF-κB. This suggested that A238L may inhibit NF-κB activity by retaining the complex in the cytoplasm (Tait *et al.*, 2000). However, detailed studies of the nuclear–cytoplasmic shuttling of A238L throughout a time course of infection have not been carried out. In this study, we showed that A238L is actively transported into the nucleus, with larger amounts present at late times p.i. We also demonstrated that a proportion of A238L is exported from the nucleus by a CRM1-mediated pathway. In addition, we showed that A238L does not inhibit nuclear import or export of p65.

METHODS

Viruses and cells. African green monkey (*Cercopithecus aethiops*) kidney (Vero) cells were maintained in Dulbecco's modified Eagle's medium containing 25 mM HEPES and supplemented with 2 mM glutamine, 50 U penicillin ml^{-1}, 50 μg streptomycin ml^{-1} and 5 % bovine fetal calf serum (FCS; PAA Laboratories GmbH).

ASFV strains were the BA71V tissue-culture-adapted ASFV isolate and recombinants of this isolate, which either had the simian virus 5 (SV5) Pk epitope tag (V5 tag) fused to the 5′ end of the A238L gene (SV5Gal) or had the coding region of A238L deleted (vIKGal). These viruses contained the β-galactosidase gene under the control of the ASFV p72 promoter inserted at the site of recombination (Miskin *et al.*, 1998).

Virus infection. Cells were washed and virus was added at an m.o.i. of 5 in serum-free medium. After incubation for 1.5 h at 37 °C, virus was removed. Cells were then washed twice and cultured in medium with FCS for various lengths of time as indicated.

Preparation of cell extracts. Cells were washed in PBS, harvested by scraping and pelleted by centrifugation. To prepare nuclear and cytoplasmic fractions, cells were resuspended in 200 μl pre-chilled fractionation buffer [150 mM Tris/HCl (pH 8.8), 10 mM KCl, 1 mM EDTA, 0.2 % NP-40, 10 % glycerol, 1 mM PMSF, 1 μg small protease inhibitors (leupeptin, pepstatin, antipain and chymostatin) ml^{-1}] and incubated on ice for 10 min. The suspension was then centrifuged for 5 min at 13 200 r.p.m. in a benchtop centrifuge to pellet the nuclei. The supernatant was removed and added to 200 μl SDS-PAGE sample buffer [100 mM Tris/HCl (pH 6.8), 4 % SDS, 0.2 % bromophenol blue, 20 % glycerol, 100 mM dithiothreitol]. The nuclear pellet was then harvested in 50 μl SDS-PAGE sample buffer and the DNA sheared by repeated passage through a 21-gauge needle. To prepare total extracts, cell pellets were resuspended in SDS-PAGE sample buffer and the DNA sheared as described above. To confirm that fractions were not cross-contaminated, parallel blots were probed with antibody against histone H1 as a nuclear marker or against α-tubulin as a cytoplasmic marker.

Western blotting. Proteins were separated by SDS-PAGE electrophoresis and transferred to nitrocellulose membranes. Membranes were blocked in blocking solution [3 % milk powder in PBS with 0.1 % Tween 20) at 4 °C overnight or at room temperature for 3 h. Membranes were incubated with antibodies in blocking solution for 1 h at room temperature and then washed in PBS plus 0.05 %

Tween 20, before incubation with HRP-conjugated protein A (ab7456-1, diluted 1 : 2000; Abcam). Bound antibodies were detected by enhanced chemiluminescence (ECL). Digital images of gels were collected using a Bio-Rad GS-710 densitometer.

Indirect immunofluorescence. Cells were grown on glass coverslips to approximately 90 % confluence and then transfected for 4 h using Lipofectamine 2000 (Invitrogen). Following transfection, cells were washed in serum-free medium and then, where appropriate, infected with ASFV following the above protocol. At the appropriate times p.i., the coverslips were washed with PBS, fixed in 4 % paraformaldehyde for 30 min and permeabilized for internal staining with PBS containing 0.2 % Triton X-100 (Sigma) for 15 min. Cells were blocked in PBS containing 3 % BSA (Sigma) for 1 h and then incubated with primary antibody diluted in PBS/3 % BSA. V5-tagged proteins were detected with mouse anti-Pk tag (diluted 1 : 100; Serotec) and p65 was detected using anti-p65 (sc-372, diluted 1 : 200; Santa-Cruz). After 30 min, the cells were washed three times in PBS plus 0.2 % Tween 20 (Sigma) and then incubated with secondary antibodies diluted 1 : 300 in PBS/3 % BSA for 30 min. Primary mouse antibodies were detected using Alexa 488-conjugated goat anti-mouse IgG and rabbit polyclonal serum was detected using Alexa 568-conjugated goat anti-rabbit IgG secondary antibody (Molecular Probes). Cells were washed twice in PBS/0.2 % Tween and three times in PBS. The coverslips were mounted onto slides with Vectashield containing DAPI (Vector Laboratories). The cells were visualized using a Leica TCS SP2 confocal laser scanning microscope. Data were collected sequentially to prevent cross-talk between detection channels and were analysed using LCS (Leica Confocal Software). The images shown are representative of three independent experiments.

RESULTS

A238L accumulates in the nucleus at late times p.i.

The subcellular localization of the 28 and 32 kDa forms of the A238L protein at various times p.i. was investigated. To do this, Vero cells were infected with a recombinant ASFV (SV5Gal) in which the wild-type A238L gene had been replaced with an A238L gene containing the Pk tag from SV5 fused to the 5′ end. This fusion has previously been shown not to affect either function of A238L (Miskin *et al.*, 1998). At various times p.i., cell extracts were separated into nuclear and cytoplasmic fractions. These fractions were separated by SDS-PAGE, blotted onto nitrocellulose membranes and probed with an antibody against the Pk tag to detect the A238L protein. As shown in Fig. 1(a), both the 28 and 32 kDa forms of the A238L protein were detected early in infection (3 or 4 h p.i.). At early times, most of the A238L protein was present in the cytoplasm, although overexposure of the gels showed that small amounts of A238L could be detected in the nucleus from 3 h p.i. (Fig. 1b). Increasing amounts of A238L could be detected in the nuclear fraction from 16 h p.i., reaching a maximum at 16–24 h p.i. Slightly more of the 28 kDa form of A238L was detected at early times p.i. compared with the 32 kDa form, but from 16 h p.i. onwards, the 32 kDa form of the protein was the main form detected, particularly in the nuclear fraction. The protein detected in the nucleus at late times p.i. ran slightly more slowly than the form detected in the cytoplasm, raising the possibility that it had been modified further. Parallel infected cultures were incubated for 16 h in the presence of cytosine arabinoside, an inhibitor of virus DNA replication and late virus gene expression. Similar amounts of both forms of the A238L protein were detected in the nuclear and cytoplasmic fractions compared with cultures incubated without cytosine arabinoside (Fig. 1c). This showed that most of the A238L protein was synthesized early in infection and that late virus gene expression was not required for nuclear accumulation of A238L or for the increase in the relative amount of the 32 kDa form at late times p.i.

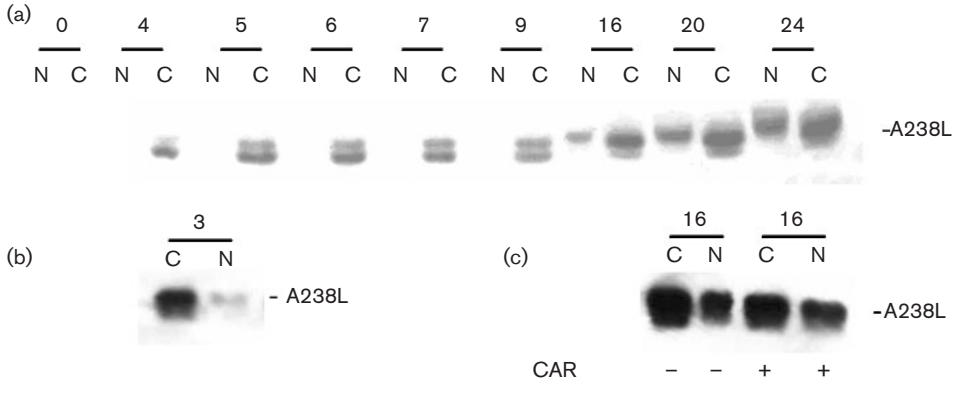

Fig. 1. Localization of the A238L protein in different subcellular fractions during ASFV infection. (a) Vero cells were infected with SV5Gal. At various times after infection, cells were harvested and separated into nuclear and cytoplasmic fractions. Proteins from each fraction were separated by SDS-PAGE, transferred to nitrocellulose membranes and probed with anti-Pk tag antibodies followed by HRP-conjugated anti-mouse secondary antibodies. Bound antibodies were detected by ECL. The time (h p.i.) at which extracts were harvested is indicated. (b) Overexposure of extracts harvested 3 h p.i. (c) Extracts harvested from cells at 16 h p.i. in the presence (+) or absence (–) of cytosine arabinoside. N, Nuclear fraction; C, cytoplasmic fraction.

A238L is exported from the nucleus by a CRM1-mediated pathway

To investigate whether A238L was exported from or retained in the nucleus, the subcellular localization of A238L was examined in the presence of leptomycin B (LMB), a specific inhibitor of the CRM1-dependent nuclear export pathway (Huang *et al.*, 2000). Levels of A238L detected in infected cells by immunofluorescence were low and difficult to quantify. Therefore, we transfected Vero cells with a plasmid containing a Pk-tagged A238L gene under the control of the A238L promoter. Cells were then infected with ASFV isolate BA71V. Three hours prior to fixation, cells were treated or not with LMB in the presence or absence of PMA and LPS. Cells transfected with a plasmid containing Pk-tagged IκBα were used as a positive control for LMB: IκBα contains a CRM1-dependent NES and has previously been shown to accumulate exclusively in the nucleus in the presence of LMB (Huang *et al.*, 2000). These cells were treated with PMA/LPS to activate NF-κB and enhance IκB nuclear import. At 8 and 16 h p.i., cell cultures were fixed, permeabilized and stained with an antibody specific to the Pk tag, followed by a fluorescently labelled secondary antibody. Cells were then examined using confocal microscopy and the subcellular localization of A238L was determined.

As shown in Fig. 2(a), in cells stimulated with PMA/LPS in the presence of LMB, all of the IκB was present in the nucleus as expected. In the absence of LMB, although most IκB was in the nucleus, a detectable amount was present in the cytoplasm. This is consistent with the nuclear export of IκB via the CRM1-mediated pathway and showed that the LMB was functionally active.

In ASFV-infected cells expressing A238L under the control of its own promoter, A238L exhibited a distribution that could be characterized into three distinct patterns of subcellular localization: preferentially nuclear, a uniform distribution throughout the cytoplasm and nucleus, or preferentially cytoplasmic [see Fig. 2b(i)]. One hundred cells were scored for these three cellular distributions under each experimental condition and in three independent experiments. In the presence of LMB, at both 8 and 16 h p.i., there was a significant increase in the number of cells exhibiting a predominantly nuclear localization compared with in the absence of LMB (∼50 % compared with <10 %) [Fig. 2b(ii)]. This demonstrated that at least a proportion of the nuclear A238L was exported to the cytoplasm using the CRM1-dependent nuclear export pathway. In cells treated with LMB, A238L was predominantly present in the nucleus in more cells; nevertheless, in approximately half of the cells

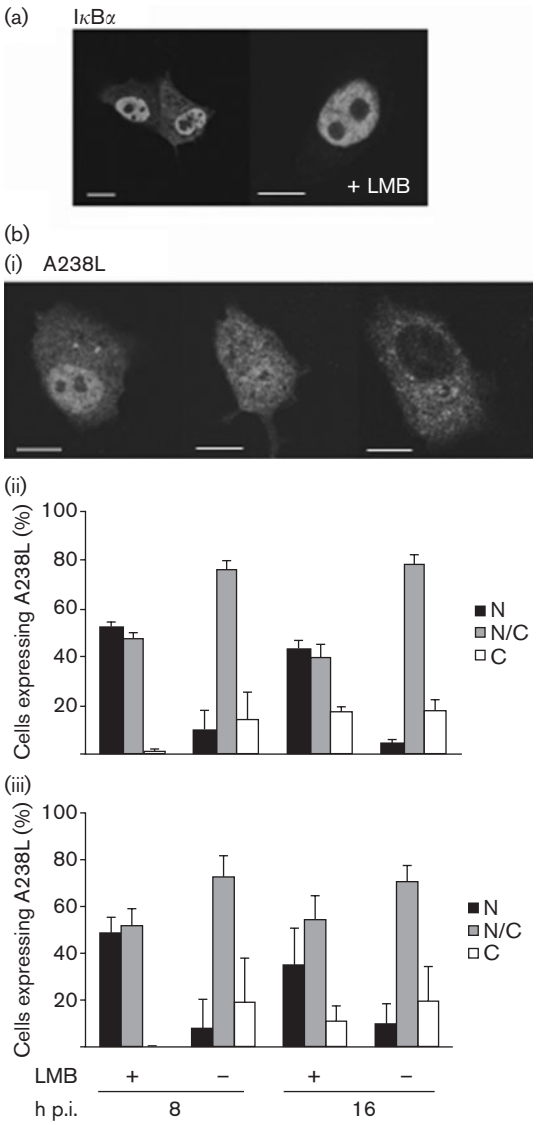

Fig. 2. A238L is exported from the nucleus by a CRM1-mediated pathway. (a) Vero cells were transfected for 16 h with a plasmid expressing Pk-tagged IκBα. Three hours prior to fixation, cells were treated with LPS (10 μg ml^{-1}) and PMA (100 nM) in the presence or absence of LMB (40 nM). (b) BA71V-infected Vero cells expressing Pk-tagged A238L under the control of its own promoter. Three hours prior to fixation, cells were treated with or without LPS and PMA in the presence or absence of LMB, as above. At 8 or 16 h p.i., cells were fixed and stained. In both (a) and (b), Pk-tagged proteins were detected with anti-Pk antibody, followed by Alexa 488-conjugated goat anti-mouse IgG secondary antibody, and imaged using confocal microscopy. The subcellular localization of Pk-tagged A238L was characterized as preferentially nuclear (N), both nuclear and cytoplasmic (N/C) or preferentially cytoplasmic (C). Representative images are shown (i). For each condition tested, 100 cells were counted and the percentages of cells exhibiting N, N/C and C distributions were determined. Cells were examined in the absence (ii) or presence (iii) of PMA/LPS, with or without LMB as indicated. Data presented is the mean (±SD) of three independent experiments. Bars, 10 μm.

treated with LMB, A238L exhibited an even distribution of A238L throughout the nucleus and cytoplasm. It is possible that a proportion of A238L was either not imported into the nucleus and remained in the cytoplasm, or, if it was imported into the nucleus and then exported, a CRM1-independent nuclear export pathway may have been involved.

Infection of cells is likely to activate a number of signalling pathways and this probably explains why no difference was observed in the distribution of A238L in PMA/LPS-treated cells compared with untreated cells. The Western blot results shown in Fig. 1 indicated that at 9 h p.i. most A238L was in the cytoplasm. In contrast, the results from the immunofluorescence experiments shown in Fig. 2 suggested that similar amounts of A238L were present in the nucleus at 8 compared with 16 h p.i. One possible explanation is that protein expression was higher from the plasmid transfected into infected cells in the immunofluorescence experiments. The complex interactions of A238L with components of the NF-κB and calcineurin signalling pathways and with nuclear import and export machinery mean that altering expression levels of A238L may alter its distribution. Nevertheless, our key conclusion regarding the nuclear export of A238L remained valid.

Nuclear import of A238L occurs by an energy-dependent process

Both forms of A238L are less than 60 kDa, which is the diffusion exclusion limit of the nuclear pore complex. To determine whether A238L is imported into the nucleus by an active process, cells were treated with cycloheximide to block protein synthesis and then incubated at 37 or 4 °C. At 4 °C, all active transport processes are blocked, whereas diffusion is unaffected. In the majority of cells at 4 °C, A238L was found to be evenly distributed between the nucleus and cytoplasm, both in the presence and absence of LMB. However, when cells were incubated at 37 °C, the results were dramatically different and A238L exhibited a predominantly nuclear localization in almost 50 % of the cells examined (Fig. 3). This suggested that, although passive diffusion may play a role in the nuclear import of A238L, an additional active nuclear transport process is involved.

This comparison also showed that there was no significant difference in the distribution of A238L in cells treated with cycloheximide compared with untreated cells (see Fig. 3).

As inhibition of protein synthesis did not prevent the nuclear accumulation of A238L, we concluded that a pool of pre-existing cytoplasmic A238L was imported into the nucleus.

Expression of A238L does not inhibit nuclear translocation of NF-κB

To investigate whether expression of A238L inhibited nuclear translocation of NF-κB, we compared nuclear translocation of the p65 and p50 subunits of NF-κB in cells infected with ASFV BA71V isolate expressing the Pk-tagged

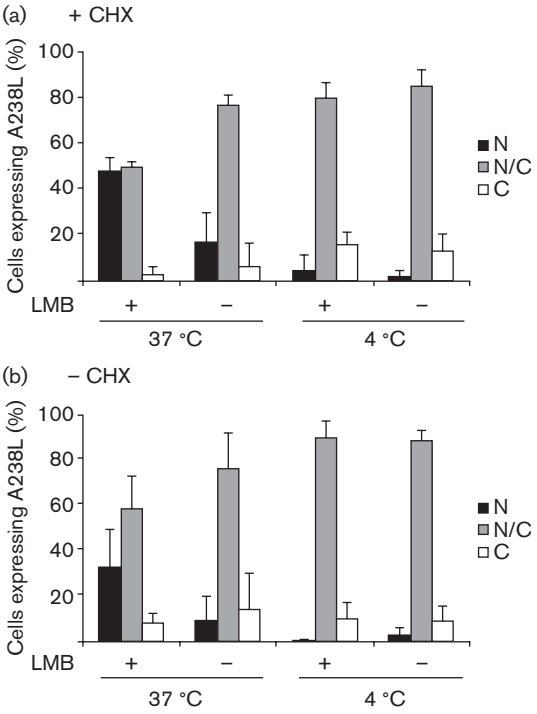

Fig. 3. Movement of A238L is energy-dependent. ASFV-infected Vero cells expressing Pk-tagged A238L under the control of its promoter were treated with cycloheximide (CHX; 100 μg ml^{-1}) (a) or were left untreated (b). Three hours prior to fixation, cells were treated with or without LMB (40 nM) and incubated at either 37 or 4 °C. Pk-tagged A238L was detected by indirect immunofluorescence. The percentages of cells exhibiting the N, N/C and C phenotypes were determined for each condition tested. Data represent the mean of three independent experiments (± SD).

A238L gene (SV5Gal) or a recombinant BA71V isolate from which the A238L gene had been deleted (vIKGal). Deletion of the A238L gene has been shown previously not to affect virus replication in cells and, as demonstrated in Fig. 4(b), the patterns of virus protein synthesis were not significantly different during a time course of infection with these viruses. To determine whether the total cellular pool of the p65 and p50 proteins was altered following infection with SV5Gal or vIKGal virus, total cell extracts were separated by SDS-PAGE, blotted and probed with antibody against p65 or p50. No change was detected in the total cellular pool of p50 during infection with either virus (Fig. 4a). In contrast, an increase in the amount of p65 was detected at 3 h p.i. Total amounts of p65 decreased at 6 and 9 h p.i. but increased again at 12 and 18 h p.i. These results suggested that regulation of the total cellular pool of p65 may contribute to regulation of NF-κB activity during ASFV infection. However, similar changes in amounts of p65 were observed in cells infected with both wild-type BA71V and the deletion mutant lacking A238L, suggesting that A238L expression does not regulate the amount of p65.

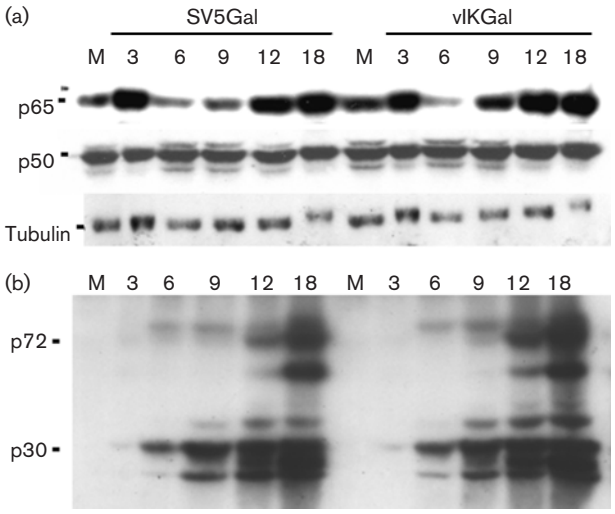

Fig. 4. Expression of the p50 and p65 subunits of NF-κB at different times after infection with recombinant ASFV either expressing A238L (SV5Gal) or with the A238L gene deleted (vIKGal). Vero cells were infected with the SV5Gal or vIKGal recombinant strains of ASFV isolate BA71V. At different times p.i., total cell extracts were harvested, separated by SDS-PAGE and blotted onto nitrocellulose membranes. Blots were probed with antibodies against the p65 or p50 subunits of NF-κB or against α-tubulin (a), or with hyperimmune serum from an ASFV-infected pig (b). Appropriate HRP-conjugated secondary antibodies were used and bound antibodies were detected by ECL. The positions of the major capsid protein, p72, and of the major early and late protein p30 are indicated. Lane M, mock-infected cells.

At various times after infection, cells were fractionated into nuclear and cytoplasmic extracts and these were separated by SDS-PAGE, blotted onto nitrocellulose membranes and probed with antibodies that recognized either the p50 or the p65 NF-κB subunit. Fig. 5(a) shows that in cells infected with SV5Gal, which expressed A238L, the p65 subunit of NF-κB was detected in both nuclear and cytoplasmic fractions throughout infection. Larger amounts were detected in the nucleus at late times (16–24 h p.i.). At early times, the p50 subunit was detected almost exclusively in the cytoplasm but was detected in both nuclear and cytoplasmic fractions at late times (16–24 h p.i.). Fig. 5(b) shows the distribution of the p65 and p50 subunits following infection with the vIKGal ASFV A238L deletion mutant. There was no significant difference in the distribution of p65 and p50 between the nucleus and cytoplasm when results were compared with those from cells infected with virus expressing A238L. At 16 and 24 h p.i., an additional 55 kDa form of p65 was detected in the nucleus. The appearance of this band is consistent with cleavage of p65 late in infection by caspase-3 (Kang *et al.*, 2001), which has been shown to be induced in ASFV-infected cells (Nogal *et al.*, 2001).

Fig. 6 shows cells that were infected with ASFV and stained with antibodies against an early ASFV protein, p30 (green), and the p65 subunit of NF-κB (red); nuclei are shown in blue. Translocation of p65 to the nucleus was observed in cells that were stained with the anti-p30 antibody. There was no difference in the amount of p65 in the nucleus of uninfected cells that did not show positive staining with the anti-p30 antibody, demonstrating that nuclear translocation of p65 was not inhibited in cells infected with ASFV. To determine whether expression of A238L inhibited nuclear export of p65, we compared localization of p65 in cells infected with BA71V or vIKGal ASFV in the presence and absence of LMB. The results showed that, as expected, treatment of cells with LMB resulted in an increase in the percentage of cells showing a predominantly nuclear localization of p65. In the absence of LMB, an increase in the amount of cytoplasmic p65 was observed, showing that p65 is exported from the nucleus to the cytoplasm by a

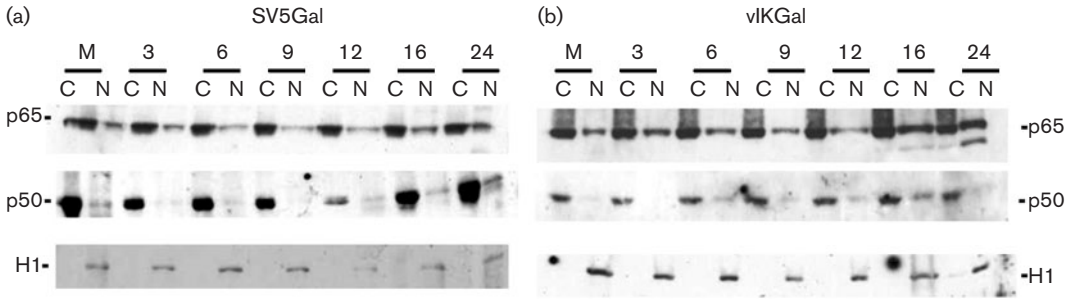

Fig. 5. Localization of the p50 and p65 subunits of NF-κB at different times after infection with recombinant ASFV either expressing A238L (SV5Gal) or with the A238L gene deleted (vIKGal). Vero cells were infected with the SV5Gal (a) or vIKGal (b) recombinant strains of the ASFV BA71V isolate. At different times p.i., cells were harvested and separated into nuclear and cytoplasmic fractions. These were separated by SDS-PAGE and blotted onto nitrocellulose membranes. Blots were probed with antibodies against the p65 or p50 subunit of NF-κB, or with an antibody against histone H1 as a control for the fractionation. After reaction with an appropriate secondary antibody, bound antibodies were detected by ECL. The time (h p.i.) at which extracts were harvested is indicated. N, nuclear fraction; C, cytoplasmic fraction. Lane M, mock-infected cells.

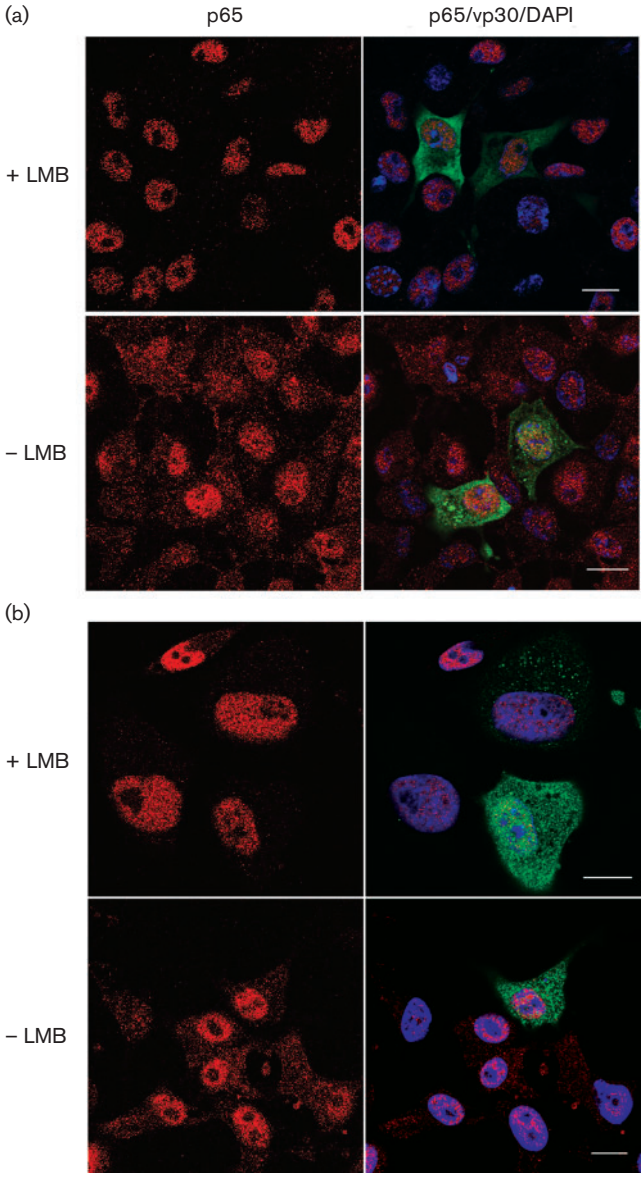

Fig. 6. p65 nuclear import and export is not inhibited in ASFV-infected cells. Vero cells were fixed 8 h after infection with BA71V (a) or vIKGal isolates (b). Three hours prior to fixation, cells were stimulated with PMA (100 nM) and LPS (10 μg ml^{-1}) in the presence or absence of LMB. Cells were incubated with an antibody against cellular p65 (red) and with an antibody specific for the early viral protein p30 (green). DNA was labelled with DAPI (blue). Bars, 10 μm.

CRM1-mediated pathway. No difference was observed in the cells infected with the two viruses, demonstrating that A238L does not inhibit nuclear export of p65.

DISCUSSION

The A238L protein of ASFV inhibits activation of the NF-κB transcription factor and the phosphatase activity of calcineurin. In addition, A238L has been shown to inhibit transcription from the TNF-α promoter by a mechanism involving the CBP/p300 transcriptional co-activators. The A238L protein thus has the potential to act as a potent immunosuppressant by inhibiting transcriptional activation of the many immune response genes regulated by these factors (Miskin *et al.*, 1998, 2000; Powell *et al.*, 1996; Revilla *et al.*, 1998). Evidence to date has shown that, in a T-cell line, A238L inhibition of cyclo-oxygenase 2 (COX2) gene transcription is dependent on an NFAT element within the gene promoter and involves inhibition of the p300 transcriptional co-activator (Granja *et al.*, 2004a). Similarly, inhibition of TNF-α expression has been shown to involve inhibition of CBP/p300 function (Granja *et al.*, 2006). The NF-κB and NFAT pathways are targeted by other viruses (Bowie *et al.*, 2004; Camus-Bouclainville *et al.*, 2004; Li *et al.*, 2004; Scott *et al.*, 2001), although A238L is the only protein known to combine both of these functions in a single protein.

Little is known of the detailed mechanism by which A238L functions. Previous work has suggested that the protein may function in both the cytoplasm and the nucleus (Granja *et al.*, 2006; Revilla *et al.*, 1998; Tait *et al.*, 2000), but a detailed study of the location and cytoplasmic nuclear shuttling of A238L during ASFV infection has not previously been carried out.

The similarity between the ankyrin repeats of A238L and those of members of the IκB family suggests that A238L may make direct contact via these ankyrin repeats with NF-κB subunits. The observation that A238L can be co-precipitated with the NF-κB p65 subunit supports this hypothesis, although direct contact between A238L and p65 has not been demonstrated. IκB proteins contain between five and seven ankyrin repeats, and crystallographic structures of IκBα and IκBβ in complex with p65/p50 NF-κB heterodimers show that the IκB ankyrin repeats make multiple contacts with NF-κB, blocking both the NLS and DNA-binding domain on the p65 subunit (Huxford *et al.*, 1998; Jacobs & Harrison, 1998; Malek *et al.*, 1998, 2003). In contrast, A238L contains only four ankyrin repeats, and protein structure modelling (D. Chapman & L. K. Dixon, unpublished data), based on the structure of IκB in complex with NF-κB, suggests that A238L may block the DNA-binding site but not the nuclear localization signal on p65, and vice versa.

In this study, we have shown that A238L is imported into the nucleus by an active process in virus-infected cells. Western blotting of nuclear and cytoplasmic cell extracts suggested that the 32 kDa higher molecular mass form of A238L predominantly accumulated in the nucleus at later times post-infection. Previous data has shown that this form of the protein is co-precipitated with the NF-κB p65 subunit, suggesting that, particularly at late times p.i., A238L functions within the nucleus to inhibit NF-κB. The difference between the two forms of A238L has been suggested to be due to post-translational modification of the

protein, although the nature of the modification has not been defined (Tait *et al.*, 2000). Possible explanations for accumulation of the 32 kDa form of A238L in the nucleus are that the modification to the protein takes place in the nucleus or that this modification is required for nuclear translocation of the protein. NLSs on A238L have not been defined to date. However, sequence analysis of A238L using PSORT (Horton *et al.*, 2006), which predicts possible subcellular localization sites, has identified two putative NLSs. These consist of single, short stretches of amino acids highly enriched in basic residues. One of these is located at the N terminus towards the tail end of the first ankyrin repeat domain and the second is located at the C terminus within the PxIxITxC/S calcineurin-binding domain. A proportion of the A238L protein is also present in the cytoplasm. We showed a greater nuclear accumulation of A238L in cells when LMB was added to inhibit CRM1-mediated nuclear export. Thus, we concluded that A238L is exported actively from the nucleus by a CRM1-mediated pathway. No NESs were identified and it is not known whether A238L interacts directly with the nuclear export pathways or translocates in association with another protein that contains a NES.

Our experiments indicated that the cytoplasmic A238L protein comprises both molecules that do not enter the nucleus and molecules that are actively exported from the nucleus. If the higher molecular mass 32 kDa form of A238L shuttles between the nucleus and cytoplasm, this could explain why both forms are present in the cytoplasm. The 28 kDa form of A238L is not co-precipitated with p65, suggesting that this may be the form of the protein that binds to and inhibits calcineurin (Tait *et al.*, 2000). If the predicted NLS within the calcineurin-docking motif in the A238L protein is functional, then this would be masked when A238L binds to calcineurin. Hence, this A238L–calcineurin complex would be predicted to remain in the cytoplasm. Calcineurin is not thought to contain specific NLSs and instead is thought to shuttle into the nucleus in a complex with other proteins such as NFAT (Crabtree & Olson, 2002).

Our data also showed that expression of A238L did not inhibit nuclear translocation of the NF-κB p50 and p65 subunits. This is consistent with a model whereby A238L may act within the nucleus to inhibit binding of NF-κB to DNA. Previous experiments have shown that recombinant A238L, when added to nuclear extracts from stimulated cells, inhibits binding of NF-κB to κB enhancer sequences and can also displace preformed NF-κB transcription complexes from DNA (Revilla *et al.*, 1998).

p65 can be exported from the nucleus either using NESs contained in the p65 protein or as part of a complex with IκB utilizing export signals on IκB (Huang *et al.*, 2000). Our data showed that A238L did not inhibit nuclear export of p65, although we did not define the form in which p65 is exported in ASFV-infected cells.

Accumulating evidence suggests that IκB proteins play critical roles within the nucleus in regulating NF-κB-dependent gene transcription. IκBζ acts within the nucleus and can either inhibit or activate NF-κB transcriptional activity. IκBζ binds to the p50 subunit of NF-κB in both p50/p50 and p50/p65 NF-κB dimers. Transcription of the IκBζ gene has been shown to be activated in response to IL-1 and signalling through Toll-like receptors. Evidence from IκBζ-deficient cells shows that IκBζ is required for transcriptional activation of IL-6 and a number of other immune response genes (Yamamoto *et al.*, 2004; Yamazaki *et al.*, 2001). Evidence to date suggests that A238L acts as an inhibitor of NF-κB-dependent gene transcription. However, we cannot exclude the possibility that A238L may also have some role in activating gene transcription. This may be revealed by global transcription profiling.

As both NF-κB and calcineurin are important targets for immunomodulatory drugs, there is considerable interest in defining how a single protein can mediate inhibition of both of these pathways. Understanding how the two functions of A238L are regulated is also important for understanding its role during ASFV infection.

ACKNOWLEDGEMENTS

We would like to thank Professor Ron Hay, University of Dundee, UK, for providing the Pk-tagged IκB plasmid and Dr Paul Monaghan and Pippa Hawes from the Bioimaging Department at IAH, Pirbright, UK, for advice. We acknowledge funding from BBSRC.

REFERENCES

Aubareda, A., Mulero, M. C. & Pérez-Riba, M. (2006). Functional characterization of the calcipressin motif that suppresses calcineurin-mediated NFAT-dependent cytokine gene expression in human T cells. *Cell Signal* **18**, 1430–1438.

Bowie, A. G., Zhan, J. & Marshal, W. L. (2004). Viral appropriation of apoptotic and NF-κB signaling pathways. *J Cell Biochem* **91**, 1099–1108.

Camus-Bouclainville, C., Fiette, L., Bouchiha, S., Pignolet, A., Counor, D., Filipe, U., Gelfi, J. & Messud-Petit, F. (2004). A virulence factor of myxoma virus colocalizes with NF-κB in the nucleus and interferes with inflammation. *J Virol* **78**, 2510–2516.

Crabtree, G. R. & Olson, E. N. (2002). NFAT signaling: choreographing the social lives of cells. *Cell* **109**, S67–S79.

Dixon, L. K., Abrams, C. C., Bowick, G., Goatley, L. C., Kay-Jackson, P. C., Chapman, D., Liverani, E., Nix, R., Silk, R. & Zhang, F. (2004). African swine fever virus proteins involved in evading host defence systems. *Vet Immunol Immunopathol* **100**, 117–134.

Dixon, L. K., Escribano, J. M., Martins, C., Rock, D. L., Salas, M. L. & Wilkinson, P. J. (2005). Asfarviridae. In *Virus Taxonomy: Eighth Report of the International Committee on Taxonomy of Viruses*, pp. 135–143. Edited by C. M. Fauquet, M. A. Mayo, J. Maniloff, U. Desselberger & L. A. Ball. London: Elsevier/Academic Press.

Granja, A. G., Nogal, M. L., Hurtado, C., Salas, J., Salas, M. L., Carrascosa, A. L. & Revilla, Y. (2004a). Modulation of p53 cellular function and cell death by African swine fever virus. *J Virol* **78**, 7165–7174.

Granja, A. G., Nogal, M. L., Hurtado, C., Vila, V., Carrascosa, A. L., Salas, M. L., Fresno, M. & Revilla, Y. (2004b). The viral protein A238L inhibits cyclooxygenase-2 expression through a nuclear factor of activated T cell-dependent transactivation pathway. *J Biol Chem* **279**, 53736–53746.

Granja, A. G., Nogal, M. L., Hurtado, C., del Aguila, C., Carrascosa, A. L., Salas, M. L., Fresno, M. & Revilla, Y. (2006). The viral protein A238L inhibits TNF-α expression through a CBP/p300 transcriptional coactivators pathway. *J Immunol* **176**, 451–462.

Hayden, M. S. & Ghosh, S. (2004). Signaling to NF-κB. *Genes Dev* **18**, 2195–2224.

Horton, P., Park, K.-J., Obayashi, T. & Nakai, K. (2006). *Protein Subcellular Localization Prediction with WoLF PSORT. Proceedings of the 4th Annual Asia Pacific Bioinformatics Conference APBC06, Taipei, Taiwan*, pp. 39–48.

Huang, T. T. & Miyamoto, S. (2001). Postrepression activation of NF-κB requires the amino-terminal nuclear export signal specific to IκBα. *Mol Cell Biol* **21**, 4737–4747.

Huang, T. T., Kudo, N., Yoshida, M. & Miyamoto, S. (2000). A nuclear export signal in the N-terminal regulatory domain of IκBα controls cytoplasmic localization of inactive NF-κB/IκBα complexes. *Proc Natl Acad Sci U S A* **97**, 1014–1019.

Huxford, T., Huang, D.-B., Malek, S. & Ghosh, G. (1998). The crystal structure of the IκBα/NF-κB complex reveals mechanisms of NF-κB inactivation. *Cell* **95**, 759–770.

Israel, A. (2000). The IKK complex: an integrator of all signals that activate NF-κB? *Trends Cell Biol* **10**, 129–133.

Jacobs, M. D. & Harrison, S. C. (1998). Structure of an IκBα/NF-κB complex. *Cell* **95**, 749–758.

Johnson, C., Van Antwerp, D. & Hope, T. J. (1999). An N-terminal nuclear export signal is required for the nucleocytoplasmic shuttling of IκBα. *EMBO J* **18**, 6682–6693.

Kang, K.-H., Lee, K.-H., Kim, M.-Y. & Choi, K.-H. (2001). Caspase-3-mediated cleavage of the NF-κB subunit p65 at the NH_2 terminus potentiates naphthoquinone analog-induced apoptosis. *J Biol Chem* **276**, 24638–24644.

Li, H., Rao, A. J. & Hogan, P. G. (2004). Structural delineation of the calcineurin–NFAT interaction and its parallels to PP1 targeting interactions. *J Mol Biol* **342**, 1659–1674.

Malek, S., Huxford, T. & Ghosh, G. (1998). IκBα functions through direct contacts with the nuclear localization signals and the DNA binding sequences of NF-κB. *J Biol Chem* **273**, 25427–25435.

Malek, S., Chen, Y., Huxford, T. & Ghosh, G. (2001). IκBβ, but not IκBα, functions as a classical cytoplasmic inhibitor of NF-κB dimers by masking both NF-κB nuclear localization sequences in resting cells. *J Biol Chem* **276**, 45225–45235.

Malek, S., Huang, D.-B., Huxford, T., Ghosh, S. & Ghosh, G. (2003). X-ray crystal structure of an IκBβ center dot NF-κB p65 homodimer complex. *J Biol Chem* **278**, 23094–23100.

Martinez-Martinez, S. & Redondo, J. M. (2004). Inhibitors of the calcineurin/NFAT pathway. *Curr Med Chem* **11**, 997–1007.

Miskin, J. E., Abrams, C. C., Goatley, L. C. & Dixon, L. K. (1998). A viral mechanism for inhibition of the cellular phosphatase calcineurin. *Science* **281**, 562–565.

Miskin, J. E., Abrams, C. C. & Dixon, L. K. (2000). African swine fever virus protein A238L interacts with the cellular phosphatase calcineurin via a binding domain similar to that of NFAT. *J Virol* **74**, 9412–9420.

Neilan, J. G., Lu, Z., Kutish, G. F., Zsak, L., Lewis, T. L. & Rock, D. L. (1997). A conserved African swine fever virus I kappa B homolog, 5EL, is nonessential for growth *in vitro* and virulence in domestic swine. *Virology* **235**, 377–385.

Nogal, M. L., de Buitrago, G. G., Rodriguez, C., Cubelos, B., Carrascosa, A. L., Salas, M. L. & Revilla, Y. (2001). African swine fever virus IAP homologue inhibits caspase activation and promotes cell survival in mammalian cells. *J Virol* **75**, 2535–2543.

Powell, P. P., Dixon, L. K. & Parkhouse, R. M. E. (1996). An IκB homolog encoded by African swine fever virus provides a novel mechanism for downregulation of proinflammatory cytokine responses in host macrophages. *J Virol* **70**, 8527–8533.

Revilla, Y., Callejo, M., Rodríguez, J. M., Culebras, E., Nogal, M. L., Salas, M. L., Viñuela, E. & Fresno, M. (1998). Inhibition of nuclear factor κB activation by a virus-encoded IκB-like protein. *J Biol Chem* **273**, 5405–5411.

Scott, E. S., Malcomber, S. & O'Hare, P. (2001). Nuclear translocation and activation of the transcription factor NFAT is blocked by herpes simplex virus infection. *J Virol* **75**, 9955–9965.

Tait, S. W. G., Reid, E. B., Greaves, D. R., Wileman, T. E. & Powell, P. P. (2000). Mechanism of inactivation of NF-κB by a viral homologue of IκBα: signal-induced release of IκBα results in binding of the viral homologue to NF-κB. *J Biol Chem* **275**, 34656–34664.

Upton, C., Slack, S., Hunter, A. L., Ehlers, A. & Roper, R. L. (2003). Poxvirus orthologous clusters: toward defining the minimum essential poxvirus genome. *J Virol* **77**, 7590–7600.

Yamamoto, M., Yamazaki, S., Uematsu, S., Sato, S., Hemmi, H., Hoshino, K., Kaisho, T., Kuwata, H., Takeuchi, O. & other authors (2004). Regulation of Toll/IL-1-receptor-mediated gene expression by the inducible nuclear protein IκBζ. *Nature* **430**, 218–222.

Yamazaki, S., Muta, T. & Takeshige, K. (2001). A novel IκB protein, IκBζ, induced by proinflammatory stimuli, negatively regulates nuclear factor-κB in the nuclei. *J Biol Chem* **276**, 27657–27662.

Available online at www.sciencedirect.com
ScienceDirect
Virology 374 (2008) 477–486
VIROLOGY
www.elsevier.com/locate/yviro

Domains involved in calcineurin phosphatase inhibition and nuclear localisation in the African swine fever virus A238L protein

Charles C. Abrams, Dave A.G. Chapman, Rhiannon Silk, Elisabetta Liverani, Linda K. Dixon *

Institute for Animal Health Pirbright Laboratory, Pirbright, UK

Received 19 November 2007; returned to author for revision 4 January 2008; accepted 7 January 2008
Available online 7 February 2008

Abstract

The African swine fever virus A238L protein inhibits calcineurin phosphatase activity and activation of NF-κB and p300 co-activator. An 82 amino acid domain containing residues 157 to 238 at the C-terminus of A238L was expressed in *E. coli* and purified. This purified A238L fragment acted as a potent inhibitor of calcineurin phosphatase *in vitro* with an IC_{50} of approximately 70 nM. Two putative nuclear localisation signals were identified between residues 80 to 86 (NLS-1) and between residues 203 to 207 overlapping with the N-terminus of the calcineurin docking motif (NLS-2). Mutation of these motifs independently did not reduce nuclear localisation compared to the wild type A238L protein, whereas mutation of both motifs significantly reduced nuclear localisation of A238L. Mutation of the calcineurin docking motif resulted in a dramatic increase in the nuclear localisation of A238L provided an intact NLS was present. We propose that binding of calcineurin to A238L masks NLS-2 contributing to the cytoplasmic retention of A238L.

Keywords: African swine fever virus; Calcineurin phosphatase inhibitor; NF-κB inhibitor; Immune evasion; Macrophage; Nuclear localisation

Introduction

African swine fever virus (ASFV) is a large, cytoplasmic DNA virus and is the only member of the *Asfarviridae* family. The virus encodes between 156 and 167 ORFs, many of which are not essential for virus replication in cells but have important roles in virus/host interactions. These include a number encoding proteins which inhibit host defence pathways (Dixon et al., 2005). One of these, the A238L protein, has been reported to inhibit signalling pathways in infected cells by three different mechanisms; inhibition of NF-κB activation, inhibition of the activity of calcineurin (CaN) phosphatase (now known as protein phosphatase 3C or PP3C) resulting in inhibition of pathways dependent on CaN including activation of NFAT transcription factor (Hogan et al., 2003) and inhibition of the transcriptional co-activator p300 (Granja et al., 2004, 2006b; Miskin et al., 1998; Powell et al., 1996; Revilla et al., 1998). A238L is predicted to act as a potent immunosuppressive protein by inhibiting transcriptional activation of the broad range of immunomodulatory genes dependent on these pathways. So far reports have shown that A238L is involved in inhibiting transcription from the TNF-α, cycloxygenase-2 and inducible nitric oxide synthase genes which results in reduced production of inflammatory mediators NO, prostaglandins and TNF-α from infected cells (Granja et al., 2006a, 2004, 2006b; Miskin et al., 1998; Powell et al., 1996; Revilla et al., 1998). The A238L gene is conserved in all ASFV isolates analysed. Deletion of the A238L gene from the genome of a virulent isolate did not reduce virus virulence in pigs (Neilan et al., 1997), possibly other genes may compensate for the loss of A238L. The A238L protein is 238 amino acids long and contains a central region encoding 4 ankyrin-like repeats, an N-terminal domain of unknown function and a C-terminal domain which contains a docking motif involved in binding to CaN (Miskin et al., 2000; Neilan et al., 1997; Revilla et al., 1998). The ankyrin repeats in the A238L protein resemble those in the IκBα inhibitor of NF-κB activation. In resting cells NF-κB is present in a complex with IκB inhibitor proteins (Wietek and O'Neill, 2007). Activation by a

* Corresponding author. Institute for Animal Health Pirbright Laboratory, Ash Road, Pirbright, Surrey GU24 0NF, UK. Fax: +44 1483 232448.
E-mail address: linda.dixon@bbsrc.ac.uk (L.K. Dixon).

0042-6822/$ - see front matter.
doi:10.1016/j.virol.2008.01.005

variety of stimuli leads to phosphorylation dependent ubiquitinylation of IκB and degradation by the proteasome. Nuclear localisation signals on NF-κB are exposed resulting in its translocation into the nucleus and activation of genes containing the NF-κB binding sites in the promoter. The similarity between the ankyrin repeats in A238L and those in IκB suggested that A238L may act as a homologue of IκB to inhibit the stimulus induced activation of NF-κB that occurs following virus infection. This was supported by experiments which demonstrated that expression of A238L inhibits transcriptional activation of an NF-κB dependent luciferase reporter gene (Powell et al., 1996; Revilla et al., 1998). The A238L protein was shown, by co-precipitation, to be present in a complex with the p65 subunit of NF-κB, although, direct interaction between A238L and the p65 subunit of NF-κB has not been demonstrated (Revilla et al., 1998; Tait et al., 2000). In one study A238L was shown to be predominantly localised in the cytoplasm at 8 h post-infection (Tait et al., 2000). However, our data showed that the A238L protein is present in both the cytoplasm and nucleus of cells and accumulates in the nucleus at later times post-infection (from 10 to 18 hpi). A238L was shown to be actively imported into the nucleus and exported by a CRM-1 dependent pathway (Silk et al., 2007). Two forms of the A238L protein are expressed during infection, a 28 kDa and 32 kDa form. These are thought to differ by post-translational modification, although the nature of the modification has not been defined (Tait et al., 2000). The higher molecular weight form accumulates in the nucleus and is preferentially co-precipitated with the p65 subunit of NF-κB (Tait et al., 2000). Expression of A238L does not inhibit nuclear accumulation of NF-κB p50 or p65 subunits. Recombinant A238L added to nuclear extracts inhibits binding of NF-κB to its binding elements in gene promoters in electromobility shift assays and displaced prebound NF-κB from DNA (Revilla et al., 1998). These data provide support for a model whereby A238L acts in the nucleus to inhibit NF-κB activation.

Evidence that A238L acts by modulating the function of the transcriptional co-activator CREB binding protein/p300 comes from studies using cell lines expressing A238L. In a Jurkat T cell line A238L inhibited expression from the TNF-α promoter by modulating NF-κB, NFAT and c-Jun transactivation by a mechanism that involves CREB binding protein/p300 function (Granja et al., 2006a). A238L inhibition of transcription from the cyclooxygenase-2 promoter depended on NFAT elements within the promoter and was reversed by a constitutively active CaN. This suggested that inhibition of CaN was involved in this process. However, the data showed that binding of NFAT to DNA was not inhibited, but that transactivation of p300 by a GAL4/NFAT fusion protein was inhibited (Granja et al., 2004). LPS and IFN-γ stimulated transcription of the inducible nitric oxide synthase (iNOS) gene promoter was inhibited in the RAW 264.7 mouse macrophage cell line expressing A238L. In this study A238L was shown to inhibit p65 and p300 interaction and inhibited p65/rel A and p300 binding to distal NF-κB sequence in the iNOS promoter. In these experiments A238L also abrogated p300 transactivation mediated by a GAL4 p300 fusion protein. These results also suggest that A238L acts within the nucleus possibly by interfering with the activation of the transcriptional co-activator CREB binding protein/p300 (Granja et al., 2006b). The mode of A238L action may depend on the stimulus delivered, cell and promoter type.

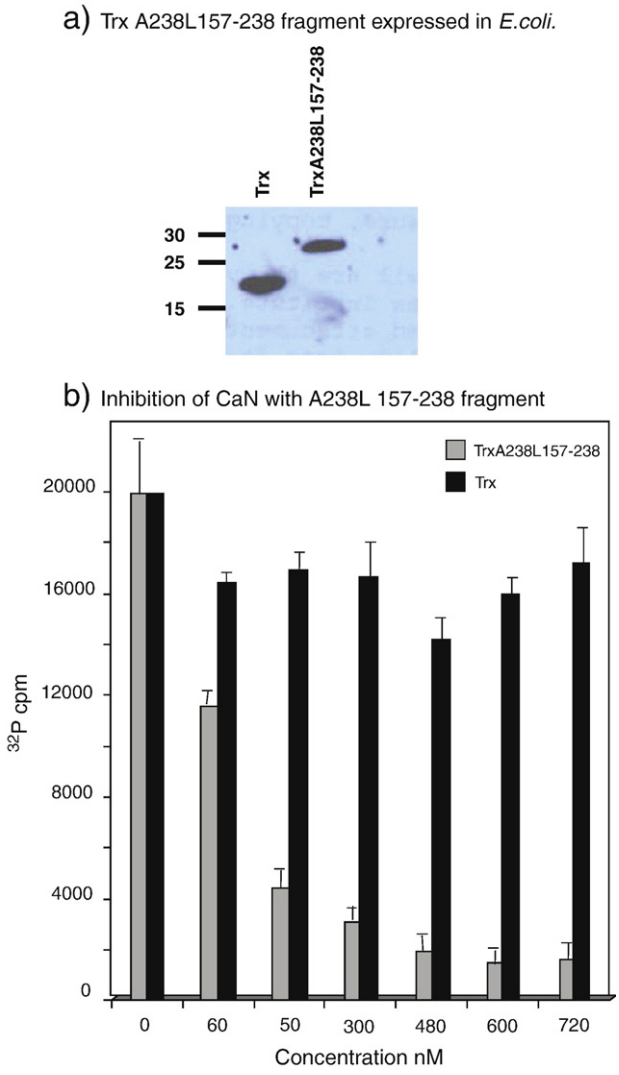

Fig. 1. Inhibition of CaN phosphatase activity by the A238L157–238 fragment. Panel a) shows proteins purified from *E. coli* strain BL21 which were transformed with either pET32a vector alone or pET32a containing A238L fragment encoding residues 157 to 238. Protein expression was induced by addition of IPTG and the His-tagged proteins were purified from extracts by nickel affinity chromatography. Purified proteins were separated by SDS-PAGE and blotted onto PVDF membranes. The His-tagged proteins were detected using ant-His antibodies followed by HRP-conjugated Protein A. Bound antibodies were detected by enhanced chemiluminescence. Lane 1 shows the Trx protein tag purified from bacteria transformed with pET32a vector and lane 2 shows the Trx-A238L157–238 fusion protein purified from bacteria transformed with the vector containing the A238L insert. The position of molecular weight markers run in parallel is indicated. In Panel b) the effect of varying concentrations of these proteins on CaN phosphatase activity is shown. The concentration (nM) of either the Trx-A238L157–238 fusion protein or the Trx protein alone added to each reaction is indicated on the X-axis. The CaN phosphatase activity measured in cpm of [^{32}P] released from a phosphorylated substrate peptide is indicated on the y-axis. Data from a representative experiment is shown and represents means from 3 replicates. Standard deviation error bars are shown.

a)

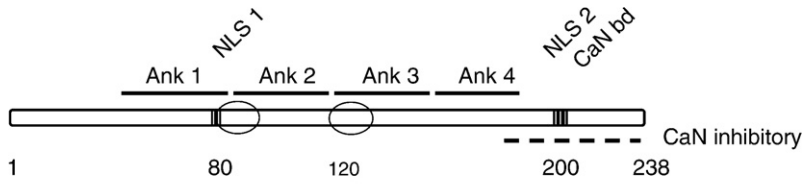

b)

```
Malawi: 158 YLKGFTTWDWAVFTGHADLVKTLNKGYQKPLFMHFPLYKLDV 199
Ba71v:  157 YHRGFTAWDWAVFTGNMELVKSLNHDYQKPLYMHFPLYKLDV 198
            * :***:********: :***:**:.*****:**********

MAlawi: 200 FHRRFKKKPKIIITGCEDNVYEKLPEQNSNFLCVKKLNKYGK 239
Ba71v:  199 FHRWFKKKPKIIITGCKNNVYEKLPEQNPNFLCVKKLNKYGK 238
            *** ************::**********.*************
```

c)

A238L Form	NLS 1 (aa 80 – 86)	NLS 2/CaN bd (aa 202 – 213)	CaN Binding
WT-A238L	PHRRDKDGNS	KKK**P**K**I**I**I**T G**C**	Yes
W13-A238L	PHRRDKDGNS	TTTSK**I**I**I**T G**S**	No
W20-A238L	PHRRDKDGNS	KKKSK**I**T I A G**S**	No
B19-A238L	PHRRDKDGNS	TTT**P**K**I**I**I**T G**C**	Yes
WT-A238L-NLS 1	PHRRGGGGGS	KKK**P**K**I**I**I**T G**C**	Yes
W13-A238L-NLS 1	PHRRGGGGGS	TTTSK**I**I**I**T G**S**	No
W20-A238L-NLS 1	PHRRGGGGGS	KKKSK**I**T I A G**C**	No
B19-A238L-NLS 1	PHRRGGGGGS	TTT**P**K**I**I**I**T G**C**	Yes

Fig. 2. Domains and mutant forms of A238L used in studies of its subcellular localisation. Panel a) schematically illustrates the structure of A238L illustrating the position of the ankyrin repeats (Ank1 to 4), predicted NLS (NLS-1 and -2), CaN binding domain (CaN bd) and CaN inhibitory domains. Panel b) shows the sequence of the CaN inhibitory domain including residues 157 to 238 from the A238L protein of the BA71V strain and the Malawi LIL20/1 strain. Panel c) shows the sequence of the NLS-1, NLS-2 and CaN binding domain from the wild type A238L and mutant forms used in these studies. The ability of the expressed proteins to bind to CaN as determined previously is indicated by 'Yes' or 'No'.

A number of key questions remain regarding the mechanism by which A238L functions. In particular little is known about functional domains within the A238L protein. A peptide containing the motif which is essential for binding of A238L to CaN did not inhibit phosphatase activity, suggesting that additional sequences from A238L are required for this inhibition (Miskin et al., 2000). Here we demonstrate that the C-terminal 82 amino acid domain of A238L effectively inhibits CaN phosphatase activity. Previously we showed that the A238L protein is actively imported into the nucleus and exported by a CRM-1 dependent pathway. Here we evaluate the role of two putative nuclear localisation signals (NLS) in the nuclear translocation of A238L. Our results show that mutation of either NLS alone does not alter the nuclear accumulation of A238L but that mutation of both significantly reduces nuclear import. In addition we show that mutating the CaN docking motif of A238L results in increased accumulation into the nucleus providing an intact NLS is present. Thus binding of A238L to CaN may result in increased retention of A238L in the cytoplasm.

Results

A238L calcineurin phosphatase inhibitory domain

Our previous data identified critical residues that are required for binding to CaN, PxIxITxC/S within the sequence PKIIITGC at residues 206 to 213 close to the C-terminus of A238L. A 14 amino acid peptide containing residues 200 to 213, which included these residues, bound with high affinity to CaN but did not inhibit its phosphatase activity (Miskin et al., 2000). This suggested that other residues from A238L or possibly another protein, are required to inhibit CaN. In order to identify this domain, we cloned the 3′ end of the A238L gene encoding the C-terminal 82 amino acids from residues 157 to 238 in the bacterial expression vector pET32a. The A238L sequences were fused downstream from the 100 amino acid Trx tag from the thioredoxin gene. Polyhistidine tags were also present in frame with the A238L fragment. The plasmid was transformed into *E. coli* strain BL21 and, following induction of expression, a protein of molecular weight 27 kDa was detected in extracts from bacteria transformed with the plasmid expressing 157–238-A238L-polyhistidine. This protein was not detected in extracts from bacteria transformed with the vector plasmid alone, instead an additional protein of 17 kDa was detected following induction of expression. These proteins were detected by western blotting using an antibody which binds to the polyhistidine tag, confirming that they were the proteins expressed from the pET32a vector (see Fig. 1a). The 157–238-A238L-Trx fusion protein and the Trx tag expressed from the vector alone were purified by Nickel affinity chromatography and the amount of protein quantified. Varying concentrations of this purified A238L-polyhistidine fusion protein, ranging between 60 nM to 720 nM, were added to *in vitro*

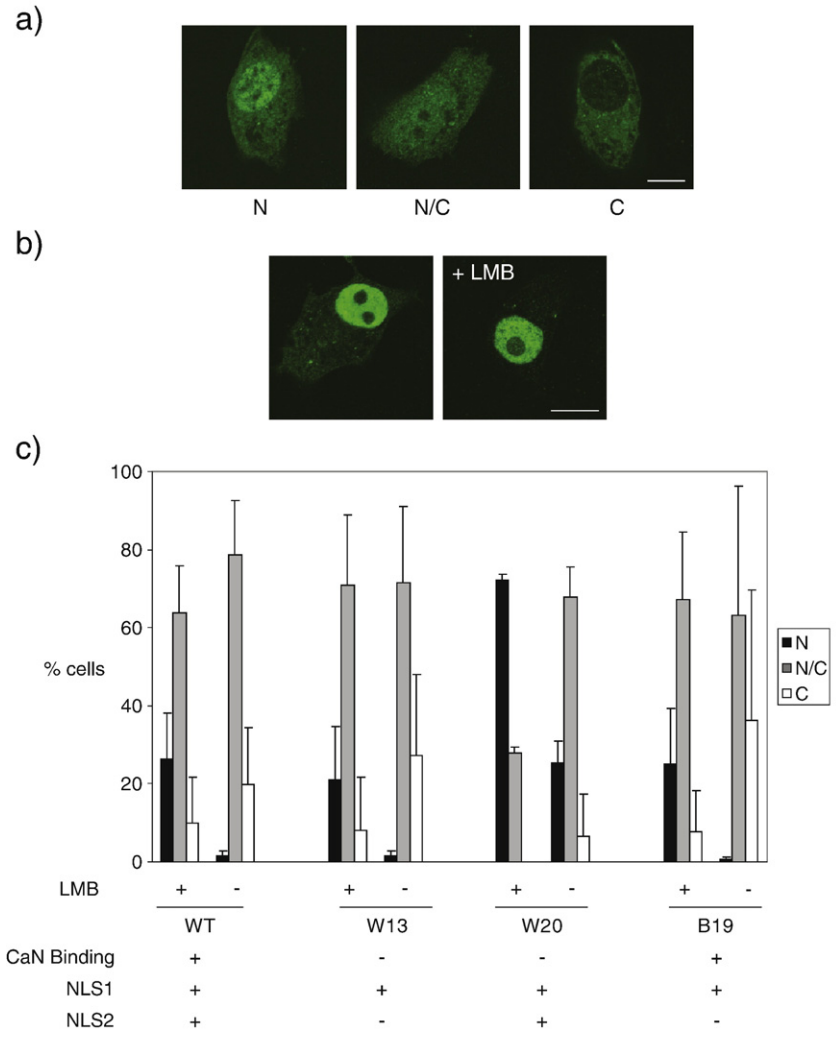

Fig. 3. Effect of mutating NLS-2 and the CaN binding domain on the subcellular distribution of A238L. Vero cells were transfected with plasmids expressing different versions of PK-tagged A238L under the control of the A238L promoter and infected with ASFV BA71V VIKGal strain. After incubation for 13 h cells were treated with or without LMB (40 nM) 3 h prior to fixation. Permeabilised cells were incubated with antibodies against the PK-tag to detect the A238L proteins, followed by Alexa Fluor 488 conjugated goat anti-mouse IgG secondary antibody and imaged using confocal microscopy. Panel a) shows representative images of the subcellular localisation of PK-tagged A238L. This was characterised as either, preferentially nuclear (N), both nuclear and cytoplasmic (N/C) or preferentially cytoplasmic (C). Panel b) shows images from control experiments in which a plasmid expressing IκB fused to the PK-tag was transfected into cells and these were either treated or untreated with LMB. Panel c) shows the percentage of cells exhibiting predominantly nuclear (N), predominantly cytoplasmic (C), or nuclear and cytoplasmic (N/C) distributions for each A238L constructed and tested and under each condition. Data represents 3 independent experiments for which 100 cells were counted for each treatment. Means and standard deviation error bars are shown. The properties of each plasmid tested are shown beneath the graph. A cross (+) represents a functional CaN binding site, NLS-1 and NLS-2 and a bar (−) represents non-functional motifs.

calcineurin phosphatase assays. The ability of these fragments to inhibit the release of [^{32} P] from a phosphorylated substrate of CaN was measured in reactions containing 100 nM concentration of CaN (Fig. 1b). This showed that the 157–238-A238L-polyhistidine protein inhibited CaN in a dose dependent manner varying from 45% inhibition at 60 nM concentration to 80% at 150 nM and more than 90% at 720 nM. The IC_{50} was estimated to be 70 nM. In contrast, no inhibition was observed when comparable amounts of control Trx tag protein purified from bacteria transformed with the pET32a vector without insert was added to the CaN phosphatase assays. A similar percentage inhibition was observed when either the CaN autoinhibitory peptide or cyclosporine A, cyclophilin complexes were added to reactions (data not shown). These results show that the C-terminal domain of A238L containing residues 157 and 238 alone is a very effective inhibitor of CaN phosphatase and that no additional proteins are required. The estimated IC_{50} is comparable to that reported for other inhibitors of CaN including carabin, cyclosporine A/cyclophilin complexes and calcipressin. Attempts were made to further define the domain of A238L required to inhibit CaN phosphatase by subcloning a fragment containing residues 157 to 213 and testing in *in vitro* assays using the same strategy. The results showed this fragment did not inhibit CaN even at concentrations up to 600 nM (data not shown). A peptide was synthesised which contained residues 191 to 220 from A238L. This was tested for its ability to inhibit CaN phosphatase activity but no inhibition was observed even at concentrations up to 600 nM (data not shown). Although no inhibition of CaN activity was observed with these fragments of A238L, we cannot exclude the

possibility that this was because the fragments did not fold in their native format.

Sequences involved in the nuclear localisation of A238L

Previous data had suggested that A238L is present both in the cytoplasm and in the nucleus and that a proportion of the protein is actively transported into the nucleus and exported by a CRM-1 dependent pathway (Silk et al., 2007). In order to define signals in A238L that may be involved in nuclear localisation and to determine if interaction with CaN may affect the localisation of A238L, we observed the subcellular localisation of a series of mutants of the A238L protein by confocal microscopy. Analysis of the A238L protein sequence using the PSORT programme (Horton et al., 2006), which predicts putative nuclear localisation signals (NLS), identified two (see Fig. 2). These NLSs consist of short stretches of amino acids, highly enriched in basic residues. One of these (NLS-1) is located close to the N-terminus of A238L near the C-terminus of the first ankyrin repeat domain and includes amino acids 80 to 86 (PHRRDKD). The second (NLS-2), which includes the sequence KKKPK between amino acids 202 to 206, is located close to the C-terminus adjacent to and overlapping the PxIxITxC/S CaN binding domain. Mapping the NLS-1 motif onto the model of the predicted structure of A238L, suggests it is on the surface of the A238L protein. The NLS-2 sequence is also predicted to be located on the surface since it overlaps the CaN binding site.

To determine if the predicted signals NLS-1 and NLS-2 are involved in the nuclear localisation of A238L, mutations were generated in each of these sites separately and in both sites (Fig. 2). The subcellular localisation of the expressed A238L proteins was examined by confocal microscopy by using antibodies against the PK-epitope tag fused at the N-terminus of the gene. Plasmids expressing A238L under the control of the A238L promoter and containing mutations within the CaN binding motif have been described previously (Miskin et al., 2000). Plasmids W13-A238L and B19-A238L contain mutations within the predicted NLS-2. Although plasmid W20-A238L contains a P to S mutation, this is not predicted to disrupt NLS-2. The proteins W20-A238L and W13-A238L do not bind to CaN whereas the WT-A238L and B19-A238L proteins bind CaN (Fig. 2) (Miskin et al., 2000).

An additional plasmid was constructed which had mutations within the predicted NLS-1. This plasmid (pcDNA3-A238L 84–88) encodes 5 G residues at amino acid positions 84–88, instead of the wild type sequence, DKDGN. This was predicted by the PSORT programme to inactivate the NLS-1 sequence present between residues 80–86. This mutant form of the A238L protein was cloned under control of its own promoter and fused to the PK-epitope tag (pFlanks-WT-NLS-1). A 310 bp N-terminal fragment of A238L containing these mutations in NLS-1, was inserted into the plasmids described above which contain mutations within the predicted NLS-2 and CaN binding domain. The amino acid sequence of the regions including NLS-1 and NLS-2 and the CaN binding properties of all of these plasmids are described in Fig. 2.

The effect of disrupting NLS-2 was first examined by transfection of plasmids expressing wild type and mutant A238L proteins under control of their own promoter into ASFV-infected Vero cells. The subcellular distribution of A238L was examined at late times post-infection by confocal microscopy in both the presence and absence of leptomycin B (LMB) to inhibit CRM-1 mediated nuclear export (Fig. 3a and b). All of these plasmids encode an intact NLS-1. Plasmids pFlanks-W13-A238L and B19-A238L contain mutations which are predicted to disrupt NLS-2; W13-A238L encodes a protein which does not bind CaN and B19-A238L binds to CaN. As mentioned above, the P to S mutation in plasmid W20-A238L does not disrupt NLS-2, but the expressed protein does not bind to CaN. The distribution of A238L was scored as predominantly nuclear, predominantly cytoplasmic or distributed between the nucleus and cytoplasm. Three independent experiments were performed and distributions were scored in 100 cells for each treatment (see Fig. 3.).

Both W13-A238L and B19-A238L showed a similar subcellular distribution to wild type A238L in both the absence and presence of LMB (Fig. 3c). This showed that disruption of the NLS-2 motif alone was not sufficient to alter or prevent the nuclear accumulation of A238L. Surprisingly, in cells transfected with the plasmid expressing W20-A238L, which has an intact NLS-2 but disrupted CaN binding motif, a dramatic increase in the number of cells exhibiting a predominantly nuclear distribution was observed compared to the wild type protein, both in untreated cells and cells treated with LMB. This observation was particularly dramatic in cells treated with LMB since the proportion of cells showing a nuclear distribution of A238L increased from approximately 25% for wild type A238L to greater than 70% for W20-A238L. The number of cells showing a predominantly nuclear distribution was also significantly increased in the absence of LMB: from approximately 2% for wild type A238L to approximately 30% for W20-A238L. Since disruption of the CaN binding site significantly increases the nuclear accumulation of A238L a likely hypothesis is that the interaction between wild type A238L and CaN masks NLS-2, contributing to the retention of a proportion of A238L in the cytoplasm of ASFV-infected cells. The difference observed between untreated cells and those treated with LMB confirm our previous results (Silk et al., 2007) and indicate that a proportion of A238L is exported from the nucleus by a CRM-1 mediated pathway.

The effect of mutating NLS-1 alone, and in combination with NLS-2, was also examined. The subcellular localisation of A238L in the presence and absence of LMB was examined following transfection of 4 plasmids expressing forms of A238L which all had mutations in NLS-1 (A238L-NLS-1, W13-A238L-NLS-1, W20-A238L-NLS-1 and B19-A238L-NLS-1). A238L-NLS-1 does not contain mutations in NLS-2 and, although W20-A238L-NLS-1 has a mutation of the P to S residue (see Fig. 2), this is not predicted to interfere with the function of NLS-2. WT-A238L-NLS-1 and B19-A238L-NLS-1 bind CaN whereas W20-A238L-NLS-1 and W13-A238L-NLS-1 do not bind CaN. W13-A238L-NLS-1 and B19-A238L-NLS-1 both contain a disrupted NLS-2; W13-A238L-NLS-1 does not bind CaN whereas B19-A238L-NLS-1 does bind CaN. As shown

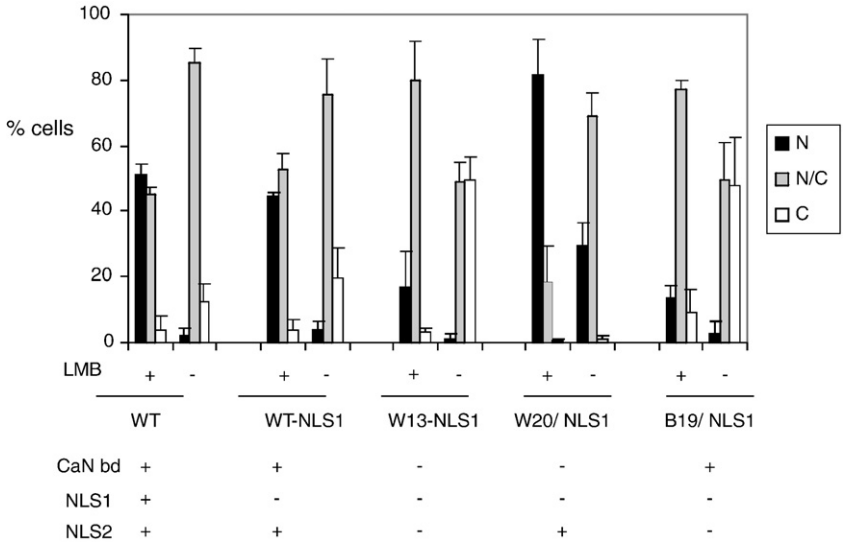

Fig. 4. Effect of mutating NLS-1, NLS-2 and the CaN binding domain on the subcellular distribution of A238L. Vero cells were transfected with plasmids expressing different versions of PK-tagged A238L under the control of its promoter and infected with ASFV BA71V vIKGal strain. After incubation for 13 h cells were treated with or without LMB (40 nM) 3 h prior to fixation. Permeabilised cells were incubated with antibodies against the PK-tag to detect the A238L proteins, followed by Alexa Fluor 488 conjugated secondary antibody. A238L was detected by indirect immunofluorescence. Cells were imaged using confocal microscopy. The percent of cells exhibiting predominantly nuclear (N), predominantly cytoplasmic (C), or nuclear and cytoplasmic (N/C) distributions was determined for each A238L constructed and tested and under each condition. Data represents 3 independent experiments for which 100 cells were counted for each treatment. Means and standard deviation error bars are shown. The properties of each plasmid tested are shown beneath the graph. A cross (+) represents a functional CaN binding site, NLS-1 and NLS-2 and a bar (−) represents non-functional motifs.

(Fig. 4), the expressed WT-A238L-NLS-1 protein showed a similar subcellular distribution to wild type A238L, indicating that disruption of NLS-1 alone was not sufficient to alter the nuclear accumulation of A238L. The protein expressed from plasmid W20-A238L-NLS-1 showed a similar distribution to that expressed from the parental W20 plasmid, (see Figs. 3c and 4) and, as discussed above, a significant increase was detected in the nuclear accumulation of these A238L proteins compared to WT A238L. This supports our hypothesis that disruption of the CaN binding domain results in increased nuclear accumulation of A238L, provided that a functional NLS is present.

In contrast to these results, when cells were transfected with plasmids expressing W13-A238L-NLS-1 and B19-A238L-NLS-1, which contain mutations within both NLS-1 and NLS-2, a dramatic decrease in the number of cells exhibiting a predominately nuclear distribution was observed. In the presence of LMB, less than 15% of the cells examined showed a predominately nuclear distribution for both W13-NLS-1-A238L and B19-NLS-1-A238L, compared to greater than 50% for WT-A238L. In the absence of LMB a significantly higher proportion of cells transfected with W13-A238L-NLS-1 and B19-A238L-NLS-1 exhibited a predominantly cytoplasmic distribution (approximately 50%) compared to those transfected with a plasmid expressing WT-A238L (<10%). Therefore mutation of both NLS-1 and NLS-2 together significantly reduced the nuclear accumulation of A238L, although nuclear translocation of A238L was not completely abolished. This suggests that, in addition to NLS-1 and NLS-2, another mechanism may operate to facilitate the nuclear localisation of A238L. Taken together these results indicate that both of these NLS play a significant role in the nuclear localisation of A238L, and appear to act independently with one compensating for the loss of the other.

Mutation of residues within the A238L ankyrin repeats does not alter the ability to inhibit NF-κB dependent gene expression

The mechanism by which A238L inhibits NF-κB activity has not been defined. Although A238L has been shown to be co-precipitated from cells with the p65 subunit of NF-κB (Revilla et al., 1998; Tait et al., 2000), direct interaction of these proteins has not been demonstrated. However, the presence of ankyrin repeats in A238L suggests that these may make direct contact with NF-κB, as has been reported for IκB. Determination of the structure of IκB in complex with NF-κB (Huxford et al., 1998) showed that non-contacting amino acids play a role in the formation of this complex. The most important of these residues are found within 20 Å of residues Asn 202 and Ser 203 of the P65 subunit of NF-κB (Huxford et al., 1998). The structure of the central domain of A238L containing the ankyrin repeats was modelled using the DeepView software and the structure of IκBα as substrate. Comparison of this model of A238L with that of IκBα identified those residues on A238L which were predicted to be within a 20 Å radius of the 202 and 203 residues of p65 and potentially to make contact with p65. These included two groups of residues between 84 to 88 and 121 to 125 which were highly conserved in the A238L sequences from all ASFV isolates. These residues are located within the ankyrin repeats and are predicted to be solvent exposed on the loop structures.

To determine if mutation of these residues altered the ability of A238L to inhibit NF-κB dependent gene transcription, three mutant forms of A238L were tested. The residues 84 to 88

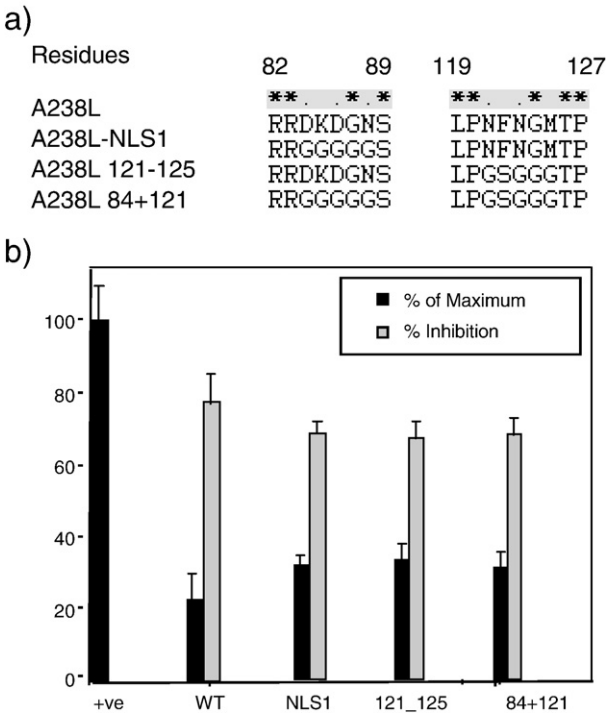

Fig. 5. Effect of mutations in A238L protein on inhibition of NF-κB activation. Sequences encoding residues 84–88 and 121–125 of A238L were mutated as shown in panel a). Plasmids expressing A238L proteins containing these mutations were co-transfected into LPK15a cells with a plasmid expressing the luciferase reporter gene under control of an NF-κB dependent element. Cells were stimulated with PMA, LPS and ionomycin and after 4 h extracts were prepared and tested for luciferase activity. The plasmid transfected is indicated on the x-axis. The y-axis indicates luciferase activity as a percentage of that observed in stimulated cells transfected with vector alone and also shows the percentage inhibition of this activity. Results from a typical experiment including triplicate samples are shown in panel b). Mean and standard deviation error bars are shown.

include sequences within the predicted NLS-1. Mutation of these residues to Gs was described above (A238L-NLS-1). Two additional mutant forms of A238L were constructed. One of these had mutated sequences encoding residues 121 to 125 to either G or S (A238L 121_125). The third mutant (A238L 84+121) combined both sets of mutations in residues 84 to 88 and 121 to 125. To test the effect of these mutant forms of A238L on activation of NF-κB dependent transcription, the plasmids expressing mutant forms or wild type A238L were co-transfected into PK15a cells with an NF-κB dependent luciferase reporter construct. Cells were stimulated with PMA, LPS and ionomycin to activate NF-κB and the level of activation assayed by measuring luciferase activity in cell extracts. The expression of wild type A238L inhibited the activation of NF-κB dependent gene transcription by 78% compared to stimulated cells (Fig. 5) whereas expression of A238L-NLS-1 inhibited NF-κB activation by 68% and expression of A238L 121_125 inhibited NF-κB activation by 69%. Expression of the A238L mutant, A238L 84+121, which combined both of these mutations, also inhibited NF-κB activation by 69%. Therefore mutation of these groups of residues both individually and combined had a comparatively small effect on the ability of A238L to inhibit NF-κB activation.

Discussion

A238L is the only protein known to combine the functions of inhibiting both CaN phosphatase activity and activation of NF-κB. The importance of these pathways as targets for immunosuppressive drugs means that there is considerable interest in defining the molecular mechanisms by which these dual functions of A238L are mediated and the functional consequences. Previously a CaN docking motif of sequence PKIIITGC was identified in the C-terminal domain of A238L. This domain contains critical residues PxIxITxC/S required for binding of A238L to CaN. A 14 amino acid peptide, including this motif and adjacent residues, bound to CaN with high affinity (K_d 600 nM) but did not inhibit its phosphatase activity, suggesting that additional residues were required for inhibition. These might be either from A238L or another protein which might associate with A238L (Miskin et al., 2000a). Here we show that an 82 amino acid C-terminal domain of A238L very effectively inhibits CaN phosphatase activity at low concentrations (IC_{50} is approximately 70 nM) indicating that this fragment binds to CaN with high affinity to inhibit its phosphatase activity.

The CaN docking motif in A238L closely resembles those in substrate proteins of CaN including NFAT 1–4 (Aramburu et al., 1998, 1999) and the yeast transcription factor Crz1 (Roy et al., 2007) as well as cellular inhibitors of CaN including members of the calcipressin family and cabin/cain (Aubareda et al., 2006; Liu, 2003; Martinez-Martinez and Redondo, 2004; Sun et al., 1998).

Although all of these proteins share the conserved residues PxIxIT in their CaN docking sequence, other residues both in the core motif and surrounding residues differ considerably. There is strong evidence supporting a model whereby the sequence of these other residues in the docking motif determines the affinity of binding to CaN. A random screening approach identified the peptide containing core residues PVIVIT which bound to CaN with higher affinity than the docking peptide identified in NFAT (PRIEIT) (Aramburu et al., 1998, 1999). Replacement of the CaN docking motif in the CaN substrates NFAT and the yeast Crz1 protein with the PVIVIT sequence resulted in their constitutive dephosphorylation and activation (Aramburu et al., 1998; Roy et al., 2007). In the NFAT protein a second site involved in binding to CaN has been identified and it is proposed that this is a lower affinity interaction which is brought into contact with CaN following initial binding to the PRIEIT sequence. This brings the hyperphosphorylated residues on NFAT in contact with the active site following displacement of the autoinhibitory peptide of CaN (Garcia-Cozar et al., 1998; Park et al., 2000). The structure of the PVIVIT peptide in complex with CaN has recently been solved by NMR. These results showed that the PVIVIT peptide binds as a β-strand on the edge of a β-sheet of CaN. The side chains of the core residues PxIxIT make extensive interactions with conserved residues in CaN. Non-conserved residues are solvent exposed and sequence variations can modulate the K_d of the interaction (between 1 μM to 1 mM) (Li et al., 2007; Takeuchi et al., 2007). We showed previously that a 14 amino acid residue peptide containing the docking motif from A238L competed more strongly for binding

to CaN than the comparable peptide from porcine NFAT-2 supporting the hypothesis that A238L may bind to CaN via this docking motif with higher affinity than NFAT (Miskin et al., 2000). We propose that this interaction brings additional residues from A238L into contact with CaN, resulting in inhibition of phosphatase activity, possibly by blocking access to the active site. Other possibilities such as conformational changes in CaN induced by the binding cannot be excluded. Our demonstration that a purified recombinant protein containing the C-terminal 82 amino acids of A238L inhibits CaN phosphatase activity very effectively with an IC_{50} comparable to other defined CaN inhibitors (IC_{50} in the nM range) shows that no other proteins are required for the inhibition. We have not further defined the sequences in A238L required for inhibiting CaN. There is no obvious sequence similarity with the second site in NFAT (Cn B) that is required for binding to CaN or with inhibitory domains from the defined CaN endogenous inhibitors (Hogan et al., 2003). Sequence comparison of A238L proteins from 9 different isolates show that these share between 75 and 100% identity (Neilan et al., 1997) and residues in the C-terminal domain are very well conserved.

Previous data has shown that A238L is present in both the cytoplasm and nucleus of cells and that a proportion is actively imported into the nucleus and exported by a CRM-1 mediated pathway (Silk et al., 2007). Here we have examined the role of two predicted NLS signals, one located within the first ankyrin repeat and the other immediately adjacent to the CaN docking motif. We showed that mutation of each of these independently did not significantly alter the nuclear accumulation of A238L when compared to the wild type A238L. However, when both of these putative NLS were mutated, nuclear accumulation of A238L was significantly reduced compared to mutation of either NLS alone or the wild type A238L. This suggests that both of these putative NLS are involved in nuclear import of A238L and that one can compensate for loss of the other. Mutation of the CaN docking motif, which is adjacent to and partially overlaps with the NLS-2, resulted in a dramatic increase in nuclear accumulation of A238L when the NLS-2 signal was intact. In contrast expression of mutant A238L, with both a disrupted CaN docking motif and NLS-2 signal did not result in any increased nuclear accumulation compared to wild type A238L. An attractive hypothesis is that binding of CaN to A238L masks this NLS-2 and this contributes to retention of A238L in the cytoplasm. In this case the NLS-1, which is close to the N-terminus of A238L and distant from the CaN binding domain, may be exposed and direct nuclear translocation of A238L. We observed increased nuclear accumulation of the higher molecular weight form of A238L at late times post-infection compared to early times (Silk et al., 2007). This form of A238L was shown to be preferentially co-precipitated with the p65 subunit of NF-κB suggesting it may function primarily to inhibit NF-κB activity. Possibly post-translational modification of A238L may disrupt its binding to CaN exposing NLS-2 and enhancing the nuclear localisation of this modified form of A238L. Binding of CaN to the lower molecular weight form of A238L may enhance cytoplasmic retention of this form of the protein.

The detailed mechanism by which A238L inhibits NF-κB activation remains unclear. Although A238L can be co-precipitated with the p65 subunit of NF-κB, direct interaction between the proteins has not been demonstrated. Here we have mutated residues of A238L predicted to be important for interaction with p65 and shown that there was no dramatic effect of these mutations on the ability of A238L to inhibit NF-κB activation.

No other proteins have been described which have the dual functions of inhibiting both CaN and NF-κB pathways. However endogenous inhibitors of CaN combined with other pathways have been described. One such endogenous inhibitor is the ubiquitously expressed Cabin 1/cain CaN protein. This consists of more than 2200 amino acids and contains functional domains in addition to the CaN inhibitory domain. A region containing multiple ligands for SH3 domains is required for binding of Cabin 1/cain to amphiphysin, a component of a protein complex responsible for calcium dependent synaptic vesicle release. A model was proposed in which Cabin 1/cain serves as a negative regulator of CaN and neurotransmitter endocytosis. In addition to its function as a negative regulator of CaN, Cabin 1/cain was shown to act as a transcriptional repressor of the myocyte enhancing factor (MEF)-2 family of transcription factors. This may provide a mechanism to integrate regulation of both CaN dependent and MEF2 pathways. An endogenous inhibitor of CaN, named Carabin, has recently been identified, which also inhibits the Ras signalling pathway through its intrinsic Ras GTPase-activating protein (GAP) activity. Expression of this inhibitor is induced through the T cell signalling pathway. As a negative feedback inhibitor of the CaN signalling pathway that also mediates cross-talk between CaN and Ras, Carabin may provide a mechanism for feedback regulation of pathways including T cell activation (Pan et al., 2007). Evidence suggests that the main role of the A238L protein is to inhibit the activation of host defence pathways dependent on CaN and NF-κB which occurs in response to virus infection. Targeting of these pathways by A238L emphasises their importance in regulating the host's defences in infected macrophages.

CaN and NF-κB pathways are important targets for immunosuppressive drugs. Understanding how A238L inhibits both pathways will provide new leads for drug discovery. Here we have identified a short domain of 82 amino acids which acts as a potent inhibitor of CaN.

Materials and methods

Viruses and cells

The Vero cell-adapted ASFV strain BA71V with the A238L gene deleted, vIKGAL, has been described previously (Miskin et al., 1998). Vero cells were used for infections with ASFV. Vero cells and PK15a (Gilpin et al., 2003) cells were used for transfections.

Construction of plasmids

The fragments of A238L encoding residues 157 to 238 and 157 to 213 from the Malawi LIL 20/1 isolate were amplified by

PCR, including restriction enzyme sites *Bam* HI and *Hind* III at the 5′ and 3′ ends respectively. These fragments were digested with *Bam* HI and *Hind* III and cloned into the pET32a vector (Novagen), which had been digested with the same enzymes.

Sequences encoding residues 84 to 88 and 121 to 125 of A238L were mutated using the Stratagene quick change system. The respective fragments were amplified by PCR from plasmid pcDNA3-A238L (Miskin et al., 1998) using oligonucleotides CTCATAGGAGGGGTGGAGGTGGAGGCTCTGC TTTACATTATTTAG and CTAAATAATGTAAAGCAGAGCCTCCACCTCCACCCCTCCTATGAG or GGGACCAAAATTTGTTTACCGGGTTCTGGTGGGGGGACTCCTGTG and CACAGGAGTCCCCCCACCAGAACC CGGTAAACAAATTTTGGTCCC. These oligonucleotides introduce the following mutations, residues 84 to 88 change from DKDGN to GGGGG and residues 121–125 are changed from NFNGM to GSGGG, respectively.

The plasmids pFlanks-A238L, pFlanks-W13-A238L, pFlanks-W20-A238L, and pFlanks-B19-A238L have been described previously (Miskin et al., 2000). These contain upstream promoter sequences of the A238L gene and either the wild type A238L gene from Malawi LIL 20/1 isolate or forms of the gene containing mutations in the CaN docking motif as described previously (Miskin et al., 2000). The PK-tag is fused at the N-terminus of the A238L gene in all plasmids. The plasmids pFlanks-WT-A238L-NLS-1, pFlanks-W13-A238L-NLS-1, pFlanks-W20-A238L-NLS-1, and pFlanks-B19-A238L-NLS-1 were constructed by inserting a fragment containing the mutated version of the predicted NLS-1 site into plasmids pFlanks-A238L, pFlanks-W13-A238L, pFlanks-W20-A238L, and pFlanks-B19-A238L. This was achieved by PCR amplification of a fragment encoding amino acids 1 to 103 from the pcDNA3-A238L84–88 plasmid using forward and reverse primers containing an *Xho1* site and *EcoN1* site respectively. The resulting PCR product was digested with *Xho1* and *EcoN1* and ligated into the appropriate backbone plasmid from which the same fragment had been removed by digestion. The sequence of all plasmids was confirmed. The NF-κB dependent luciferase reporter plasmid was a gift from Prof. Ron Hay, University of Dundee and was used previously to measure the effect of A238L.

Expression and purification of proteins from E. coli

The pET32a vector containing fragments from A238L and the vector without insert, were transformed into *E. coli* strain BL21 and cultures incubated at 37 °C. Expression of the proteins was induced by addition of IPTG and 2 h after induction bacteria were pelleted and lysed by suspension in buffer containing 50 mM Tris pH 8.0, 1 mM DTT, 10 mM imidazole, 300 mM NaCl, 0.1% NP40 and a mixture of protease inhibitors (Sigma), followed by sonication for 5 bursts of 30 s. The expressed proteins were purified using His Trap columns (GEHealthcare) according to the manufacturer's instructions. Purified proteins were stored at −80 °C in aliquots. The amount of protein present was determined using the Protein Assay Kit (Biorad) and by comparison with a known amount of protein markers run on SDS-PAGE and detected by silver staining. Proteins samples were separated by SDS-PAGE and either detected by silver staining or blotted onto Hybond C membranes (GE Health care) and detected with anti-His antibody (GE Healthcare) followed by secondary antibodies. Bound antibodies were detected by enhanced chemiluminescence.

CaN phosphatase assays

Purified CaN (100 nM Sigma) and calmodulin (600 nm Sigma) were incubated for 30 min. with ^{32}P-labelled RII phosphopeptide in 60 μl reactions containing 12 mM Tris–HCl (pH 7.5), 3.5 mM $MgCl_2$, 17 mM $CaCl_2$, 8 mM 2-mercaptoethanol, and 58 μg/ml bovine serum albumin. CaN phosphatase activity was measured by release of [^{32}P]-phosphate from the RII phosphopeptide (Fruman et al., 1996). Where indicated recombinant proteins were added to the reactions.

Infection and transfection

Vero cells or PK15a cells were seeded into 35 mm wells of a 6 well plate at a density of 1×10^6 and incubated at 37 °C, 5% CO_2, for 24 h. Vero cells were infected with ASFV for 2 h then transfected with 5 μg of plasmid DNA using lipofectin or lipofectamine according to the manufacturer's recommendations (Invitrogen). After transfection for 5 h at 37 °C, 5% CO_2, the transfection reagent was replaced with 3 ml of antibiotic free DMEM and incubated for further periods as indicated.

SDS-PAGE gel electrophoresis and Western blotting

Protein samples were prepared in SDS-PAGE sample loading buffer and heated at 90 °C for 5 min to denature the protein sample. Proteins were resolved at 100 V on 12.5% Tricine SDS-PAGE gels. Where appropriate a small aliquot of the protein sample was removed for quantification prior to the addition of loading buffer. Gels were either silver stained or transferred to PVDF membrane, 0.2 μm, for Western blot analysis. Western blots were probed with anti-His antibody (GE Healthcare) at a dilution of 1/1000 followed by HRP-conjugated Protein A. Bound antibodies were detected by enhanced chemiluminescence.

Confocal microscopy

Cell monolayers were grown on 22 × 22 mm glass cover slips in 35 mm wells and fixed for 20 min in PBSe containing 4% paraformaldehyde. The cells were permeabilised in 1% Triton X-100 in PBSe for 15 min then incubated in 0.5% BSA in PBSe for 30 min to inhibit non-specific antibody binding. They were incubated with primary antibody diluted in 0.5% BSA/PBSe for 1 h and after washing in secondary antibody diluted in 0.5% BSA/PBSe for 1 h. After washing cells were mounted onto glass slides using VectaShield mounting medium with Dapi (Vector Laboratories). The cells were visualised using Leica TCS SP2 confocal microscopy. The primary antibody used was mouse anti-PK-tag (Serotec) 20 μg/ml and the secondary antibody was Alexa Fluor 488 goat anti-mouse 10 μg/ml.

Luciferase assays

PK15a cells were transfected with either a NF-κB luciferase expression plasmid or both the NF-κB luciferase expression plasmid and an A238L expression plasmid, as previously described. After incubation for 18 h post-transfection cells were stimulated by the addition of 100 nM Phorbol 12-myristate 13-acetate (PMA), 10 μg/ml Lipopolysacharide (LPS) and 4 nM Ionomycin for 4 h to induce NF-κB activity. The cells were then harvested using the Promega (USA) Luciferase assay system according to the manufacturer's instructions. Sample measurement was performed using a BioOrbit 1253 luminometer (Turku, Finland) according to the instructions provided by Promega.

Protein modelling

The structure of A238L was modelled using the DeepView software package (Guex and Peitsch, 1997). The model of A238L is based upon the atomic coordinates from the crystal structure of IκB, as these two proteins share significant homology within the region of the ankyrin repeats. As the significant homology only encompasses the central region of A238L, the model lacks the first 52 amino acids from the N-terminus and last 55 amino acids from the C-terminus.

Acknowledgments

We thank Drs. Gavin Bowick, Fuquan Zhang and Lynnette Goatley for helpful discussions and acknowledge financial support from BBSRC and DEFRA.

References

Aramburu, J., Garcia-Cozar, F., Raghavan, A., Okamura, H., Rao, A., Hogan, P.G., 1998. Selective inhibition of NFAT activation by a peptide spanning the calcineurin targeting site of NFAT. Mol. Cell 1 (5), 627–637.

Aramburu, J., Yaffe, M.B., Lopez-Rodriguez, C., Cantley, L.C., Hogan, P.G., Rao, A., 1999. Affinity-driven peptide selection of an NFAT inhibitor more selective than cyclosporin A. Science 285 (5436), 2129–2133.

Aubareda, A., Mulero, M.C., Perez-Riba, M., 2006. Functional characterization of the calcipressin motif that suppresses calcineurin-mediated NFAT-dependent cytokine gene expression in human T cells. Cell. Signal. 18 (9), 1430–1438.

Dixon, L.K., Escribano, J.M., Martins, C., Rock, D.L., Salas, M.L., Wilkinson, P.J., 2005. Asfarviridae (2005). Asfarviridae In: Fauquet, C.M., Mayo, M.A., Maniloff, J., Desselberger, U., Ball, L.A. (Eds.), Virus Taxonomy, VIIIth Report of the ICTV. Elsevier/Academic Press, London, pp. 135–143.

Fruman, D.A., Pai, S.Y., Klee, C.B., Burakoff, S.J., Bierer, B.E., 1996. Measurement of calcineurin phosphatase activity in cell extracts. METHODS: A Companion to Methods in Enzymology 9 (2), 146–154.

Garcia-Cozar, F.J., Okamura, H., Aramburu, J.F., Shaw, K.T.Y., Pelletier, L., Showalter, R., Villafranca, E., Rao, A., 1998. Two-site interaction of nuclear factor of activated T cells with activated calcineurin. J. Biol. Chem. 273 (37), 23877–23883.

Gilpin, D.F., McCullough, K., Meehan, B.M., McNeilly, F., McNair, I., Stevenson, L.S., Foster, J.C., Ellis, J.A., Krakowka, S., Adair, B.M., Allan, G.M., 2003. *In vitro* studies on the infection and replication of porcine circovirus type 2 in cells of the porcine immune system. Vet. Immunol. Immunopathol. 94 (3–4), 149–161.

Granja, A.G., Nogal, M.L., Hurtado, C., del Aguila, C., Carrascosa, A.L., Salas, M.L., Fresno, M., Revilla, Y., 2006a. The viral protein A238L inhibits TNF-alpha expression through a CBP/p300 transcriptional coactivators pathway. J. Immunol. 176 (1), 451–462.

Granja, A.G., Nogal, M.L., Hurtado, C., Vila, V., Carrascosa, A.L., Salas, M.L., Fresno, M., Revilla, Y., 2004. The viral protein A238L inhibits cyclooxygenase-2 expression through a nuclear factor of activated T cell-dependent transactivation pathway. J. Biol. Chem. 279 (51), 53736–53746.

Granja, A.G., Sabina, P., Salas, M.L., Fresno, M., Revilla, Y., 2006b. Regulation of inducible nitric oxide synthase expression by viral A238L-mediated inhibition of p65/RelA acetylation and p300 transactivation. J. Virol. 80 (21), 10487–10496.

Guex, N., Peitsch, M.C., 1997. SWISS-MODEL and the Swiss-PdbViewer: an environment for comparative protein modeling. Electrophoresis 18 (15), 2714–2723.

Hogan, P.G., Chen, L., Nardone, J., Rao, A., 2003. Transcriptional regulation by calcium, calcineurin, and NFAT. Genes Dev. 17 (18), 2205–2232.

Horton, P., Park, K.-J., Obayashi, T., Nakai, K., 2006. Protein subcellular localization prediction with WoLF PSORT. Proceedings of the 4th Annual Asia Pacific Bioinformatics Conference APBC06, Taipei, Taiwan, pp. 39–48.

Huxford, T., Huang, D.B., Malek, S., Ghosh, G., 1998. The crystal structure of the I kappa B alpha/NF-kappa B complex reveals mechanisms of NF-kappa B inactivation. Cell 95 (6), 759–770.

Li, H.M., Zhang, L., Rao, A., Harrison, S.C., Hogan, P.G., 2007. Structure of calcineurin in complex with PVIVIT peptide: portrait of a low-affinity signalling interaction. J. Mol. Biol. 369 (5), 1296–1306.

Liu, J.O., 2003. Endogenous protein inhibitors of calcineurin. Biochem. Biophys. Res. Commun. 311 (4), 1103–1109.

Martinez-Martinez, S., Redondo, J.M., 2004. Inhibitors of the calcineurin/NFAT pathway. Curr. Med. Chem. 11 (8), 997–1007.

Miskin, J.E., Abrams, C.C., Goatley, L.C., Dixon, L.K., 1998. A viral mechanism for inhibition of the cellular phosphatase calcineurin. Science 281 (5376), 562–565.

Miskin, J.E., Abrams, C.C., Dixon, L.K., 2000. African swine fever virus protein A238L interacts with the cellular phosphatase calcineurin via a binding domain similar to that of NFAT. J. Virol. 74 (20), 9412–9420.

Neilan, J.G., Lu, Z., Kutish, G.F., Zsak, L., Lewis, T.L., Rock, D.L., 1997. A conserved African swine fever virus I kappa B homolog, 5EL, is nonessential for growth in vitro and virulence in domestic swine. Virology 235 (2), 377–385.

Pan, F., Sun, L., Kardian, D.B., Whartenby, K.A., Pardoll, D.M., Liu, J.O., 2007. Feedback inhibition of calcineurin and Ras by a dual inhibitory protein Carabin. Nature 445 (7126), 433–436.

Park, S., Uesugi, M., Verdine, G.L., 2000. A second calcineurin binding site on the NFAT regulatory domain. Proc. Natl. Acad. Sci. U. S. A. 97 (13), 7130–7135.

Powell, P.P., Dixon, L.K., Parkhouse, R.M.E., 1996. An I kappa B homolog encoded by African swine fever virus provides a novel mechanism for downregulation of proinflammatory cytokine responses in host macrophages. J. Virol. 70 (12), 8527–8533.

Revilla, Y., Callejo, M., Rodriguez, J.M., Culebras, E., Nogal, M.L., Salas, M.L., Vinuela, E., Fresno, M., 1998. Inhibition of nuclear factor kappa B activation by a virus-encoded I kappa B-like protein. J. Biol. Chem. 273 (9), 5405–5411.

Roy, J., Li, H.M., Hogan, P.G., Cyert, M.S., 2007. A conserved docking site modulates substrate affinity for calcineurin, signaling output, and in vivo function. Mol. Cell 25 (6), 889–901.

Silk, R.N., Bowick, G.C., Abrams, C.C., Dixon, L.K., 2007. African swine fever virus A238L inhibitor of NF-kappa B and of calcineurin phosphatase is imported actively into the nucleus and exported by a CRM1-mediated pathway. J. Gen. Virol. 88, 411–419.

Sun, L., Youn, H.D., Loh, C., Stolow, M., He, W.W., Liu, J.O., 1998. Cabin 1, a negative regulator for calcineurin signaling in T lymphocytes. Immunity 8 (6), 703–711.

Tait, S.W.G., Reid, E.B., Greaves, D.R., Wileman, T.E., Powell, P.P., 2000. Mechanism of inactivation of NF-kappa B by a viral homologue of I kappa B alpha—signal-induced release of I kappa B alpha results in binding of the viral homologue to NF-kappa B. J. Biol. Chem. 275 (44), 34656–34664.

Takeuchi, K., Roehrl, M.H.A., Sun, Z.Y.J., Wagner, G., 2007. Structure of the calcineurin–NFAT complex: defining a T cell activation switch using solution NMR and crystal coordinates. Structure 15 (5), 587–597.

Wietek, C., O'Neill, L.A.J., 2007. Diversity and regulation in the NF-κB system. Trends Biochem. Sci. 32 (7), 211–219.

Appendix 2

Genes differentially regulated by baculovirus, LPS, PMA and ionomycin treatment.

APPENDIX 2 Genes differentialy regulated by baculovirus, LPS, PMA and ionomycin treatment

Accession No.	Description	1 hour Average	CI -ve	CI +ve	4 hours Average	CI -ve	CI +ve
Genes up regulated by baculovirus treatment followed by LPS, PMA and ionomycin stimulation at 1 hr post stimulation							
NM_020858	sema domain, transmembrane domain (TM), and cytoplasmic domain, (semaphorin) 6D (SEM	1.88	(1.52	, 2.24)			
NM_003246	thrombospondin 1 (THBS1), mRNA	1.63	(1.19	, 2.07)			
NM_020747	zinc finger protein 608 (ZNF608), mRNA	1.37	(1.02	, 1.72)			
NM_000014	alpha-2-macroglobulin (A2M), mRNA	1.34	(1.21	, 1.46)			
NM_014622	loss of heterozygosity, 11, chromosomal region 2, gene A (LOH11CR2A), transcript vari	1.31	(1	, 1.62)			
NM_000856	guanylate cyclase 1, soluble, alpha 3 (GUCY1A3), mRNA	1.29	(1.19	, 1.38)			
NM_002224	inositol 1,4,5-triphosphate receptor, type 3 (ITPR3), mRNA	1.26	(1.22	, 1.29)			
NM_004183	vitelliform macular dystrophy (Best disease, bestrophin) (VMD2), mRNA	1.25	(0.75	, 1.75)			
NM_003931	WAS protein family, member 1 (WASF1), mRNA	1.21	(0.7	, 1.73)			
NM_002885	RAP1, GTPase activating protein 1 (RAP1GA1), mRNA	1.2	(1.07	, 1.34)			
NM_002603	phosphodiesterase 7A (PDE7A), transcript variant 1, mRNA	1.19	(0.38	, 2.01)			
NM_002356	myristoylated alanine-rich protein kinase C substrate (MARCKS), mRNA	1.18	(0.84	, 1.52)			
NM_005447	peptidylglycine alpha-amidating monooxygenase COOH-terminal interactor (PAMCI), mRNA	1.14	(0.68	, 1.6)			
NM_003243	transforming growth factor, beta receptor III (betaglycan, 300kDa) (TGFBR3), mRNA	1.11	(0.81	, 1.41)			
NM_020732	AT rich interactive domain 1B (SWI1-like) (ARID1B), transcript variant 2, mRNA	1.1	(0.86	, 1.33)			
NM_006887	zinc finger protein 36, C3H type-like 2 (ZFP36L2), mRNA	1.09	(0.79	, 1.39)			
NM_181673	O-linked N-acetylglucosamine (GlcNAc) transferase (UDP-N-acetylglucosamine:polypeptid	1.07	(0.76	, 1.38)			
NM_018243	septin 11 (SEPT11), mRNA	1.06	(0.51	, 1.61)			
NM_014606	hect domain and RLD 3 (HERC3), mRNA	1.06	(0.82	, 1.29)			
NM_004910	phosphatidylinositol transfer protein, membrane-associated 1 (PITPNM1), mRNA	1.06	(0.74	, 1.38)			
NM_020918	glycerol-3-phosphate acyltransferase, mitochondrial (GPAM), mRNA	1.05	(0.74	, 1.36)			
NM_032772	zinc finger protein 503 (ZNF503), mRNA	1.04	(0.62	, 1.47)			
NM_020770	cingulin (CGN), mRNA	1.04	(0.77	, 1.32)			
NM_001006665	ribosomal protein S6 kinase, 90kDa, polypeptide 1 (RPS6KA1), transcript variant 2, mR	1.03	(0.72	, 1.35)			
NM_021070	latent transforming growth factor beta binding protein 3 (LTBP3), mRNA	1.02	(0.8	, 1.24)			
NM_006044	histone deacetylase 6 (HDAC6), mRNA	1.01	(0.88	, 1.13)			

NM_033632	F-box and WD-40 domain protein 7 (archipelago homolog, Drosophila) (FBXW7), transcrip	1	(	0.54	,	1.46	)
NM_001005404	yippee-like 2 (Drosophila) (YPEL2), mRNA	0.99	(	0.72	,	1.26	)
NM_006079	Cbp/p300-interacting transactivator, with Glu/Asp-rich carboxy-terminal domain, 2 (CI	0.99	(	0.61	,	1.37	)
NM_002589	BH-protocadherin (brain-heart) (PCDH7), transcript variant a, mRNA	0.99	(	0.86	,	1.11	)
NM_000293	phosphorylase kinase, beta (PHKB), mRNA	0.98	(	0.75	,	1.22	)
NM_145175	NSE1 (NSE1), mRNA	0.98	(	0.68	,	1.28	)
NM_006469	influenza virus NS1A binding protein (IVNS1ABP), transcript variant 1, mRNA	0.97	(	0.84	,	1.11	)
NM_024613	pleckstrin homology domain containing, family F (with FYVE domain) member 2 (PLEKHF2)	0.97	(	0.53	,	1.4	)
NM_138615	DEAH (Asp-Glu-Ala-His) box polypeptide 30 (DHX30), transcript variant 1, mRNA	0.95	(	0.7	,	1.2	)
NM_021056	tuberous sclerosis 2 (TSC2), transcript variant 3, mRNA	0.95	(	0.82	,	1.07	)
NM_145341	programmed cell death 4 (neoplastic transformation inhibitor) (PDCD4), transcript var	0.94	(	0.69	,	1.19	)
NM_002166	inhibitor of DNA binding 2, dominant negative helix-loop-helix protein (ID2), mRNA	0.93	(	0.85	,	1.01	)
NM_004926	zinc finger protein 36, C3H type-like 1 (ZFP36L1), mRNA	0.92	(	0.57	,	1.28	)
NM_014452	tumor necrosis factor receptor superfamily, member 21 (TNFRSF21), mRNA	0.92	(	0.66	,	1.18	)
NM_006820	interferon-induced protein 44 (IFI44L), mRNA	0.92	(	0.77	,	1.06	)
NM_144729	dual specificity phosphatase 10 (DUSP10), transcript variant 3, mRNA	0.92	(	0.59	,	1.24	)
NM_000455	serine/threonine kinase 11 (Peutz-Jeghers syndrome) (STK11), mRNA	0.91	(	0.52	,	1.3	)
NM_004071	CDC-like kinase 1 (CLK1), mRNA	0.9	(	0.74	,	1.07	)
NM_033104	stonin 2 (STN2), mRNA	0.89	(	0.55	,	1.24	)
NM_206943	latent transforming growth factor beta binding protein 1 (LTBP1), transcript variant	0.89	(	0.44	,	1.34	)
NM_013392	nuclear receptor binding protein (NRBP), mRNA	0.89	(	0.62	,	1.16	)
NM_032457	BH-protocadherin (brain-heart) (PCDH7), transcript variant c, mRNA	0.89	(	0.76	,	1.01	)
NM_020801	arrestin domain containing 3 (ARRDC3), mRNA	0.88	(	0.3	,	1.46	)
NM_133635	protein O-fucosyltransferase 2 (POFUT2), transcript variant 3, mRNA	0.88	(	0.62	,	1.14	)
NM_173694	ATPase, Class VI, type 11C (ATP11C), mRNA	0.87	(	0.76	,	0.99	)
NM_012235	SREBP cleavage-activating protein (SCAP), mRNA	0.87	(	0.58	,	1.16	)
NM_015246	mahogunin, ring finger 1 (MGRN1), mRNA	0.86	(	0.72	,	1.01	)
NM_172060	eyes absent homolog 1 (Drosophila) (EYA1), transcript variant 1, mRNA	0.86	(	0.41	,	1.31	)
NM_001418	eukaryotic translation initiation factor 4 gamma, 2 (EIF4G2), mRNA	0.86	(	0.5	,	1.22	)
NM_020654	SUMO1/sentrin specific protease 7 (SENP7), mRNA	0.86	(	0.61	,	1.11	)
NM_005966	NGFI-A binding protein 1 (EGR1 binding protein 1) (NAB1), mRNA	0.85	(	0.81	,	0.88	)
NM_018364	round spermatid basic protein 1 (RSBN1), mRNA	0.84	(	0.59	,	1.1	)
NM_198501	FLJ42461 protein (FLJ42461), mRNA	0.84	(	0.34	,	1.34	)

NM_003688	calcium/calmodulin-dependent serine protein kinase (MAGUK family) (CASK), mRNA	0.83	(	0.54	,	1.12	)
NM_018490	leucine-rich repeat-containing G protein-coupled receptor 4 (LGR4), mRNA	0.83	(	0.37	,	1.3	)
NM_012199	eukaryotic translation initiation factor 2C, 1 (EIF2C1), mRNA	0.82	(	0.49	,	1.16	)
NM_001627	activated leukocyte cell adhesion molecule (ALCAM), mRNA	0.82	(	0.66	,	0.98	)
NM_000340	solute carrier family 2 (facilitated glucose transporter), member 2 (SLC2A2), mRNA	0.82	(	0.4	,	1.24	)
NM_000259	myosin VA (heavy polypeptide 12, myoxin) (MYO5A), mRNA	0.82	(	0.66	,	0.98	)
NM_002821	PTK7 protein tyrosine kinase 7 (PTK7), transcript variant PTK7-1, mRNA	0.81	(	0.72	,	0.9	)
NM_002569	furin (paired basic amino acid cleaving enzyme) (FURIN), mRNA	0.8	(	0.74	,	0.85	)
NM_001287	chloride channel 7 (CLCN7), mRNA	0.8	(	0.64	,	0.95	)
NM_017641	kinesin family member 21A (KIF21A), mRNA	0.79	(	0.09	,	1.5	)
NM_053064	guanine nucleotide binding protein (G protein), gamma 2 (GNG2), mRNA	0.79	(	0.65	,	0.94	)
NM_152754	sema domain, immunoglobulin domain (Ig), short basic domain, secreted, (semaphorin) 3	0.79	(	0.55	,	1.03	)
NM_016275	selenoprotein T (SELT), mRNA	0.79	(	0.62	,	0.95	)
NM_014707	histone deacetylase 9 (HDAC9), transcript variant 3, mRNA	0.79	(	0.57	,	1	)
NM_016061	yippee-like 5 (Drosophila) (YPEL5), mRNA	0.79	(	0.48	,	1.09	)
NM_000341	solute carrier family 3 (cystine, dibasic and neutral amino acid transporters, activa	0.79	(	-0.15	,	1.72	)
NM_080685	protein tyrosine phosphatase, non-receptor type 13 (APO-1/CD95 (Fas)-associated phosp	0.78	(	0.71	,	0.85	)
NM_007191	WNT inhibitory factor 1 (WIF1), mRNA	0.78	(	0.23	,	1.33	)
NM_198968	DAZ interacting protein 1 (DZIP1), mRNA	0.78	(	-0.06	,	1.61	)
NM_004162	RAB5A, member RAS oncogene family (RAB5A), mRNA	0.78	(	0.69	,	0.86	)
NM_015662	selective LIM binding factor, rat homolog (SLB), mRNA	0.77	(	0.47	,	1.08	)
NM_005630	solute carrier organic anion transporter family, member 2A1 (SLCO2A1), mRNA	0.77	(	0.64	,	0.9	)
NM_005581	Lutheran blood group (Auberger b antigen included) (LU), mRNA	0.77	(	0.55	,	0.99	)
NM_013291	cleavage and polyadenylation specific factor 1, 160kDa (CPSF1), mRNA	0.77	(	0.53	,	1.01	)
NM_032547	short coiled-coil protein (SCOC), mRNA	0.77	(	0.44	,	1.1	)
NM_002291	laminin, beta 1 (LAMB1), mRNA	0.77	(	0.22	,	1.31	)
NM_170662	Cas-Br-M (murine) ecotropic retroviral transforming sequence b (CBLB), mRNA	0.77	(	0.45	,	1.09	)
NM_145740	glutathione S-transferase A1 (GSTA1), mRNA	0.77	(	0.58	,	0.96	)
NM_030791	sphingosine-1-phosphate phosphatase 1 (SGPP1), mRNA	0.77	(	0.47	,	1.06	)
NM_002971	special AT-rich sequence binding protein 1 (binds to nuclear matrix/scaffold-associat	0.77	(	0.71	,	0.82	)
NM_016824	adducin 3 (gamma) (ADD3), transcript variant 1, mRNA	0.76	(	0.62	,	0.9	)
NM_002111	huntingtin (Huntington disease) (HD), mRNA	0.76	(	0.54	,	0.98	)
NM_003020	secretory granule, neuroendocrine protein 1 (7B2 protein) (SGNE1), mRNA	0.76	(	0.59	,	0.93	)

NM_007222	zinc fingers and homeoboxes 1 (ZHX1), mRNA	0.76	(	0.59	,	0.92	)
NM_016357	epithelial protein lost in neoplasm beta (EPLIN), mRNA	0.76	(	0.45	,	1.07	)
NM_080792	protein tyrosine phosphatase, non-receptor type substrate 1 (PTPNS1), mRNA	0.76	(	0.33	,	1.18	)
NM_000166	gap junction protein, beta 1, 32kDa (connexin 32, Charcot-Marie-Tooth neuropathy, X-l	0.76	(	0.65	,	0.86	)
NM_022171	T-cell leukemia translocation altered gene (TCTA), mRNA	0.75	(	0.71	,	0.79	)
NM_001256	cell division cycle 27 (CDC27), mRNA	0.75	(	0.5	,	0.99	)
NM_002210	integrin, alpha V (vitronectin receptor, alpha polypeptide, antigen CD51) (ITGAV), mR	0.75	(	0.49	,	1.01	)
NM_006648	protein kinase, lysine deficient 2 (PRKWNK2), mRNA	0.75	(	0.05	,	1.44	)
NM_001343	disabled homolog 2, mitogen-responsive phosphoprotein (Drosophila) (DAB2), mRNA	0.75	(	0.6	,	0.89	)
NM_004225	malignant fibrous histiocytoma amplified sequence 1 (MFHAS1), mRNA	0.74	(	0.38	,	1.11	)
NM_006835	cyclin I (CCNI), mRNA	0.74	(	0.66	,	0.83	)
NM_021005	nuclear receptor subfamily 2, group F, member 2 (NR2F2), mRNA	0.74	(	0.6	,	0.88	)
NM_015640	PAI-1 mRNA-binding protein (PAI-RBP1), mRNA	0.74	(	0.69	,	0.79	)
NM_003128	spectrin, beta, non-erythrocytic 1 (SPTBN1), transcript variant 1, mRNA	0.74	(	0.64	,	0.83	)
NM_001418	eukaryotic translation initiation factor 4 gamma, 2 (EIF4G2), mRNA	0.73	(	0.64	,	0.82	)
NM_130839	ubiquitin protein ligase E3A (human papilloma virus E6-associated protein, Angelman s	0.73	(	0.66	,	0.8	)
NM_153280	ubiquitin-activating enzyme E1 (A1S9T and BN75 temperature sensitivity complementing)	0.73	(	0.67	,	0.78	)
NM_000110	dihydropyrimidine dehydrogenase (DPYD), mRNA	0.73	(	0.55	,	0.9	)
NM_025188	tripartite motif-containing 45 (TRIM45), mRNA	0.72	(	0.45	,	1	)
NM_014729	thymus high mobility group box protein TOX (TOX), mRNA	0.72	(	0.05	,	1.4	)
NM_013231	fibronectin leucine rich transmembrane protein 2 (FLRT2), mRNA	0.72	(	0.43	,	1.01	)
NM_006614	cell adhesion molecule with homology to L1CAM (close homolog of L1) (CHL1), mRNA	0.72	(	0.16	,	1.29	)
NM_000362	tissue inhibitor of metalloproteinase 3 (Sorsby fundus dystrophy, pseudoinflammatory)	0.72	(	0.59	,	0.85	)
NM_052886	mal, T-cell differentiation protein 2 (MAL2), mRNA	0.72	(	0.56	,	0.88	)
NM_032995	Rho guanine nucleotide exchange factor (GEF) 4 (ARHGEF4), transcript variant 2, mRNA	0.72	(	0.51	,	0.92	)
NM_198576	agrin (AGRN), mRNA	0.72	(	0.46	,	0.97	)
NM_003601	SWI/SNF related, matrix associated, actin dependent regulator of chromatin, subfamily	0.72	(	0.47	,	0.96	)
NM_015964	brain specific protein (CGI-38), mRNA	0.72	(	0.11	,	1.32	)
NM_002979	sterol carrier protein 2 (SCP2), transcript variant 1, mRNA	0.71	(	0.37	,	1.06	)
NM_022157	Ras-related GTP binding C (RRAGC), mRNA	0.71	(	0.32	,	1.1	)
NM_032383	Hermansky-Pudlak syndrome 3 (HPS3), mRNA	0.71	(	0.49	,	0.92	)
NM_148169	F-box protein 17 (FBXO17), transcript variant 1, mRNA	0.7	(	0.06	,	1.35	)
NM_000042	apolipoprotein H (beta-2-glycoprotein I) (APOH), mRNA	0.7	(	0.52	,	0.89	)

NM_199462	receptor interacting protein kinase 5 (RIPK5), transcript variant 2, mRNA	0.7	(	0.14	,	1.26	)
NM_173853	keratinocyte associated protein 3 (KRTCAP3), mRNA	0.7	(	0.58	,	0.81	)
NM_002959	sortilin 1 (SORT1), mRNA	0.7	(	0.43	,	0.96	)
NM_052932	pro-oncosis receptor inducing membrane injury gene (PORIMIN), mRNA	0.7	(	0.49	,	0.9	)
NM_212472	protein kinase, cAMP-dependent, regulatory, type I, alpha (tissue specific extinguish	0.69	(	0.54	,	0.85	)
NM_015141	glycerol-3-phosphate dehydrogenase 1-like (GPD1L), mRNA	0.69	(	0.55	,	0.84	)
NM_004723	rho/rac guanine nucleotide exchange factor (GEF) 2 (ARHGEF2), mRNA	0.69	(	0.53	,	0.86	)
NM_020861	zinc finger and BTB domain containing 2 (ZBTB2), mRNA	0.69	(	0.49	,	0.89	)
NM_005924	mesenchyme homeo box 2 (growth arrest-specific homeo box) (MEOX2), mRNA	0.69	(	0.5	,	0.88	)
NM_207035	NPD014 protein (NPD014), transcript variant 1, mRNA	0.69	(	0.56	,	0.82	)
NM_012089	ATP-binding cassette, sub-family B (MDR/TAP), member 10 (ABCB10), nuclear gene encodi	0.69	(	0.3	,	1.08	)
NM_000186	complement factor H (CFH), mRNA	0.69	(	0.52	,	0.85	)
NM_016596	histone deacetylase 7A (HDAC7A), transcript variant 2, mRNA	0.68	(	0.64	,	0.73	)
NM_003640	inhibitor of kappa light polypeptide gene enhancer in B-cells, kinase complex-associa	0.68	(	0.55	,	0.81	)
NM_139321	attractin (ATRN), transcript variant 1, mRNA	0.68	(	0.51	,	0.85	)
NM_000314	phosphatase and tensin homolog (mutated in multiple advanced cancers 1) (PTEN), mRNA	0.68	(	0.53	,	0.83	)
NM_003972	BTAF1 RNA polymerase II, B-TFIID transcription factor-associated, 170kDa (Mot1 homolo	0.67	(	0.31	,	1.04	)
NM_005197	checkpoint suppressor 1 (CHES1), mRNA	0.67	(	0.27	,	1.07	)
NM_006275	splicing factor, arginine/serine-rich 6 (SFRS6), mRNA	0.67	(	0.56	,	0.78	)
NM_002856	poliovirus receptor-related 2 (herpesvirus entry mediator B) (PVRL2), mRNA	0.67	(	0.48	,	0.85	)
NM_002227	Janus kinase 1 (a protein tyrosine kinase) (JAK1), mRNA	0.67	(	0.47	,	0.86	)
NM_207040	transcription factor 12 (HTF4, helix-loop-helix transcription factors 4) (TCF12), tra	0.67	(	0.35	,	0.99	)
NM_020169	latexin (LXN), mRNA	0.67	(	0.11	,	1.23	)
NM_021913	AXL receptor tyrosine kinase (AXL), transcript variant 1, mRNA	0.67	(	0.27	,	1.06	)
NM_032451	spire homolog 2 (Drosophila) (SPIRE2), mRNA	0.66	(	0.46	,	0.86	)
NM_000945	protein phosphatase 3 (formerly 2B), regulatory subunit B, 19kDa, alpha isoform (calc	0.66	(	0.52	,	0.81	)
NM_021906	ubiquitin specific protease 9, X-linked (fat facets-like, Drosophila) (USP9X), transc	0.66	(	0.3	,	1.02	)
NM_003629	phosphoinositide-3-kinase, regulatory subunit 3 (p55, gamma) (PIK3R3), mRNA	0.66	(	0.35	,	0.97	)
NM_024658	importin 4 (IPO4), mRNA	0.66	(	0.5	,	0.82	)
NM_145906	RIO kinase 3 (yeast) (RIOK3), transcript variant 2, mRNA	0.66	(	0.41	,	0.91	)
NM_006664	chemokine (C-C motif) ligand 27 (CCL27), mRNA	0.66	(	0.53	,	0.78	)
NM_001846	collagen, type IV, alpha 2 (COL4A2), mRNA	0.66	(	0.63	,	0.68	)
NM_016235	G protein-coupled receptor, family C, group 5, member B (GPRC5B), mRNA	0.66	(	0.5	,	0.81	)

NM_177414	phosphatidic acid phosphatase type 2B (PPAP2B), transcript variant 2, mRNA	0.66	(	0.24	,	1.07	)
NM_012406	PR domain containing 4 (PRDM4), mRNA	0.66	(	0.57	,	0.74	)
NM_006243	protein phosphatase 2, regulatory subunit B (B56), alpha isoform (PPP2R5A), mRNA	0.65	(	0.41	,	0.89	)
NM_003479	protein tyrosine phosphatase type IVA, member 2 (PTP4A2), transcript variant 1, mRNA	0.65	(	0.18	,	1.12	)
NM_000927	ATP-binding cassette, sub-family B (MDR/TAP), member 1 (ABCB1), mRNA	0.65	(	0.57	,	0.73	)
NM_138730	high mobility group nucleosomal binding domain 3 (HMGN3), transcript variant 2, mRNA	0.65	(	0.42	,	0.87	)
NM_018085	importin 9 (IPO9), mRNA	0.64	(	0.26	,	1.03	)
NM_020166	methylcrotonoyl-Coenzyme A carboxylase 1 (alpha) (MCCC1), mRNA	0.64	(	0.44	,	0.85	)
NM_004438	EPH receptor A4 (EPHA4), mRNA	0.64	(	0.43	,	0.86	)
NM_003635	N-deacetylase/N-sulfotransferase (heparan glucosaminyl) 2 (NDST2), mRNA	0.64	(	0.4	,	0.89	)
NM_001690	ATPase, H+ transporting, lysosomal 70kDa, V1 subunit A (ATP6V1A), mRNA	0.64	(	0.44	,	0.84	)
NM_001005502	carboxypeptidase M (CPM), transcript variant 3, mRNA	0.64	(	-0.18	,	1.46	)
NM_005967	NGFI-A binding protein 2 (EGR1 binding protein 2) (NAB2), mRNA	0.64	(	0.45	,	0.83	)
NM_016035	coenzyme Q4 homolog (yeast) (COQ4), mRNA	0.64	(	0.13	,	1.15	)
NM_199368	transient receptor potential cation channel, subfamily C, member 4 associated protein	0.64	(	0.57	,	0.71	)
NM_001001560	golgi associated, gamma adaptin ear containing, ARF binding protein 1 (GGA1), transcr	0.63	(	0.4	,	0.87	)
NM_014454	sestrin 1 (SESN1), mRNA	0.63	(	0.56	,	0.7	)
NM_001418	eukaryotic translation initiation factor 4 gamma, 2 (EIF4G2), mRNA	0.63	(	0.54	,	0.71	)
NM_000084	chloride channel 5 (nephrolithiasis 2, X-linked, Dent disease) (CLCN5), mRNA	0.63	(	0.42	,	0.84	)
NM_198976	TH1-like (Drosophila) (TH1L), transcript variant 1, mRNA	0.63	(	0.47	,	0.78	)
NM_181524	phosphoinositide-3-kinase, regulatory subunit 1 (p85 alpha) (PIK3R1), transcript vari	0.62	(	0.48	,	0.77	)
NM_001901	connective tissue growth factor (CTGF), mRNA	0.62	(	0.44	,	0.81	)
NM_015518	DKFZP434C131 protein (DKFZP434C131), mRNA	0.62	(	0.47	,	0.78	)
NM_000038	adenomatosis polyposis coli (APC), mRNA	0.62	(	0.24	,	1.01	)
NM_012287	centaurin, beta 2 (CENTB2), mRNA	0.62	(	0.35	,	0.9	)
NM_012414	rab3 GTPase-activating protein, non-catalytic subunit (150kD) (RAB3-GAP150), mRNA	0.62	(	0.45	,	0.8	)
NM_003128	spectrin, beta, non-erythrocytic 1 (SPTBN1), transcript variant 1, mRNA	0.62	(	0.45	,	0.79	)
NM_000689	aldehyde dehydrogenase 1 family, member A1 (ALDH1A1), mRNA	0.62	(	0.45	,	0.79	)
NM_005313	glucose regulated protein, 58kDa (GRP58), mRNA	0.62	(	0.46	,	0.78	)
NM_004776	UDP-Gal:betaGlcNAc beta 1,4- galactosyltransferase, polypeptide 5 (B4GALT5), mRNA	0.62	(	0.36	,	0.87	)
NM_002703	phosphoribosyl pyrophosphate amidotransferase (PPAT), mRNA	0.62	(	0.36	,	0.88	)
NM_014014	activating signal cointegrator 1 complex subunit 3-like 1 (ASCC3L1), mRNA	0.62	(	0.44	,	0.79	)
NM_020385	XPMC2 prevents mitotic catastrophe 2 homolog (Xenopus laevis) (XPMC2H), mRNA	0.62	(	0.54	,	0.69	)

NM_005474	histone deacetylase 5 (HDAC5), transcript variant 1, mRNA	0.61	(	0.49	,	0.74	)
NM_001008493	enabled homolog (Drosophila) (ENAH), transcript variant 1, mRNA	0.61	(	0.25	,	0.98	)
NM_203372	acyl-CoA synthetase long-chain family member 3 (ACSL3), transcript variant 2, mRNA	0.61	(	0.55	,	0.68	)
NM_194298	solute carrier family 16 (monocarboxylic acid transporters), member 9 (SLC16A9), mRNA	0.61	(	0.5	,	0.73	)
NM_014633	SH2 domain binding protein 1 (tetratricopeptide repeat containing) (SH2BP1), mRNA	0.61	(	0.29	,	0.93	)
NM_004521	kinesin family member 5B (KIF5B), mRNA	0.61	(	0.39	,	0.83	)
NM_004529	myeloid/lymphoid or mixed-lineage leukemia (trithorax homolog, Drosophila); transloca	0.61	(	0.33	,	0.89	)
NM_002291	laminin, beta 1 (LAMB1), mRNA	0.61	(	0.39	,	0.82	)
NM_006378	sema domain, immunoglobulin domain (Ig), transmembrane domain (TM) and short cytoplas	0.6	(	0.51	,	0.7	)
NM_022776	oxysterol binding protein-like 11 (OSBPL11), mRNA	0.6	(	0.55	,	0.65	)
NM_006805	heterogeneous nuclear ribonucleoprotein A0 (HNRPA0), mRNA	0.6	(	0.46	,	0.74	)
NM_145059	fucokinase (FUK), mRNA	0.6	(	0.2	,	0.99	)
NM_018303	SEC5-like 1 (S. cerevisiae) (SEC5L1), mRNA	0.6	(	0.41	,	0.78	)
NM_006622	polo-like kinase 2 (Drosophila) (PLK2), mRNA	0.59	(	0.37	,	0.81	)
NM_000903	NAD(P)H dehydrogenase, quinone 1 (NQO1), mRNA	0.59	(	0.38	,	0.8	)
NM_006751	sperm specific antigen 2 (SSFA2), mRNA	0.59	(	0.34	,	0.84	)
NM_002687	pinin, desmosome associated protein (PNN), mRNA	0.59	(	0.44	,	0.74	)
NM_013449	bromodomain adjacent to zinc finger domain, 2A (BAZ2A), mRNA	0.59	(	0.43	,	0.75	)
NM_145720	tigger transposable element derived 4 (TIGD4), mRNA	0.58	(	0.4	,	0.77	)
NM_033140	caldesmon 1 (CALD1), transcript variant 5, mRNA	0.58	(	0.52	,	0.65	)
NM_207297	muscleblind-like (Drosophila) (MBNL1), transcript variant 7, mRNA	0.58	(	0.38	,	0.78	)
NM_212482	fibronectin 1 (FN1), transcript variant 1, mRNA	0.58	(	0.52	,	0.65	)
NM_006243	protein phosphatase 2, regulatory subunit B (B56), alpha isoform (PPP2R5A), mRNA	0.58	(	0.44	,	0.73	)
NM_003565	unc-51-like kinase 1 (C. elegans) (ULK1), mRNA	0.58	(	0.32	,	0.85	)
NM_002293	laminin, gamma 1 (formerly LAMB2) (LAMC1), mRNA	0.58	(	0.31	,	0.85	)
NM_002568	poly(A) binding protein, cytoplasmic 1 (PABPC1), mRNA	0.58	(	0.56	,	0.6	)
NM_000263	N-acetylglucosaminidase, alpha- (Sanfilippo disease IIIB) (NAGLU), mRNA	0.58	(	0.16	,	0.99	)
NM_004157	protein kinase, cAMP-dependent, regulatory, type II, alpha (PRKAR2A), mRNA	0.58	(	0.34	,	0.82	)
NM_013374	programmed cell death 6 interacting protein (PDCD6IP), mRNA	0.58	(	0.43	,	0.73	)
NM_016357	epithelial protein lost in neoplasm beta (EPLIN), mRNA	0.57	(	0.26	,	0.89	)
NM_017436	alpha 1,4-galactosyltransferase (A4GALT), mRNA	0.57	(	0.13	,	1.02	)
NM_004656	BRCA1 associated protein-1 (ubiquitin carboxy-terminal hydrolase) (BAP1), mRNA	0.57	(	0.41	,	0.74	)
NM_004449	v-ets erythroblastosis virus E26 oncogene like (avian) (ERG), transcript variant 2, m	0.57	(	0.34	,	0.8	)

NM_003506	frizzled homolog 6 (Drosophila) (FZD6), mRNA	0.57	(	0.46	,	0.68	)
NM_000790	dopa decarboxylase (aromatic L-amino acid decarboxylase) (DDC), mRNA	0.57	(	0.22	,	0.92	)
NM_003635	N-deacetylase/N-sulfotransferase (heparan glucosaminyl) 2 (NDST2), mRNA	0.57	(	0.35	,	0.79	)
NM_003861	WD repeat domain 22 (WDR22), mRNA	0.57	(	0.49	,	0.66	)
NM_003070	SWI/SNF related, matrix associated, actin dependent regulator of chromatin, subfamily	0.57	(	0.16	,	0.98	)
NM_001007553	upstream of NRAS (UNR), transcript variant 1, mRNA	0.57	(	0.44	,	0.7	)
NM_005316	general transcription factor IIH, polypeptide 1 (62kD subunit) (GTF2H1), mRNA	0.57	(	0.29	,	0.85	)
NM_022575	vacuolar protein sorting 16 (yeast) (VPS16), transcript variant 1, mRNA	0.57	(	0.34	,	0.8	)
NM_025160	WD repeat domain 26 (WDR26), mRNA	0.57	(	0.28	,	0.86	)
NM_001304	carboxypeptidase D (CPD), mRNA	0.57	(	0.27	,	0.86	)
NM_006357	ubiquitin-conjugating enzyme E2E 3 (UBC4/5 homolog, yeast) (UBE2E3), transcript varia	0.57	(	0.46	,	0.67	)
NM_000722	calcium channel, voltage-dependent, alpha 2/delta subunit 1 (CACNA2D1), mRNA	0.57	(	0.33	,	0.8	)
NM_014862	aryl-hydrocarbon receptor nuclear translocator 2 (ARNT2), mRNA	0.57	(	0.32	,	0.81	)
NM_004667	hect domain and RLD 2 (HERC2), mRNA	0.57	(	0.34	,	0.79	)
NM_058172	anthrax toxin receptor 2 (ANTXR2), mRNA	0.56	(	0.34	,	0.79	)
NM_014892	RNA binding motif protein 16 (RBM16), mRNA	0.56	(	0.36	,	0.77	)
NM_016322	RAB14, member RAS oncogene family (RAB14), mRNA	0.56	(	0.45	,	0.68	)
NM_015200	SCC-112 protein (SCC-112), mRNA	0.56	(	0.5	,	0.62	)
NM_018482	development and differentiation enhancing factor 1 (DDEF1), mRNA	0.56	(	0.25	,	0.87	)
NM_025132	WD repeat domain 19 (WDR19), mRNA	0.56	(	0.08	,	1.04	)
NM_006887	zinc finger protein 36, C3H type-like 2 (ZFP36L2), mRNA	0.56	(	0.14	,	0.98	)
NM_173561	unc-5 homolog C (C. elegans)-like (UNC5CL), mRNA	0.56	(	0.52	,	0.59	)
NM_015885	pre-mRNA cleavage complex II protein Pcf11 (PCF11), mRNA	0.56	(	0.27	,	0.84	)
NM_024085	APG9 autophagy 9-like 1 (S. cerevisiae) (APG9L1), mRNA	0.56	(	0.17	,	0.94	)
NM_005847	solute carrier family 23 (nucleobase transporters), member 1 (SLC23A1), transcript va	0.56	(	0.4	,	0.71	)
NM_001618	poly (ADP-ribose) polymerase family, member 1 (PARP1), mRNA	0.55	(	0.35	,	0.76	)
NM_020150	SAR1a gene homolog 1 (S. cerevisiae) (SARA1), mRNA	0.55	(	0.4	,	0.71	)
NM_003385	visinin-like 1 (VSNL1), mRNA	0.55	(	0.35	,	0.75	)
NM_014727	myeloid/lymphoid or mixed-lineage leukemia 4 (MLL4), mRNA	0.55	(	0.45	,	0.65	)
NM_020132	1-acylglycerol-3-phosphate O-acyltransferase 3 (AGPAT3), mRNA	0.55	(	0.52	,	0.58	)
NM_138729	suppression of tumorigenicity 7 like (ST7L), transcript variant 4, mRNA	0.55	(	0.25	,	0.85	)
NM_006763	BTG family, member 2 (BTG2), mRNA	0.55	(	0.25	,	0.85	)
NM_014991	WD repeat and FYVE domain containing 3 (WDFY3), transcript variant 1, mRNA	0.55	(	0.21	,	0.89	)

NM_144996	ADP-ribosylation factor-like 2-like 1 (ARL2L1), transcript variant 2, mRNA	0.55	(	0.36	,	0.74	)
NM_181354	oxidation resistance 1 (OXR1), mRNA	0.55	(	0.4	,	0.69	)
NM_006565	CCCTC-binding factor (zinc finger protein) (CTCF), mRNA	0.55	(	0.28	,	0.82	)
NM_006822	RAB40B, member RAS oncogene family (RAB40B), mRNA	0.54	(	0.36	,	0.73	)
NM_172218	sperm associated antigen 1 (SPAG1), transcript variant 2, mRNA	0.54	(	0.43	,	0.66	)
NM_033271	BTB (POZ) domain containing 6 (BTBD6), mRNA	0.54	(	0.18	,	0.91	)
NM_019610	similar to RNA binding motif protein, X-linked (LOC494115), mRNA	0.54	(	0.31	,	0.77	)
NM_000359	transglutaminase 1 (K polypeptide epidermal type I, protein-glutamine-gamma-glutamylt	0.54	(	0.39	,	0.7	)
NM_025109	myosin head domain containing 1 (MYOHD1), mRNA	0.54	(	0.47	,	0.61	)
NM_015989	cysteine sulfinic acid decarboxylase (CSAD), mRNA	0.54	(	0.09	,	0.99	)
NM_021962	active BCR-related gene (ABR), transcript variant 1, mRNA	0.54	(	0.51	,	0.57	)
NM_014947	forkhead box J3 (FOXJ3), mRNA	0.54	(	0.44	,	0.63	)
NM_005502	ATP-binding cassette, sub-family A (ABC1), member 1 (ABCA1), mRNA	0.54	(	0.43	,	0.65	)
NM_003216	thyrotrophic embryonic factor (TEF), mRNA	0.54	(	0.47	,	0.6	)
NM_005271	glutamate dehydrogenase 1 (GLUD1), mRNA	0.54	(	0.39	,	0.69	)
NM_024712	engulfment and cell motility 3 (ced-12 homolog, C. elegans) (ELMO3), mRNA	0.54	(	0.22	,	0.85	)
NM_005077	transducin-like enhancer of split 1 (E(sp1) homolog, Drosophila) (TLE1), mRNA	0.54	(	0.38	,	0.69	)
NM_004124	glia maturation factor, beta (GMFB), mRNA	0.53	(	0.38	,	0.69	)
NM_017761	proline-rich nuclear receptor coactivator 2 (PNRC2), mRNA	0.53	(	0.43	,	0.63	)
NM_004705	protein-kinase, interferon-inducible double stranded RNA dependent inhibitor, repress	0.53	(	0.46	,	0.61	)
NM_002271	RAN binding protein 5 (RANBP5), mRNA	0.53	(	0.41	,	0.66	)
NM_002945	replication protein A1, 70kDa (RPA1), mRNA	0.53	(	0.38	,	0.68	)
NM_018847	kelch-like 9 (Drosophila) (KLHL9), mRNA	0.53	(	0.47	,	0.59	)
NM_006016	CD164 antigen, sialomucin (CD164), mRNA	0.53	(	0.32	,	0.75	)
NM_000176	nuclear receptor subfamily 3, group C, member 1 (glucocorticoid receptor) (NR3C1), mR	0.53	(	0.18	,	0.89	)
NM_020440	prostaglandin F2 receptor negative regulator (PTGFRN), mRNA	0.53	(	0.44	,	0.63	)
NM_014735	PHD finger protein 16 (PHF16), mRNA	0.53	(	0.18	,	0.88	)
NM_003922	hect (homologous to the E6-AP (UBE3A) carboxyl terminus) domain and RCC1 (CHC1)-like	0.53	(	0.42	,	0.64	)
NM_001987	ets variant gene 6 (TEL oncogene) (ETV6), mRNA	0.53	(	0.15	,	0.91	)
NM_032409	PTEN induced putative kinase 1 (PINK1), mRNA	0.53	(	0.24	,	0.81	)
NM_004120	guanylate binding protein 2, interferon-inducible (GBP2), mRNA	0.53	(	0.29	,	0.77	)
NM_012330	MYST histone acetyltransferase (monocytic leukemia) 4 (MYST4), mRNA	0.53	(	0.43	,	0.63	)
NM_020383	X-prolyl aminopeptidase (aminopeptidase P) 1, soluble (XPNPEP1), mRNA	0.53	(	0.44	,	0.62	)

NM_018695	erbb2 interacting protein (ERBB2IP), transcript variant 2, mRNA	0.53	(	0.38	,	0.67	)
NM_021009	ubiquitin C (UBC), mRNA	0.53	(	0.36	,	0.69	)
NM_020899	zinc finger and BTB domain containing 4 (ZBTB4), mRNA	0.53	(	0.19	,	0.86	)
NM_017922	PRP39 pre-mRNA processing factor 39 homolog (yeast) (PRPF39), mRNA	0.52	(	0.34	,	0.71	)
NM_017944	ubiquitin specific protease 47 (USP47), mRNA	0.52	(	0.16	,	0.89	)
NM_016081	palladin (KIAA0992), mRNA	0.52	(	0.36	,	0.69	)
NM_005595	nuclear factor I/A (NFIA), mRNA	0.52	(	0.37	,	0.68	)
NM_183381	ring finger protein 13 (RNF13), transcript variant 4, mRNA	0.52	(	0.12	,	0.93	)
NM_005766	FERM, RhoGEF (ARHGEF) and pleckstrin domain protein 1 (chondrocyte-derived) (FARP1),	0.52	(	0.24	,	0.8	)
NM_020773	TBC1 domain family, member 14 (TBC1D14), mRNA	0.52	(	0.29	,	0.75	)
NM_014950	zinc finger and BTB domain containing 1 (ZBTB1), mRNA	0.52	(	0.43	,	0.61	)
NM_025238	BTB (POZ) domain containing 1 (BTBD1), mRNA	0.52	(	0.35	,	0.69	)
NM_020965	membrane-associated guanylate kinase-related (MAGI-3) (MAGI-3), mRNA	0.52	(	0.41	,	0.63	)
NM_138973	beta-site APP-cleaving enzyme 1 (BACE1), transcript variant d, mRNA	0.52	(	0.45	,	0.59	)
NM_004170	solute carrier family 1 (neuronal/epithelial high affinity glutamate transporter, sys	0.52	(	0.41	,	0.63	)
NM_205842	NCK-associated protein 1 (NCKAP1), transcript variant 2, mRNA	0.52	(	0.42	,	0.61	)
NM_014038	basic leucine zipper and W2 domains 2 (BZW2), mRNA	0.52	(	0.39	,	0.65	)
NM_003982	solute carrier family 7 (cationic amino acid transporter, y+ system), member 7 (SLC7A	0.52	(	0.3	,	0.74	)
NM_015153	PHD finger protein 3 (PHF3), mRNA	0.52	(	0.39	,	0.64	)
NM_014604	Tax1 (human T-cell leukemia virus type I) binding protein 3 (TAX1BP3), mRNA	0.51	(	0.08	,	0.95	)
NM_014314	DEAD (Asp-Glu-Ala-Asp) box polypeptide 58 (DDX58), mRNA	0.51	(	0.39	,	0.64	)
NM_002647	phosphoinositide-3-kinase, class 3 (PIK3C3), mRNA	0.51	(	0.21	,	0.82	)
NM_147233	nuclear receptor coactivator 1 (NCOA1), transcript variant 3, mRNA	0.51	(	0.32	,	0.71	)
NM_019063	echinoderm microtubule associated protein like 4 (EML4), mRNA	0.51	(	0.23	,	0.8	)
NM_002065	glutamate-ammonia ligase (glutamine synthase) (GLUL), mRNA	0.51	(	0.37	,	0.66	)
NM_019023	protein arginine N-methyltransferase 7 (PRMT7), mRNA	0.51	(	0.35	,	0.68	)
NM_005445	chondroitin sulfate proteoglycan 6 (bamacan) (CSPG6), mRNA	0.51	(	0.4	,	0.62	)
NM_004396	DEAD (Asp-Glu-Ala-Asp) box polypeptide 5 (DDX5), mRNA	0.51	(	0.44	,	0.58	)
NM_001396	dual-specificity tyrosine-(Y)-phosphorylation regulated kinase 1A (DYRK1A), transcrip	0.51	(	0.21	,	0.81	)
NM_001753	caveolin 1, caveolae protein, 22kDa (CAV1), mRNA	0.51	(	0.2	,	0.82	)
NM_201281	myotubularin related protein 2 (MTMR2), transcript variant 3, mRNA	0.51	(	0.24	,	0.77	)
NM_001568	eukaryotic translation initiation factor 3, subunit 6 48kDa (EIF3S6), mRNA	0.51	(	0.32	,	0.69	)
NM_003816	a disintegrin and metalloproteinase domain 9 (meltrin gamma) (ADAM9), transcript vari	0.51	(	0.3	,	0.71	)

NM_003036	v-ski sarcoma viral oncogene homolog (avian) (SKI), mRNA	0.51	(	0.31	,	0.7	)
NM_007214	SEC63-like (S. cerevisiae) (SEC63), mRNA	0.51	(	0.29	,	0.72	)
NM_025230	WD repeat domain 23 (WDR23), transcript variant 1, mRNA	0.5	(	0.42	,	0.59	)
NM_080546	CDW92 antigen (CDW92), mRNA	0.5	(	0.33	,	0.68	)
NM_152493	FLJ25476 protein (FLJ25476), mRNA	0.5	(	0.46	,	0.55	)
NM_001280	cold inducible RNA binding protein (CIRBP), mRNA	0.5	(	0.23	,	0.77	)
NM_022470	p53 target zinc finger protein (WIG1), transcript variant 1, mRNA	0.5	(	0.17	,	0.83	)
NM_004393	dystroglycan 1 (dystrophin-associated glycoprotein 1) (DAG1), mRNA	0.5	(	0.24	,	0.76	)
NM_004476	folate hydrolase (prostate-specific membrane antigen) 1 (FOLH1), mRNA	0.5	(	0.26	,	0.74	)
NM_015393	DKFZP564O0823 protein (DKFZP564O0823), mRNA	0.5	(	0.36	,	0.63	)
NM_020142	NADH:ubiquinone oxidoreductase MLRQ subunit homolog (LOC56901), mRNA	0.5	(	0.36	,	0.63	)
NM_006646	WAS protein family, member 3 (WASF3), mRNA	0.49	(	0.12	,	0.87	)
NM_006022	transforming growth factor beta 1 induced transcript 4 (TGFB1I4), transcript variant	0.49	(	0.22	,	0.77	)
NM_031466	Tularik gene 1 (T1), mRNA	0.49	(	0.24	,	0.74	)
NM_014045	low density lipoprotein receptor-related protein 10 (LRP10), mRNA	0.49	(	0.4	,	0.58	)
NM_139276	signal transducer and activator of transcription 3 (acute-phase response factor) (STA	0.49	(	0.31	,	0.67	)
NM_016733	LIM domain kinase 2 (LIMK2), transcript variant 2b, mRNA	0.49	(	0.21	,	0.76	)
NM_000480	adenosine monophosphate deaminase (isoform E) (AMPD3), mRNA	0.49	(	0.44	,	0.53	)
NM_213618	suppression of tumorigenicity 5 (ST5), transcript variant 3, mRNA	0.49	(	0.35	,	0.62	)
NM_006633	IQ motif containing GTPase activating protein 2 (IQGAP2), mRNA	0.48	(	0.38	,	0.59	)
NM_177453	progestin and adipoQ receptor family member III (PAQR3), mRNA	0.48	(	0.24	,	0.73	)
NM_017709	family with sequence similarity 46, member C (FAM46C), mRNA	0.48	(	0.36	,	0.6	)
NM_003056	solute carrier family 19 (folate transporter), member 1 (SLC19A1), transcript variant	0.48	(	0.36	,	0.6	)
NM_032121	implantation-associated protein (DKFZp564K142), mRNA	0.48	(	0.41	,	0.55	)
NM_153427	paired-like homeodomain transcription factor 2 (PITX2), transcript variant 1, mRNA	0.48	(	0.33	,	0.62	)
NM_013995	lysosomal-associated membrane protein 2 (LAMP2), transcript variant LAMP2B, mRNA	0.48	(	0.26	,	0.7	)
NM_004360	cadherin 1, type 1, E-cadherin (epithelial) (CDH1), mRNA	0.48	(	0.27	,	0.68	)
NM_021079	N-myristoyltransferase 1 (NMT1), mRNA	0.48	(	0.31	,	0.64	)
NM_003200	transcription factor 3 (E2A immunoglobulin enhancer binding factors E12/E47) (TCF3),	0.48	(	0.42	,	0.53	)
NM_020474	UDP-N-acetyl-alpha-D-galactosamine:polypeptide N-acetylgalactosaminyltransferase 1 (G	0.48	(	0.26	,	0.69	)
NM_201274	myosin phosphatase-Rho interacting protein (M-RIP), mRNA	0.48	(	0.43	,	0.52	)
NM_031454	selenoprotein O (SELO), mRNA	0.47	(	0.41	,	0.54	)
NM_020126	sphingosine kinase 2 (SPHK2), mRNA	0.47	(	0.3	,	0.65	)

NM_145690	tyrosine 3-monooxygenase/tryptophan 5-monooxygenase activation protein, zeta polypept	0.47	(	0.42	,	0.52)
NM_001961	eukaryotic translation elongation factor 2 (EEF2), mRNA	0.47	(	0.36	,	0.58)
NM_002959	sortilin 1 (SORT1), mRNA	0.47	(	0.38	,	0.57)
NM_178822	immunoglobulin superfamily, member 10 (IGSF10), mRNA	0.47	(	0.38	,	0.56)
NM_175629	DNA (cytosine-5-)-methyltransferase 3 alpha (DNMT3A), transcript variant 1, mRNA	0.47	(	0.19	,	0.75)
NM_007085	follistatin-like 1 (FSTL1), mRNA	0.47	(	0.26	,	0.67)
NM_007043	HIV-1 rev binding protein 2 (HRB2), mRNA	0.47	(	0.46	,	0.48)
NM_145324	oxysterol binding protein-like 3 (OSBPL3), transcript variant 6, mRNA	0.47	(	0.39	,	0.54)
NM_015575	trinucleotide repeat containing 15 (TNRC15), mRNA	0.47	(	0.43	,	0.5)
NM_024525	tetratricopeptide repeat domain 13 (TTC13), mRNA	0.47	(	0.23	,	0.7)
NM_006454	MAX dimerization protein 4 (MXD4), mRNA	0.47	(	0.33	,	0.6)
NM_022830	RNA binding motif protein 21 (RBM21), mRNA	0.46	(	0.35	,	0.57)
NM_100264	WW domain containing adaptor with coiled-coil (WAC), transcript variant 2, mRNA	0.46	(	0.42	,	0.5)
NM_002499	neogenin homolog 1 (chicken) (NEO1), mRNA	0.46	(	0.33	,	0.6)
NM_022763	factor for adipocyte differentiation 104 (FAD104), mRNA	0.46	(	0.42	,	0.51)
NM_004579	mitogen-activated protein kinase kinase kinase kinase 2 (MAP4K2), mRNA	0.46	(	0.19	,	0.74)
NM_018023	YEATS domain containing 2 (YEATS2), mRNA	0.46	(	0.38	,	0.55)
NM_199320	PHD finger protein 17 (PHF17), transcript variant L, mRNA	0.46	(	0.18	,	0.74)
NM_014282	hyaluronan binding protein 4 (HABP4), mRNA	0.46	(	0.39	,	0.53)
NM_033625	ribosomal protein L34 (RPL34), transcript variant 2, mRNA	0.46	(	0.19	,	0.73)
NM_021943	testis expressed sequence 27 (TEX27), mRNA	0.46	(	0.2	,	0.72)
NM_181349	SMAD specific E3 ubiquitin protein ligase 1 (SMURF1), transcript variant 2, mRNA	0.46	(	0.3	,	0.62)
NM_001033	ribonucleotide reductase M1 polypeptide (RRM1), mRNA	0.46	(	0.39	,	0.52)
NM_181443	BTB (POZ) domain containing 3 (BTBD3), transcript variant 2, mRNA	0.46	(	0.23	,	0.68)
NM_002844	protein tyrosine phosphatase, receptor type, K (PTPRK), mRNA	0.45	(	0.22	,	0.69)
NM_005234	nuclear receptor subfamily 2, group F, member 6 (NR2F6), mRNA	0.45	(	0.26	,	0.64)
NM_016289	calcium binding protein 39 (CAB39), mRNA	0.45	(	0.36	,	0.54)
NM_005271	glutamate dehydrogenase 1 (GLUD1), mRNA	0.45	(	0.37	,	0.54)
NM_005271	glutamate dehydrogenase 1 (GLUD1), mRNA	0.45	(	0.23	,	0.67)
NM_000158	glucan (1,4-alpha-), branching enzyme 1 (glycogen branching enzyme, Andersen disease,	0.45	(	0.34	,	0.57)
NM_018230	nucleoporin 133kDa (NUP133), mRNA	0.45	(	0.31	,	0.6)
NM_201525	G protein-coupled receptor 56 (GPR56), transcript variant 3, mRNA	0.45	(	0.29	,	0.61)
NM_031483	itchy homolog E3 ubiquitin protein ligase (mouse) (ITCH), mRNA	0.45	(	0.39	,	0.51)

NM_032293	GTPase activating Rap/RanGAP domain-like 3 (GARNL3), mRNA	0.45	(	0.29	,	0.61	)
NM_152850	phosphatidylinositol glycan, class O (PIGO), transcript variant 2, mRNA	0.45	(	0.3	,	0.6	)
NM_020141	protein x 013 (AD-020), mRNA	0.45	(	0.39	,	0.51	)
NM_000093	collagen, type V, alpha 1 (COL5A1), mRNA	0.45	(	0.24	,	0.65	)
NM_020830	WD repeat and FYVE domain containing 1 (WDFY1), mRNA	0.45	(	0.36	,	0.53	)
NM_004064	cyclin-dependent kinase inhibitor 1B (p27, Kip1) (CDKN1B), mRNA	0.44	(	0.29	,	0.6	)
NM_003849	succinate-CoA ligase, GDP-forming, alpha subunit (SUCLG1), mRNA	0.44	(	0.26	,	0.63	)
NM_004613	transglutaminase 2 (C polypeptide, protein-glutamine-gamma-glutamyltransferase) (TGM2	0.44	(	0.23	,	0.65	)
NM_013239	protein phosphatase 2A 48 kDa regulatory subunit (PR48), transcript variant 1, mRNA	0.44	(	0.29	,	0.6	)
NM_012199	eukaryotic translation initiation factor 2C, 1 (EIF2C1), mRNA	0.44	(	0.25	,	0.63	)
NM_024580	elongation factor Tu GTP binding domain containing 1 (EFTUD1), mRNA	0.44	(	0.26	,	0.62	)
NM_018844	B-cell receptor-associated protein 29 (BCAP29), transcript variant 2, mRNA	0.44	(	0.22	,	0.66	)
NM_015000	serine/threonine kinase 38 like (STK38L), mRNA	0.44	(	0.26	,	0.61	)
NM_005027	phosphoinositide-3-kinase, regulatory subunit 2 (p85 beta) (PIK3R2), mRNA	0.44	(	0.33	,	0.55	)
NM_003684	MAP kinase interacting serine/threonine kinase 1 (MKNK1), mRNA	0.44	(	0.34	,	0.53	)
NM_003023	SH3-domain binding protein 2 (SH3BP2), mRNA	0.44	(	0.31	,	0.57	)
NM_013354	CCR4-NOT transcription complex, subunit 7 (CNOT7), transcript variant 1, mRNA	0.44	(	0.24	,	0.63	)
NM_004945	dynamin 2 (DNM2), transcript variant 3, mRNA	0.43	(	0.31	,	0.56	)
NM_001068	topoisomerase (DNA) II beta 180kDa (TOP2B), mRNA	0.43	(	0.24	,	0.62	)
NM_014646	lipin 2 (LPIN2), mRNA	0.43	(	0.25	,	0.61	)
NM_002693	polymerase (DNA directed), gamma (POLG), mRNA	0.43	(	0.35	,	0.51	)
NM_015392	neural proliferation, differentiation and control, 1 (NPDC1), mRNA	0.43	(	0.35	,	0.5	)
NM_003861	WD repeat domain 22 (WDR22), mRNA	0.43	(	0.3	,	0.55	)
NM_001004106	G protein-coupled receptor kinase 6 (GRK6), transcript variant 1, mRNA	0.43	(	0.25	,	0.61	)
NM_003932	suppression of tumorigenicity 13 (colon carcinoma) (Hsp70 interacting protein) (ST13)	0.43	(	0.32	,	0.53	)
NM_004768	splicing factor, arginine/serine-rich 11 (SFRS11), mRNA	0.42	(	0.31	,	0.54	)
NM_003980	microtubule-associated protein 7 (MAP7), mRNA	0.42	(	0.31	,	0.53	)
NM_001007553	upstream of NRAS (UNR), transcript variant 1, mRNA	0.42	(	0.34	,	0.5	)
NM_002899	retinol binding protein 1, cellular (RBP1), mRNA	0.42	(	0.34	,	0.5	)
NM_015954	2-deoxyribose-5-phosphate aldolase homolog (C. elegans) (DERA), mRNA	0.42	(	0.26	,	0.57	)
NM_005080	X-box binding protein 1 (XBP1), mRNA	0.41	(	0.33	,	0.5	)
NM_001200	bone morphogenetic protein 2 (BMP2), mRNA	0.41	(	0.27	,	0.55	)
NM_002556	oxysterol binding protein (OSBP), mRNA	0.41	(	0.27	,	0.55	)

NM_020441	coronin, actin binding protein, 1B (CORO1B), mRNA	0.41	(	0.35	,	0.47)
NM_138319	proprotein convertase subtilisin/kexin type 6 (PCSK6), transcript variant 2, mRNA	0.4	(	0.35	,	0.45)
NM_002856	poliovirus receptor-related 2 (herpesvirus entry mediator B) (PVRL2), mRNA	0.4	(	0.3	,	0.5)
NM_022771	TBC1 domain family, member 15 (TBC1D15), mRNA	0.4	(	0.34	,	0.45)
NM_148923	cytochrome b-5 (CYB5), transcript variant 1, mRNA	0.39	(	0.34	,	0.44)
NM_001287	chloride channel 7 (CLCN7), mRNA	0.38	(	0.37	,	0.39)

Genes down regulated by baculovirus treatment followed by LPS, PMA and ionomycin stimulation at 1 hr post stimulation

NM_012145	deoxythymidylate kinase (thymidylate kinase) (DTYMK), mRNA	-0.45	(	-0.48	,	-0.42)
NM_018686	cytidine monophosphate N-acetylneuraminic acid synthetase (CMAS), mRNA	-0.45	(	-0.5	,	-0.39)
NM_033550	TP53 regulating kinase (TP53RK), mRNA	-0.46	(	-0.53	,	-0.38)
NM_000113	torsin family 1, member A (torsin A) (TOR1A), mRNA	-0.46	(	-0.52	,	-0.4)
NM_012155	echinoderm microtubule associated protein like 2 (EML2), mRNA	-0.46	(	-0.55	,	-0.37)
NM_001305	claudin 4 (CLDN4), mRNA	-0.46	(	-0.52	,	-0.41)
NM_018412	suppression of tumorigenicity 7 (ST7), transcript variant a, mRNA	-0.46	(	-0.55	,	-0.38)
NM_012100	aspartyl aminopeptidase (DNPEP), mRNA	-0.47	(	-0.48	,	-0.45)
NM_002319	leucine-rich repeats and calponin homology (CH) domain containing 4 (LRCH4), mRNA	-0.47	(	-0.5	,	-0.43)
NM_007170	testis-specific kinase 2 (TESK2), mRNA	-0.47	(	-0.55	,	-0.39)
NM_198954	nudix (nucleoside diphosphate linked moiety X)-type motif 1 (NUDT1), transcript varia	-0.47	(	-0.51	,	-0.43)
NM_001013	ribosomal protein S9 (RPS9), mRNA	-0.47	(	-0.52	,	-0.42)
NM_006854	KDEL (Lys-Asp-Glu-Leu) endoplasmic reticulum protein retention receptor 2 (KDELR2), m	-0.47	(	-0.58	,	-0.36)
NR_002163	olfactory receptor, family 7, subfamily E, member 37 pseudogene (OR7E37P) on chromoso	-0.47	(	-0.59	,	-0.36)
NM_018367	phytoceramidase, alkaline (PHCA), mRNA	-0.47	(	-0.51	,	-0.44)
NM_001249	ectonucleoside triphosphate diphosphohydrolase 5 (ENTPD5), mRNA	-0.47	(	-0.56	,	-0.39)
NM_005488	target of myb1 (chicken) (TOM1), mRNA	-0.47	(	-0.56	,	-0.39)
NM_001050	somatostatin receptor 2 (SSTR2), mRNA	-0.48	(	-0.54	,	-0.41)
NM_007322	RAN binding protein 3 (RANBP3), transcript variant RANBP3-d, mRNA	-0.48	(	-0.56	,	-0.39)
NM_002479	myogenin (myogenic factor 4) (MYOG), mRNA	-0.48	(	-0.62	,	-0.34)
NM_014725	START domain containing 8 (STARD8), mRNA	-0.48	(	-0.61	,	-0.35)
NM_152359	carnitine palmitoyltransferase 1C (CPT1C), mRNA	-0.48	(	-0.59	,	-0.37)
NM_177543	phosphatidic acid phosphatase type 2C (PPAP2C), transcript variant 3, mRNA	-0.48	(	-0.55	,	-0.41)
NM_001122	adipose differentiation-related protein (ADFP), mRNA	-0.48	(	-0.6	,	-0.37)

NM_000599	insulin-like growth factor binding protein 5 (IGFBP5), mRNA	-0.48	(	-0.5	,	-0.46)
NM_013304	zinc finger, DHHC domain containing 1 (ZDHHC1), mRNA	-0.48	(	-0.56	,	-0.41)
NM_006854	KDEL (Lys-Asp-Glu-Leu) endoplasmic reticulum protein retention receptor 2 (KDELR2), m	-0.48	(	-0.58	,	-0.39)
NM_005626	splicing factor, arginine/serine-rich 4 (SFRS4), mRNA	-0.49	(	-0.58	,	-0.41)
NM_005318	H1 histone family, member 0 (H1F0), mRNA	-0.49	(	-0.61	,	-0.37)
NM_025080	asparaginase like 1 (ASRGL1), mRNA	-0.49	(	-0.56	,	-0.43)
NM_014224	pepsinogen 5, group I (pepsinogen A) (PGA5), mRNA	-0.5	(	-0.66	,	-0.33)
NM_002234	potassium voltage-gated channel, shaker-related subfamily, member 5 (KCNA5), mRNA	-0.5	(	-0.66	,	-0.33)
NM_005681	TATA box binding protein (TBP)-associated factor, RNA polymerase I, A, 48kDa (TAF1A),	-0.5	(	-0.68	,	-0.32)
NM_005105	RNA binding motif protein 8A (RBM8A), mRNA	-0.5	(	-0.64	,	-0.36)
NM_017634	potassium channel tetramerisation domain containing 9 (KCTD9), mRNA	-0.5	(	-0.59	,	-0.41)
NM_001658	ADP-ribosylation factor 1 (ARF1), mRNA	-0.5	(	-0.63	,	-0.38)
NM_005386	neuronatin (NNAT), transcript variant 1, mRNA	-0.5	(	-0.65	,	-0.36)
NM_004368	calponin 2 (CNN2), transcript variant 1, mRNA	-0.5	(	-0.66	,	-0.35)
NM_005721	ARP3 actin-related protein 3 homolog (yeast) (ACTR3), mRNA	-0.51	(	-0.67	,	-0.34)
NM_001361	dihydroorotate dehydrogenase (DHODH), nuclear gene encoding mitochondrial protein, mR	-0.51	(	-0.72	,	-0.3)
NM_022164	lipocalin 7 (LCN7), mRNA	-0.51	(	-0.54	,	-0.48)
NM_000145	follicle stimulating hormone receptor (FSHR), transcript variant 1, mRNA	-0.51	(	-0.62	,	-0.4)
NM_013964	neuregulin 1 (NRG1), transcript variant HRG-alpha, mRNA	-0.51	(	-0.56	,	-0.46)
NM_006155	neural precursor cell expressed, developmentally down-regulated 5 (NEDD5), transcript	-0.51	(	-0.7	,	-0.32)
NM_001678	ATPase, Na+/K+ transporting, beta 2 polypeptide (ATP1B2), mRNA	-0.51	(	-0.67	,	-0.36)
NM_003258	thymidine kinase 1, soluble (TK1), mRNA	-0.51	(	-0.62	,	-0.41)
NM_032682	forkhead box P1 (FOXP1), mRNA	-0.51	(	-0.6	,	-0.43)
NM_001069	tubulin, beta 2 (TUBB2), mRNA	-0.52	(	-0.68	,	-0.35)
NM_002999	syndecan 4 (amphiglycan, ryudocan) (SDC4), mRNA	-0.52	(	-0.65	,	-0.38)
NM_002773	protease, serine, 8 (prostasin) (PRSS8), mRNA	-0.52	(	-0.67	,	-0.37)
NM_006843	serine dehydratase (SDS), mRNA	-0.52	(	-0.61	,	-0.42)
NM_003896	sialyltransferase 9 (CMP-NeuAc:lactosylceramide alpha-2,3-sialyltransferase; GM3 synt	-0.52	(	-0.67	,	-0.37)
NM_003132	spermidine synthase (SRM), mRNA	-0.52	(	-0.54	,	-0.5)
NM_018463	uncharacterized hematopoietic stem/progenitor cells protein MDS028 (MDS028), mRNA	-0.52	(	-0.6	,	-0.44)
NM_206914	hepatocellularcarcinoma-associated antigen HCA557a (DKFZP586D0919), transcript varian	-0.52	(	-0.73	,	-0.31)
NM_013328	pyrroline-5-carboxylate reductase family, member 2 (PYCR2), mRNA	-0.52	(	-0.76	,	-0.29)
NM_020676	abhydrolase domain containing 6 (ABHD6), mRNA	-0.52	(	-0.65	,	-0.39)

NM_002373	microtubule-associated protein 1A (MAP1A), mRNA	-0.52	(	-0.7	,	-0.35)
NM_000206	interleukin 2 receptor, gamma (severe combined immunodeficiency) (IL2RG), mRNA	-0.52	(	-0.75	,	-0.29)
NM_000629	interferon (alpha, beta and omega) receptor 1 (IFNAR1), mRNA	-0.53	(	-0.78	,	-0.27)
NM_004742	BAI1-associated protein 1 (BAIAP1), mRNA	-0.53	(	-0.55	,	-0.5)
NM_003029	SHC (Src homology 2 domain containing) transforming protein 1 (SHC1), transcript vari	-0.53	(	-0.7	,	-0.36)
NM_033308	ATP-binding cassette, sub-family A (ABC1), member 7 (ABCA7), transcript variant 2, mR	-0.53	(	-0.79	,	-0.26)
NM_016042	exosome component 3 (EXOSC3), transcript variant 1, mRNA	-0.53	(	-0.63	,	-0.43)
NM_024632	Sin3A associated protein p30-like (SAP30L), mRNA	-0.53	(	-0.63	,	-0.43)
NM_006662	Snf2-related CBP activator protein (SRCAP), mRNA	-0.53	(	-0.73	,	-0.34)
NM_021626	serine carboxypeptidase 1 (SCPEP1), mRNA	-0.53	(	-0.58	,	-0.49)
NM_014476	PDZ and LIM domain 3 (PDLIM3), mRNA	-0.53	(	-0.79	,	-0.28)
NM_207411	HARL2754 (UNQ2754), mRNA	-0.53	(	-0.74	,	-0.33)
NM_005202	collagen, type VIII, alpha 2 (COL8A2), mRNA	-0.54	(	-0.63	,	-0.44)
NM_138352	atherin (LOC90378), mRNA	-0.54	(	-0.77	,	-0.31)
NM_019110	zinc finger protein 307 (ZNF307), mRNA	-0.54	(	-0.7	,	-0.38)
NM_000486	aquaporin 2 (collecting duct) (AQP2), mRNA	-0.54	(	-0.58	,	-0.51)
NM_001895	casein kinase 2, alpha 1 polypeptide (CSNK2A1), transcript variant 2, mRNA	-0.55	(	-0.66	,	-0.43)
NM_004767	G-protein coupled receptor 37 like 1 (GPR37L1), mRNA	-0.55	(	-0.82	,	-0.27)
NM_001824	creatine kinase, muscle (CKM), mRNA	-0.55	(	-0.74	,	-0.35)
NM_003142	Sjogren syndrome antigen B (autoantigen La) (SSB), mRNA	-0.55	(	-0.68	,	-0.42)
NM_213646	tryptophanyl-tRNA synthetase (WARS), transcript variant 4, mRNA	-0.55	(	-0.64	,	-0.45)
NM_031299	cell division cycle associated 3 (CDCA3), mRNA	-0.55	(	-0.59	,	-0.52)
NM_004094	eukaryotic translation initiation factor 2, subunit 1 alpha, 35kDa (EIF2S1), mRNA	-0.55	(	-0.65	,	-0.46)
NM_004161	RAB1A, member RAS oncogene family (RAB1A), mRNA	-0.55	(	-0.64	,	-0.47)
NM_032311	polymerase (DNA-directed), delta interacting protein 3 (POLDIP3), transcript variant	-0.55	(	-0.7	,	-0.41)
NM_012080	haloacid dehalogenase-like hydrolase domain containing 1A (HDHD1A), mRNA	-0.55	(	-0.75	,	-0.36)
NM_001866	cytochrome c oxidase subunit VIIb (COX7B), nuclear gene encoding mitochondrial protei	-0.56	(	-0.76	,	-0.35)
NM_006319	CDP-diacylglycerol--inositol 3-phosphatidyltransferase (phosphatidylinositol synthase	-0.56	(	-0.73	,	-0.39)
NM_017634	potassium channel tetramerisation domain containing 9 (KCTD9), mRNA	-0.56	(	-0.64	,	-0.48)
NM_052944	solute carrier family 5 (sodium/glucose cotransporter), member 11 (SLC5A11), mRNA	-0.56	(	-0.73	,	-0.39)
NM_016320	nucleoporin 98kDa (NUP98), transcript variant 1, mRNA	-0.56	(	-0.86	,	-0.26)
NM_031443	cerebral cavernous malformation 2 (CCM2), mRNA	-0.56	(	-0.68	,	-0.44)
NM_019116	similar to ubiquitin binding protein (UBPH), mRNA	-0.56	(	-0.71	,	-0.41)

NM_144564	solute carrier family 39 (zinc transporter), member 3 (SLC39A3), transcript variant 1	-0.56	(	-0.79	,	-0.34)
NM_021078	GCN5 general control of amino-acid synthesis 5-like 2 (yeast) (GCN5L2), mRNA	-0.56	(	-0.68	,	-0.44)
NM_000107	damage-specific DNA binding protein 2, 48kDa (DDB2), mRNA	-0.56	(	-0.89	,	-0.24)
NM_016282	adenylate kinase 3 like 1 (AK3L1), mRNA	-0.56	(	-0.88	,	-0.25)
NM_170691	G elongation factor, mitochondrial 2 (GFM2), nuclear gene encoding mitochondrial prot	-0.57	(	-0.72	,	-0.41)
NM_004886	amyloid beta (A4) precursor protein-binding, family A, member 3 (X11-like 2) (APBA3),	-0.57	(	-0.78	,	-0.36)
NM_153684	nucleoporin 50kDa (NUP50), transcript variant 1, mRNA	-0.57	(	-0.82	,	-0.32)
NM_053017	ADP-ribosyltransferase 5 (ART5), mRNA	-0.57	(	-0.66	,	-0.49)
NM_001129	AE binding protein 1 (AEBP1), mRNA	-0.57	(	-0.87	,	-0.28)
NM_004577	phosphoserine phosphatase (PSPH), mRNA	-0.58	(	-0.88	,	-0.27)
NM_003279	troponin C2, fast (TNNC2), mRNA	-0.58	(	-0.93	,	-0.23)
NM_018297	N-glycanase 1 (NGLY1), mRNA	-0.58	(	-0.72	,	-0.44)
NM_199204	dehydrogenase/reductase (SDR family) member 9 (DHRS9), transcript variant 2, mRNA	-0.58	(	-0.89	,	-0.27)
NM_004435	endonuclease G (ENDOG), nuclear gene encoding mitochondrial protein, mRNA	-0.58	(	-0.62	,	-0.54)
NM_006412	1-acylglycerol-3-phosphate O-acyltransferase 2 (lysophosphatidic acid acyltransferase	-0.58	(	-0.87	,	-0.29)
NM_017955	cell division cycle associated 4 (CDCA4), transcript variant 1, mRNA	-0.58	(	-0.64	,	-0.53)
NM_001003794	monoglyceride lipase (MGLL), transcript variant 2, mRNA	-0.58	(	-0.69	,	-0.47)
NM_016020	transcription factor B1, mitochondrial (TFB1M), mRNA	-0.59	(	-0.65	,	-0.52)
NM_000098	carnitine palmitoyltransferase II (CPT2), nuclear gene encoding mitochondrial protein	-0.59	(	-0.79	,	-0.39)
NM_012137	dimethylarginine dimethylaminohydrolase 1 (DDAH1), mRNA	-0.59	(	-0.73	,	-0.44)
NM_000858	guanylate kinase 1 (GUK1), mRNA	-0.59	(	-0.71	,	-0.47)
NM_024102	MEP50 protein (MEP50), mRNA	-0.59	(	-0.88	,	-0.3)
NM_014578	ras homolog gene family, member D (RHOD), mRNA	-0.59	(	-0.69	,	-0.5)
NM_000943	peptidylprolyl isomerase C (cyclophilin C) (PPIC), mRNA	-0.59	(	-0.74	,	-0.45)
NM_030984	thromboxane A synthase 1 (platelet, cytochrome P450, family 5, subfamily A) (TBXAS1),	-0.6	(	-0.92	,	-0.27)
NM_006182	discoidin domain receptor family, member 2 (DDR2), mRNA	-0.6	(	-0.91	,	-0.28)
NM_024417	ferredoxin reductase (FDXR), nuclear gene encoding mitochondrial protein, transcript	-0.6	(	-0.76	,	-0.44)
NM_014341	mitochondrial carrier homolog 1 (C. elegans) (MTCH1), nuclear gene encoding mitochond	-0.6	(	-0.76	,	-0.44)
NM_004553	NADH dehydrogenase (ubiquinone) Fe-S protein 6, 13kDa (NADH-coenzyme Q reductase) (N	-0.6	(	-0.82	,	-0.38)
NM_016319	COP9 constitutive photomorphogenic homolog subunit 7A (Arabidopsis) (COPS7A), mRNA	-0.6	(	-0.88	,	-0.33)
NM_000022	adenosine deaminase (ADA), mRNA	-0.61	(	-0.75	,	-0.46)
NM_006268	D4, zinc and double PHD fingers family 2 (DPF2), mRNA	-0.61	(	-0.85	,	-0.36)
NM_005489	SH2 domain containing 3C (SH2D3C), mRNA	-0.61	(	-1.08	,	-0.13)

NM_014020	LR8 protein (LR8), mRNA	-0.61	(	-0.7	,	-0.52)
NM_020189	e(y)2 protein (e(y)2), mRNA	-0.61	(	-0.97	,	-0.25)
NM_006449	CDC42 effector protein (Rho GTPase binding) 3 (CDC42EP3), mRNA	-0.61	(	-0.73	,	-0.5)
NM_020137	GRIP1 associated protein 1 (GRIPAP1), transcript variant 1, mRNA	-0.62	(	-1.01	,	-0.23)
NM_002710	protein phosphatase 1, catalytic subunit, gamma isoform (PPP1CC), mRNA	-0.63	(	-0.68	,	-0.57)
NM_181798	potassium voltage-gated channel, KQT-like subfamily, member 1 (KCNQ1), transcript var	-0.63	(	-0.87	,	-0.38)
NM_002659	plasminogen activator, urokinase receptor (PLAUR), transcript variant 1, mRNA	-0.63	(	-0.93	,	-0.33)
NM_022473	zinc finger protein 106 homolog (mouse) (ZFP106), mRNA	-0.63	(	-0.69	,	-0.56)
NM_005070	solute carrier family 4, anion exchanger, member 3 (SLC4A3), mRNA	-0.63	(	-0.99	,	-0.26)
NM_006745	sterol-C4-methyl oxidase-like (SC4MOL), mRNA	-0.63	(	-0.7	,	-0.56)
NM_015219	exocyst complex component 7 (EXOC7), mRNA	-0.63	(	-0.8	,	-0.47)
NM_020133	1-acylglycerol-3-phosphate O-acyltransferase 4 (lysophosphatidic acid acyltransferase	-0.64	(	-0.84	,	-0.43)
NM_000766	cytochrome P450, family 2, subfamily A, polypeptide 13 (CYP2A13), mRNA	-0.64	(	-0.98	,	-0.29)
NM_004967	integrin-binding sialoprotein (bone sialoprotein, bone sialoprotein II) (IBSP), mRNA	-0.64	(	-1.1	,	-0.18)
NM_182926	kinectin 1 (kinesin receptor) (KTN1), mRNA	-0.64	(	-0.89	,	-0.38)
NM_017436	alpha 1,4-galactosyltransferase (A4GALT), mRNA	-0.64	(	-0.78	,	-0.51)
NM_012154	eukaryotic translation initiation factor 2C, 2 (EIF2C2), mRNA	-0.65	(	-0.76	,	-0.54)
NM_014176	HSPC150 protein similar to ubiquitin-conjugating enzyme (HSPC150), mRNA	-0.65	(	-0.86	,	-0.44)
NM_002823	prothymosin, alpha (gene sequence 28) (PTMA), mRNA	-0.65	(	-1.08	,	-0.22)
NM_181745	G protein-coupled receptor 120 (GPR120), mRNA	-0.66	(	-0.82	,	-0.5)
NM_021932	likely ortholog of mouse synembryn (RIC-8), mRNA	-0.66	(	-0.84	,	-0.48)
NM_006256	protein kinase N2 (PKN2), mRNA	-0.66	(	-0.96	,	-0.37)
NM_005147	DnaJ (Hsp40) homolog, subfamily A, member 3 (DNAJA3), mRNA	-0.66	(	-0.93	,	-0.4)
NM_007188	ATP-binding cassette, sub-family B (MDR/TAP), member 8 (ABCB8), nuclear gene encoding	-0.67	(	-0.74	,	-0.6)
NM_005195	CCAAT/enhancer binding protein (C/EBP), delta (CEBPD), mRNA	-0.68	(	-1.35	,	-0.02)
NM_012214	mannosyl (alpha-1,3-)-glycoprotein beta-1,4-N-acetylglucosaminyltransferase, isoenzym	-0.68	(	-0.76	,	-0.61)
NM_001219	calumenin (CALU), mRNA	-0.68	(	-0.78	,	-0.59)
NM_181597	uridine phosphorylase 1 (UPP1), transcript variant 2, mRNA	-0.69	(	-0.79	,	-0.58)
NM_001798	cyclin-dependent kinase 2 (CDK2), transcript variant 1, mRNA	-0.69	(	-0.87	,	-0.51)
NM_002532	nucleoporin 88kDa (NUP88), mRNA	-0.7	(	-0.93	,	-0.47)
NM_001785	cytidine deaminase (CDA), mRNA	-0.71	(	-1	,	-0.41)
NM_014474	sphingomyelin phosphodiesterase, acid-like 3B (SMPDL3B), mRNA	-0.71	(	-0.95	,	-0.47)
NM_006744	retinol binding protein 4, plasma (RBP4), mRNA	-0.74	(	-0.89	,	-0.58)

NM_021127	phorbol-12-myristate-13-acetate-induced protein 1 (PMAIP1), mRNA	-0.74	(	-0.84	,	-0.64)
NM_002689	polymerase (DNA-directed), alpha (70kD) (POLA2), mRNA	-0.74	(	-0.93	,	-0.56)
NM_003943	genethonin 1 (GENX-3414), mRNA	-0.74	(	-0.92	,	-0.56)
NM_005550	kinesin family member C3 (KIFC3), mRNA	-0.74	(	-0.85	,	-0.64)
NM_003380	vimentin (VIM), mRNA	-0.75	(	-0.85	,	-0.64)
NM_182665	Ras association (RalGDS/AF-6) domain family 5 (RASSF5), transcript variant 3, mRNA	-0.75	(	-1.18	,	-0.33)
NM_001003689	l(3)mbt-like 2 (Drosophila) (L3MBTL2), transcript variant 2, mRNA	-0.77	(	-0.9	,	-0.64)
NM_001423	epithelial membrane protein 1 (EMP1), mRNA	-0.77	(	-0.93	,	-0.62)
NM_015675	growth arrest and DNA-damage-inducible, beta (GADD45B), mRNA	-0.78	(	-0.81	,	-0.75)
NM_005114	heparan sulfate (glucosamine) 3-O-sulfotransferase 1 (HS3ST1), mRNA	-0.78	(	-1.49	,	-0.06)
NM_017775	tetratricopeptide repeat domain 19 (TTC19), mRNA	-0.8	(	-1.52	,	-0.08)
NM_012385	p8 protein (candidate of metastasis 1) (P8), mRNA	-0.8	(	-0.87	,	-0.73)
NM_018264	radical S-adenosyl methionine and flavodoxin domains 1 (RSAFD1), mRNA	-0.81	(	-1.23	,	-0.38)
NM_001126	adenylosuccinate synthase (ADSS), mRNA	-0.81	(	-0.94	,	-0.68)
NM_018103	leucine rich repeat containing 5 (LRRC5), mRNA	-0.82	(	-1.16	,	-0.49)
NM_013322	sorting nexin 10 (SNX10), mRNA	-0.83	(	-0.92	,	-0.74)
NM_001008222	zinc finger, DHHC domain containing 9 (ZDHHC9), transcript variant 2, mRNA	-0.84	(	-1.17	,	-0.51)
NM_015847	methyl-CpG binding domain protein 1 (MBD1), transcript variant PCM1, mRNA	-0.86	(	-1	,	-0.71)
NM_022078	G patch domain containing 3 (GPATC3), mRNA	-0.87	(	-0.92	,	-0.82)
NM_002466	v-myb myeloblastosis viral oncogene homolog (avian)-like 2 (MYBL2), mRNA	-0.87	(	-1.26	,	-0.49)
NM_206918	degenerative spermatocyte homolog 2, lipid desaturase (Drosophila) (DEGS2), mRNA	-0.9	(	-1.16	,	-0.64)
NM_001444	fatty acid binding protein 5 (psoriasis-associated) (FABP5), mRNA	-0.91	(	-1.17	,	-0.64)
NM_006493	ceroid-lipofuscinosis, neuronal 5 (CLN5), mRNA	-0.91	(	-1.01	,	-0.81)
NM_005562	laminin, gamma 2 (LAMC2), transcript variant 1, mRNA	-0.95	(	-1.09	,	-0.8)
NM_002076	glucosamine (N-acetyl)-6-sulfatase (Sanfilippo disease IIID) (GNS), mRNA	-0.95	(	-1.2	,	-0.71)
NM_016225	Rhesus blood group, D antigen (RHD), transcript variant 2, mRNA	-1	(	-1.59	,	-0.4)
NM_005882	macrophage erythroblast attacher (MAEA), mRNA	-1.02	(	-1.31	,	-0.74)
NM_000024	adrenergic, beta-2-, receptor, surface (ADRB2), mRNA	-1.04	(	-1.33	,	-0.75)
NM_014889	pitrilysin metalloproteinase 1 (PITRM1), mRNA	-1.06	(	-1.61	,	-0.52)
NM_001110	a disintegrin and metalloproteinase domain 10 (ADAM10), mRNA	-1.15	(	-1.45	,	-0.84)
NM_017921	nuclear protein localization 4 (NPL4), mRNA	-1.2	(	-1.56	,	-0.84)
NM_000210	integrin, alpha 6 (ITGA6), mRNA	-1.27	(	-1.52	,	-1.02)
NM_006659	tubulin, gamma complex associated protein 2 (TUBGCP2), mRNA	-1.27	(	-2.22	,	-0.33)

NM_012486	presenilin 2 (Alzheimer disease 4) (PSEN2), transcript variant 2, mRNA	-1.36	(	-1.53	,	-1.18	)	

Genes Up regulated at 1 and 4 hrs

NM_000803	folate receptor 2 (fetal) (FOLR2), mRNA	1.28	(| 0.91 | , | 1.65 |)	1.89	(| 1.49 | , | 2.3 |)
NM_000900	matrix Gla protein (MGP), mRNA	1.37	(| 1.1 | , | 1.64 |)	1.61	(| 1.4 | , | 1.8 |)
NM_005025	serine (or cysteine) proteinase inhibitor, clade I (neuroserpin), member 1 (SERPINI1), mRNA	0.74	(| 0.42 | , | 1.06 |)	1.38	(| 1.11 | , | 1.7 |)
NM_004772	chromosome 5 open reading frame 13 (C5orf13), mRNA	0.95	(| 0.49 | , | 1.41 |)	1.25	(| 0.88 | , | 1.6 |)
NM_002514	nephroblastoma overexpressed gene (NOV), mRNA	1.15	(| 1.08 | , | 1.22 |)	1.22	(| 0.79 | , | 1.7 |)
NM_006988	a disintegrin-like and metalloprotease (reprolysin type) with thrombospondin type 1 motif, 1 (Al	1.63	(| 1.36 | , | 1.89 |)	1.14	(| 0.66 | , | 1.6 |)
NM_004337	chromosome 8 open reading frame 1 (C8orf1), mRNA	0.66	(| 0.53 | , | 0.79 |)	1.01	(| 0.74 | , | 1.3 |)
NM_152556	hypothetical protein FLJ31818 (FLJ31818), mRNA	0.78	(| 0.75 | , | 0.82 |)	0.97	(| 0.43 | , | 1.5 |)
NM_001889	crystallin, zeta (quinone reductase) (CRYZ), mRNA	0.68	(| 0.61 | , | 0.76 |)	0.91	(| 0.44 | , | 1.4 |)
NM_025243	solute carrier family 19, member 3 (SLC19A3), mRNA	0.7	(| 0.19 | , | 1.21 |)	0.87	(| 0.42 | , | 1.3 |)
NM_006237	POU domain, class 4, transcription factor 1 (POU4F1), mRNA	0.62	(| 0.24 | , | 1.01 |)	0.83	(| 0.55 | , | 1.1 |)
NM_003528	histone 2, H2be (HIST2H2BE), mRNA	0.78	(| 0.47 | , | 1.09 |)	0.73	(| 0.54 | , | 0.9 |)
NM_000313	protein S (alpha) (PROS1), mRNA	0.51	(| 0.43 | , | 0.6 |)	0.71	(| 0.53 | , | 0.9 |)
NM_199040	nudix (nucleoside diphosphate linked moiety X)-type motif 4 (NUDT4), transcript variant 2, mR	0.77	(| 0.52 | , | 1.02 |)	0.65	(| 0.55 | , | 0.8 |)

Genes Up regulated at 1 hr and down regulated at 4 hrs

NM_007361	nidogen 2 (osteonidogen) (NID2), mRNA	0.51	(| 0.25 | , | 0.77 |)	-0.42	(| -0.5 | , | -0.3 |)
NM_144967	hypothetical protein FLJ30058 (FLJ30058), mRNA	0.46	(| 0.28 | , | 0.65 |)	-0.42	(| -0.5 | , | -0.3 |)
NR_001564	X (inactive)-specific transcript (XIST) on chromosome X	0.83	(| 0.2 | , | 1.45 |)	-0.42	(| -0.5 | , | -0.3 |)
NM_139207	nucleosome assembly protein 1-like 1 (NAP1L1), transcript variant 1, mRNA	0.84	(| 0.62 | , | 1.05 |)	-0.43	(| -0.6 | , | -0.3 |)
NM_002467	c-myc, mRNA	0.81	(| 0.7 | , | 0.92 |)	-0.45	(| -0.6 | , | -0.3 |)
NM_175066	DEAD (Asp-Glu-Ala-Asp) box polypeptide 51 (DDX51), mRNA	0.48	(| 0.33 | , | 0.62 |)	-0.45	(| -0.5 | , | -0.4 |)
NM_017458	major vault protein (MVP), transcript variant 1, mRNA	0.51	(| 0.38 | , | 0.65 |)	-0.45	(| -0.6 | , | -0.3 |)
NM_000404	galactosidase, beta 1 (GLB1), transcript variant 1	0.52	(| 0.33 | , | 0.7 |)	-0.46	(| -0.6 | , | -0.3 |)
NM_005560	laminin, alpha 5 (LAMA5), mRNA	1.33	(| 0.85 | , | 1.8 |)	-0.46	(| -0.6 | , | -0.3 |)
NM_012334	myosin X (MYO10), mRNA	0.55	(| 0.36 | , | 0.74 |)	-0.46	(| -0.6 | , | -0.4 |)
NM_018082	polymerase (RNA) III (DNA directed) polypeptide B (POLR3B), mRNA	0.45	(| 0.23 | , | 0.66 |)	-0.47	(| -0.6 | , | -0.3 |)
NM_139124	mitogen-activated protein kinase 8 interacting protein 2 (MAPK8IP2), transcript variant 3, mRN	0.55	(| 0.39 | , | 0.72 |)	-0.47	(| -0.6 | , | -0.3 |)

NM_018834	matrin 3 (MATR3), mRNA	0.91	(	0.78 , 1.03	)	-0.47	(	-0.6 , -0.3)
NM_014787	DnaJ (Hsp40) homolog, subfamily C, member 6 (DNAJC6), mRNA	0.48	(	0.37 , 0.6	)	-0.47	(	-0.7 , -0.3)
NM_001005273	chromodomain helicase DNA binding protein 3 (CHD3), transcript variant 1, mRNA	0.59	(	0.28 , 0.89	)	-0.48	(	-0.7 , -0.2)
NM_018060	mitochondrial isoleucine tRNA synthetase (FLJ10326), mRNA	0.5	(	0.43 , 0.58	)	-0.48	(	-0.6 , -0.4)
NM_001046	solute carrier family 12 (sodium/potassium/chloride transporters), member 2 (SLC12A2), mRN	0.48	(	0.21 , 0.74	)	-0.48	(	-0.7 , -0.3)
NM_020117	leucyl-tRNA synthetase (LARS), mRNA	0.43	(	0.33 , 0.53	)	-0.48	(	-0.7 , -0.3)
NM_003758	eukaryotic translation initiation factor 3, subunit 1 alpha, 35kDa (EIF3S1), mRNA	0.43	(	0.3 , 0.56	)	-0.49	(	-0.7 , -0.2)
NM_002940	ATP-binding cassette, sub-family E (OABP), member 1 (ABCE1), mRNA	0.52	(	0.36 , 0.69	)	-0.49	(	-0.5 , -0.5)
NM_032208	anthrax toxin receptor 1 (ANTXR1), transcript variant 1, mRNA	0.97	(	0.57 , 1.37	)	-0.49	(	-0.7 , -0.3)
NM_153051	myotubularin related protein 3 (MTMR3), transcript variant 2, mRNA	0.4	(	0.36 , 0.45	)	-0.49	(	-0.7 , -0.3)
NM_004910	phosphatidylinositol transfer protein, membrane-associated 1 (PITPNM1), mRNA	0.5	(	0.24 , 0.76	)	-0.5	(	-0.6 , -0.4)
NM_004739	metastasis associated 1 family, member 2 (MTA2), mRNA	0.48	(	0.37 , 0.59	)	-0.51	(	-0.8 , -0.3)
NM_002267	karyopherin alpha 3 (importin alpha 4) (KPNA3), mRNA	0.54	(	0.06 , 1.02	)	-0.51	(	-0.7 , -0.3)
NM_022763	factor for adipocyte differentiation 104 (FAD104), mRNA	0.42	(	0.29 , 0.56	)	-0.51	(	-0.8 , -0.3)
NM_014969	WD repeat domain 47 (WDR47), mRNA	0.94	(	0.7 , 1.18	)	-0.51	(	-0.8 , -0.3)
NM_003501	acyl-Coenzyme A oxidase 3, pristanoyl (ACOX3), mRNA	1.24	(	0.4 , 2.07	)	-0.51	(	-0.8 , -0.2)
NM_002748	mitogen-activated protein kinase 6 (MAPK6), mRNA	0.86	(	0.57 , 1.15	)	-0.53	(	-0.7 , -0.3)
NM_003998	nuclear factor of kappa light polypeptide gene enhancer in B-cells 1 (p105) (NFKB1), mRNA	0.65	(	0.5 , 0.8	)	-0.53	(	-0.7 , -0.3)
M14636	glycogen phosphorylase mRNA, complete cds	0.55	(	0.43 , 0.67	)	-0.53	(	-0.9 , -0.2)
NM_015705	RUN and TBC1 domain containing 3 (RUTBC3), mRNA	0.45	(	0.35 , 0.56	)	-0.53	(	-0.8 , -0.3)
NM_005940	matrix metalloproteinase 11 (stromelysin 3) (MMP11), mRNA	0.42	(	0.29 , 0.56	)	-0.53	(	-0.8 , -0.2)
BC003562	dual specificity phosphatase 6, mRNA	0.66	(	0.5 , 0.81	)	-0.54	(	-0.9 , -0.2)
NM_018699	PR domain containing 5 (PRDM5), mRNA	0.71	(	0.47 , 0.95	)	-0.54	(	-0.9 , -0.2)
NM_021078	GCN5 general control of amino-acid synthesis 5-like 2 (yeast) (GCN5L2), mRNA	0.45	(	0.33 , 0.56	)	-0.55	(	-0.6 , -0.5)
NM_014743	KIAA0232 gene product (KIAA0232), mRNA	0.57	(	0.15 , 1	)	-0.55	(	-0.9 , -0.2)
NM_173172	nuclear receptor subfamily 4, group A, member 2 (NR4A2), transcript variant 3, mRNA	0.68	(	0.42 , 0.94	)	-0.55	(	-0.7 , -0.4)
XM_114611	omo sapiens hypothetical protein KIAA1833 (KIAA1833), mRNA	0.84	(	0.57 , 1.11	)	-0.55	(	-0.9 , -0.2)
NM_147171	A kinase (PRKA) anchor protein (yotiao) 9 (AKAP9), transcript variant 1, mRNA	0.43	(	0.35 , 0.52	)	-0.56	(	-0.7 , -0.5)
NM_018981	DnaJ (Hsp40) homolog, subfamily C, member 10 (DNAJC10), mRNA	0.51	(	0.23 , 0.79	)	-0.56	(	-0.8 , -0.3)
NM_020718	ubiquitin specific protease 31 (USP31), mRNA	0.6	(	0.45 , 0.75	)	-0.56	(	-0.6 , -0.5)
NM_018569	chromosome 4 open reading frame 16 (C4orf16), mRNA	0.59	(	0.42 , 0.76	)	-0.56	(	-0.6 , -0.5)
NM_002342	lymphotoxin beta receptor (TNFR superfamily, member 3) (LTBR), mRNA	0.38	(	0.34 , 0.43	)	-0.56	(	-0.8 , -0.4)
NM_198531	ATPase, Class II, type 9B (ATP9B), mRNA	0.6	(	0.47 , 0.72	)	-0.57	(	-0.8 , -0.3)

NM_177423	protein tyrosine phosphatase, receptor type, f polypeptide (PTPRF), interacting protein (liprin),	0.68	(	0.66 , 0.71	)	-0.57	(	-0.7 , -0.5)
NM_015534	zinc finger, ZZ domain containing 3 (ZZZ3), mRNA	0.69	(	0.34 , 1.05	)	-0.58	(	-0.9 , -0.3)
NM_014423	ALL1 fused gene from 5q31 (AF5Q31), mRNA	1.12	(	0.73 , 1.52	)	-0.58	(	-0.8 , -0.4)
NM_030580	zinc finger protein 34 (KOX 32) (ZNF34), mRNA	0.46	(	0.44 , 0.48	)	-0.58	(	-1.1 , -0.1)
NM_004747	discs, large homolog 5 (Drosophila) (DLG5), mRNA	0.57	(	0.34 , 0.8	)	-0.58	(	-0.9 , -0.3)
NM_015434	DKFZP434B168 protein (DKFZP434B168), mRNA	0.42	(	0.35 , 0.5	)	-0.58	(	-0.7 , -0.5)
NM_032870	chromosome 6 open reading frame 111 (C6orf111), mRNA	0.58	(	0.49 , 0.68	)	-0.58	(	-0.8 , -0.4)
NM_015173	TBC1 (tre-2/USP6, BUB2, cdc16) domain family, member 1 (TBC1D1), mRNA	0.65	(	0.45 , 0.85	)	-0.59	(	-0.9 , -0.3)
NM_144997	folliculin (FLCN), transcript variant 1, mRNA	0.47	(	0.2 , 0.73	)	-0.59	(	-0.7 , -0.5)
NM_018156	vacuolar protein sorting 13D (yeast) (VPS13D), transcript variant 2, mRNA	0.65	(	0.54 , 0.75	)	-0.6	(	-0.7 , -0.5)
NM_006775	quaking homolog, KH domain RNA binding (mouse) (QKI), transcript variant 1, mRNA	0.73	(	0.67 , 0.79	)	-0.6	(	-0.9 , -0.3)
NM_198597	SEC24 related gene family, member C (S. cerevisiae) (SEC24C), transcript variant 2, mRNA	0.48	(	0.26 , 0.7	)	-0.6	(	-1 , -0.2)
NM_003685	KH-type splicing regulatory protein (FUSE binding protein 2) (KHSRP), mRNA	0.46	(	0.23 , 0.69	)	-0.6	(	-0.8 , -0.4)
NM_006715	mannosidase, alpha, class 2C, member 1 (MAN2C1), mRNA	0.54	(	0.27 , 0.81	)	-0.6	(	-0.9 , -0.3)
NM_019020	TBC1 domain family, member 16 (TBC1D16), mRNA	1.17	(	0.68 , 1.66	)	-0.61	(	-1 , -0.2)
NM_002444	moesin (MSN), mRNA	0.46	(	0.21 , 0.7	)	-0.61	(	-0.9 , -0.3)
NM_015049	amyotrophic lateral sclerosis 2 (juvenile) chromosome region, candidate 3 (ALS2CR3), mRNA	0.5	(	0.44 , 0.57	)	-0.61	(	-0.8 , -0.4)
NM_022652	dual specificity phosphatase 6 (DUSP6), transcript variant 2, mRNA	1.11	(	0.94 , 1.28	)	-0.62	(	-0.9 , -0.4)
NM_017694	FLJ20160 protein (FLJ20160), mRNA	0.49	(	0.44 , 0.54	)	-0.62	(	-0.8 , -0.4)
NM_004819	symplekin (SYMPK), mRNA	0.66	(	0.25 , 1.06	)	-0.63	(	-1 , -0.3)
NM_020410	ATPase type 13A (ATP13A), mRNA	0.6	(	0.53 , 0.67	)	-0.63	(	-0.9 , -0.3)
NM_016272	transducer of ERBB2, 2 (TOB2), mRNA	0.74	(	0.57 , 0.91	)	-0.63	(	-1.1 , -0.2)
NM_001001894	tetratricopeptide repeat domain 3 (TTC3), transcript variant 2, mRNA	0.55	(	0.46 , 0.64	)	-0.63	(	-1 , -0.3)
NM_005124	nucleoporin 153kDa (NUP153), mRNA	0.62	(	0.34 , 0.89	)	-0.63	(	-1 , -0.3)
NM_016343	centromere protein F, 350/400ka (mitosin) (CENPF), mRNA	0.72	(	-0.06 , 1.5	)	-0.63	(	-1.1 , -0.2)
NM_006788	ralA binding protein 1 (RALBP1), mRNA	0.44	(	0.21 , 0.68	)	-0.63	(	-0.9 , -0.4)
NM_022553	vacuolar protein sorting 52 (yeast) (VPS52), transcript variant 2, mRNA	0.68	(	0.55 , 0.81	)	-0.63	(	-0.7 , -0.5)
NM_014666	enthoprotin (ENTH), mRNA	0.56	(	0.37 , 0.74	)	-0.64	(	-0.9 , -0.4)
NM_005596	nuclear factor I/B (NFIB), mRNA	0.42	(	0.27 , 0.58	)	-0.64	(	-0.7 , -0.6)
NM_004846	eukaryotic translation initiation factor 4E member 2 (EIF4E2), mRNA	0.76	(	0.44 , 1.07	)	-0.65	(	-1.2 , -0.1)
NM_003760	eukaryotic translation initiation factor 4 gamma, 3 (EIF4G3), mRNA	0.62	(	0.4 , 0.83	)	-0.65	(	-1.2 , -0.1)
NM_014640	tubulin tyrosine ligase-like family, member 4 (TTLL4), mRNA	0.43	(	0.39 , 0.48	)	-0.65	(	-1 , -0.3)
NM_018125	hypothetical protein FLJ10521 (FLJ10521), mRNA	0.68	(	0.51 , 0.86	)	-0.65	(	-0.9 , -0.4)

NM_001556	inhibitor of kappa light polypeptide gene enhancer in B-cells, kinase beta (IKBKB), mRNA	0.81	(	0.66 , 0.96	)	-0.66	(	-1 , -0.3)
NM_153329	hypothetical protein MGC10204 (MGC10204), mRNA	0.91	(	0.73 , 1.1	)	-0.66	(	-1.1 , -0.2)
NM_012102	arginine-glutamic acid dipeptide (RE) repeats (RERE), mRNA	0.48	(	0.4 , 0.57	)	-0.66	(	-1 , -0.3)
NM_017721	putative NFkB activating protein (FLJ20241), mRNA	0.59	(	0.45 , 0.73	)	-0.66	(	-0.9 , -0.4)
NM_144982	hypothetical protein MGC23401 (MGC23401), mRNA	0.54	(	0.4 , 0.67	)	-0.67	(	-1 , -0.4)
NM_012272	Huntingtin interacting protein C (HYPC), mRNA	0.77	(	-0.42 , 1.97	)	-0.67	(	-0.8 , -0.5)
NM_012297	Ras-GTPase activating protein SH3 domain-binding protein 2 (G3BP2), transcript variant 2, m	0.54	(	0.19 , 0.89	)	-0.67	(	-1.2 , -0.1)
NM_007110	telomerase-associated protein 1 (TEP1), mRNA	0.67	(	0.33 , 1	)	-0.67	(	-1.2 , -0.1)
XM_371575	omo sapiens formin binding protein 3 (FNBP3), mRNA	0.89	(	0.72 , 1.05	)	-0.67	(	-1 , -0.4)
NM_002268	karyopherin alpha 4 (importin alpha 3) (KPNA4), mRNA	0.68	(	0.3 , 1.06	)	-0.68	(	-1.1 , -0.3)
NM_002892	AT rich interactive domain 4A (RBP1-like) (ARID4A), transcript variant 1, mRNA	0.46	(	0.27 , 0.64	)	-0.68	(	-1.1 , -0.3)
NM_005257	GATA binding protein 6 (GATA6), mRNA	1.19	(	1.01 , 1.36	)	-0.68	(	-1.3 , -0.1)
NM_002556	oxysterol binding protein (OSBP), mRNA	0.93	(	0.79 , 1.07	)	-0.68	(	-1 , -0.4)
NM_024662	N-acetyltransferase-like protein (FLJ10774), mRNA	0.59	(	0.39 , 0.8	)	-0.68	(	-0.8 , -0.6)
NM_003935	topoisomerase (DNA) III beta (TOP3B), mRNA	0.58	(	0.46 , 0.7	)	-0.69	(	-1 , -0.4)
NM_015027	KIAA0251 protein (KIAA0251), mRNA	0.65	(	0.28 , 1.03	)	-0.69	(	-1 , -0.3)
NM_006387	calcium homeostasis endoplasmic reticulum protein (CHERP), mRNA	0.43	(	0.29 , 0.58	)	-0.69	(	-1 , -0.4)
NM_001981	epidermal growth factor receptor pathway substrate 15 (EPS15), mRNA	0.53	(	0.17 , 0.9	)	-0.7	(	-0.9 , -0.5)
NM_014925	KIAA1002 protein (KIAA1002), mRNA	0.48	(	0.33 , 0.63	)	-0.7	(	-1.2 , -0.2)
NM_018223	checkpoint with forkhead and ring finger domains (CHFR), mRNA	0.46	(	0.23 , 0.7	)	-0.7	(	-1 , -0.5)
XM_497119	omo sapiens upstream regulatory element binding protein 1 (UREB1), mRNA	0.5	(	0.43 , 0.58	)	-0.71	(	-1.2 , -0.3)
NM_018193	hypothetical protein FLJ10719 (FLJ10719), mRNA	0.49	(	0.26 , 0.73	)	-0.71	(	-1 , -0.4)
NM_145110	mitogen-activated protein kinase kinase 3 (MAP2K3), transcript variant C, mRNA	0.57	(	0.42 , 0.72	)	-0.71	(	-0.7 , -0.7)
NM_006306	SMC1 structural maintenance of chromosomes 1-like 1 (yeast) (SMC1L1), mRNA	0.52	(	0.28 , 0.77	)	-0.72	(	-1 , -0.5)
NM_080669	similar to RIKEN cDNA 1110002C08 gene (MGC9564), mRNA	0.58	(	0.41 , 0.76	)	-0.72	(	-1.2 , -0.3)
NM_024811	pre-mRNA cleavage factor I, 59 kDa subunit (FLJ12529), mRNA	0.47	(	0.21 , 0.72	)	-0.72	(	-0.9 , -0.5)
NM_017790	regulator of G-protein signalling 3 (RGS3), transcript variant 3, mRNA	0.49	(	0.21 , 0.76	)	-0.73	(	-0.9 , -0.6)
NM_014608	cytoplasmic FMR1 interacting protein 1 (CYFIP1), mRNA	0.7	(	0.48 , 0.92	)	-0.73	(	-1.3 , -0.2)
NM_006825	cytoskeleton-associated protein 4 (CKAP4), mRNA	0.62	(	0.53 , 0.71	)	-0.73	(	-0.8 , -0.7)
NM_002519	nuclear protein, ataxia-telangiectasia locus (NPAT), mRNA	0.48	(	0.32 , 0.64	)	-0.73	(	-1.1 , -0.4)
NM_016111	KIAA0683 gene product (KIAA0683), mRNA	0.64	(	0.41 , 0.86	)	-0.73	(	-0.9 , -0.6)
NM_006836	GCN1 general control of amino-acid synthesis 1-like 1 (yeast) (GCN1L1), mRNA	0.71	(	0.6 , 0.81	)	-0.74	(	-1 , -0.5)
NM_022089	putative ATPase (HSA9947), mRNA	0.67	(	0.21 , 1.14	)	-0.74	(	-1 , -0.5)

NM_002885	RAP1, GTPase activating protein 1 (RAP1GA1), mRNA	0.61	(	0.54 , 0.68	)	-0.75	(	-1.2 , -0.3)
NM_016111	KIAA0683 gene product (KIAA0683), mRNA	0.63	(	0.42 , 0.85	)	-0.75	(	-1.3 , -0.2)
NM_005347	heat shock 70kDa protein 5 (glucose-regulated protein, 78kDa) (HSPA5), mRNA	1.11	(	0.83 , 1.38	)	-0.75	(	-1.1 , -0.4)
NM_020857	vacuolar protein sorting protein 18 (VPS18), mRNA	0.56	(	0.46 , 0.65	)	-0.75	(	-0.9 , -0.6)
NM_004526	MCM2 minichromosome maintenance deficient 2, mitotin (S. cerevisiae) (MCM2), mRNA	0.52	(	0.24 , 0.8	)	-0.75	(	-1.1 , -0.4)
NM_000152	glucosidase, alpha; acid (Pompe disease, glycogen storage disease type II) (GAA), mRNA	0.78	(	0.57 , 0.99	)	-0.76	(	-1.2 , -0.3)
NM_016649	chromosome 20 open reading frame 6 (C20orf6), mRNA	0.75	(	0.28 , 1.23	)	-0.76	(	-1.1 , -0.4)
NM_016320	nucleoporin 98kDa (NUP98), transcript variant 1, mRNA	0.67	(	0.51 , 0.83	)	-0.76	(	-1.2 , -0.3)
NM_014773	KIAA0141 (KIAA0141), mRNA	0.82	(	0.8 , 0.83	)	-0.76	(	-1.1 , -0.5)
NM_015516	likely ortholog of chicken tsukushi (TSK), mRNA	0.73	(	0.71 , 0.76	)	-0.76	(	-1.3 , -0.2)
NM_006322	tubulin, gamma complex associated protein 3 (TUBGCP3), mRNA	0.83	(	0.67 , 0.99	)	-0.77	(	-1.2 , -0.3)
NM_015047	KIAA0090 protein (KIAA0090), mRNA	0.45	(	0.25 , 0.66	)	-0.78	(	-1 , -0.6)
NM_019606	hypothetical protein FLJ20257 (FLJ20257), mRNA	0.64	(	0.44 , 0.85	)	-0.78	(	-1 , -0.6)
NM_018085	importin 9 (IPO9), mRNA	0.53	(	0.5 , 0.56	)	-0.78	(	-1.2 , -0.4)
NM_198830	ATP citrate lyase (ACLY), transcript variant 2, mRNA	0.57	(	0.28 , 0.87	)	-0.78	(	-1.1 , -0.5)
NM_139181	centaurin, delta 2 (CENTD2), transcript variant 1, mRNA	1.05	(	0.95 , 1.15	)	-0.79	(	-1.5 , -0.1)
NM_015537	nasal embryonic LHRH factor (NELF), mRNA	0.46	(	0.31 , 0.62	)	-0.79	(	-1.1 , -0.5)
NM_001280	cold inducible RNA binding protein (CIRBP), mRNA	0.62	(	0.31 , 0.94	)	-0.79	(	-1.3 , -0.3)
XM_496933	omo sapiens similar to FLJ00261 protein (LOC441296), mRNA	0.76	(	0.51 , 1	)	-0.79	(	-1 , -0.6)
NM_001961	eukaryotic translation elongation factor 2 (EEF2), mRNA	0.61	(	0.16 , 1.07	)	-0.79	(	-1.4 , -0.2)
NM_003029	SHC (Src homology 2 domain containing) transforming protein 1 (SHC1), transcript variant 2, r	0.45	(	0.33 , 0.57	)	-0.8	(	-1.3 , -0.3)
NM_006129	bone morphogenetic protein 1 (BMP1), transcript variant BMP1-3, mRNA	0.48	(	0.36 , 0.61	)	-0.8	(	-1 , -0.6)
NM_003567	breast cancer anti-estrogen resistance 3 (BCAR3), mRNA	0.59	(	0.46 , 0.72	)	-0.81	(	-1.1 , -0.5)
NM_003170	suppressor of Ty 6 homolog (S. cerevisiae) (SUPT6H), mRNA	0.45	(	0.21 , 0.7	)	-0.81	(	-1.4 , -0.2)
NM_031965	haspin (GSG2), mRNA	0.4	(	0.3 , 0.51	)	-0.81	(	-1.2 , -0.4)
NM_024663	aminopeptidase-like 1 (NPEPL1), mRNA	0.73	(	0.42 , 1.03	)	-0.81	(	-1.3 , -0.3)
NM_033200	hypothetical protein BC002942 (BC002942), mRNA	0.76	(	0.43 , 1.08	)	-0.82	(	-1.2 , -0.5)
NR_001564	X (inactive)-specific transcript (XIST) on chromosome X	0.94	(	0.67 , 1.2	)	-0.82	(	-1.1 , -0.6)
NM_000148	fucosyltransferase 1 (galactoside 2-alpha-L-fucosyltransferase) (FUT1), mRNA	0.86	(	0.76 , 0.97	)	-0.82	(	-1.3 , -0.3)
NM_170707	lamin A/C (LMNA), transcript variant 1, mRNA	0.48	(	0.43 , 0.54	)	-0.82	(	-0.9 , -0.8)
NM_015335	thyroid hormone receptor associated protein 2 (THRAP2)	0.8	(	0.6 , 1.01	)	-0.82	(	-1 , -0.6)
NM_005993	tubulin-specific chaperone d (TBCD), mRNA	0.63	(	0.43 , 0.82	)	-0.82	(	-1 , -0.6)
NM_181351	neural cell adhesion molecule 1 (NCAM1), mRNA	0.44	(	0.26 , 0.63	)	-0.83	(	-1.3 , -0.4)

NM_002081	glypican 1 (GPC1), mRNA	0.45	(	0.39	,	0.51	)	-0.83	(	-1.2 , -0.4)
NM_015631	chromosome 10 open reading frame 61 (C10orf61), mRNA	1.05	(	1.02	,	1.08	)	-0.83	(	-1.1 , -0.6)
NM_173555	trypsin domain containing 1 (TYSND1), mRNA	0.69	(	0.44	,	0.94	)	-0.83	(	-1.2 , -0.5)
NM_002130	3-hydroxy-3-methylglutaryl-Coenzyme A synthase 1 (soluble) (HMGCS1), mRNA	0.46	(	0.28	,	0.65	)	-0.84	(	-1.1 , -0.6)
NM_152383	hypothetical protein MGC42174 (MGC42174), mRNA	0.85	(	0.71	,	0.98	)	-0.84	(	-1.5 , -0.2)
NM_017758	hypothetical protein FLJ20308 (FLJ20308), mRNA	0.84	(	0.65	,	1.03	)	-0.85	(	-1.1 , -0.6)
NM_015425	polymerase (RNA) I polypeptide A, 194kDa (POLR1A), mRNA	0.52	(	0.48	,	0.57	)	-0.85	(	-1 , -0.7)
NM_001681	ATPase, Ca++ transporting, cardiac muscle, slow twitch 2 (ATP2A2), transcript variant 2, mR	0.52	(	0.32	,	0.71	)	-0.86	(	-1 , -0.7)
XM_496255	KIAA0563-related gene (LOC440472), mRNA	0.6	(	0.35	,	0.85	)	-0.86	(	-1.3 , -0.4)
XM_374768	USP6 N-terminal like (USP6NL), mRNA	0.68	(	0.51	,	0.85	)	-0.86	(	-1.2 , -0.5)
NM_013432	nuclear factor of kappa light polypeptide gene enhancer in B-cells inhibitor-like 2 (NFKBIL2), m	0.5	(	0.37	,	0.63	)	-0.86	(	-1.2 , -0.5)
NM_007055	polymerase (RNA) III (DNA directed) polypeptide A, 155kDa (POLR3A), mRNA	0.56	(	0.26	,	0.86	)	-0.87	(	-1.3 , -0.5)
NM_003400	exportin 1 (CRM1 homolog, yeast) (XPO1), mRNA	0.61	(	0.22	,	1	)	-0.87	(	-1.1 , -0.7)
NM_014661	family with sequence similarity 53, member B (FAM53B), mRNA	0.44	(	0.31	,	0.58	)	-0.87	(	-1.5 , -0.3)
NM_005779	lipoma HMGIC fusion partner-like 2 (LHFPL2), mRNA	1.19	(	1.11	,	1.26	)	-0.87	(	-1.3 , -0.5)
NM_020832	KIAA1441 protein (KIAA1441), mRNA	0.54	(	0.26	,	0.81	)	-0.88	(	-1.3 , -0.4)
NM_003481	ubiquitin specific protease 5 (isopeptidase T) (USP5), mRNA	0.69	(	0.52	,	0.85	)	-0.88	(	-1.1 , -0.6)
NM_024519	hypothetical protein FLJ13725 (FLJ13725), mRNA	0.5	(	0.29	,	0.71	)	-0.89	(	-1.8 , 0)
NM_017747	ankyrin repeat and KH domain containing 1 (ANKHD1), transcript variant 1, mRNA	0.57	(	0.49	,	0.65	)	-0.89	(	-1.3 , -0.5)
NM_021174	KIAA1967 (KIAA1967), transcript variant 1, mRNA	0.72	(	0.45	,	0.99	)	-0.9	(	-1.5 , -0.3)
NM_030792	hypothetical protein PP1665 (PP1665), mRNA	0.63	(	0.55	,	0.71	)	-0.9	(	-1.2 , -0.6)
NM_032259	WD repeat domain 24 (WDR24), mRNA	0.73	(	0.46	,	1.01	)	-0.91	(	-1.3 , -0.5)
NM_207197	a disintegrin and metalloproteinase domain 15 (metargidin) (ADAM15), transcript variant 6, mR	0.66	(	0.61	,	0.72	)	-0.91	(	-1.3 , -0.6)
NM_020461	tubulin, gamma complex associated protein 6 (TUBGCP6), transcript variant 1, mRNA	0.69	(	0.41	,	0.97	)	-0.92	(	-1.1 , -0.7)
NM_012305	adaptor-related protein complex 2, alpha 2 subunit (AP2A2), mRNA	0.61	(	0.43	,	0.79	)	-0.93	(	-1.2 , -0.7)
NM_002332	low density lipoprotein-related protein 1 (alpha-2-macroglobulin receptor) (LRP1), mRNA	0.47	(	0.4	,	0.55	)	-0.93	(	-1.6 , -0.3)
NM_015329	KIAA0892 (KIAA0892), mRNA	0.55	(	0.39	,	0.71	)	-0.94	(	-1.4 , -0.5)
NM_001270	chromodomain helicase DNA binding protein 1 (CHD1), mRNA	0.66	(	0.07	,	1.24	)	-0.94	(	-1.3 , -0.5)
NM_001084	procollagen-lysine, 2-oxoglutarate 5-dioxygenase 3 (PLOD3), mRNA	0.74	(	0.66	,	0.83	)	-0.95	(	-1.4 , -0.5)
NM_014918	carbohydrate (chondroitin) synthase 1 (CHSY1), mRNA	0.7	(	0.49	,	0.91	)	-0.95	(	-1.3 , -0.6)
NM_005245	FAT tumor suppressor homolog 1 (Drosophila) (FAT), mRNA	0.49	(	0.41	,	0.57	)	-0.96	(	-1.3 , -0.7)
NM_004341	carbamoyl-phosphate synthetase 2, aspartate transcarbamylase, and dihydroorotase (CAD), r	0.46	(	0.39	,	0.54	)	-0.97	(	-1.1 , -0.8)
NM_030628	KIAA1698 protein (KIAA1698), mRNA	0.63	(	0.49	,	0.78	)	-0.97	(	-1.5 , -0.5)

NM_206937	ligase IV, DNA, ATP-dependent (LIG4), mRNA	0.84	(	0.65 , 1.03	)	-0.97	(	-1.2 , -0.8)
NM_198066	glucosamine-phosphate N-acetyltransferase 1 (GNPNAT1), mRNA	0.44	(	0.25 , 0.63	)	-0.98	(	-1.2 , -0.7)
NM_004634	bromodomain and PHD finger containing, 1 (BRPF1), transcript variant 2, mRNA	0.58	(	0.35 , 0.81	)	-1	(	-1.5 , -0.5)
NM_014045	low density lipoprotein receptor-related protein 10 (LRP10), mRNA	0.87	(	0.66 , 1.07	)	-1	(	-1.4 , -0.7)
NM_005163	v-akt murine thymoma viral oncogene homolog 1 (AKT1), mRNA	0.62	(	0.57 , 0.66	)	-1.01	(	-1.3 , -0.7)
NM_004687	myotubularin related protein 4 (MTMR4), mRNA	0.93	(	0.78 , 1.08	)	-1.02	(	-1.3 , -0.7)
NM_002663	phospholipase D2 (PLD2), mRNA	0.51	(	0.33 , 0.69	)	-1.04	(	-1.9 , -0.2)
NM_006038	spermatogenesis associated 2 (SPATA2), mRNA	0.63	(	0.21 , 1.06	)	-1.04	(	-1.4 , -0.7)
NM_033407	dedicator of cytokinesis 7 (DOCK7), mRNA	0.55	(	0.05 , 1.05	)	-1.04	(	-1.1 , -1)
NM_138619	golgi associated, gamma adaptin ear containing, ARF binding protein 3 (GGA3), transcript var	0.98	(	0.57 , 1.39	)	-1.08	(	-1.5 , -0.6)
NR_001564	X (inactive)-specific transcript (XIST) on chromosome X	0.74	(	0.4 , 1.08	)	-1.08	(	-1.3 , -0.9)
NM_004941	DEAH (Asp-Glu-Ala-His) box polypeptide 8 (DHX8), mRNA	1.11	(	0.95 , 1.26	)	-1.1	(	-1.3 , -0.9)
NM_012294	Rap guanine nucleotide exchange factor (GEF) 5 (RAPGEF5), mRNA	0.45	(	0.21 , 0.7	)	-1.13	(	-1.8 , -0.5)
NM_173602	KIAA1463 protein (KIAA1463), mRNA	0.47	(	0.25 , 0.69	)	-1.14	(	-1.4 , -0.9)
NM_006295	valyl-tRNA synthetase 2 (VARS2), mRNA	1.13	(	0.86 , 1.4	)	-1.14	(	-1.6 , -0.7)
NM_014287	NODAL modulator 1 (NOMO1), mRNA	0.99	(	0.78 , 1.2	)	-1.14	(	-1.5 , -0.8)
NM_004716	proprotein convertase subtilisin/kexin type 7 (PCSK7), mRNA	1.12	(	1.05 , 1.19	)	-1.16	(	-1.4 , -0.9)
NM_002447	macrophage stimulating 1 receptor (c-met-related tyrosine kinase) (MST1R), mRNA	0.82	(	0.66 , 0.98	)	-1.16	(	-1.6 , -0.7)
NM_134269	smoothelin (SMTN), transcript variant 2, mRNA	0.71	(	0.63 , 0.78	)	-1.16	(	-1.6 , -0.7)
NM_002691	polymerase (DNA directed), delta 1, catalytic subunit 125kDa (POLD1), mRNA	0.78	(	0.47 , 1.09	)	-1.21	(	-1.9 , -0.5)
NM_004383	c-src tyrosine kinase (CSK), mRNA	0.84	(	0.55 , 1.12	)	-1.25	(	-2.2 , -0.3)
NM_004260	RecQ protein-like 4 (RECQL4), mRNA	0.47	(	0.45 , 0.5	)	-1.3	(	-1.7 , -1)
NM_024757	euchromatic histone methyltransferase 1 (EHMT1), mRNA	0.69	(	0.42 , 0.95	)	-1.33	(	-1.9 , -0.7)
NM_024997	activating transcription factor 7 interacting protein 2 (ATF7IP2), mRNA	1.02	(	0.46 , 1.59	)	-1.33	(	-1.7 , -1)
NM_014685	homocysteine-inducible, endoplasmic reticulum stress-inducible, ubiquitin-like domain membe	0.75	(	0.62 , 0.89	)	-1.37	(	-1.7 , -1.1)
NM_000455	serine/threonine kinase 11 (Peutz-Jeghers syndrome) (STK11), mRNA	1.02	(	0.65 , 1.39	)	-1.39	(	-1.9 , -0.9)
NM_203346	high density lipoprotein binding protein (vigilin) (HDLBP), mRNA	0.86	(	0.58 , 1.14	)	-1.41	(	-1.5 , -1.3)

Genes down regulated at 1 and 4 hrs

NM_006649	UTP14, U3 small nucleolar ribonucleoprotein, homolog A (yeast) (UTP14A), mRNA	-2.12	(	-2.24 , -2	)	1.95	(	1.13 , 2.8)
NM_032991	caspase 3, apoptosis-related cysteine protease (CASP3), transcript variant beta, mRNA	-1.2	(	-1.37 , -1.03	)	1.74	(	0.59 , 2.9)
NM_018842	insulin receptor tyrosine kinase substrate (LOC55971), mRNA	-1.35	(	-1.41 , -1.28	)	1.48	(	0.79 , 2.2)

NM_013366	anaphase promoting complex subunit 2 (ANAPC2), mRNA	-1.96	(	-2.33 , -1.59	)	1.46	(	1.2 , 1.7)
NM_004433	E74-like factor 3 (ets domain transcription factor, epithelial-specific) (ELF3), mRNA	-0.99	(	-1.27 , -0.71	)	1.38	(	1.15 , 1.6)
NM_004157	protein kinase, cAMP-dependent, regulatory, type II, alpha (PRKAR2A), mRNA	-0.63	(	-0.78 , -0.47	)	1.35	(	0.17 , 2.5)
NM_006764	interferon-related developmental regulator 2 (IFRD2), mRNA	-0.77	(	-0.97 , -0.57	)	1.23	(	0.27 , 2.2)
NM_003383	very low density lipoprotein receptor (VLDLR), mRNA	-1.43	(	-1.56 , -1.31	)	1.21	(	1.04 , 1.4)
NM_002137	heterogeneous nuclear ribonucleoprotein A2/B1 (HNRPA2B1), transcript variant A2, mRNA	-0.9	(	-1.18 , -0.62	)	1.19	(	0.65 , 1.7)
NM_005346	heat shock 70kDa protein 1B (HSPA1B), mRNA	-1.05	(	-1.12 , -0.97	)	1.13	(	0.82 , 1.4)
NM_001005386	ARP2 actin-related protein 2 homolog (yeast) (ACTR2), transcript variant 1, mRNA	-0.59	(	-0.68 , -0.5	)	1.09	(	0.43 , 1.8)
NM_001005386	ARP2 actin-related protein 2 homolog (yeast) (ACTR2), transcript variant 1, mRNA	-0.78	(	-1.08 , -0.47	)	1.08	(	0.58 , 1.6)
NM_005826	heterogeneous nuclear ribonucleoprotein R (HNRPR), mRNA	-0.78	(	-0.97 , -0.6	)	1.07	(	0.49 , 1.7)
NM_003379	villin 2 (ezrin) (VIL2), mRNA	-1.52	(	-1.72 , -1.32	)	1.06	(	0.71 , 1.4)
NM_005346	heat shock 70kDa protein 1B (HSPA1B), mRNA	-1.3	(	-1.44 , -1.17	)	1.06	(	0.76 , 1.4)
NM_014570	ADP-ribosylation factor GTPase activating protein 3 (ARFGAP3), mRNA	-0.94	(	-1.1 , -0.79	)	1.04	(	0.49 , 1.6)
NM_002298	lymphocyte cytosolic protein 1 (L-plastin) (LCP1), mRNA	-1.33	(	-2.04 , -0.63	)	1.01	(	0.47 , 1.6)
NM_001539	DnaJ (Hsp40) homolog, subfamily A, member 1 (DNAJA1), mRNA	-0.61	(	-0.79 , -0.44	)	0.99	(	0.43 , 1.6)
NM_005346	heat shock 70kDa protein 1B (HSPA1B), mRNA	-1.01	(	-1.07 , -0.94	)	0.95	(	0.71 , 1.2)
NM_024419	phosphatidylglycerophosphate synthase (PGS1), mRNA	-1.3	(	-1.37 , -1.23	)	0.93	(	0.43 , 1.4)
NM_017722	hypothetical protein FLJ20244 (FLJ20244), mRNA	-1.07	(	-1.32 , -0.81	)	0.92	(	0.41 , 1.4)
NM_005346	heat shock 70kDa protein 1B (HSPA1B), mRNA	-1.39	(	-1.46 , -1.31	)	0.89	(	0.73 , 1.1)
NM_005346	heat shock 70kDa protein 1B (HSPA1B), mRNA	-1.27	(	-1.35 , -1.18	)	0.87	(	0.68 , 1.1)
NM_007357	component of oligomeric golgi complex 2 (COG2), mRNA	-0.66	(	-0.77 , -0.55	)	0.84	(	0.44 , 1.3)
NM_002356	myristoylated alanine-rich protein kinase C substrate (MARCKS), mRNA	-0.69	(	-0.84 , -0.54	)	0.82	(	0.55 , 1.1)
NM_005346	heat shock 70kDa protein 1B (HSPA1B), mRNA	-1.43	(	-1.56 , -1.3	)	0.81	(	0.42 , 1.2)
NM_005346	heat shock 70kDa protein 1B (HSPA1B), mRNA	-1.03	(	-1.11 , -0.95	)	0.79	(	0.54 , 1)
NM_005346	heat shock 70kDa protein 1B (HSPA1B), mRNA	-1.13	(	-1.23 , -1.03	)	0.79	(	0.47 , 1.1)
NM_005346	heat shock 70kDa protein 1B (HSPA1B), mRNA	-0.96	(	-1.08 , -0.83	)	0.78	(	0.41 , 1.1)
NM_014437	solute carrier family 39 (zinc transporter), member 1 (SLC39A1), mRNA	-0.89	(	-1.07 , -0.7	)	0.74	(	0.64 , 0.8)
NM_005346	heat shock 70kDa protein 1B (HSPA1B), mRNA	-1.08	(	-1.25 , -0.91	)	0.73	(	0.43 , 1)
NM_005346	heat shock 70kDa protein 1B (HSPA1B), mRNA	-1.36	(	-1.45 , -1.27	)	0.68	(	0.46 , 0.9)
NM_005346	heat shock 70kDa protein 1B (HSPA1B), mRNA	-0.49	(	-0.65 , -0.33	)	0.38	(	0.23 , 0.5)

Genes down regulated at 1 and 4 hrs

NM_005345	heat shock 70kDa protein 1A (HSPA1A), mRNA	-0.56	(-0.73 , -0.39)	-0.21 (-0.4 , -0)
NM_005345	heat shock 70kDa protein 1A (HSPA1A), mRNA	-0.59	(-0.67 , -0.5)	-0.25 (-0.5 , 0.1)
NM_002659	plasminogen activator, urokinase receptor (PLAUR)	-0.71	(-0.81 , -0.61)	-0.52 (-0.7 , -0.3)
NM_001270	chromodomain helicase DNA binding protein 1 (CHD1), mRNA	-0.52	(-0.73 , -0.32)	-0.54 (-0.7 , -0.4)
XM_377072	similar to LINE-1 reverse transcriptase homolog (LOC401623), mRNA	-1.36	(-1.77 , -0.94)	-0.55 (-1 , -0.2)
NM_005194	CCAAT/enhancer binding protein (C/EBP), beta (CEBPB), mRNA	-0.59	(-0.96 , -0.22)	-0.58 (-0.7 , -0.5)
NM_203418	Down syndrome critical region gene 1 (DSCR1), transcript variant 3, mRNA	-0.86	(-1.2 , -0.52)	-0.62 (-0.8 , -0.5)
NM_016522	neurotrimin (HNT), mRNA	-0.71	(-1.34 , -0.07)	-0.63 (-0.9 , -0.4)
NM_002659	plasminogen activator, urokinase receptor (PLAUR), transcript variant 1, mRNA	-0.79	(-0.88 , -0.7)	-0.7 (-0.9 , -0.5)
NM_000045	arginase, liver (ARG1), mRNA	-1.64	(-2.33 , -0.96)	-0.71 (-1 , -0.4)
NM_012118	CCR4 carbon catabolite repression 4-like (S. cerevisiae) (CCRN4L), mRNA	-0.59	(-0.71 , -0.47)	-0.71 (-1.1 , -0.3)
NM_020529	nuclear factor of kappa light polypeptide gene enhancer in B-cells inhibitor, alpha (NFKBIA), m	-1.04	(-1.14 , -0.94)	-0.76 (-0.9 , -0.6)
NM_006216	serine (or cysteine) proteinase inhibitor, clade E (nexin, plasminogen activator inhibitor type 1)	-1.17	(-1.33 , -1.01)	-0.8 (-0.9 , -0.7)
NM_001008490	Kruppel-like factor 6 (KLF6), transcript variant 1, mRNA	-0.56	(-0.63 , -0.49)	-0.81 (-1.1 , -0.5)
NM_002133	heme oxygenase (decycling) 1 (HMOX1), mRNA	-0.81	(-0.89 , -0.74)	-0.81 (-1.4 , -0.2)
NM_002089	chemokine (C-X-C motif) ligand 2 (CXCL2), mRNA.	-1	(-1.62 , -0.38)	-0.91 (-1.1 , -0.8)
NM_005946	metallothionein 1A (functional) (MT1A), mRNA	-0.65	(-0.92 , -0.39)	-0.94 (-1.3 , -0.6)
BC088358	eukaryotic translation termination factor 1, mRNA	-1.08	(-1.56 , -0.6)	-1.07 (-2.4 , 0.3)
NM_000758	colony stimulating factor 2 (granulocyte-macrophage) (CSF2), mRNA	-1.21	(-1.57 , -0.86)	-1.11 (-1.4 , -0.9)
NM_080645	collagen, type XII, alpha 1 (COL12A1), transcript variant short, mRNA	-0.78	(-1.14 , -0.41)	-1.13 (-1.4 , -0.9)
NM_001550	interferon-related developmental regulator 1 (IFRD1), transcript variant 1, mRNA	-0.46	(-0.5 , -0.41)	-0.78 (-1 , -0.5)

Genes up regulated by baculovirus treatment followed by LPS, PMA and ionomycin stimulation at 4 hrs post stimulation

NM_001001992	ubiquitin specific protease 16 (USP16), transcript variant 2, mRNA	1.63	(0.33 , 2.9)
NM_000341	solute carrier family 3 (cystine, dibasic and neutral amino acid transporters, activator of cystine	1.28	(0.55 , 2)
NM_004396	DEAD (Asp-Glu-Ala-Asp) box polypeptide 5 (DDX5), mRNA	1.08	(0.47 , 1.7)
NM_002165	inhibitor of DNA binding 1, dominant negative helix-loop-helix protein (ID1), transcript variant 1	0.98	(0.9 , 1.1)
NM_014618	deleted in bladder cancer 1 (DBC1), mRNA	0.94	(0.7 , 1.2)
NM_001359	2,4-dienoyl CoA reductase 1, mitochondrial (DECR1), nuclear gene encoding mitochondrial pr	0.88	(0.54 , 1.2)
NM_004058	calcyphosine (CAPS), transcript variant 1, mRNA	0.87	(0.5 , 1.2)
NM_006406	peroxiredoxin 4 (PRDX4), mRNA	0.77	(0.62 , 0.9)
NM_020899	zinc finger and BTB domain containing 4 (ZBTB4), mRNA	0.76	(0.67 , 0.9)

NM_000055	butyrylcholinesterase (BCHE), mRNA	0.72	(0.6 , 0.8)
NM_000029	angiotensinogen (serine (or cysteine) proteinase inhibitor, clade A (alpha-1 antiproteinase, ant	0.72	(0.62 , 0.8)
NM_018337	zinc finger protein 444 (ZNF444), mRNA	0.7	(0.64 , 0.8)
NM_006953	uroplakin 3A (UPK3A), mRNA	0.65	(0.58 , 0.7)
NM_177925	H2A histone family, member J (H2AFJ), transcript variant 2, mRNA	0.62	(0.62 , 0.6)

Genes down regulated by baculovirus treatment followed by LPS, PMA and ionomycin stimulation at 4 hrs post stim

NM_000575	interleukin 1, alpha (IL1A), mRNA	-1.48	(-1.7 , -1.2)
NM_000358	transforming growth factor, beta-induced, 68kDa (TGFBI), mRNA	-1.13	(-2 , -0.3)
NM_000499	cytochrome P450, family 1, subfamily A, polypeptide 1 (CYP1A1), mRNA	-1.13	(-1.4 , -0.9)
NM_012291	extra spindle poles like 1 (S. cerevisiae) (ESPL1), mRNA	-1.1	(-1.2 , -1)
NM_032010	microtubule-associated protein 1B (MAP1B), transcript variant 2, mRNA	-1.1	(-1.8 , -0.4)
NM_002502	nuclear factor of kappa light polypeptide gene enhancer in B-cells 2 (p49/p100) (NFKB2), mR	-1.1	(-1.6 , -0.6)
NM_007171	protein-O-mannosyltransferase 1 (POMT1), mRNA	-1.08	(-1.8 , -0.4)
NM_015633	FGFR1 oncogene partner 2 (FGFR1OP2), mRNA	-1.07	(-1.4 , -0.7)
NM_001986	ets variant gene 4 (E1A enhancer binding protein, E1AF) (ETV4), mRNA	-1.06	(-1.3 , -0.8)
NM_007353	guanine nucleotide binding protein (G protein) alpha 12 (GNA12), mRNA	-1.03	(-1.4 , -0.7)
BC113560	IBR domain containing 3, mRNA	-1.03	(-1.5 , -0.6)
NM_019902	ATP-binding cassette, sub-family C (CFTR/MRP), member 1 (ABCC1), transcript variant 7, mF	-0.99	(-1.3 , -0.7)
NM_014674	ER degradation enhancer, mannosidase alpha-like 1 (EDEM1), mRNA	-0.99	(-1.1 , -0.8)
NM_003376	vascular endothelial growth factor (VEGF), mRNA	-0.99	(-1.3 , -0.7)
NM_020443	neuron navigator 1 (NAV1), mRNA	-0.97	(-1.5 , -0.5)
NM_015361	R3H domain (binds single-stranded nucleic acids) containing (R3HDM), mRNA	-0.97	(-1.4 , -0.6)
NM_001431	erythrocyte membrane protein band 4.1-like 2 (EPB41L2), mRNA	-0.96	(-1.3 , -0.6)
NM_004670	3'-phosphoadenosine 5'-phosphosulfate synthase 2 (PAPSS2), mRNA	-0.95	(-1.2 , -0.7)
NM_015355	suppressor of zeste 12 homolog (Drosophila) (SUZ12), mRNA	-0.95	(-1 , -0.9)
NM_201533	diacylglycerol kinase, zeta 104kDa (DGKZ), transcript variant 3, mRNA	-0.92	(-1.4 , -0.5)
NM_016936	ubinuclein 1 (UBN1), mRNA	-0.91	(-1.4 , -0.4)
NM_006845	kinesin family member 2C (KIF2C), mRNA	-0.9	(-1.4 , -0.5)
NM_000358	transforming growth factor, beta-induced, 68kDa (TGFBI), mRNA	-0.9	(-1.1 , -0.7)
NM_015120	Alstrom syndrome 1 (ALMS1), mRNA	-0.89	(-1.2 , -0.6)
NM_002155	heat shock 70kDa protein 6 (HSP70B') (HSPA6), mRNA	-0.87	(-1.6 , -0.2)

NM_018069	centrosomal protein 192 kDa (Cep192), transcript variant 2, mRNA	-0.87	(-1.1 , -0.6)
NM_001423	epithelial membrane protein 1 (EMP1), mRNA	-0.87	(-1.3 , -0.5)
NM_152829	testis derived transcript (3 LIM domains) (TES), transcript variant 2, mRNA	-0.87	(-1 , -0.7)
NM_002019	fms-related tyrosine kinase 1 (vascular endothelial growth factor/vascular permeability factor r	-0.86	(-1.2 , -0.5)
NM_014727	myeloid/lymphoid or mixed-lineage leukemia 4 (MLL4), mRNA	-0.86	(-1.4 , -0.3)
NM_006453	transducin (beta)-like 3 (TBL3), mRNA	-0.86	(-1.2 , -0.5)
NM_000419	integrin, alpha 2b (platelet glycoprotein IIb of IIb/IIIa complex, antigen CD41B) (ITGA2B), mRNA	-0.85	(-1.2 , -0.5)
NM_017641	kinesin family member 21A (KIF21A), mRNA	-0.85	(-1.1 , -0.6)
NM_173555	trypsin domain containing 1 (TYSND1), mRNA	-0.85	(-1.1 , -0.6)
NM_002155	heat shock 70kDa protein 6 (HSP70B') (HSPA6), mRNA	-0.84	(-1.3 , -0.4)
NM_002155	heat shock 70kDa protein 6 (HSP70B') (HSPA6), mRNA	-0.84	(-1.1 , -0.5)
NM_003580	neutral sphingomyelinase (N-SMase) activation associated factor (NSMAF), mRNA	-0.84	(-1.2 , -0.5)
NM_002155	heat shock 70kDa protein 6 (HSP70B') (HSPA6), mRNA	-0.83	(-1.6 , -0.1)
NM_001521	general transcription factor IIIC, polypeptide 2, beta 110kDa (GTF3C2), mRNA	-0.83	(-1.1 , -0.5)
NM_021229	netrin 4 (NTN4), mRNA	-0.83	(-1 , -0.7)
NM_015349	KIAA0240 (KIAA0240), mRNA	-0.83	(-1.4 , -0.3)
NM_001876	carnitine palmitoyltransferase 1A (liver) (CPT1A), nuclear gene encoding mitochondrial protein	-0.82	(-1 , -0.6)
NM_015904	eukaryotic translation initiation factor 5B (EIF5B), mRNA	-0.82	(-1.3 , -0.4)
NM_006389	hypoxia up-regulated 1 (HYOU1), mRNA	-0.81	(-1.2 , -0.5)
NM_004867	integral membrane protein 2A (ITM2A), mRNA	-0.81	(-1.3 , -0.3)
NM_006715	mannosidase, alpha, class 2C, member 1 (MAN2C1), mRNA	-0.81	(-1.1 , -0.5)
NM_017790	regulator of G-protein signalling 3 (RGS3), transcript variant 3, mRNA	-0.81	(-0.9 , -0.7)
NM_003557	phosphatidylinositol-4-phosphate 5-kinase, type I, alpha (PIP5K1A), mRNA	-0.81	(-1 , -0.6)
NM_018201	TBC1 domain family, member 13 (TBC1D13), mRNA	-0.8	(-1.4 , -0.3)
NM_003028	SHB (Src homology 2 domain containing) adaptor protein B (SHB), mRNA	-0.8	(-1.7 , 0.1)
NM_001819	chromogranin B (secretogranin 1) (CHGB), mRNA	-0.8	(-1.1 , -0.6)
NM_002155	heat shock 70kDa protein 6 (HSP70B') (HSPA6), mRNA	-0.8	(-1.2 , -0.5)
NM_001605	alanyl-tRNA synthetase (AARS), mRNA	-0.79	(-1 , -0.6)
NM_015172	HBxAg transactivated protein 2 (XTP2), mRNA	-0.79	(-0.9 , -0.7)
NM_014649	scaffold attachment factor B2 (SAFB2), mRNA	-0.79	(-1.3 , -0.3)
NM_172230	synovial apoptosis inhibitor 1, synoviolin (SYVN1), transcript variant 2, mRNA	-0.78	(-1.1 , -0.5)
NM_002155	heat shock 70kDa protein 6 (HSP70B') (HSPA6), mRNA	-0.78	(-1 , -0.6)
NM_006089	sex comb on midleg-like 2 (Drosophila) (SCML2), mRNA	-0.78	(-1.2 , -0.4)

NM_002627	phosphofructokinase, platelet (PFKP), mRNA	-0.77	(	-1.1	,	-0.5)
NM_004941	DEAH (Asp-Glu-Ala-His) box polypeptide 8 (DHX8), mRNA	-0.77	(	-1.2	,	-0.4)
NM_019054	family with sequence similarity 35, member A (FAM35A), mRNA	-0.77	(	-0.9	,	-0.6)
NM_001006642	solute carrier family 25 (mitochondrial carrier; phosphate carrier), member 25 (SLC25A25), nu	-0.77	(	-1	,	-0.5)
NM_016252	baculoviral IAP repeat-containing 6 (apollon) (BIRC6), mRNA	-0.77	(	-1	,	-0.5)
NM_152221	casein kinase 1, epsilon (CSNK1E), transcript variant 1, mRNA	-0.76	(	-1	,	-0.5)
NM_002155	heat shock 70kDa protein 6 (HSP70B') (HSPA6), mRNA	-0.76	(	-1.3	,	-0.3)
NM_007183	plakophilin 3 (PKP3), mRNA	-0.76	(	-1.3	,	-0.3)
NM_014292	chromobox homolog 6 (CBX6), mRNA	-0.76	(	-0.9	,	-0.6)
NM_004817	tight junction protein 2 (zona occludens 2) (TJP2), transcript variant 1, mRNA	-0.75	(	-1	,	-0.6)
NM_020432	putative homeodomain transcription factor 2 (PHTF2), mRNA	-0.75	(	-1	,	-0.5)
NM_203351	mitogen-activated protein kinase kinase kinase 3 (MAP3K3), transcript variant 1, mRNA	-0.75	(	-1.3	,	-0.2)
NM_032960	mitogen-activated protein kinase-activated protein kinase 2 (MAPKAPK2), transcript variant 2,	-0.75	(	-1.2	,	-0.3)
NM_033512	TSPY-like 5 (TSPYL5), mRNA	-0.75	(	-1.1	,	-0.4)
NM_016076	CGI-146 protein (PNAS-4), mRNA	-0.74	(	-0.9	,	-0.6)
NM_017553	homolog of yeast INO80 (INO80), transcript variant 1, mRNA	-0.74	(	-1.1	,	-0.4)
NM_005134	protein phosphatase 4, regulatory subunit 1 (PPP4R1), mRNA	-0.74	(	-1	,	-0.5)
NM_014786	Rho guanine nucleotide exchange factor (GEF) 17 (ARHGEF17), mRNA	-0.74	(	-1.3	,	-0.2)
NM_014611	MDN1, midasin homolog (yeast) (MDN1), mRNA	-0.74	(	-0.9	,	-0.6)
NM_018671	smooth muscle cell associated protein-1 (SMAP-1), mRNA	-0.73	(	-1.2	,	-0.3)
NM_018201	TBC1 domain family, member 13 (TBC1D13), mRNA	-0.73	(	-0.8	,	-0.7)
NM_002155	heat shock 70kDa protein 6 (HSP70B') (HSPA6), mRNA	-0.73	(	-1.2	,	-0.3)
NM_178819	putative lysophosphatidic acid acyltransferase (DKFZp586M1819), mRNA	-0.73	(	-0.8	,	-0.7)
NM_004638	HLA-B associated transcript 2 (BAT2), transcript variant 2, mRNA	-0.72	(	-1.1	,	-0.3)
NM_033046	rhotekin (RTKN), mRNA	-0.72	(	-1	,	-0.4)
NM_000617	solute carrier family 11 (proton-coupled divalent metal ion transporters), member 2 (SLC11A2)	-0.72	(	-0.9	,	-0.6)
NM_002466	v-myb myeloblastosis viral oncogene homolog (avian)-like 2 (MYBL2), mRNA	-0.72	(	-1.1	,	-0.3)
NM_005647	transducin (beta)-like 1X-linked (TBL1X), mRNA	-0.72	(	-1.1	,	-0.3)
NM_022070	amplified in breast cancer 1 (ABC1), mRNA	-0.72	(	-1.1	,	-0.3)
NM_005700	dipeptidylpeptidase 3 (DPP3), transcript variant 1, mRNA	-0.72	(	-0.9	,	-0.5)
NM_017565	family with sequence similarity 20, member A (FAM20A), mRNA	-0.72	(	-1.1	,	-0.3)
NM_002359	v-maf musculoaponeurotic fibrosarcoma oncogene homolog G (avian) (MAFG), transcript varia	-0.72	(	-1	,	-0.5)
NM_001457	filamin B, beta (actin binding protein 278) (FLNB), mRNA	-0.71	(	-1	,	-0.4)

NM_030884	microtubule-associated protein 4 (MAP4), transcript variant 2, mRNA	-0.71	(-1.4 , -0.1)
NM_000211	integrin, beta 2 (antigen CD18 (p95), lymphocyte function-associated antigen 1; macrophage a	-0.71	(-1.4 , -0.1)
NM_014631	SH3 multiple domains 1 (SH3MD1), mRNA	-0.71	(-1.4 , -0.1)
NM_005628	solute carrier family 1 (neutral amino acid transporter), member 5 (SLC1A5), mRNA	-0.71	(-1.1 , -0.4)
NM_015382	HECT domain containing 1 (HECTD1), mRNA	-0.71	(-0.8 , -0.6)
NM_006827	transmembrane trafficking protein (TMP21), mRNA	-0.7	(-0.9 , -0.5)
NM_006026	H1 histone family, member X (H1FX), mRNA	-0.7	(-1.3 , -0.1)
NM_020438	dolichyl pyrophosphate phosphatase 1 (DOLPP1), mRNA	-0.69	(-1 , -0.4)
NM_030884	microtubule-associated protein 4 (MAP4), transcript variant 2, mRNA	-0.69	(-1 , -0.4)
NM_002874	RAD23 homolog B (S. cerevisiae) (RAD23B), mRNA	-0.69	(-1 , -0.4)
NM_006267	RAN binding protein 2 (RANBP2), mRNA	-0.69	(-0.8 , -0.6)
NM_015229	KIAA0664 protein (KIAA0664), mRNA	-0.69	(-1 , -0.4)
NM_018703	retinoblastoma binding protein 6 (RBBP6), transcript variant 2, mRNA	-0.69	(-0.8 , -0.6)
NM_014305	TDP-glucose 4,6-dehydratase (TGDS), mRNA	-0.69	(-0.8 , -0.6)
NM_018639	WD repeat and SOCS box-containing 2 (WSB2), mRNA	-0.69	(-1 , -0.4)
NM_003088	fascin homolog 1, actin-bundling protein (Strongylocentrotus purpuratus) (FSCN1), mRNA	-0.69	(-0.9 , -0.5)
NM_024745	SHC SH2-domain binding protein 1 (SHCBP1), mRNA	-0.69	(-0.9 , -0.5)
NM_007126	valosin-containing protein (VCP), mRNA	-0.69	(-0.9 , -0.4)
NM_004427	polyhomeotic-like 2 (Drosophila) (PHC2), transcript variant 2, mRNA	-0.68	(-0.9 , -0.5)
NM_004229	cofactor required for Sp1 transcriptional activation, subunit 2, 150kDa (CRSP2), mRNA	-0.68	(-0.9 , -0.4)
NM_182984	HpaII tiny fragments locus 9C (HTF9C), transcript variant 2, mRNA	-0.68	(-1.2 , -0.2)
NM_006767	leucine-zipper-like transcription regulator 1 (LZTR1), mRNA	-0.68	(-0.9 , -0.4)
NM_003255	tissue inhibitor of metalloproteinase 2 (TIMP2), mRNA	-0.68	(-1 , -0.3)
NM_024658	importin 4 (IPO4), mRNA	-0.68	(-1 , -0.4)
NM_001254	CDC6 cell division cycle 6 homolog (S. cerevisiae) (CDC6), mRNA	-0.67	(-0.8 , -0.6)
NM_005607	PTK2 protein tyrosine kinase 2 (PTK2), transcript variant 2, mRNA	-0.67	(-0.9 , -0.4)
NM_020824	Rho GTPase activating protein 21 (ARHGAP21), mRNA	-0.67	(-1.1 , -0.3)
NM_006314	connector enhancer of kinase suppressor of Ras 1 (CNKSR1), mRNA	-0.67	(-1.2 , -0.1)
NM_017921	nuclear protein localization 4 (NPL4), mRNA	-0.67	(-0.8 , -0.5)
NM_003144	signal sequence receptor, alpha (translocon-associated protein alpha) (SSR1), mRNA	-0.67	(-0.8 , -0.5)
NM_031284	ADP-dependent glucokinase (ADPGK), mRNA	-0.66	(-0.9 , -0.5)
NM_032621	brain expressed X-linked 2 (BEX2), mRNA	-0.66	(-0.8 , -0.5)
NM_004494	hepatoma-derived growth factor (high-mobility group protein 1-like) (HDGF), mRNA	-0.66	(-1 , -0.3)

NM_014940	HSV-1 stimulation-related gene 1 (HSRG1), mRNA	-0.66	(	-0.8	,	-0.5)
NM_002336	low density lipoprotein receptor-related protein 6 (LRP6), mRNA	-0.66	(	-1	,	-0.4)
NM_006702	neuropathy target esterase (NTE), mRNA	-0.66	(	-0.9	,	-0.4)
NM_014884	splicing factor, arginine/serine-rich 14 (SFRS14), mRNA	-0.66	(	-1	,	-0.3)
NM_206835	TNF receptor-associated factor 7 (TRAF7), transcript variant 2, mRNA	-0.66	(	-1	,	-0.4)
NM_182800	arsenate resistance protein ARS2 (ARS2), transcript variant 2, mRNA	-0.65	(	-0.9	,	-0.4)
NM_020379	mannosidase, alpha, class 1C, member 1 (MAN1C1), mRNA	-0.65	(	-0.7	,	-0.6)
NM_014669	nucleoporin 93kDa (NUP93), mRNA	-0.65	(	-1.2	,	-0.1)
NM_014679	translokin (KIAA0092), mRNA	-0.65	(	-1	,	-0.4)
NM_000598	insulin-like growth factor binding protein 3 (IGFBP3), mRNA	-0.65	(	-0.9	,	-0.4)
NM_015057	MYC binding protein 2 (MYCBP2), mRNA	-0.65	(	-1	,	-0.3)
NM_001618	poly (ADP-ribose) polymerase family, member 1 (PARP1), mRNA	-0.65	(	-1	,	-0.3)
NM_015289	vacuolar protein sorting 39 (yeast) (VPS39), mRNA	-0.65	(	-0.9	,	-0.5)
NM_005104	bromodomain containing 2 (BRD2), mRNA	-0.65	(	-0.9	,	-0.5)
NM_033271	BTB (POZ) domain containing 6 (BTBD6), mRNA	-0.65	(	-0.9	,	-0.4)
NM_003829	multiple PDZ domain protein (MPDZ), mRNA	-0.65	(	-0.8	,	-0.5)
NM_001211	BUB1 budding uninhibited by benzimidazoles 1 homolog beta (yeast) (BUB1B), mRNA	-0.64	(	-0.8	,	-0.5)
NM_145689	amyloid beta (A4) precursor protein-binding, family B, member 1 (Fe65) (APBB1), transcript va	-0.64	(	-1	,	-0.3)
NM_015925	liver-specific bHLH-Zip transcription factor (LISCH7), transcript variant 1, mRNA	-0.64	(	-1.1	,	-0.2)
NM_003900	sequestosome 1 (SQSTM1), mRNA	-0.64	(	-0.8	,	-0.5)
NM_006818	ALL1-fused gene from chromosome 1q (AF1Q), mRNA	-0.64	(	-1	,	-0.3)
NM_001904	catenin (cadherin-associated protein), beta 1, 88kDa (CTNNB1), mRNA	-0.64	(	-0.8	,	-0.5)
NM_002155	heat shock 70kDa protein 6 (HSP70B') (HSPA6), mRNA	-0.64	(	-0.7	,	-0.6)
NM_023002	hyaluronan and proteoglycan link protein 4 (HAPLN4), mRNA	-0.64	(	-0.9	,	-0.3)
NM_005085	nucleoporin 214kDa (NUP214), mRNA	-0.64	(	-0.8	,	-0.5)
NM_182648	bromodomain adjacent to zinc finger domain, 1A (BAZ1A), transcript variant 2, mRNA	-0.63	(	-0.9	,	-0.4)
NM_177438	Dicer1, Dcr-1 homolog (Drosophila) (DICER1), transcript variant 1, mRNA	-0.63	(	-0.8	,	-0.5)
NM_207521	reticulon 4 (RTN4), transcript variant 5, mRNA	-0.63	(	-1	,	-0.3)
NM_012470	transportin 3 (TNPO3), mRNA	-0.63	(	-0.9	,	-0.4)
NM_006594	adaptor-related protein complex 4, beta 1 subunit (AP4B1), mRNA	-0.63	(	-0.7	,	-0.5)
NM_016376	ankyrin repeat and FYVE domain containing 1 (ANKFY1), transcript variant 1, mRNA	-0.63	(	-1	,	-0.3)
NM_182712	eukaryotic translation initiation factor 3, subunit 9 eta, 116kDa (EIF3S9), transcript variant 2, m	-0.63	(	-0.9	,	-0.4)
NM_013241	formin homology 2 domain containing 1 (FHOD1), mRNA	-0.63	(	-0.9	,	-0.3)

NM_020338	retinoic acid induced 17 (RAI17), mRNA	-0.63	(-0.8 , -0.4)
NM_002575	serine (or cysteine) proteinase inhibitor, clade B (ovalbumin), member 2 (SERPINB2), mRNA	-0.63	(-1.1 , -0.1)
NM_001067	topoisomerase (DNA) II alpha 170kDa (TOP2A), mRNA	-0.63	(-1 , -0.3)
NM_033083	ELL associated factor 1 (EAF1), mRNA	-0.63	(-0.9 , -0.4)
NM_014329	autoantigen (RCD-8), mRNA	-0.62	(-0.9 , -0.4)
NM_006145	DnaJ (Hsp40) homolog, subfamily B, member 1 (DNAJB1), mRNA	-0.62	(-0.9 , -0.4)
NM_004540	neural cell adhesion molecule 2 (NCAM2), mRNA	-0.62	(-0.9 , -0.4)
NM_020123	SM-11044 binding protein (SMBP), mRNA	-0.62	(-1.1 , -0.1)
NM_182919	TIR domain containing adaptor inducing interferon-beta (TRIF), mRNA	-0.62	(-1 , -0.2)
NM_016128	coatomer protein complex, subunit gamma (COPG), mRNA	-0.62	(-1 , -0.3)
NM_015292	likely ortholog of mouse membrane bound C2 domain containing protein (MBC2), mRNA	-0.62	(-0.8 , -0.5)
NM_145693	lipin 1 (LPIN1), mRNA	-0.62	(-0.9 , -0.3)
NM_000484	amyloid beta (A4) precursor protein (protease nexin-II, Alzheimer disease) (APP), transcript va	-0.62	(-1 , -0.2)
NM_013312	hook homolog 2 (Drosophila) (HOOK2), mRNA	-0.62	(-0.8 , -0.5)
NM_030884	microtubule-associated protein 4 (MAP4), transcript variant 2, mRNA	-0.62	(-0.9 , -0.3)
NM_170692	RAS protein activator like 2 (RASAL2), transcript variant 2, mRNA	-0.62	(-0.9 , -0.4)
NM_003359	UDP-glucose dehydrogenase (UGDH), mRNA	-0.62	(-0.8 , -0.5)
NM_004926	zinc finger protein 36, C3H type-like 1 (ZFP36L1), mRNA	-0.62	(-0.7 , -0.6)
NM_001105	activin A receptor, type I (ACVR1), mRNA	-0.61	(-0.7 , -0.5)
NM_145730	adaptor-related protein complex 1, beta 1 subunit (AP1B1), transcript variant 2, mRNA	-0.61	(-0.9 , -0.4)
NM_014774	KIAA0494 gene product (KIAA0494), mRNA	-0.61	(-0.8 , -0.4)
NM_012432	SET domain, bifurcated 1 (SETDB1), mRNA	-0.61	(-0.8 , -0.5)
NM_058243	bromodomain containing 4 (BRD4), transcript variant long, mRNA	-0.61	(-0.9 , -0.4)
NM_002018	flightless I homolog (Drosophila) (FLII), mRNA	-0.61	(-0.9 , -0.3)
NM_005540	inositol polyphosphate-5-phosphatase, 75kDa (INPP5B), mRNA	-0.61	(-0.8 , -0.4)
NM_198129	laminin, alpha 3 (LAMA3), transcript variant 1, mRNA	-0.61	(-0.6 , -0.6)
NM_006464	trans-golgi network protein 2 (TGOLN2), mRNA	-0.61	(-1 , -0.2)
NM_002155	heat shock 70kDa protein 6 (HSP70B') (HSPA6), mRNA	-0.61	(-1 , -0.2)
NM_018445	selenoprotein S (SELS), transcript variant 2, mRNA	-0.61	(-0.7 , -0.5)
NM_001725	bactericidal/permeability-increasing protein (BPI), mRNA	-0.6	(-0.8 , -0.4)
NM_023924	bromodomain containing 9 (BRD9), mRNA	-0.6	(-0.7 , -0.5)
NM_000918	procollagen-proline, 2-oxoglutarate 4-dioxygenase (proline 4-hydroxylase), beta polypeptide (p	-0.6	(-0.6 , -0.6)
NM_020967	nuclear receptor coactivator 5 (NCOA5), mRNA	-0.6	(-0.8 , -0.4)

NM_002859	paxillin (PXN), mRNA	-0.6	(	-1	,	-0.2)
NM_001102	actinin, alpha 1 (ACTN1), mRNA	-0.6	(	-0.9	,	-0.3)
NM_153719	nucleoporin 62kDa (NUP62), transcript variant 1, mRNA	-0.6	(	-0.7	,	-0.5)
NM_004587	ribosome binding protein 1 homolog 180kDa (dog) (RRBP1), mRNA	-0.6	(	-0.7	,	-0.5)
NM_004749	transforming growth factor beta regulator 4 (TBRG4), transcript variant 1, mRNA	-0.59	(	-0.8	,	-0.4)
BC016365	transmembrane emp24 protein transport domain containing 5	-0.59	(	-0.7	,	-0.5)
NM_018188	ATPase family, AAA domain containing 3A (ATAD3A), mRNA	-0.59	(	-0.8	,	-0.3)
NM_019058	DNA-damage-inducible transcript 4 (DDIT4), mRNA	-0.59	(	-0.8	,	-0.4)
NM_002228	v-jun sarcoma virus 17 oncogene homolog (avian) (JUN), mRNA	-0.59	(	-0.7	,	-0.5)
NM_001670	armadillo repeat gene deletes in velocardiofacial syndrome (ARVCF), mRNA	-0.59	(	-0.8	,	-0.3)
NM_002155	heat shock 70kDa protein 6 (HSP70B') (HSPA6), mRNA	-0.59	(	-0.7	,	-0.5)
NM_004417	dual specificity phosphatase 1 (DUSP1), mRNA	-0.58	(	-0.6	,	-0.6)
NM_015171	exportin 6 (XPO6), mRNA	-0.58	(	-0.8	,	-0.4)
NM_000942	peptidylprolyl isomerase B (cyclophilin B) (PPIB), mRNA	-0.58	(	-0.7	,	-0.5)
NM_007027	topoisomerase (DNA) II binding protein 1 (TOPBP1), mRNA	-0.58	(	-0.8	,	-0.4)
NM_005194	CCAAT/enhancer binding protein (C/EBP), beta (CEBPB), mRNA	-0.58	(	-0.9	,	-0.3)
NM_002074	guanine nucleotide binding protein (G protein), beta polypeptide 1 (GNB1), mRNA	-0.58	(	-0.8	,	-0.3)
NM_002394	solute carrier family 3 (activators of dibasic and neutral amino acid transport), member 2 (SLC	-0.58	(	-0.9	,	-0.3)
NM_001273	chromodomain helicase DNA binding protein 4 (CHD4), mRNA	-0.58	(	-0.6	,	-0.5)
NM_182712	eukaryotic translation initiation factor 3, subunit 9 eta, 116kDa (EIF3S9), transcript variant 2, mRNA	-0.58	(	-0.7	,	-0.5)
NM_014753	BMS1-like, ribosome assembly protein (yeast) (BMS1L), mRNA	-0.57	(	-0.7	,	-0.5)
NM_013449	bromodomain adjacent to zinc finger domain, 2A (BAZ2A), mRNA	-0.57	(	-0.8	,	-0.4)
NM_002265	karyopherin (importin) beta 1 (KPNB1), mRNA	-0.57	(	-0.8	,	-0.3)
NM_005898	membrane component, chromosome 11, surface marker 1 (M11S1), transcript variant 1, mRNA	-0.57	(	-0.9	,	-0.2)
NM_002911	regulator of nonsense transcripts 1 (RENT1), mRNA	-0.57	(	-0.8	,	-0.4)
NM_003129	squalene epoxidase (SQLE), mRNA	-0.57	(	-0.6	,	-0.6)
NM_005184	calmodulin 3 (phosphorylase kinase, delta) (CALM3), mRNA	-0.57	(	-1	,	-0.2)
NM_004417	dual specificity phosphatase 1 (DUSP1), mRNA	-0.57	(	-0.9	,	-0.2)
NM_005505	scavenger receptor class B, member 1 (SCARB1), mRNA	-0.57	(	-0.9	,	-0.3)
NM_024700	Smad nuclear interacting protein (SNIP1), mRNA	-0.57	(	-0.9	,	-0.3)
NM_006015	AT rich interactive domain 1A (SWI- like) (ARID1A), transcript variant 1, mRNA	-0.56	(	-0.7	,	-0.4)
NM_004380	CREB binding protein (Rubinstein-Taybi syndrome) (CREBBP), mRNA	-0.56	(	-0.9	,	-0.2)
NM_016604	jumonji domain containing 1B (JMJD1B), mRNA	-0.56	(	-0.7	,	-0.4)

NM_016612	mitochondrial solute carrier protein (MSCP), mRNA	-0.56	(	-0.9 ,	-0.2)
NM_033505	selenoprotein I (SELI), mRNA	-0.56	(	-0.8 ,	-0.4)
NM_001905	CTP synthase (CTPS), mRNA	-0.56	(	-0.7 ,	-0.5)
NM_024072	DEAD (Asp-Glu-Ala-Asp) box polypeptide 54 (DDX54), mRNA	-0.56	(	-0.8 ,	-0.3)
NM_005324	H3 histone, family 3B (H3.3B) (H3F3B), mRNA	-0.56	(	-0.8 ,	-0.3)
NM_020850	RAN binding protein 10 (RANBP10), mRNA	-0.56	(	-0.6 ,	-0.5)
NM_173079	RUN domain containing 1 (RUNDC1), mRNA	-0.56	(	-0.7 ,	-0.4)
NM_009643	AHNAK nucleoprotein (desmoyokin) (Ahnak)	-0.56	(	-0.7 ,	-0.4)
NM_005388	phosducin-like (PDCL), mRNA	-0.56	(	-0.7 ,	-0.4)
NM_006147	interferon regulatory factor 6 (IRF6), mRNA	-0.55	(	-0.6 ,	-0.5)
NM_001219	calumenin (CALU), mRNA	-0.55	(	-0.8 ,	-0.4)
NM_014756	KIAA0097 gene product (ch-TOG), mRNA	-0.55	(	-0.8 ,	-0.3)
NM_005034	polymerase (RNA) II (DNA directed) polypeptide K, 7.0kDa (POLR2K), mRNA	-0.55	(	-0.7 ,	-0.4)
NM_004336	BUB1 budding uninhibited by benzimidazoles 1 homolog (yeast) (BUB1), mRNA	-0.55	(	-0.7 ,	-0.4)
NM_022842	CUB domain-containing protein 1 (CDCP1), transcript variant 1, mRNA	-0.55	(	-0.7 ,	-0.4)
NM_015296	dedicator of cytokinesis 9 (DOCK9), mRNA	-0.55	(	-0.9 ,	-0.2)
NM_004827	ATP-binding cassette, sub-family G (WHITE), member 2 (ABCG2), mRNA	-0.54	(	-0.8 ,	-0.3)
NM_152221	casein kinase 1, epsilon (CSNK1E), transcript variant 1, mRNA	-0.54	(	-0.8 ,	-0.3)
NM_198316	tensin like C1 domain containing phosphatase (TENC1), transcript variant 3, mRNA	-0.54	(	-0.8 ,	-0.2)
NM_005587	MADS box transcription enhancer factor 2, polypeptide A (myocyte enhancer factor 2A) (MEF2	-0.54	(	-0.7 ,	-0.4)
NM_133370	splicing factor YT521-B (YT521), mRNA	-0.54	(	-0.8 ,	-0.3)
NM_004424	E4F transcription factor 1 (E4F1), mRNA	-0.54	(	-0.6 ,	-0.5)
NM_002540	outer dense fiber of sperm tails 2 (ODF2), transcript variant 1, mRNA	-0.54	(	-0.7 ,	-0.4)
NM_005628	solute carrier family 1 (neutral amino acid transporter), member 5 (SLC1A5), mRNA	-0.54	(	-0.8 ,	-0.3)
NM_014445	stress-associated endoplasmic reticulum protein 1 (SERP1), mRNA	-0.54	(	-0.6 ,	-0.5)
NM_001091	amiloride binding protein 1 (amine oxidase (copper-containing)) (ABP1), mRNA	-0.53	(	-0.8 ,	-0.3)
NM_014652	importin 13 (IPO13), mRNA	-0.53	(	-0.8 ,	-0.2)
NM_003819	poly(A) binding protein, cytoplasmic 4 (inducible form) (PABPC4), mRNA	-0.53	(	-0.7 ,	-0.4)
NM_003376	vascular endothelial growth factor (VEGF), mRNA	-0.53	(	-0.8 ,	-0.3)
NM_000210	integrin, alpha 6 (ITGA6), mRNA	-0.53	(	-0.8 ,	-0.2)
NM_003576	serine/threonine kinase 24 (STE20 homolog, yeast) (STK24), mRNA	-0.53	(	-0.7 ,	-0.4)
NM_032259	WD repeat domain 24 (WDR24), mRNA	-0.53	(	-0.7 ,	-0.4)
NM_003311	pleckstrin homology-like domain, family A, member 2 (PHLDA2), mRNA	-0.53	(	-0.6 ,	-0.4)

NM_020765	retinoblastoma-associated factor 600 (RBAF600), mRNA	-0.53	(-0.8 , -0.2)
NM_006595	apoptosis inhibitor 5 (API5), mRNA	-0.52	(-0.7 , -0.3)
NM_002689	polymerase (DNA-directed), alpha (70kD) (POLA2), mRNA	-0.52	(-0.8 , -0.3)
NM_014847	ubiquitin associated protein 2-like (UBAP2L), mRNA	-0.52	(-0.7 , -0.4)
NM_033671	cyclin B3 (CCNB3), transcript variant 2, mRNA	-0.52	(-0.8 , -0.3)
NM_006924	splicing factor, arginine/serine-rich 1 (splicing factor 2, alternate splicing factor) (SFRS1), mRNA	-0.52	(-0.6 , -0.5)
NM_007292	acyl-Coenzyme A oxidase 1, palmitoyl (ACOX1), transcript variant 2, mRNA	-0.52	(-0.7 , -0.4)
NM_002155	heat shock 70kDa protein 6 (HSP70B') (HSPA6), mRNA	-0.52	(-0.7 , -0.3)
NM_176800	PRP4 pre-mRNA processing factor 4 homolog B (yeast) (PRPF4B), transcript variant 2, mRNA	-0.52	(-0.7 , -0.4)
NM_003579	RAD54-like (S. cerevisiae) (RAD54L), mRNA	-0.52	(-0.8 , -0.3)
NM_175852	taxilin (DKFZp451J0118), mRNA	-0.52	(-0.8 , -0.3)
NM_001008697	tuftelin interacting protein 11 (TFIP11), transcript variant 1, mRNA	-0.52	(-0.8 , -0.3)
NM_005088	DNA segment on chromosome X and Y (unique) 155 expressed sequence (DXYS155E), trans	-0.51	(-0.6 , -0.4)
NM_004462	farnesyl-diphosphate farnesyltransferase 1 (FDFT1), mRNA	-0.51	(-0.6 , -0.5)
NM_006979	solute carrier family 39 (zinc transporter), member 7 (SLC39A7), mRNA	-0.51	(-0.8 , -0.3)
NM_003368	ubiquitin specific protease 1 (USP1), mRNA	-0.51	(-0.7 , -0.4)
NM_003379	villin 2 (ezrin) (VIL2), mRNA	-0.51	(-0.7 , -0.4)
NM_012197	RAB GTPase activating protein 1 (RABGAP1), mRNA	-0.51	(-0.7 , -0.4)
NM_004584	RAD9 homolog A (S. pombe) (RAD9A), mRNA	-0.51	(-0.6 , -0.4)
NM_023071	spermatogenesis associated, serine-rich 2 (SPATS2), mRNA	-0.51	(-0.7 , -0.4)
NM_015518	DKFZP434C131 protein (DKFZP434C131), mRNA	-0.51	(-0.8 , -0.2)
NM_006145	DnaJ (Hsp40) homolog, subfamily B, member 1 (DNAJB1), mRNA	-0.51	(-0.6 , -0.4)
NM_025164	KIAA0999 protein (KIAA0999), mRNA	-0.51	(-0.8 , -0.3)
NM_017857	slingshot homolog 3 (Drosophila) (SSH3), mRNA	-0.51	(-0.7 , -0.3)
NM_004618	topoisomerase (DNA) III alpha (TOP3A), mRNA	-0.51	(-0.6 , -0.4)
NM_001379	DNA (cytosine-5-)-methyltransferase 1 (DNMT1), mRNA	-0.5	(-0.7 , -0.3)
NM_003760	eukaryotic translation initiation factor 4 gamma, 3 (EIF4G3), mRNA	-0.5	(-0.7 , -0.3)
NM_000600	interleukin 6 (interferon, beta 2) (IL6), mRNA	-0.5	(-0.6 , -0.4)
NM_012289	kelch-like ECH-associated protein 1 (KEAP1), transcript variant 2, mRNA	-0.5	(-0.7 , -0.3)
NM_006868	RAB31, member RAS oncogene family (RAB31), mRNA	-0.5	(-0.8 , -0.3)
NM_000201	intercellular adhesion molecule 1 (CD54), human rhinovirus receptor (ICAM1), mRNA	-0.5	(-0.6 , -0.4)
NM_002745	mitogen-activated protein kinase 1 (MAPK1), transcript variant 1, mRNA	-0.5	(-0.6 , -0.4)
NM_013277	Rac GTPase activating protein 1 (RACGAP1), mRNA	-0.5	(-0.8 , -0.3)

NM_203327	solute carrier family 23 (nucleobase transporters), member 2 (SLC23A2), transcript variant 2, mRNA	-0.5	(-0.7 , -0.3)
NM_003330	thioredoxin reductase 1 (TXNRD1), transcript variant 1, mRNA	-0.5	(-0.6 , -0.4)
NM_021996	globoside alpha-1,3-N-acetylgalactosaminyltransferase 1 (GBGT1), mRNA	-0.5	(-0.7 , -0.3)
NM_173470	transmembrane protein 32 (TMEM32), mRNA	-0.49	(-0.7 , -0.3)
NM_007118	triple functional domain (PTPRF interacting) (TRIO), mRNA	-0.49	(-0.6 , -0.4)
NM_000389	cyclin-dependent kinase inhibitor 1A (p21, Cip1) (CDKN1A), transcript variant 1, mRNA	-0.49	(-0.6 , -0.4)
NM_001696	ATPase, H+ transporting, lysosomal 31kDa, V1 subunit E isoform 1 (ATP6V1E1), mRNA	-0.49	(-0.7 , -0.3)
NM_019063	echinoderm microtubule associated protein like 4 (EML4), mRNA	-0.49	(-0.6 , -0.4)
NM_007189	ATP-binding cassette, sub-family F (GCN20), member 2 (ABCF2), nuclear gene encoding mit	-0.48	(-0.6 , -0.3)
NM_178155	fucosyltransferase 8 (alpha (1,6) fucosyltransferase) (FUT8), transcript variant 1, mRNA	-0.48	(-0.6 , -0.4)
NM_018428	hepatocellular carcinoma-associated antigen 66 (HCA66), mRNA	-0.48	(-0.6 , -0.4)
NM_015922	NAD(P) dependent steroid dehydrogenase-like (NSDHL), mRNA	-0.48	(-0.6 , -0.4)
NM_020440	prostaglandin F2 receptor negative regulator (PTGFRN), mRNA	-0.48	(-0.7 , -0.3)
NM_033291	midline 1 (Opitz/BBB syndrome) (MID1), transcript variant 2, mRNA	-0.48	(-0.6 , -0.4)
NM_032985	Sec23 homolog B (S. cerevisiae) (SEC23B), transcript variant 2, mRNA	-0.48	(-0.5 , -0.5)
NM_145690	tyrosine 3-monooxygenase/tryptophan 5-monooxygenase activation protein, zeta polypeptide	-0.48	(-0.6 , -0.4)
NM_005225	E2F transcription factor 1 (E2F1), mRNA	-0.48	(-0.7 , -0.3)
NM_005665	ecotropic viral integration site 5 (EVI5), mRNA	-0.48	(-0.7 , -0.3)
NM_198244	eukaryotic translation initiation factor 4 gamma, 1 (EIF4G1), transcript variant 3, mRNA	-0.48	(-0.7 , -0.3)
NM_016320	nucleoporin 98kDa (NUP98), transcript variant 1, mRNA	-0.48	(-0.6 , -0.4)
NM_207113	solute carrier family 37 (glycerol-3-phosphate transporter), member 3 (SLC37A3), transcript va	-0.48	(-0.7 , -0.3)
NM_015214	DDHD domain containing 2 (DDHD2), mRNA	-0.47	(-0.6 , -0.3)
NM_012289	kelch-like ECH-associated protein 1 (KEAP1), transcript variant 2, mRNA	-0.47	(-0.6 , -0.3)
NM_017859	uridine-cytidine kinase 1-like 1 (UCKL1), mRNA	-0.47	(-0.6 , -0.4)
NM_001933	dihydrolipoamide S-succinyltransferase (E2 component of 2-oxo-glutarate complex) (DLST), m	-0.47	(-0.6 , -0.3)
NM_002073	guanine nucleotide binding protein (G protein), alpha z polypeptide (GNAZ), mRNA	-0.47	(-0.6 , -0.4)
NM_005552	kinesin 2 60/70kDa (KNS2), mRNA	-0.47	(-0.6 , -0.4)
NM_003139	signal recognition particle receptor ('docking protein') (SRPR), mRNA	-0.47	(-0.6 , -0.3)
NM_007174	citron (rho-interacting, serine/threonine kinase 21) (CIT), mRNA	-0.46	(-0.6 , -0.4)
NM_177926	CSRP2 binding protein (CSRP2BP), transcript variant 2, mRNA	-0.46	(-0.6 , -0.3)
NM_005467	N-acetylated alpha-linked acidic dipeptidase 2 (NAALAD2), mRNA	-0.46	(-0.6 , -0.3)
NM_030782	cisplatin resistance related protein CRR9p (CRR9), mRNA	-0.46	(-0.6 , -0.3)
NM_006231	polymerase (DNA directed), epsilon (POLE), mRNA	-0.46	(-0.5 , -0.4)

NM_006947	signal recognition particle 72kDa (SRP72), mRNA	-0.46	(	-0.6	,	-0.3)
NM_025154	unc-84 homolog A (C. elegans) (UNC84A), mRNA	-0.46	(	-0.6	,	-0.3)
BC016365	transmembrane emp24 protein transport domain containing 5	-0.46	(	-0.6	,	-0.4)
NM_015120	Alstrom syndrome 1 (ALMS1), mRNA	-0.45	(	-0.6	,	-0.3)
NM_182751	MCM10 minichromosome maintenance deficient 10 (S. cerevisiae) (MCM10), transcript varian	-0.45	(	-0.5	,	-0.5)
NM_018383	WD repeat domain 33 (WDR33), transcript variant 1, mRNA	-0.45	(	-0.5	,	-0.4)
NM_182643	deleted in liver cancer 1 (DLC1), transcript variant 1, mRNA	-0.45	(	-0.5	,	-0.4)
NM_004461	phenylalanine-tRNA synthetase-like, alpha subunit (FARSLA), mRNA	-0.45	(	-0.5	,	-0.4)
NM_001969	eukaryotic translation initiation factor 5 (EIF5), transcript variant 1, mRNA	-0.44	(	-0.6	,	-0.3)
NM_015635	DKFZP434C212 protein (DKFZP434C212), mRNA	-0.44	(	-0.5	,	-0.4)
NM_001809	centromere protein A, 17kDa (CENPA), mRNA	-0.44	(	-0.5	,	-0.4)
NM_006145	DnaJ (Hsp40) homolog, subfamily B, member 1 (DNAJB1), mRNA	-0.44	(	-0.5	,	-0.4)
NM_014949	KIAA0907 protein (KIAA0907), mRNA	-0.44	(	-0.5	,	-0.3)
NM_003938	adaptor-related protein complex 3, delta 1 subunit (AP3D1), mRNA	-0.43	(	-0.6	,	-0.3)
NM_013402	fatty acid desaturase 1 (FADS1), mRNA	-0.43	(	-0.5	,	-0.4)
NM_007190	SEC23 interacting protein (SEC23IP), mRNA	-0.43	(	-0.5	,	-0.3)
NM_003185	TAF4 RNA polymerase II, TATA box binding protein (TBP)-associated factor, 135kDa (TAF4),	-0.43	(	-0.5	,	-0.4)
NM_003716	Ca2+-dependent secretion activator (CADPS), transcript variant 1, mRNA	-0.43	(	-0.5	,	-0.4)
NM_006310	aminopeptidase puromycin sensitive (NPEPPS), mRNA	-0.43	(	-0.5	,	-0.3)
NM_021259	transmembrane protein 8 (five membrane-spanning domains) (TMEM8), mRNA	-0.43	(	-0.5	,	-0.4)
NM_198896	RAB6A, member RAS oncogene family (RAB6A), transcript variant 2, mRNA	-0.42	(	-0.5	,	-0.4)
NM_006990	WAS protein family, member 2 (WASF2), mRNA	-0.42	(	-0.5	,	-0.4)
NM_020728	chr2 synaptotagmin (CHR2SYT), mRNA	-0.41	(	-0.5	,	-0.4)
NM_017801	chemokine-like factor super family 6 (CKLFSF6), mRNA	-0.4	(	-0.5	,	-0.4)
NM_018206	vacuolar protein sorting 35 (yeast) (VPS35), mRNA	-0.4	(	-0.4	,	-0.4)

##

References

Abe, T., Takahashi, H., Hamazaki, H., Miyano-Kurosaki, N., Matsuura, Y. & Takaku, H. (2003). Baculovirus induces an innate immune response and confers protection from lethal influenza virus infection in mice. *J Immunol* **171**, 1133-1139.

Abramovitch, R., Tavor, E., Jacob-Hirsch, J., Zeira, E., Amariglio, N., Pappo, O., Rechavi, G., Galun, E. & Honigman, A. (2004). A pivotal role of cyclic AMP-responsive element binding protein in tumor progression. *Cancer Res* **64**, 1338-1346.

Abrams, C. C., Chapman, D. A., Silk, R., Liverani, E. & Dixon, L. K. (2008). Domains involved in calcineurin phosphatase inhibition and nuclear localisation in the African swine fever virus A238L protein. *Virology* **374**, 477-486.

Acuto, O. & Cantrell, D. (2000). T cell activation and the cytoskeleton. *Annu Rev Immunol* **18**, 165-184.

Afonso, C. L., Piccone, M. E., Zaffuto, K. M., Neilan, J., Kutish, G. F., Lu, Z., Balinsky, C. A., Gibb, T. R., Bean, T. J., Zsak, L. & Rock, D. L. (2004). African swine fever virus multigene family 360 and 530 genes affect host interferon response. *J Virol* **78**, 1858-1864.

Alejo, A., Andres, G. & Salas, M. L. (2003). African Swine Fever virus proteinase is essential for core maturation and infectivity. *J Virol* **77**, 5571-5577.

Alfonso, P., Quetglas, J. I., Escribano, J. M. & Alonso, C. (2007). Protein pE120R of African swine fever virus is post-translationally acetylated as revealed by post-source decay MALDI mass spectrometry. *Virus Genes* **35**, 81-85.

Almazan, F., Rodriguez, J. M., Andres, G., Perez, R., Vinuela, E. & Rodriguez, J. F. (1992). Transcriptional analysis of multigene family 110 of African swine fever virus. *J Virol* **66**, 6655-6667.

Andres, G., Garcia-Escudero, R., Simon-Mateo, C. & Vinuela, E. (1998). African swine fever virus is enveloped by a two-membraned collapsed cisterna derived from the endoplasmic reticulum. *J Virol* **72**, 8988-9001.

Andres, G., Simon-Mateo, C. & Vinuela, E. (1997). Assembly of African swine fever virus: role of polyprotein pp220. *J Virol* **71**, 2331-2341.

Aramburu, J., Garcia-Cozar, F., Raghavan, A., Okamura, H., Rao, A. & Hogan, P. G. (1998). Selective inhibition of NFAT activation by a peptide spanning the calcineurin targeting site of NFAT. *Mol Cell* **1**, 627-637.

Aramburu, J., Yaffe, M. B., Lopez-Rodriguez, C., Cantley, L. C., Hogan, P. G. & Rao, A. (1999). Affinity-driven peptide selection of an NFAT inhibitor more selective than cyclosporin A. *Science* **285**, 2129-2133.

Baeuerle, P. A. (1998). IkappaB-NF-kappaB structures: at the interface of inflammation control. *Cell* **95**, 729-731.

Baichwal, V. R. & Baeuerle, P. A. (1997). Activate NF-kappa B or die? *Curr Biol* **7**, R94-96.

Bantignies, F., Goodman, R. H. & Smolik, S. M. (2002). The interaction between the coactivator dCBP and Modulo, a chromatin-associated factor, affects

segmentation and melanotic tumor formation in Drosophila. *Proc Natl Acad Sci U S A* **99**, 2895-2900.

Berrebi, D., Bruscoli, S., Cohen, N., Foussat, A., Migliorati, G., Bouchet-Delbos, L., Maillot, M. C., Portier, A., Couderc, J., Galanaud, P., Peuchmaur, M., Riccardi, C. & Emilie, D. (2003). Synthesis of glucocorticoid-induced leucine zipper (GILZ) by macrophages: an anti-inflammatory and immunosuppressive mechanism shared by glucocorticoids and IL-10. *Blood* **101**, 729-738.

Bernet J, Mullick J, Singh AK & Sahu A.(2003). Viral mimicry of the complement system. J Biosci.**28**, 49-64. **Bjorkbacka, H., Fitzgerald, K. A., Huet, F., Li, X., Gregory, J. A., Lee, M. A., Ordija, C. M., Dowley, N. E., Golenbock, D. T. & Freeman, M. W. (2004).** The induction of macrophage gene expression by LPS predominantly utilizes Myd88-independent signaling cascades. *Physiol Genomics* **19**, 319-330.

Boinas, F. S., Hutchings, G. H., Dixon, L. K. & Wilkinson, P. J. (2004). Characterization of pathogenic and non-pathogenic African swine fever virus isolates from Ornithodoros erraticus inhabiting pig premises in Portugal. *J Gen Virol* **85**, 2177-2187.

Bork, P., (1993). Hundreds of ankyrin-like repeats in functionally diverse proteins: mobile modules that cross phyla horizontally? *Proteins* **17**(4): 363-74.

Boldrick, J. C., Alizadeh, A. A., Diehn, M., Dudoit, S., Liu, C. L., Belcher, C. E., Botstein, D., Staudt, L. M., Brown, P. O. & Relman, D. A. (2002). Stereotyped and specific gene expression programs in human innate immune responses to bacteria. *Proc Natl Acad Sci U S A* **99**, 972-977.

Borca, M. V., Carrillo, C., Zsak, L., Laegreid, W. W., Kutish, G. F., Neilan, J. G., Burrage, T. G. & Rock, D. L. (1998). Deletion of a CD2-like gene, 8-DR, from African swine fever virus affects viral infection in domestic swine. *J Virol* **72**, 2881-2889.

Borca, M. V., Kutish, G. F., Afonso, C. L., Irusta, P., Carrillo, C., Brun, A., Sussman, M. & Rock, D. L. (1994). An African swine fever virus gene with similarity to the T-lymphocyte surface antigen CD2 mediates hemadsorption. *Virology* **199**, 463-468.

Bouillet, P. & Strasser, A. (2002). Bax and Bak: back-bone of T cell death. *Nat Immunol* **3**, 893-894.

Bowick, G. (2004). Mechanism of Action of A238L: An Immune evasion protein of African Swine Fever. In *School of biomedical and life sciences*: University of Surrey.

Brookes, S. M., Dixon, L. K. & Parkhouse, R. M. (1996). Assembly of African Swine fever virus: quantitative ultrastructural analysis in vitro and in vivo. *Virology* **224**, 84-92.

Brun, A., Rivas, C., Esteban, M., Escribano, J. M. & Alonso, C. (1996). African swine fever virus gene A179L, a viral homologue of bcl-2, protects cells from programmed cell death. *Virology* **225**, 227-230.

Buchman, A. R. & Berg, P. (1988). Comparison of intron-dependent and intron-independent gene expression. *Mol Cell Biol* **8**, 4395-4405.

Buck, M., Burgess, A., Stirzaker, R., Krauer, K. & Sculley, T. (2006). Epstein-Barr virus nuclear antigen 3A contains six nuclear-localization signals. *J Gen Virol* **87**, 2879-2884.

Burke B, L. C., (ed) (2002). *The Macrophage*: Oxford University Press.

Burrage, T. G., Lu, Z., Neilan, J. G., Rock, D. L. & Zsak, L. (2004). African swine fever virus multigene family 360 genes affect virus replication and generalization of infection in Ornithodoros porcinus ticks. *J Virol* **78**, 2445-2453.

Callendret, B., Lorin, V., Charneau, P., Marianneau, P., Contamin, H., Betton, J. M., van der Werf, S. & Escriou, N. (2007). Heterologous viral RNA export elements improve expression of severe acute respiratory syndrome (SARS) coronavirus spike protein and protective efficacy of DNA vaccines against SARS. *Virology* **363**, 288-302.

Calvano, S. E., Xiao, W., Richards, D. R., Felciano, R. M., Baker, H. V., Cho, R. J., Chen, R. O., Brownstein, B. H., Cobb, J. P., Tschoeke, S. K., Miller-Graziano, C., Moldawer, L. L., Mindrinos, M. N., Davis, R. W., Tompkins, R. G. & Lowry, S. F. (2005). A network-based analysis of systemic inflammation in humans. *Nature* **437**, 1032-1037.

Camus-Bouclainville, C., Fiette, L., Bouchiha, S., Pignolet, B., Counor, D., Filipe, C., Gelfi, J. & Messud-Petit, F. (2004). A virulence factor of myxoma virus colocalizes with NF-kappaB in the nucleus and interferes with inflammation. *J Virol* **78**, 2510-2516.

Carlotti, F., Dower, S. K. & Qwarnstrom, E. E. (2000). Dynamic shuttling of nuclear factor kappa B between the nucleus and cytoplasm as a consequence of inhibitor dissociation. *J Biol Chem* **275**, 41028-41034.

Carrasco, L., Nunez, A., Salguero, F. J., Diaz San Segundo, F., Sanchez-Cordon, P., Gomez-Villamandos, J. C. & Sierra, M. A. (2002). African swine fever: Expression of interleukin-1 alpha and tumour necrosis factor-alpha by pulmonary intravascular macrophages. *J Comp Pathol* **126**, 194-201.

Carrascosa, J. L., Carazo, J. M., Carrascosa, A. L., Garcia, N., Santisteban, A. & Vinuela, E. (1984). General morphology and capsid fine structure of African swine fever virus particles. *Virology* **132**, 160-172.

Carrillo, C., Borca, M. V., Afonso, C. L., Onisk, D. V. & Rock, D. L. (1994). Long-term persistent infection of swine monocytes/macrophages with African swine fever virus. *J Virol* **68**, 580-583.

Chacon, M. R., Almazan, F., Nogal, M. L., Vinuela, E. & Rodriguez, J. F. (1995). The African swine fever virus IAP homolog is a late structural polypeptide. *Virology* **214**, 670-674.

Chakravarti, D., LaMorte, V. J., Nelson, M. C., Nakajima, T., Schulman, I. G., Juguilon, H., Montminy, M. & Evans, R. M. (1996). Role of CBP/P300 in nuclear receptor signalling. *Nature* **383**, 99-103.

Chakravarti, D., Ogryzko, V., Kao, H. Y., Nash, A., Chen, H., Nakatani, Y. & Evans, R. M. (1999). A viral mechanism for inhibition of p300 and PCAF acetyltransferase activity. *Cell* **96**, 393-403.

Chan, H. M. & La Thangue, N. B. (2001). p300/CBP proteins: HATs for transcriptional bridges and scaffolds. *J Cell Sci* **114**, 2363-2373.

Chapman, D. A., Tcherepanov, V., Upton, C. & Dixon, L. K. (2008). Comparison of the genome sequences of non-pathogenic and pathogenic African swine fever virus isolates. *J Gen Virol* **89**, 397-408.

Chawla, S., Hardingham, G. E., Quinn, D. R. & Bading, H. (1998). CBP: a signal-regulated transcriptional coactivator controlled by nuclear calcium and CaM kinase IV. *Science* **281**, 1505-1509.

Chen, F., Lu, Y., Zhang, Z., Vallyathan, V., Ding, M., Castranova, V. & Shi, X. (2001a). Opposite effect of NF-kappa B and c-Jun N-terminal kinase on p53-independent GADD45 induction by arsenite. *J Biol Chem* **276**, 11414-11419.

Chen, L., Fischle, W., Verdin, E. & Greene, W. C. (2001b). Duration of nuclear NF-kappaB action regulated by reversible acetylation. *Science* **293**, 1653-1657.

Chen, L. F. & Greene, W. C. (2004). Shaping the nuclear action of NF-kappaB. *Nat Rev Mol Cell Biol* **5**, 392-401.

Chen, L. F., Mu, Y. & Greene, W. C. (2002). Acetylation of RelA at discrete sites regulates distinct nuclear functions of NF-kappaB. *EMBO J* **21**, 6539-6548.

Chung KM, Liszewski MK, Nybakken G, Davis AE, Townsend RR, Fremont DH, Atkinson JP & Diamond MS. (2006). West Nile virus nonstructural protein NS1 inhibits complement activation by binding the regulatory protein factor H. Proc Natl Acad Sci U S A. **103**, 19111-6.

Consortium, G. O. (2006). The Gene Ontology (GO) project in 2006. *Nucleic Acids Res* **34**, D322-326.

Crabtree, G. R. & Olson, E. N. (2002). NFAT signaling: choreographing the social lives of cells. *Cell* **109 Suppl**, S67-79.

Dennis, G., Jr., Sherman, B. T., Hosack, D. A., Yang, J., Gao, W., Lane, H. C. & Lempicki, R. A. (2003). DAVID: Database for Annotation, Visualization, and Integrated Discovery. *Genome Biol* **4**, P3.

Der, S. D., Zhou, A., Williams, B. R. & Silverman, R. H. (1998). Identification of genes differentially regulated by interferon alpha, beta, or gamma using oligonucleotide arrays. *Proc Natl Acad Sci U S A* **95**, 15623-15628.

Dixon, L. (2005). Part Three: The viruses family Asfarviridae. In *Virus Taxonomy: Eighth report of the International committee on Taxonomy of Viruses*. Edited by A. Press: In Press.

Dixon, L. & Chapman, D. (2008). African Swine Fever Virus. In *Encyclopidia of Virology*, pp. 43-51. Edited by M. B. W. J. a. V. R. M.H.V.: Oxford: Elisveir.

Dixon, L. K., Abrams, C. C., Bowick, G., Goatley, L. C., Kay-Jackson, P. C., Chapman, D., Liverani, E., Nix, R., Silk, R. & Zhang, F. (2004). African swine fever virus proteins involved in evading host defence systems. *Vet Immunol Immunopathol* **100**, 117-134.

Dixon, L. K. & Wilkinson, P. J. (1988). Genetic diversity of African swine fever virus isolates from soft ticks (Ornithodoros moubata) inhabiting warthog burrows in Zambia. *J Gen Virol* **69 (Pt 12)**, 2981-2993.

Dong, C., Davis, R. J. & Flavell, R. A. (2002). MAP kinases in the immune response. *Annu Rev Immunol* **20**, 55-72.

Earnshaw, W. C., Martins, L. M. & Kaufmann, S. H. (1999). Mammalian caspases: structure, activation, substrates, and functions during apoptosis. *Annu Rev Biochem* **68**, 383-424.

Eckner, R., Ludlow, J. W., Lill, N. L., Oldread, E., Arany, Z., Modjtahedi, N., DeCaprio, J. A., Livingston, D. M. & Morgan, J. A. (1996). Association of p300 and CBP with simian virus 40 large T antigen. *Mol Cell Biol* **16**, 3454-3464.

Ekerot, M., Stavridis, M. P., Delavaine, L., Mitchell, M. P., Staples, C., Owens, D. M., Keenan, I. D., Dickinson, R. J., Storey, K. G. & Keyse, S. M. (2008). Negative-feedback regulation of FGF signalling by DUSP6/MKP-3 is driven by ERK1/2 and mediated by Ets factor binding to a conserved site within the DUSP6/MKP-3 gene promoter. *Biochem J* **412**, 287-298.

Enjuanes, L., Carrascosa, A. L., Moreno, M. A. & Vinuela, E. (1976). Titration of African swine fever (ASF) virus. *J Gen Virol* **32**, 471-477.

Ernst, P. & Smale, S. T. (1995). Combinatorial regulation of transcription. I: General aspects of transcriptional control. *Immunity* **2**, 311-319.

Esparza, I., Gonzalez, J. C. & Vinuela, E. (1988). Effect of interferon-alpha, interferon-gamma and tumour necrosis factor on African swine fever virus replication in porcine monocytes and macrophages. *J Gen Virol* **69 (Pt 12)**, 2973-2980.

Eulalio, A., Nunes-Correia, I., Carvalho, A. L., Faro, C., Citovsky, V., Salas, J., Salas, M. L., Simoes, S. & de Lima, M. C. (2006). Nuclear export of African swine fever virus p37 protein occurs through two distinct pathways and is mediated by three independent signals. *J Virol* **80**, 1393-1404.

Favoreel HW, Van de Walle GR, Nauwynck HJ & Pensaert MB. (2003). Virus complement evasion strategies. J Gen Virol. **84**(Pt 1), 1-15.

Feldmann, H., Volchkov, V. E., Volchkova, V. A. & Klenk, H. D. (1999). The glycoproteins of Marburg and Ebola virus and their potential roles in pathogenesis. *Arch Virol Suppl* **15**, 159-169.

Feske, S., Giltnane, J., Dolmetsch, R., Staudt, L. M. & Rao, A. (2001). Gene regulation mediated by calcium signals in T lymphocytes. *Nat Immunol* **2**, 316-324.

Foletta, V. C., Segal, D. H. & Cohen, D. R. (1998). Transcriptional regulation in the immune system: all roads lead to AP-1. *J Leukoc Biol* **63**, 139-152.

Furst, R., Zahler, S. & Vollmar, A. M. (2008). Dexamethasone-induced expression of endothelial MKP-1 involves activation of the transcription factors AP-1 and CREB and the generation of ROS. *Endocrinology*.

Galindo, I., Hernaez, B., Diaz-Gil, G., Escribano, J. M. & Alonso, C. (2008). A179L, a viral Bcl-2 homologue, targets the core Bcl-2 apoptotic machinery and its upstream BH3 activators with selective binding restrictions for Bid and Noxa. *Virology* **375**, 561-572.

Garcia-Rodriguez, C. & Rao, A. (1998). Nuclear factor of activated T cells (NFAT)-dependent transactivation regulated by the coactivators p300/CREB-binding protein (CBP). *J Exp Med* **187**, 2031-2036.

Garg, S., Oran, A. E., Hon, H. & Jacob, J. (2004). The hybrid cytomegalovirus enhancer/chicken beta-actin promoter along with woodchuck hepatitis virus posttranscriptional regulatory element enhances the protective efficacy of DNA vaccines. *J Immunol* **173**, 550-558.

Geiger, T. R., Sharma, N., Kim, Y. M. & Nyborg, J. K. (2008). The human T-cell leukemia virus type 1 tax protein confers CBP/p300 recruitment and transcriptional activation properties to phosphorylated CREB. *Mol Cell Biol* **28**, 1383-1392.

Geisbert, T. W., Hensley, L. E., Gibb, T. R., Steele, K. E., Jaax, N. K. & Jahrling, P. B. (2000). Apoptosis induced in vitro and in vivo during infection by Ebola and Marburg viruses. *Lab Invest* **80**, 171-186.

Ghosh, S. & Karin, M. (2002). Missing pieces in the NF-kappaB puzzle. *Cell* **109 Suppl**, S81-96.

Ghosh, S., May, M. J. & Kopp, E. B. (1998). NF-kappa B and Rel proteins: evolutionarily conserved mediators of immune responses. *Annu Rev Immunol* **16**, 225-260.

Goatley, L. C., Twigg, S. R., Miskin, J. E., Monaghan, P., St-Arnaud, R., Smith, G. L. & Dixon, L. K. (2002). The African swine fever virus protein j4R binds to the alpha chain of nascent polypeptide-associated complex. *J Virol* **76**, 9991-9999.

Gomez del Moral, M., Ortuno, E., Fernandez-Zapatero, P., Alonso, F., Alonso, C., Ezquerra, A. & Dominguez, J. (1999). African swine fever virus infection induces tumor necrosis factor alpha production: implications in pathogenesis. *J Virol* **73**, 2173-2180.

Gonzalez, A., Talavera, A., Almendral, J. M. & Vinuela, E. (1986). Hairpin loop structure of African swine fever virus DNA. *Nucleic Acids Res* **14**, 6835-6844.

Goodman, R. H. & Smolik, S. (2000). CBP/p300 in cell growth, transformation, and development. *Genes Dev* **14**, 1553-1577.

Granja, A. G., Nogal, M. L., Hurtado, C., Del Aguila, C., Carrascosa, A. L., Salas, M. L., Fresno, M. & Revilla, Y. (2006a). The viral protein A238L inhibits TNF-alpha expression through a CBP/p300 transcriptional coactivators pathway. *J Immunol* **176**, 451-462.

Granja, A. G., Nogal, M. L., Hurtado, C., Vila, V., Carrascosa, A. L., Salas, M. L., Fresno, M. & Revilla, Y. (2004a). The viral protein A238L inhibits cyclooxygenase-2 expression through a nuclear factor of activated T cell-dependent transactivation pathway. *J Biol Chem* **279**, 53736-53746.

Granja, A. G., Perkins, N. D. & Revilla, Y. (2008). A238L inhibits NF-ATc2, NF-kappa B, and c-Jun activation through a novel mechanism involving protein kinase C-theta-mediated up-regulation of the amino-terminal transactivation domain of p300. *J Immunol* **180**, 2429-2442.

Granja, A. G., Sabina, P., Salas, M. L., Fresno, M. & Revilla, Y. (2006b). Regulation of inducible nitric oxide synthase expression by viral A238L-mediated inhibition of p65/RelA acetylation and p300 transactivation. *J Virol* **80**, 10487-10496.

Gronowski, A. M., Hilbert, D. M., Sheehan, K. C., Garotta, G. & Schreiber, R. D. (1999). Baculovirus stimulates antiviral effects in mammalian cells. *J Virol* **73**, 9944-9951.

Gruter, P., Tabernero, C., von Kobbe, C., Schmitt, C., Saavedra, C., Bachi, A., Wilm, M., Felber, B. K. & Izaurralde, E. (1998). TAP, the human homolog of Mex67p, mediates CTE-dependent RNA export from the nucleus. *Mol Cell* **1**, 649-659.

Guha, M. & Mackman, N. (2001). LPS induction of gene expression in human monocytes. *Cell Signal* **13**, 85-94.

Hamdy, F. M. & Dardiri, A. H. (1984). Clinical and immunologic responses of pigs to African swine fever virus isolated from the Western Hemisphere. *Am J Vet Res* **45**, 711-714.

Harhaj, E. W. & Sun, S. C. (1999). Regulation of RelA subcellular localization by a putative nuclear export signal and p50. *Mol Cell Biol* **19**, 7088-7095.

Harris, M. A., Clark, J., Ireland, A., Lomax, J., Ashburner, M., Foulger, R., Eilbeck, K., Lewis, S., Marshall, B., Mungall, C., Richter, J., Rubin, G. M., Blake, J. A., Bult, C., Dolan, M., Drabkin, H., Eppig, J. T., Hill, D. P., Ni, L., Ringwald, M., Balakrishnan, R., Cherry, J. M., Christie, K. R., Costanzo, M. C., Dwight, S. S., Engel, S., Fisk, D. G., Hirschman, J. E., Hong, E. L., Nash, R. S., Sethuraman, A., Theesfeld, C. L., Botstein, D., Dolinski, K., Feierbach, B., Berardini, T., Mundodi, S., Rhee, S. Y., Apweiler, R., Barrell, D., Camon, E., Dimmer, E., Lee, V., Chisholm, R., Gaudet, P., Kibbe, W., Kishore, R., Schwarz, E. M., Sternberg, P., Gwinn, M., Hannick, L., Wortman, J., Berriman, M., Wood, V., de la Cruz, N., Tonellato, P., Jaiswal, P., Seigfried, T. & White, R. (2004). The Gene Ontology (GO) database and informatics resource. *Nucleic Acids Res* **32**, D258-261.

Heath, C. M., Windsor, M. & Wileman, T. (2001). Aggresomes resemble sites specialized for virus assembly. *J Cell Biol* **153**, 449-455.

Hegde, N. R., Tomazin, R. A., Wisner, T. W., Dunn, C., Boname, J. M., Lewinsohn, D. M., Johnson, D. C. (2002). Inhibition of HLA-DR assembly, transport, and loading by human cytomegalovirus glycoprotein US3: a novel mechanism for evading major histocompatibility complex class II antigen presentation *J. Virol.* **76**,10929-10941.

Hess, W. R. (1981). African swine fever - a reassessment. *Adv Vet Sci Comp Med* **25**, 39-69.

Hewitt EW, Gupta SS & Lehner PJ. (2001). The human cytomegalovirus gene product US6 inhibits ATP binding by TAP. EMBO J **20**:387-396.

Horton, P., Park, K.J., Obayashi, T. and Nakai, K. (2006). Protein Subcellular localisation prediction with WoLF PSORT. In *Proceedings of the 4th Annual Asia Pacific bioinformatics conference APBC06*, pp. 39-48. Taipei, Taiwan.

Hosack, D. A., Dennis, G., Jr., Sherman, B. T., Lane, H. C. & Lempicki, R. A. (2003). Identifying biological themes within lists of genes with EASE. *Genome Biol* **4**, R70.

Huang, T. T., Kudo, N., Yoshida, M. & Miyamoto, S. (2000). A nuclear export signal in the N-terminal regulatory domain of IkappaBalpha controls cytoplasmic localization of inactive NF-kappaB/IkappaBalpha complexes. *Proc Natl Acad Sci U S A* **97**, 1014-1019.

Huang, W. C., Ju, T. K., Hung, M. C. & Chen, C. C. (2007). Phosphorylation of CBP by IKKalpha promotes cell growth by switching the binding preference of CBP from p53 to NF-kappaB. *Mol Cell* **26**, 75-87.

Iyer, L. M., L. Aravind, et al. (2001). Common origin of four diverse families of large eukaryotic DNA viruses. *J Virol* **75**(23): 11720-34.

Iyer, L. M., S. Balaji, et al. (2006). Evolutionary genomics of nucleo-cytoplasmic large DNA viruses. *Virus Res* **117**(1): 156-84.

Janknecht, R. & Hunter, T. (1996). Transcription. A growing coactivator network. *Nature* **383**, 22-23.

Janknecht, R. & Hunter, T. (1997). Convergence of MAP kinase pathways on the ternary complex factor Sap-1a. *EMBO J* **16**, 1620-1627.

Johnston JB & McFadden G. (2003). Poxvirus immunomodulatory strategies: current perspectives. J Virol. **77**, 6093-100.

Jouvenet, N., Monaghan, P., Way, M. & Wileman, T. (2004). Transport of African swine fever virus from assembly sites to the plasma membrane is dependent on microtubules and conventional kinesin. *J Virol* **78**, 7990-8001.

Jouvenet, N., Windsor, M., Rietdorf, J., Hawes, P., Monaghan, P., Way, M. & Wileman, T. (2006). African swine fever virus induces filopodia-like projections at the plasma membrane. *Cell Microbiol* **8**, 1803-1811.

Kanehisa, M., Araki, M., Goto, S., Hattori, M., Hirakawa, M., Itoh, M., Katayama, T., Kawashima, S., Okuda, S., Tokimatsu, T. & Yamanishi, Y. (2008). KEGG for linking genomes to life and the environment. *Nucleic Acids Res* **36**, D480-484.

Karin, M. (1995). The regulation of AP-1 activity by mitogen-activated protein kinases. *J Biol Chem* **270**, 16483-16486.

Karin, M. & Ben-Neriah, Y. (2000). Phosphorylation meets ubiquitination: the control of NF-[kappa]B activity. *Annu Rev Immunol* **18**, 621-663.

Kim, T. K., Lee, J. S., Oh, S. Y., Jin, X., Choi, Y. J., Lee, T. H., Lee, E., Choi, Y. K., You, S., Chung, Y. G., Lee, J. B., DePinho, R. A., Chin, L. & Kim, H. (2007). Direct transcriptional activation of promyelocytic leukemia protein by IFN regulatory factor 3 induces the p53-dependent growth inhibition of cancer cells. *Cancer Res* **67**, 11133-11140.

Kim, Y., Moon, J. S., Lee, K. S., Park, S. Y., Cheong, J., Kang, H. S., Lee, H. Y. & Kim, H. D. (2004). Ca2+/calmodulin-dependent protein phosphatase calcineurin mediates the expression of iNOS through IKK and NF-kappaB activity in LPS-stimulated mouse peritoneal macrophages and RAW 264.7 cells. *Biochem Biophys Res Commun* **314**, 695-703.

Kissinger, C. R., Parge, H. E., Knighton, D. R., Lewis, C. T., Pelletier, L. A., Tempczyk, A., Kalish, V. J., Tucker, K. D., Showalter, R. E., Moomaw, E. W. & et al. (1995). Crystal structures of human calcineurin and the human FKBP12-FK506-calcineurin complex. *Nature* **378**, 641-644.

Kitts, P. A. & Possee, R. D. (1993). A method for producing recombinant baculovirus expression vectors at high frequency. *Biotechniques* **14**, 810-817.

Kost, T. A. & Condreay, J. P. (2002). Recombinant baculoviruses as mammalian cell gene-delivery vectors. *Trends Biotechnol* **20**, 173-180.

Kost, T. A., Condreay, J. P. & Jarvis, D. L. (2005). Baculovirus as versatile vectors for protein expression in insect and mammalian cells. *Nat Biotechnol* **23**, 567-575.

Kudo, N., Wolff, B., Sekimoto, T., Schreiner, E. P., Yoneda, Y., Yanagida, M., Horinouchi, S. & Yoshida, M. (1998). Leptomycin B inhibition of signal-mediated nuclear export by direct binding to CRM1. *Exp Cell Res* **242**, 540-547.

Le Hir, H., Nott, A. & Moore, M. J. (2003). How introns influence and enhance eukaryotic gene expression. *Trends Biochem Sci* **28**, 215-220.

Legembre, P., Schickel, R., Barnhart, B. C. & Peter, M. E. (2004). Identification of SNF1/AMP kinase-related kinase as an NF-kappaB-regulated anti-apoptotic kinase involved in CD95-induced motility and invasiveness. *J Biol Chem* **279**, 46742-46747.

Leitao, A., Cartaxeiro, C., Coelho, R., Cruz, B., Parkhouse, R. M., Portugal, F., Vigario, J. D. & Martins, C. L. (2001). The non-haemadsorbing African swine fever virus isolate ASFV/NH/P68 provides a model for defining the protective anti-virus immune response. *J Gen Virol* **82**, 513-523.

Li, J., Mahajan A. & Tsai MD. (2006). Ankyrin repeat: a unique motif mediating protein-protein interactions. *Biochemistry* **45**(51): 15168-78.

Liu, Y. Z., Thomas, N. S. & Latchman, D. S. (1999). CBP associates with the p42/p44 MAPK enzymes and is phosphorylated following NGF treatment. *Neuroreport* **10**, 1239-1243.

Long, G., Pan, X., Kormelink, R. & Vlak, J. M. (2006). Functional entry of baculovirus into insect and mammalian cells is dependent on clathrin-mediated endocytosis. *J Virol* **80**, 8830-8833.

Macian, F., Garcia-Cozar, F., Im, S. H., Horton, H. F., Byrne, M. C. & Rao, A. (2002). Transcriptional mechanisms underlying lymphocyte tolerance. *Cell* **109**, 719-731.

Macian, F., Garcia-Rodriguez, C. & Rao, A. (2000). Gene expression elicited by NFAT in the presence or absence of cooperative recruitment of Fos and Jun. *EMBO J* **19**, 4783-4795.

Mantovani, A., Bussolino, F. and Introna, M. (1997). Cytokine regulation of endothelial cell function: from molecular level to the bedside. *Immunol Today* **18**, 231-240.

Martins, C. L., Lawman, M. J., Scholl, T., Mebus, C. A. & Lunney, J. K. (1993). African swine fever virus specific porcine cytotoxic T cell activity. *Arch Virol* **129**, 211-225.

Martins, C. L., Scholl, T., Mebus, C. A., Fisch, H. & Lawman, M. J. (1987). Modulation of porcine peripheral blood-derived macrophage functions by in vitro infection with African swine fever virus (ASFV) isolates of different virulence. *Viral Immunol* **1**, 177-190.

Miskin, J. E., Abrams, C. C. & Dixon, L. K. (2000). African swine fever virus protein A238L interacts with the cellular phosphatase calcineurin via a binding domain similar to that of NFAT. *J Virol* **74**, 9412-9420.

Miskin, J. E., Abrams, C. C., Goatley, L. C. & Dixon, L. K. (1998). A viral mechanism for inhibition of the cellular phosphatase calcineurin. *Science* **281**, 562-565.

Monaco, C., Andreakos, E., Kiriakidis, S., Mauri, C., Bicknell, C., Foxwell, B., Cheshire, N., Paleolog, E. & Feldmann, M. (2004). Canonical pathway of nuclear factor kappa B activation selectively regulates proinflammatory and prothrombotic responses in human atherosclerosis. *Proc Natl Acad Sci U S A* **101**, 5634-5639.

Montgomery, R. (1921). On a form of swine fever ocuuring in British East Africa (Kenya Colony). *J Comp Pathol* **34**, 159-191.

Moss, B. (2001). *Poxviridae*: The Viruses and Their Replication. In *Fundamental Virology*

4edn, pp. 1249-1284. Edited by D. M. Knipe & P. M. Howley: Lippincott, Williams & Wilkins.

Mossman, K. L., Macgregor, P. F., Rozmus, J. J., Goryachev, A. B., Edwards, A. M. & Smiley, J. R. (2001). Herpes simplex virus triggers and then disarms a host antiviral response. *J Virol* **75**, 750-758.

Motoyama, M., Yamazaki, S., Eto-Kimura, A., Takeshige, K. & Muta, T. (2005). Positive and negative regulation of nuclear factor-kappaB-mediated transcription by IkappaB-zeta, an inducible nuclear protein. *J Biol Chem* **280**, 7444-7451.

Murphy, L. O., Smith, S., Chen, R. H., Fingar, D. C. & Blenis, J. (2002). Molecular interpretation of ERK signal duration by immediate early gene products. *Nat Cell Biol* **4**, 556-564.

Neilan, J. G., Lu, Z., Afonso, C. L., Kutish, G. F., Sussman, M. D. & Rock, D. L. (1993). An African swine fever virus gene with similarity to the proto-oncogene bcl-2 and the Epstein-Barr virus gene BHRF1. *J Virol* **67**, 4391-4394.

Neilan, J. G., Lu, Z., Kutish, G. F., Zsak, L., Lewis, T. L. & Rock, D. L. (1997). A conserved African swine fever virus IkappaB homolog, 5EL, is nonessential for growth in vitro and virulence in domestic swine. *Virology* **235**, 377-385.

Niwa, H., Yamamura, K. & Miyazaki, J. (1991). Efficient selection for high-expression transfectants with a novel eukaryotic vector. *Gene* **108**, 193-199.

Nogal, M. L., Gonzalez de Buitrago, G., Rodriguez, C., Cubelos, B., Carrascosa, A. L., Salas, M. L. & Revilla, Y. (2001). African swine fever virus IAP homologue inhibits caspase activation and promotes cell survival in mammalian cells. *J Virol* **75**, 2535-2543.

Northoff, E. (2007). Georgia severely hit by African Swine Fever. In *FAONewsroom*. www.FAO.org/newsroom/en/news/2007/1000594/index.html.

Nott, A., Meislin, S. H. & Moore, M. J. (2003). A quantitative analysis of intron effects on mammalian gene expression. *RNA* **9**, 607-617.

Oura, C. A., Denyer, M. S., Takamatsu, H. & Parkhouse, R. M. (2005). In vivo depletion of CD8+ T lymphocytes abrogates protective immunity to African swine fever virus. *J Gen Virol* **86**, 2445-2450.

Oura, C. A., Powell, P. P. & Parkhouse, R. M. (1998). African swine fever: a disease characterized by apoptosis. *J Gen Virol* **79 (Pt 6)**, 1427-1438.

Paez, E., Garcia, F. & Gil Fernandez, C. (1990). Interferon cures cells lytically and persistently infected with African swine fever virus in vitro. *Arch Virol* **112**, 115-127.

Papa, S., Monti, S. M., Vitale, R. M., Bubici, C., Jayawardena, S., Alvarez, K., De Smaele, E., Dathan, N., Pedone, C., Ruvo, M. & Franzoso, G. (2007). Insights into the structural basis of the GADD45beta-mediated inactivation of the JNK kinase, MKK7/JNKK2. *J Biol Chem* **282**, 19029-19041.

Park, H. S., Lee, J. S., Huh, S. H., Seo, J. S. & Choi, E. J. (2001). Hsp72 functions as a natural inhibitory protein of c-Jun N-terminal kinase. *EMBO J* **20**, 446-456.

Perez-Sanchez, R., Astigarraga, A., Oleaga-Perez, A. & Encinas-Grandes, A. (1994). Relationship between the persistence of African swine fever and the distribution of Ornithodoros erraticus in the province of Salamanca, Spain *The Veterinary Record* **135**, 207-209.

Petros, A. M., Olejniczak, E. T. & Fesik, S. W. (2004). Structural biology of the Bcl-2 family of proteins. *Biochim Biophys Acta* **1644**, 83-94.

Popa, I., Harris, M. E., Donello, J. E. & Hope, T. J. (2002). CRM1-dependent function of a cis-acting RNA export element. *Mol Cell Biol* **22**, 2057-2067.

Possee, R. D., Sun, T. P., Howard, S. C., Ayres, M. D., Hill-Perkins, M. & Gearing, K. L. (1991). Nucleotide sequence of the Autographa californica nuclear polyhedrosis 9.4 kbp EcoRI-I and -R (polyhedrin gene) region. *Virology* **185**, 229-241.

Powell, P. P., Dixon, L. K. & Parkhouse, R. M. (1996). An IkappaB homolog encoded by African swine fever virus provides a novel mechanism for downregulation of proinflammatory cytokine responses in host macrophages. *J Virol* **70**, 8527-8533.

Rajabi, H. N., Baluchamy, S., Kolli, S., Nag, A., Srinivas, R., Raychaudhuri, P. & Thimmapaya, B. (2005). Effects of depletion of CREB-binding protein on c-Myc regulation and cell cycle G1-S transition. *J Biol Chem* **280**, 361-374.

Rao, A., Luo, C. & Hogan, P. G. (1997). Transcription factors of the NFAT family: regulation and function. *Annu Rev Immunol* **15**, 707-747.

Raoult, D., S. Audic, et al. (2004). The 1.2-megabase genome sequence of Mimivirus. *Science* **306**(5700): 1344-50.

Reed, L. J. & Muench, H. (1938). A Simple Method of Estimating Fifty Per Cent Endpoints. *American Journal of Hygiene* **27**, 493-497.

Reffas, S. & Schlegel, W. (2000). Compartment-specific regulation of extracellular signal-regulated kinase (ERK) and c-Jun N-terminal kinase (JNK) mitogen-activated protein kinases (MAPKs) by ERK-dependent and non-ERK-dependent inductions of MAPK phosphatase (MKP)-3 and MKP-1 in differentiating P19 cells. *Biochem J* **352 Pt 3**, 701-708.

Revilla, Y., Callejo, M., Rodriguez, J. M., Culebras, E., Nogal, M. L., Salas, M. L., Vinuela, E. & Fresno, M. (1998). Inhibition of nuclear factor kappaB activation by a virus-encoded IkappaB-like protein. *J Biol Chem* **273**, 5405-5411.

Rodriguez, J. M., Salas, M. L. & Vinuela, E. (1996). Intermediate class of mRNAs in African swine fever virus. *J Virol* **70**, 8584-8589.

Rodriguez, J. M., Yanez, R. J., Almazan, F., Vinuela, E. & Rodriguez, J. F. (1993). African swine fever virus encodes a CD2 homolog responsible for the adhesion of erythrocytes to infected cells. *J Virol* **67**, 5312-5320.

Rojo, G., Garcia-Beato, R., Vinuela, E., Salas, M. L. & Salas, J. (1999). Replication of African swine fever virus DNA in infected cells. *Virology* **257**, 524-536.

Ruiz Gonzalvo, F., Caballero, C., Martinez, J. & Carnero, M. E. (1986a). Neutralization of African swine fever virus by sera from African swine fever-resistant pigs. *Am J Vet Res* **47**, 1858-1862.

Ruiz Gonzalvo, F., Carnero, M. E., Caballero, C. & Martinez, J. (1986b). Inhibition of African swine fever infection in the presence of immune sera in vivo and in vitro. *Am J Vet Res* **47**, 1249-1252.

Sachdev, S., Hoffmann, A. & Hannink, M. (1998). Nuclear localization of IkappaB alpha is mediated by the second ankyrin repeat: the IkappaB alpha ankyrin repeats define a novel class of cis-acting nuclear import sequences. *Mol Cell Biol* **18**, 2524-2534.

Saeed, A. I., Bhagabati, N. K., Braisted, J. C., Liang, W., Sharov, V., Howe, E. A., Li, J., Thiagarajan, M., White, J. A. & Quackenbush, J. (2006). TM4 microarray software suite. *Methods Enzymol* **411**, 134-193.

Salas, M. J. (1999). African Swine Fever Virus. In *Encyclopedia of Virology*, pp. 30-38. Edited by G. A & W. R.G: Academic Press.

Salguero, F. J., Gil, S., Revilla, Y., Gallardo, C., Arias, M. & Martins, C. (2008). Cytokine mRNA expression and pathological findings in pigs inoculated with African swine fever virus (E-70) deleted on A238L. *Vet Immunol Immunopathol* **124**, 107-119.

Salguero, F. J., Ruiz-Villamor, E., Bautista, M. J., Sanchez-Cordon, P. J., Carrasco, L. & Gomez-Villamandos, J. C. (2002). Changes in macrophages in spleen and lymph nodes during acute African swine fever: expression of cytokines. *Vet Immunol Immunopathol* **90**, 11-22.

Sanchez-Torres, C., Gomez-Puertas, P., Gomez-del-Moral, M., Alonso, F., Escribano, J. M., Ezquerra, A. & Dominguez, J. (2003). Expression of porcine CD163 on monocytes/macrophages correlates with permissiveness to African swine fever infection. *Arch Virol* **148**, 2307-2323.

Sawicki, J. A., Morris, R. J., Monks, B., Sakai, K. & Miyazaki, J. (1998). A composite CMV-IE enhancer/beta-actin promoter is ubiquitously expressed in mouse cutaneous epithelium. *Exp Cell Res* **244**, 367-369.

Schambach, A., Wodrich, H., Hildinger, M., Bohne, J., Krausslich, H. G. & Baum, C. (2000). Context dependence of different modules for posttranscriptional enhancement of gene expression from retroviral vectors. *Mol Ther* **2**, 435-445.

Schreiber, S. L. & Crabtree, G. R. (1992). The mechanism of action of cyclosporin A and FK506. *Immunol Today* **13**, 136-142.

Sherman, M. P., de Noronha, C. M., Heusch, M. I., Greene, S. & Greene, W. C. (2001). Nucleocytoplasmic shuttling by human immunodeficiency virus type 1 Vpr. *J Virol* **75**, 1522-1532.

Shi, Y. (2002). Mechanisms of caspase activation and inhibition during apoptosis. *Mol Cell* **9**, 459-470.

Shibasaki, F., Price, E. R., Milan, D. & McKeon, F. (1996). Role of kinases and the phosphatase calcineurin in the nuclear shuttling of transcription factor NF-AT4. *Nature* **382**, 370-373.

Shoji, I., Aizaki, H., Tani, H., Ishii, K., Chiba, T., Saito, I., Miyamura, T. & Matsuura, Y. (1997). Efficient gene transfer into various mammalian cells, including non-hepatic cells, by baculovirus vectors. *J Gen Virol* **78 (Pt 10)**, 2657-2664.

Silk, R. N., Bowick, G. C., Abrams, C. C. & Dixon, L. K. (2007). African swine fever virus A238L inhibitor of NF-kappaB and of calcineurin phosphatase is imported actively into the nucleus and exported by a CRM1-mediated pathway. *J Gen Virol* **88**, 411-419.

Simmons, A., Aluvihare, V. & McMichael, A. (2001). Nef triggers a transcriptional program in T cells imitating single-signal T cell activation and inducing HIV virulence mediators. *Immunity* **14**, 763-777.

Simon-Mateo, C., Andres, G., Almazan, F. & Vinuela, E. (1997). Proteolytic processing in African swine fever virus: evidence for a new structural polyprotein, pp62. *J Virol* **71**, 5799-5804.

Sogo, J. M., Almendral, J. M., Talavera, A. & Vinuela, E. (1984). Terminal and internal inverted repetitions in African swine fever virus DNA. *Virology* **133**, 271-275.

Stewart, M. (2007). Ratcheting mRNA out of the nucleus. *Mol Cell* **25**, 327-330.

Stiehl, D. P., Fath, D. M., Liang, D., Jiang, Y. & Sang, N. (2007). Histone deacetylase inhibitors synergize p300 autoacetylation that regulates its transactivation activity and complex formation. *Cancer Res* **67**, 2256-2264.

Stoddard, B. L. & Flick, K. E. (1996). Calcineurin-immunosuppressor complexes. *Curr Opin Struct Biol* **6**, 770-775.

Swope, D. L., Mueller, C. L. & Chrivia, J. C. (1996). CREB-binding protein activates transcription through multiple domains. *J Biol Chem* **271**, 28138-28145.

Tait, S. W., Reid, E. B., Greaves, D. R., Wileman, T. E. & Powell, P. P. (2000). Mechanism of inactivation of NF-kappa B by a viral homologue of I kappa b alpha. Signal-induced release of i kappa b alpha results in binding of the viral homologue to NF-kappa B. *J Biol Chem* **275**, 34656-34664.

Takamatsu, H., Denyer, M. S., Oura, C., Childerstone, A., Andersen, J. K., Pullen, L. & Parkhouse, R. M. (1999). African swine fever virus: a B cell-mitogenic virus in vivo and in vitro. *J Gen Virol* **80 (Pt 6)**, 1453-1461.

Teng, C. H., Huang, W. N. & Meng, T. C. (2007). Several dual specificity phosphatases coordinate to control the magnitude and duration of JNK activation in signaling response to oxidative stress. *J Biol Chem* **282**, 28395-28407.

Thomas, M. C. & Chiang, C. M. (2005). E6 oncoprotein represses p53-dependent gene activation via inhibition of protein acetylation independently of inducing p53 degradation. *Mol Cell* **17**, 251-264.

Tournier, C., Dong, C., Turner, T. K., Jones, S. N., Flavell, R. A. & Davis, R. J. (2001). MKK7 is an essential component of the JNK signal transduction pathway activated by proinflammatory cytokines. *Genes Dev* **15**, 1419-1426.

Trushin, S. A., Pennington, K. N., Algeciras-Schimnich, A. & Paya, C. V. (1999). Protein kinase C and calcineurin synergize to activate IkappaB kinase and NF-kappaB in T lymphocytes. *J Biol Chem* **274**, 22923-22931.

Tusher, V. G., Tibshirani, R. & Chu, G. (2001). Significance analysis of microarrays applied to the ionizing radiation response. *Proc Natl Acad Sci U S A* **98**, 5116-5121.

Valdeira, M. L., Bernardes, C., Cruz, B. & Geraldes, A. (1998). Entry of African swine fever virus into Vero cells and uncoating. *Vet Microbiol* **60**, 131-140.

Vo, N. & Goodman, R. H. (2001). CREB-binding protein and p300 in transcriptional regulation. *J Biol Chem* **276**, 13505-13508.

Vossen MT, Westerhout EM, Söderberg-Nauclér C & Wiertz EJ.(2002). Viral immune evasion: a masterpiece of evolution. Immunogenetics. **54**, 527-42.

Wadgaonkar, R., Pierce, J. W., Somnay, K., Damico, R. L., Crow, M. T., Collins, T. & Garcia, J. G. (2004). Regulation of c-Jun N-terminal kinase and p38 kinase pathways in endothelial cells. *Am J Respir Cell Mol Biol* **31**, 423-431.

Wang, C. Y., Mayo, M. W., Korneluk, R. G., Goeddel, D. V. & Baldwin, A. S., Jr. (1998). NF-kappaB antiapoptosis: induction of TRAF1 and TRAF2 and c-IAP1 and c-IAP2 to suppress caspase-8 activation. *Science* **281**, 1680-1683.

Wang, H. G., Pathan, N., Ethell, I. M., Krajewski, S., Yamaguchi, Y., Shibasaki, F., McKeon, F., Bobo, T., Franke, T. F. & Reed, J. C. (1999). Ca2+-induced apoptosis through calcineurin dephosphorylation of BAD. *Science* **284**, 339-343.

Wardley, R. C., Andrade, C. D., Black, D. N., Portugal, F. L. D., Enjuanes, L., Hess, W. R., Mebus, C., Ordas, A., Rutili, D., Vizcaino, J. S., Vigario, J. D., Wilkinson, P. J., Nunes, J. F. M. & Thomson, G. (1983). African swine fever virus. *Arch Virol* **76**, 73-90.

Wardley, R. C., Norley, S. G., Wilkinson, P. J. & Williams, S. (1985). The role of antibody in protection against African swine fever virus. *Vet Immunol Immunopathol* **9**, 201-212.

Warton, K., Foster, N. C., Gold, W. A. & Stanley, K. K. (2004). A novel gene family induced by acute inflammation in endothelial cells. *Gene* **342**, 85-95.

Weil, R., Sirma, H., Giannini, C., Kremsdorf, D., Bessia, C., Dargemont, C., Brechot, C. & Israel, A. (1999). Direct association and nuclear import of the hepatitis B virus X protein with the NF-kappaB inhibitor IkappaBalpha. *Mol Cell Biol* **19**, 6345-6354.

Weingartl, H. M., Sabara, M., Pasick, J., van Moorlehem, E. & Babiuk, L. (2002). Continuous porcine cell lines developed from alveolar macrophages: partial characterization and virus susceptibility. *J Virol Methods* **104**, 203-216.

Werlen, G., Jacinto, E., Xia, Y. & Karin, M. (1998). Calcineurin preferentially synergizes with PKC-theta to activate JNK and IL-2 promoter in T lymphocytes. *EMBO J* **17**, 3101-3111.

Whittall, J. T. & Parkhouse, R. M. (1997). Changes in swine macrophage phenotype after infection with African swine fever virus: cytokine production and responsiveness to interferon-gamma and lipopolysaccharide. *Immunology* **91**, 444-449.

Wilkinson GW, Tomasec P, Stanton RJ, Armstrong M, Prod'homme V, Aicheler R, McSharry BP, Rickards CR, Cochrane D, Llewellyn-Lacey S, Wang EC, Griffin CA & Davison AJ.(2008). Modulation of natural killer cells by human cytomegalovirus. J Clin Virol. **41**(3), 206-12.

Wilkinson, P. J. (1989). African Swine Fever Virus. In *Virus Infections of Porcines*, pp. 17-35. Edited by M. B. Pensaert: Elsevier.

Windheim M, Hilgendorf A & Burgert HG.(2004). Immune evasion by adenovirus E3 proteins: exploitation of intracellular trafficking pathways. Curr Top Microbiol Immunol.**273**, 29-85.

Wodrich, H., Cassany, A., D'Angelo, M. A., Guan, T., Nemerow, G. & Gerace, L. (2006). Adenovirus core protein pVII is translocated into the nucleus by multiple import receptor pathways. *J Virol* **80**, 9608-9618.

Wu, J. J. & Bennett, A. M. (2005). Essential role for mitogen-activated protein (MAP) kinase phosphatase-1 in stress-responsive MAP kinase and cell survival signaling. *J Biol Chem* **280**, 16461-16466.

Wu, W. S., Xu, Z. X., Hittelman, W. N., Salomoni, P., Pandolfi, P. P. & Chang, K. S. (2003). Promyelocytic leukemia protein sensitizes tumor necrosis factor alpha-induced apoptosis by inhibiting the NF-kappaB survival pathway. *J Biol Chem* **278**, 12294-12304.

Xu, W., Chen, H., Du, K., Asahara, H., Tini, M., Emerson, B. M., Montminy, M. & Evans, R. M. (2001). A transcriptional switch mediated by cofactor methylation. *Science* **294**, 2507-2511.

Yaglom, J., O'Callaghan-Sunol, C., Gabai, V. & Sherman, M. Y. (2003). Inactivation of dual-specificity phosphatases is involved in the regulation of extracellular signal-regulated kinases by heat shock and hsp72. *Mol Cell Biol* **23**, 3813-3824.

Yamamoto, M., Yamazaki, S., Uematsu, S., Sato, S., Hemmi, H., Hoshino, K., Kaisho, T., Kuwata, H., Takeuchi, O., Takeshige, K., Saitoh, T., Yamaoka, S., Yamamoto, N., Yamamoto, S., Muta, T., Takeda, K. & Akira, S. (2004). Regulation of Toll/IL-1-receptor-mediated gene expression by the inducible nuclear protein IkappaBzeta. *Nature* **430**, 218-222.

Yamazaki, S., Muta, T. & Takeshige, K. (2001). A novel IkappaB protein, IkappaB-zeta, induced by proinflammatory stimuli, negatively regulates nuclear factor-kappaB in the nuclei. *J Biol Chem* **276**, 27657-27662.

Yanez, R. J., Rodriguez, J. M., Nogal, M. L., Yuste, L., Enriquez, C., Rodriguez, J. F. & Vinuela, E. (1995). Analysis of the complete nucleotide sequence of African swine fever virus. *Virology* **208**, 249-278.

Yeh, P. Y., Kuo, S. H., Yeh, K. H., Chuang, S. E., Hsu, C. H., Chang, W. C., Lin, H. I., Gao, M. & Cheng, A. L. (2006). A pathway for tumor necrosis factor-alpha-induced Bcl10 nuclear translocation. Bcl10 is up-regulated by NF-kappaB and phosphorylated by Akt1 and then complexes with Bcl3 to enter the nucleus. *J Biol Chem* **281**, 167-175.

Yoneyama, M., Suhara, W., Fukuhara, Y., Fukuda, M., Nishida, E. & Fujita, T. (1998). Direct triggering of the type I interferon system by virus infection:

activation of a transcription factor complex containing IRF-3 and CBP/p300. *EMBO J* **17**, 1087-1095.

Zhang, D., Song, L., Li, J., Wu, K. & Huang, C. (2006a). Coordination of JNK1 and JNK2 is critical for GADD45alpha induction and its mediated cell apoptosis in arsenite responses. *J Biol Chem* **281**, 34113-34123.

Zhang, F., Hopwood, P., Abrams, C. C., Downing, A., Murray, F., Talbot, R., Archibald, A., Lowden, S. & Dixon, L. K. (2006b). Macrophage transcriptional responses following in vitro infection with a highly virulent African swine fever virus isolate. *J Virol* **80**, 10514-10521.

Zhang, N., Ahsan, M. H., Zhu, L., Sambucetti, L. C., Purchio, A. F. & West, D. B. (2005). NF-kappaB and not the MAPK signaling pathway regulates GADD45beta expression during acute inflammation. *J Biol Chem* **280**, 21400-21408.

Zhao, Y., Chapman, D. A. & Jones, I. M. (2003). Improving baculovirus recombination. *Nucleic Acids Res* **31**, E6-6.

Zsak, L., Lu, Z., Burrage, T. G., Neilan, J. G., Kutish, G. F., Moore, D. M. & Rock, D. L. (2001). African swine fever virus multigene family 360 and 530 genes are novel macrophage host range determinants. *J Virol* **75**, 3066-3076.

Zufferey, R., Donello, J. E., Trono, D. & Hope, T. J. (1999). Woodchuck hepatitis virus posttranscriptional regulatory element enhances expression of transgenes delivered by retroviral vectors. *J Virol* **73**, 2886-2892.